	Document:	D1.4. Handbook of protocols and methods		
	Author	UJAEN	Version	6
	Reference	D1.4	Date	24/03/2023



**SUSTAIN  
OLIVE**



**PRIMA**  
EUROPEAN PARTNERSHIP FOR  
IN THE MEDITERRANEAN AREA



Co-funded by the  
Horizon 2020 Framework  
Programme of the European Union

This project is part of the PRIMA programme supported by the European Union


# SUSTAINOLIVE

## Handbook of protocols and methods of SUSTAINOLIVE


Deliverable D 1.4

WP1. Project management and governance



	Document:	D1.4. Handbook of protocols and methods		
	Author	UJAEN	Version	6
	Reference	D1.4	Date	24/03/2023

## Novel approaches to promote the SUSTAINability of OLIVE cultivation in the Mediterranean

	Document:	D1.4. Handbook of protocols and methods		
	Author	UJAEN	Version	6
	Reference	D1.4	Date	24/03/2023

### DELIVERABLE FACTSHEET

Deliverable nº: D 1.4

Deliverable type: Report


Responsible Partner: UJA

WP nº and title: 1. Project management and governance

Version: 6

Version Date: 24/03/2023

Dissemination level	
	PU = Public, fully open
X	CO = Confidential, restricted under conditions set out in Model Grant Agreement

	Document:	D1.4. Handbook of protocols and methods		
	Author	UJAEN	Version	6
	Reference	D1.4	Date	24/03/2023

## Approvals

### Author/s

Roberto García Ruiz, Julio Antonio Calero González, Tomás Fernández del Castillo, Francisco Moya Giménez, Manuel López Vicente, Milagros Torrús Castillo, Juan Bautista Barroso Albarracín, Ramón González Ruiz, J.A. Gómez Guzmán, M<sup>a</sup> Pilar Cordovilla Palomares, Anna Irene De Luca and Ignacio Jesús Lorite Torres, José Liétor Gallego.


### Task Leader

Roberto García Ruiz

### WP leader:

Roberto García Ruiz

Version	Date	Status	Authors	Description
v1	02/03/2020	Draft	Roberto García Ruiz	Table of contents and content description for each section
v2	25/05/2020	Draft	Roberto García Ruiz, Julio Antonio Calero González, Tomás Fernández del Castillo Francisco Moya Giménez, Manuel López Vicente, Milagros Torrús Castillo, Juan Baustista Barroso Albarracín, Ramón González Ruiz, J.A. Gómez Guzmán, M <sup>a</sup> Pilar Cordovilla Palomares, Anna Irene De Luca and Ignacio Jesús Lorite Torres	First complete draft
V3	15/07/2020	Draft	Elena Guzmán Jiménez	Reviewed and formatted
V4	15/09/2020	Draft	General Assembly SUSTAINOLIVE	Reviewed and commented
v5	30/09/2020	Final	Roberto García Ruiz	Finalised draft
v6	23/03/2023	Final updated	Anna Irene De Luca, Giacomo Falcone, Nathalie Iofrida, Emanuele Spada, Manuel González de Molina, Pablo Domouso de Agar, Guiomar Carranza Gallego, Gloria Guzmán Casado	Incorporation of a widely detailed methodology on the Socio-economic and Life-Cycle assessment of the STSs (WP5)
v6	24/03/2023	Final updated	Jose Liétor Gallego	Addition of an extended version of the section 8 and review of the report format

	Document:	D1.4. Handbook of protocols and methods		
	Author	UJAEN	Version	6
	Reference	D1.4	Date	24/03/2023

### Disclaimer

This document contains a description of the SUSTAINOLIVE project work and findings. The authors of this document have taken any available measure in order for its content to be accurate, consistent and lawful. However, neither the project consortium as a whole nor the individual partners that implicitly or explicitly participated in the creation and publication of this document hold any responsibility for actions that might occur as a result of using its content.


The content of this publication is the sole responsibility of the SUSTAINOLIVE consortium and can in no way be taken to reflect the views of the European Union and PRIMA Foundation.

### All rights reserved

This document may not be copied, reproduced or modified in whole or in part for any purpose without the written permission from the SUSTAINOLIVE Consortium. In addition to such written permission to copy, reproduce or modify this document in whole or part, an acknowledgement of the authors of the document and all applicable portions of the copyright must be clearly referenced.

### Acknowledgement


The work described in this report has been funded by PRIMA Foundation H2020 Section 1 Framework Programme.

	Document:	D1.4. Handbook of protocols and methods		
	Author	UJAEN	Version	6
	Reference	D1.4	Date	24/03/2023

## Executive Summary


This document contains an overview and details on the main methods and protocols to be use in most of the tasks related to ecosystems services evaluation and monitoring (WP3) and on the socio-economic and life-cycle assessments of olive grove with sustainable technological solution (STS and comparable olive grove without the implementation of STS. This handbook, which will be updated in subsequent version to be adapted to each of the STS and non-STs olive groves and the limitation of the partners, compile the methodologies to asses and monitoring: abiotic stress, pest and diseases, soil functional quality, nutrient balance and retention, soil erosion, C footprint and C sequestration, resilience and resistance to climate change, and Life cycle, life cycle costing, life cycle sustainability and socio-ecological metabolism assessment.

The document has been prepared as part of SUSTAINOLIVE Work Package WP1 and correspond to the deliverable 1.4 of SUSTAINOLIVE “Handbook of protocols and methods” . This handbook is intended to guide the consortium partners on evaluating and monitoring most of the ecosystems services.


	Document:	D1.4. Handbook of protocols and methods		
	Author	UJAEN	Version	6
	Reference	D1.4	Date	24/03/2023

## TABLE OF CONTENTS

<b>1. Abiotic stress monitoring.....</b>	<b>9</b>
1.1. Considerations for samples collection .....	9
1.2. Fresh weight determination .....	10
1.3. Pigment contents: chlorophyll a, chlorophyll b, carotenoids and anthocyanins.....	11
1.4. Photosynthesis rate .....	11
1.5. Relative water content (RWC) .....	12
1.6. Hydrogen peroxide (H <sub>2</sub> O <sub>2</sub> ) quantification .....	12
1.7. Hydrogen peroxide (H <sub>2</sub> O <sub>2</sub> ) content .....	12
1.8. Free proline content .....	13
1.9. Soluble sugar (SS) content .....	13
1.10. RNA isolation and semi-quantitative RT-PCR for aquaporin (AQP), dehydrin (DHN) and heat-shock protein (HSP) genes. ....	14
1.11. Ascorbate determination .....	15
1.12. Glutathione determination .....	16
1.13. Total antioxidant activity (protocols 1 and 2) .....	16
1.14. Malondialdehyde (MDA) determination .....	17
1.15. Gene expression analysis by RNA-seq .....	18
<b>2. Biotic stresses: pests and diseases monitoring.....</b>	<b>20</b>
2.1. Overview of the biology of <i>Bactrocera oleae</i> .....	20
2.2. Fruit sampling and processing procedure.....	22
2.3. <i>B. oleae</i> , larvae and pupae (first generation: end-summer). Assessment of fruit infestation.....	24
2.4. Assessment of the incidence of <i>Prays oleae</i> and monitoring the impact of natural enemies.....	26
2.5. Assessment of the incidence of olive bark beetle <i>Phloeotribus scarabaeoides</i> .....	31
2.6. Sampling and determination of the infection rate of <i>Pseudomonas savastanoi</i> .....	36
2.6.1. Diagnosis .....	36
2.6.2. Infection rate assessment .....	36
2.6.3. Isolation of the pathogen.....	37
<b>3. Soil functional quality .....</b>	<b>37</b>
3.1. Assessment of the diatom community in STS and non-STS olive farms.....	37
3.2. Assessment of the soil quality in soils of STSs and non-STSs olive farms .....	38
3.2.1. Acid and alkaline phosphomonoesterase activity with the substrate p-nitrophenyl phosphate .....	39
3.2.2. $\beta$ -glucosidase activity: an enzyme involved in the easily-to-decompose organic carbon.....	43
3.2.3. Arylsulfatase activity: an enzyme involved in the sulphur metabolism .....	45
3.2.4. Dehydrogenase: and enzyme indicator of the intracellular metabolism.....	47


	Document:	D1.4. Handbook of protocols and methods		
	Author	UJAEN	Version	6
	Reference	D1.4	Date	24/03/2023

3.2.5. Potential nitrification rate .....	49
3.2.6. Potential soil N mineralization (waterlogged method) .....	51
3.2.7. Microbial community level physiological profiling .....	52
<b>4. Nutrient balance and retention .....</b>	<b>56</b>
4.1. General features of the model .....	56
4.2. N, P and K inputs .....	57
4.2.1. Natural N, P and K inputs .....	57
4.2.2. Inputs of N, K and P by rainfall .....	57
4.2.3. Inputs by formation of new soil .....	59
4.2.4. Inputs of N by natural N fixation .....	60
4.2.5. Symbiotic N fixation (plant-associated) .....	60
4.2.6. Non symbiotic N fixation (free-living) .....	63
4.2.7. Anthropogenic N, P and K inputs .....	64
4.2.8. N, P and K entries through irrigation .....	64
4.2.9. N, P and K entries by seeds application .....	64
4.2.10. N, P and K inputs by fertilization .....	65
4.3. N, P and K outputs .....	66
4.3.1. N, P and K outputs by harvesting .....	66
4.3.2. N outputs by burning olive tree pruning .....	66
4.3.3. N, P and K outputs by soil erosion .....	66
4.3.4. N outputs due to denitrification .....	67
4.3.5. N losses through volatilization of NH <sub>3</sub> .....	69
4.3.6. N losses through leaching .....	73
<b>5. Soil erosion .....</b>	<b>75</b>
5.1. Introduction .....	75
5.2. Information sources and Geographical Information System software .....	76
5.3. R Factor .....	79
5.4. K Factor .....	81
5.5. LS Factor .....	88
5.6. C Factor .....	93
5.7. P Factor .....	107
5.8. Sediment yield in olive groves with GIS .....	109
<b>6. Carbon sequestration and C footprint .....</b>	<b>117</b>
6.1. Introduction .....	117
6.2. Carbon footprint .....	118
6.2.1. Annual C inflows .....	119
6.2.2. Volume of trees .....	119
6.2.3. Wood density .....	120
6.2.4. Tree biovolume and mass .....	120
6.2.5. Annual C accumulation rate .....	121

	Document:	D1.4. Handbook of protocols and methods		
	Author	UJAEN	Version	6
	Reference	D1.4	Date	24/03/2023

6.2.6. Annual C outflows .....	123
6.3. Carbon sequestration.....	125
6.3.1. Disturbed samples (top 30cm) .....	126
6.3.2. Undisturbed samples and bulk density sampling and determination.....	127
6.3.3. Determination of soil organic matter .....	130
6.3.4. Determination of equivalent calcium carbonate.....	132
6.3.5. Carbon stocks.....	134
<b>7. Assessment of resilience to climate change .....</b>	<b>136</b>
7.1. General considerations.....	136
7.2. Flowering phenology evaluation .....	137
7.3. Fruit traits and oil quality assessment .....	137
<b>8. Social agrarian metabolism, social life cycle and life cycle sustainability assessments .....</b>	<b>140</b>
8.1. General introduction to WP5 methodologies.....	140
8.2. Social Agrarian Metabolism (SAM) .....	144
8.2.1. Origin, background, and theoretical principles.....	144
8.2.2. Funds and flows in agrarian metabolism .....	145
8.2.3. The organization and dynamics of agrarian metabolism.....	147
8.2.4. State of the art of sam in agricultural field and its application to olive growing.....	149
8.2.5. Methodological application to SUSTAINOLIVE project .....	151
8.3. Life cycle methodologies (LCA, LCC, SLCA).....	162
8.3.1. Origin, background, and theoretical principles.....	162
8.3.2. State of the art in agricultural field and olive growing.....	167
8.3.3. Methodological application to sustainolive project (data, elaborations, indicators, results typology, etc.).....	174
8.4. Bibliographical references.....	177



	Document:	D1.4. Handbook of protocols and methods		
	Author	UJAEN	Version	6
	Reference	D1.4	Date	24/03/2023

## 1. Abiotic stress monitoring

### WP3. Task 3.2. Monitoring for abiotic stress

Leader: Juan Bautista Barroso Albarracin (University of Jaen)

For further clarification contact: jbarroso@ujaen.es

As a Mediterranean tree, olive is exposed to a plethora of stress conditions such as high solar radiation, drought, drastic temperature changes, high salinity, etc., which can induce nitro-oxidative stress situations that seriously threaten crop productivity and quality and deteriorate the environment. The early detection of stress symptoms is essential to prevent further more devastating effects. In this task, abiotic stress will be monitored in selected non-STs and STs olive groves (about 4 olive groves per country).


The selection of comparable non-STs and STs olive groves and the battery of stress markers, which include among others non-enzymatic antioxidants (glutathione and ascorbate content), malondialdehyde, oxidative lipid injury marker and hydrogen peroxide, will be accompanied by the initial analysis of some ecophysiological parameters such as fresh weight, photosynthesis rate and chlorophyll content, among others.

In addition, gene expression studies will be carried out by analysing mass sequencing transcriptomics (RNA-seq) profiles of RNA samples from olive leaves using Illumina PE150 sequencing technology. These assays will be carried out in 4 olive groves (2 with non-STs and in 2 comparable olive groves but with STs) per country. Gene expression determinations (protocols 9 and 15) will be analyzed by the UJA for selected non-STs and STs olive groves of Portugal, Spain and Morocco, whereas UNIPR will oversee abiotic stress monitoring of olive groves of Italy, Greece and Tunisia, with close collaboration of the olive farmer associations.

*Outcomes:* Through these analyses we will obtain a data set of abiotic stress levels in STs and comparable non-STs olive groves.

### 1.1. Considerations for samples collection

It would be desirable to diminish to a minimum the environment variability, apart from the variables that we want to study. Obviously, samples will be collected at different olive groves but the weather conditions should not be too different between STs and non-STs olive farms. We strongly suggest that olive leave samples should be taken at the end of spring or

	Document:	D1.4. Handbook of protocols and methods			
	Author	UJAEN	Version	6	
	Reference	D1.4	Date	24/03/2023	

beginning of summer, at this time the tree is active and the weather is more stable with long sunny days.

In general, for the analyses described below, the following observations should be maintained whenever possible, unless other indications are specified. Otherwise, any deviations from the standard protocol will be noted.

- We need sampling at least three different trees per olive farm
- Take around 8-10 leaves per tree at least 1.5 m high to avoid juvenile tissues.
- Leaves may be around 15-20 cm from the branch tips.
- Leaves of different trees should be taken always with the same orientation, southern branches the better.

-Be careful that leaves are healthy, unbitten and not damaged.


**- Please pay special attention in cases where immediate freezing with liquid nitrogen or dry ice until processing is required and subsequent storage in a freezer (-80 °C).**

## 1.2. Fresh weight determination

Representative and homogeneous leaf samples will be randomly collected from 3 trees of each olive grove. Samples should be harvested at the same time and the same weekday along three weeks. The experimental material will be weighted as soon as possible and the next table will be filled in with the required information:

Country:

Area of study (name)	Olive cultivar	Replica number	Sampling date	Temperature in the sampling date	Sample size (number of leaves)	Fresh sample weight (g)
1		1				
		2				
		3				
2		1				
		2				
		3				
3		1				
		2				
		3				
4		1				
		2				
		3				

	Document:	D1.4. Handbook of protocols and methods		
	Author	UJAEN	Version	6
	Reference	D1.4	Date	24/03/2023

Notes:

- 4 olive grove/country will be analysed.
- If the sample collection was done in different seasons of the year, the table would have to be modified. Right now, it is configured to make three collections at any given time of the year.

### 1.3. Pigment contents: chlorophyll a, chlorophyll b, carotenoids and anthocyanins

The contents of chlorophyll a, chlorophyll b, total carotenoids and total anthocyanins will be quantified and calculated according to Sims and Gamon, 2002 and Silva et al., 2018. For chlorophylls and total carotenoids, leaves will be homogenised with acetone: Tris 50mM pH 7.8 (80 : 20, v/v); for total anthocyanins, leaves will be homogenised with methanol :HCl 1%: water (90 : 1:1, v/v/v). The homogenates will be centrifuged at 5000xg for 5 min at 4°C. Absorbance will be read in a spectrophotometer at 663, 537, 647 and 470 nm for chlorophylls and total carotenoids, and at 529 and 650 nm for total anthocyanins.

$$\text{Chl}_a = 0.01373 A_{663} - 0.000897 A_{537} - 0.003046 A_{647}$$

$$\text{Chl}_b = 0.02405 A_{647} - 0.004305 A_{537} - 0.005507 A_{663}$$

$$\text{Anthocyanin} = A_{529} - (0.288 A_{650})$$


$$\text{Carotenoids} = (A_{470} - (17.1 \times (\text{Chl}_a + \text{Chl}_b) - 9.479 \times \text{Anthocyanin})) / 119.26$$

- Sims and Gamon, 2002; doi: 10.1016/S0034-4257(02)00010-X
- Silva et al., 2018; <https://doi.org/10.1071/FP18026>

### 1.4. Photosynthesis rate

The determination of the photosynthesis rate **is optional**. We have to discuss on the **feasibility to assess for photosynthesis rate**.

Photosynthetic rate can be determined by means a portable infrared gas analyzer (IRGA). An advisable model should be a LI-COR 6400. This equipment is fitted with a “clamp” sensor which consists of a 6 cm<sup>2</sup> measurement chamber area inside which several leaves of the seedling can be placed for determinations. The appropriate corrections depending on the area of the analyzed leaf should be done in the case of small size leaves. In order to obtain data from IRGA, the Win FxFile Transfer program was used.

	Document:	D1.4. Handbook of protocols and methods		
	Author	UJAEN	Version	6
	Reference	D1.4	Date	24/03/2023

## 1.5. Relative water content (RWC)

The leaf samples of olive trees will be used for RWC assay according to Smart and Bingham (1974) and Golmohammadi et al. (2019). After fresh weight (FW) determination, leaves will be floated on distilled water in the dark for 24 h. Then the turgid weights (TW) will be recorded and the samples will be transferred into oven drying at 70 ° C for 48 h. After determination of dry weights (DW). The RWC will be estimated by the following equation:  

$$RWC\% = 100 \times (FW-DW)/(TW-DW)$$

- Smart and Bingham, 1974; URL: <http://www.jstor.org/stable/4263508>
- Golmohammadi et al., 2019; Doi: <http://dx.doi.org/10.14715/cmb/2019.65.7.9>

## 1.6. Hydrogen peroxide (H<sub>2</sub>O<sub>2</sub>) quantification


Note: the hydrogen peroxide content shall be carried out by means of Protocol 5 or 6.

For hydrogen peroxide, olive leaves should be processed fresh, if not possible, within 24 hours of collection. Half gram of a leaf tissue will be ground in 5 ml precooled 5% trichloroacetic acid (TCA) (w/v) and 0,15 g activated charcoal to remove pigments and other interfering substances in plant extracts (Dias et al., 2011). After centrifugation at 15,000 g for 20 min at 4 ° C, the pH of the supernatant will be adjusted to 8.4 with 17 M ammonia. Then, the extracts will be divided in two aliquots of 1 ml: a) in both aliquots 1 ml of colorimetric reagent (4-aminoantipyrine + phenol + peroxidase 150 U mg<sup>-1</sup> in 100 mM acetic acid buffer at pH 5.6 will be added, and b) Blank containing 8 μg catalase will only added to one aliquot. After 10 min at 30 ° C, the absorbance will be read at 505 nm, and H<sub>2</sub>O<sub>2</sub> will be calculated against a H<sub>2</sub>O<sub>2</sub> standard curve. Six to eight replicates per treatment will be used.

- Dias et al., 2011; DOI: 10.1007/s11099-011-0028-9

## 1.7. Hydrogen peroxide (H<sub>2</sub>O<sub>2</sub>) content

The H<sub>2</sub>O<sub>2</sub> concentration will be measured on fresh tissue (if not possible, within 24 hours of collection). 500 mg of leaves will be grounded to a powder in a mortar in presence of liquid nitrogen. After that, 5 ml of 0.1% (w/v) cold TCA, and then centrifuged for 15 min at 12,000 × g at 4 ° C. The supernatant (0.5 mL) will bge added to 0.5 ml 10 mM phosphate buffer (pH 7.0) and 1 ml 1 M of iodate potassium (KI) solution; the corresponding absorbance will be measured at 390 nm (Sergiev et al., 1997). The amount of hydrogen

	Document:	D1.4. Handbook of protocols and methods		
	Author	UJAEN	Version	6
	Reference	D1.4	Date	24/03/2023

peroxide is calculated using a standard curve prepared with known concentration values of H<sub>2</sub>O<sub>2</sub>.

- Ben Abdallah et al., 2018; doi.org/10.1016/j.jplph.2017.10.009
- Kong-Ngern et al., 2012; doi: 10.3923/ijb.2012.54.65 (Detailed protocol)

## 1.8. Free proline content


Free proline content was determined according to Bates et al. (1973) using L-proline for the standard curve. Frozen leaf samples (0,5 g) were ground to a powder in a mortar in presence of liquid nitrogen. After that, 10 ml of 3% (w/v) aqueous sulfosalicylic acid. Then, the homogenate will be centrifuged at 10.000 xg for 10 min. Two ml of the extract will be reacted with 2 ml ice-cold acid-ninhydrin and 2 ml of ice-cold glacial acetic acid in a test tube for 1 hour at 100° C, and the reaction will be stopped by placing the tubes in ice. After that, the reaction mixture will be extracted with 4 ml toluene, mixed vigorously with a test tube stirrer for 15-20 sec and left until separation into two phases. The chromophore containing toluene (upper phase) will be aspirated from the aqueous phase, warmed to room temperature and the absorbance read at 520 nm using toluene for a blank. The proline concentration will be determined from a standard curve and calculated on a fresh weight basis as follows: [(g proline/ml × ml toluene) / 115.5 g/ mole]/[(g sample)/5] = moles proline/g of fresh weight material.

Acid-ninhydrin is prepared by warming 1.25 g ninhydrin in 30 ml glacial acetic acid and 20 ml 6 M phosphoric acid, with agitation, until dissolved. Kept cool (stored at 4° C) the reagent remains stable 24 hours.

- Ben Abdallah et al., 2018; doi.org/10.1016/j.jplph.2017.10.009
- Bates et al., 1973 (Plant and Soil 39, 205-207)
- Silva et al., 2018; http://doi.org/10.1071/FP18026

## 1.9. Soluble sugar (SS) content

Total SS (TSS) is extracted in 80% ethanol, according to Irigoyen et al. (1992). A sample of 0.5 g of freshly harvested leaves is crushed in 5 ml of 80% (v/v) ethanol. The soluble fraction is centrifuged at 3500 xg for 10 min. The supernatants are collected and stored at 4° C for TSS determination. TSS is analyzed by reacting 0.2 ml of the alcoholic extract with 3 ml freshly prepared anthrone (150 mg anthrone + 100 ml 72% v/v] H<sub>2</sub>SO<sub>4</sub>) and placed in a

	Document:	D1.4. Handbook of protocols and methods		
	Author	UJAEN	Version	6
	Reference	D1.4	Date	24/03/2023

boiling water bath for 10 min. After cooling, the absorbance at 625 nm is determined in a spectrophotometer.

- Barcelar et al., 2007; doi: 10.1007/s11104-006-9088-1
- Irigoyen et al., 1992; doi.org/10.1111/j.1399-3054.1992.tb08764.x

### 1.10. RNA isolation and semi-quantitative RT-PCR for aquaporin (AQP), dehydrin (DHN) and heat-shock protein (HSP) genes

Total RNA will be extracted with Trizol Reagent (Gibco-BRL, Life Technologies, Grand Island, NY) as described in the manufacturer's manual, and the samples will be stored at  $-80^{\circ}\text{C}$ . Before cDNA synthesis, 2  $\mu\text{g}$  of total RNA will be incubated with 1U DNase I Amplification grade (Life Technologies, Carlsbad, CA, USA) to remove any contaminating genomic DNA. Prior and after this treatment, total RNA will be quantified on a Thermo Fisher Scientific spectrophotometer (NanoDrop 1000). After DNase I treatment, 2  $\mu\text{g}$  of total RNA will be reverse transcribed with 1  $\mu\text{M}$  Oligo (dT)18, using the Omniscript RT Kit (Qiagen, Hilden, Germany). cDNA samples will be diluted in ultrapure Milli-Q water (1:20). qPCR will be performed as described by Araújo et al. (2019). All qPCR reactions will be performed in 12  $\mu\text{L}$  volumes containing iTaq SYBR Green Supermix (Bio-Rad, Hercules, CA, USA), 150 nM each gene-specific primer (Table 1), and 3  $\mu\text{L}$  pre-diluted cDNA (1:20). The reactions will be subjected to an initial denaturation of 30 s at  $95^{\circ}\text{C}$ , followed by two cycles of 1 min at  $95^{\circ}\text{C}$ , 1 cycle of 6 s at  $95^{\circ}\text{C}$ , 60 cycles at  $94^{\circ}\text{C}$  for 5 s,  $58^{\circ}\text{C}$  for 15 s,  $72^{\circ}\text{C}$  for 15 s, and  $68^{\circ}\text{C}$  for 6 s. A melting program will be performed at the end of qPCR. Average PCR efficiency values and cycle thresholds will be estimated from the fluorescence data using the algorithm Real-Time PCR Miner (Zhao and Fernald 2005). qPCR will be carried out at least three times, and in triplicate. Gene-specific primers (Table 1) were designed from the published *O. europaea* coding sequences using the Primer3 design tool according to Rozen and Skaletsky 1999 and Araújo et al. (2019). Gene expression levels of target genes will be calculated relative to control and normalised with OeACT1 and OeGAPB reference genes according to the  $\Delta\Delta\text{CT}$  method (Applied Biosystems 2008), after cycle threshold transformation with efficiency values.

- Zhao and Fernald 2005; doi: 10.1089/cmb.2005.12.1047.
- Rozen and Skaletsky 1999; DOI: 10.1385/1-59259-192-2:365
- Araújo et al., 2019; <https://doi.org/10.1007/s00425-019-03109-2>


	Document:	D1.4. Handbook of protocols and methods		
	Author	UJAEN	Version	6
	Reference	D1.4	Date	24/03/2023

Table 1. Primers used for qPCR.


	Gene name	GenBank accession n°.	Primer sequence (5'–3')
PCR Control (Actin)	OeACT1	AF545569.1	F: GAG AGG GTA TAT GTT CAC CAC CTC A R: GGA CTT CTG GAC AAC GGA ATCT
PCR Control	OeGAPB	EF506494.1	F: GCT CAA GGG CAA GCT CAA R: ATC GCA TAC GGC CAA TAC AC
Dehydrins	OeDHN1	KR349290.1	F: CCC ACC ACC ACC ATA TCA G R: CCT TTT CCT TCT CTT CCT CAGTC
HSP	OeHSP18.3	FN554869.1	F: CAG CCG TCT CTG CTC CAA R: CTC CCT GCT CCT CTC TCC TC
Aquaporins	OePIP1.1	DQ202708.1	F: GGC TGT TTT TGG GGA GGA R: CCA TCG CCC TTG GTG TAA
Aquaporins	OePIP2.1	DQ202709.2	F: GGT TGG TTT GGG TGC TGA R: GCA GGG TTG ATG CCA GTT

### 1.1.1. Ascorbate determination

Total ascorbate (AsA + DHA) and reduced AsA contents are determined according to Silva et al. (2013). Samples of frozen leaf powder (0.5 g leaves) are homogenized with a mortar and pestle with 8 ml ice-cold 6% (w/v) TCA and centrifuged at 10.000 xg 10 min 2 °C. Total ascorbate, AsA + DHA, is determined in a reaction mixture containing 100 µl of the supernatant, 250 µl 150 mM phosphate buffer (pH 7.4) (with 5 mM EDTA) and 0.1 ml 10 mM dithiothreitol for 10 min. Then, 0.05 ml N-ethylmaleimide (0.5%, w/v) is added to the reaction. The same procedure is done to AsA determination, but instead of dithiothreitol, ultra-pure water is added. After addition 0.2 ml TCA 10% (w/v), 0.2 ml phosphoric acid 44% (v/v), 0.2 ml 4,4'-dipyridyl in 70% (v/v) ethanol, and 0.1 ml FeCl<sub>3</sub> 3% (w/v) the mixture is incubated at 40 °C for 40 min and then the absorbance is read at 532 nm using AsA as a standard. Standard curves for total AsA and AsA are established. DHA is estimated from the difference between total AsA (AsA + DHA) and AsA.

- Dias et al., 2020; <https://doi.org/10.1016/j.phytochem.2019.112199>
- Silva et al., 2013; <http://doi.org/10.1016/j.jplph.2013.01.015>
- Jin et al., 2008; doi: 10.1002/tox.20362
- Ma et al., 2008; doi: 10.1016/j.plantsci.2008.07.010



	Document:	D1.4. Handbook of protocols and methods		
	Author	UJAEN	Version	6
	Reference	D1.4	Date	24/03/2023

### 1.12. Glutathione determination

For total glutathione (GSH + GSSG) and GSSG, samples of frozen leaf powder (0.5 g leaves) are homogenized with a mortar and pestle with 8 ml ice-cold 7% (w/v) 5-sulphosalicylic acid and then centrifuged at 10.000 xg 10 min 2 °C (Silva et al., 2013). Total glutathione is quantified in a reaction mixture (1 ml) containing 100 µl of the supernatant, 200 mM phosphate buffer solution (pH 7.2, with 5 mM EDTA and 1 mM 5,5'-dithiobis-(2-nitrobenzoic acid), 0.2 mM NADPH and 1 U GR (EC 1.6.4.2)). After incubation at 27 °C for 30 min, the mixture is read at 412 nm. The same procedure is followed for GSSG, but the supernatant is previously incubated with 0.17 M 2-vinylpyridine and 3.6% triethanolamine at 27 °C for 1 h. Standard curves for GSH and GSSG are established in 7% (w/v) 5-sulphosalicylic acid diluted appropriately with 0.2 M phosphate buffer solution (pH 7.2). GSH is calculated from the difference between total glutathione and GSSG.

- Dias et al., 2020; <https://doi.org/10.1016/j.phytochem.2019.112199>
- Silva et al., 2013; <http://dx.doi.org/10.1016/j.jplph.2013.01.015>
- Ma et al., 2008 Apple; doi: 10.1016/j.plantsci.2008.07.010


### 1.13. Total antioxidant activity (protocols 1 and 2)

**Note:** the total antioxidant activity shall be carried out by means of Protocols 1 or 2.

#### Protocol 1

Experiments will be performed on the spectrophotometer fitted with temperature control. For the determination of the antioxidant activity, leaf powders will be mixed with methanol and sonicated in a 40°C bath for 30 min. After centrifugation (15,000 g for 15 min at 4 °C) the supernatant is added to an ABTS [2,20-azino-bis (3-ethylbenzothiazoline-6-sulphonic acid)] (Sigma) solution prepared prior according to Re et al. (1999). ABTS will be dissolved in water to a 7 mM concentration. ABTS radical cation (ABTS 1) will be produced by reacting ABTS stock solution with 2.45 mM potassium persulfate (final concentration) and allowing the mixture to stand in the dark at room temperature for 12 – 16 h before use. Because ABTS and potassium persulfate react stoichiometrically at a ratio of 1:0.5, this will result in incomplete oxidation of the ABTS. Oxidation of the ABTS commenced immediately, but the absorbance was not maximal and stable until more than 6 h had elapsed. The radical is stable in this form for more than two days when stored in the dark at room temperature. The ABTS 1 solution will be diluted with PBS, pH 7.4, to an absorbance of 0.70 (±0.02) at 734 nm and equilibrated at 30 °C. After addition of 1.0 ml of diluted ABTS 1 solution ( $A_{734nm} = 0.700 \pm 0.020$ ) to 10 µl (we have to test different volumes) of supernatant the



	Document:	D1.4. Handbook of protocols and methods		
	Author	UJAEN	Version	6
	Reference	D1.4	Date	24/03/2023

absorbance reading will be taken at 30° C exactly 1 min after initial mixing and up to 6 min. The antioxidant activity will be calculated using a gallic acid standard curve (Araújo et al., 2019). All determinations will be carried out at least three times, and in triplicate.

- Re et al. 1999; DOI: 10.1016/s0891-5849(98)00315-3
- Araújo et al., 2019; <https://doi.org/10.1007/s00425-019-03109-2>

## Protocol 2

The total antioxidant ability of *Olea europaea* L. extracts is analyzed by means of the determination of its 1,1 – diphenyl – 2 – picrylhydrazyl (DPPH) free radical scavenging activity. The scavenging of DPPH (stable free radical) is estimated by the reduction of the color reaction between DPPH solution and sample extracts (Bois, 1958).


Leaves are homogenized in a buffer containing 100 mM Tris-HCl pH 8.0, 1 mM EGTA, 1 mM EDTA, 0.1 M NaCl, 7% (w/v) PVPP, 15 mM DTT, 15 mM PMSF, and 10X commercial plants protease inhibitor cocktail (SIGMA). Samples are ground to a powder in a mortar in presence of liquid nitrogen and after that the previous homogenization buffer is added (1:2; w/v). The soluble fraction is centrifuged at 3000xg, 5 minutes, 4 C. Supernatants re desalted through NAP-10 columns. Next, 2 mL of 0.12 mM solution DPPH in methanol is added to 1 mL of various concentrations of extract (50 - 1000 µg/mL) to be tested. After 30 min at room temperature, the absorbance of the reaction mixture is measured at 517 nm using a spectrophotometer. Ascorbic acid (2- 20 µg/mL) was used as positive controls.

The degree of DPPH radical scavenging activity is calculated as a percentage of inhibition (% inhibition), where: % Inhibition = I% = ((A Control-A Sample)/ A Control) \* 100. Where A Control is the absorbance of the blank sample (t = 0 min) and A Sample is the absorbance of the test extract or standard (t = 30 min). The tests were carried out in triplicate.

- Ayoub et al., 2019; doi: 10.6062/97320630015226
- Bois MS. Nature 1958 26: 1199
- Kitts et al., 2000; doi: 10.1023/a:1007078414639

### 1.14. Malondialdehyde (MDA) determination

Malondialdehyde will be measured as a lipid peroxidation index according to the method of Stewart and Bewley (1980) and Ahmadipor et al. (2018). 0.5 gram of fresh leaves will be homogenized with liquid nitrogen in a porcelain mortar. Five ml of 50 mM phosphate buffer pH 7 will be added to prepared powder in a 15 ml test tube. Then, the samples will be centrifuged at 14000 g for 30 min at 4°C. The supernatant will be mixed with an equal

	Document:	D1.4. Handbook of protocols and methods		
	Author	UJAEN	Version	6
	Reference	D1.4	Date	24/03/2023

volume of 0.5% TBA (2-thiobarbituric acid) in 20% trichloroacetic acid then incubated at 95°C for 30 min. Test tubes will be put in an ice bucket for stopping the reaction immediately. Samples will be centrifuged at 14000 g for 30 min at 4°C. Absorbance will be measured at 532nm and 600 nm, and in order to correct for background absorption, absorbance values at 600 nm will be subtracted from those at 532 nm, with the latter representing the absorption maximum of the TBA:MDA adduct. The extinction coefficient of 155 mM<sup>-1</sup> cm<sup>-1</sup> will be used. All determinations will be performed at least three times, and in triplicate, and expressed in pmolMDA/g fresh weight.

- Stewart and Bewley, 1980; <http://www.jstor.org/stable/4266117>
- Ahmadipor et al., 2018; <http://dx.doi.org/10.14715/cmb/2017.64.15.4>


### 1.15. Gene expression analysis by RNA-seq

#### Samples collection

It would be desirable to diminish to a minimum the environment variability, apart from the variables that we want to study. Obviously, samples will be collected at different olive groves but the climate and weather conditions should not be too different. I would suggest the end of spring or beginning of summer, at this time the plant is active and the weather is more stable with long sunny days.

For gene expression analysis, we just need a few leaves. They must be quickly frozen to avoid changes of the gene expression induce by the injury.

- We need sampling three different trees from each olive groves.
- Take around 8-10 leaves at least 1.5 m high to avoid juvenile tissues.
- Leaves may be around 15-20 cm from the branch tips.
- We would suggest taking the samples always with the same orientation, and suggesting the south branches.
- Be careful that leaves are healthy, unbitten and not damaged.
- Prior to proceed to sample collection, a unified system of sample labelling should be designed.
- Additionally, a database should be made in which recording relevant data as olive variety, country, date of sampling, coordinates of the trees or precise location, label of the sample, water irrigated or not, conventional or sustainable agriculture, any other relevant data.
- Collect them in 50 ml Falcon tubes and freeze them immediately in liquid nitrogen. If it were not possible to use liquid nitrogen, it is essential to freeze the samples in dry ice immediately.

	Document:	D1.4. Handbook of protocols and methods		
	Author	UJAEN	Version	6
	Reference	D1.4	Date	24/03/2023

- According to my experience, I would suggest labelling the Falcon tubes with permanent ink, but also I would include inside the tube a small piece of paper with the label written with a pencil.
- Use dry ice to transport samples to the laboratory. It is essential to avoid thawing the samples.
- Keep the samples at -80 °C until they are sent to our lab.
- Samples must be in dry ice during the transport to our lab for the gene expression analysis.

### Gene expression by RNAseq


- For RNA isolation, the Spectrum Plant Total RNA kit (Sigma-Aldrich, St. Louis, MO, USA) will be used following the manufacturer's instructions.
- Any DNA contamination will be removed by a column DNase I treatment step (Roche, Basel, Switzerland).
- RNA quality tests will be performed with the Agilent 2100 Bioanalyzer (Agilent Technologies, Santa Clara, CA, USA) employing an RNA 6000 Pico assay kit (Agilent Technologies), and all the samples' RIN values will have to be ranged around 8.
- RNAseq will be carried out by NGS sequencing.
- A cDNA library of poly A+ RNA will be made from each RNA sample according to the Illumina instructions.
- cDNA libraries will be sequenced by paired-end sequencing (150 x 2) with an Illumina NovaSeq 6000 sequencer. Each biological replicate will be loaded twice on two different lanes in the flow cell.

### Data Pre-processing

- The raw Illumina RNA-seq reads will be first preprocessed using FastqMcf [1] by discarding the primers and reads with adaptors, unknown nucleotides, and poor-quality or short-length reads, which increased the Q score to more than 30 for all the libraries and filtering for lengths longer than 50 bp (Q30L50).
- Sequencing quality control was performed with the NGS QC software [2].
- The trimming and cleaning of the obtained reads were carried out by the Trim Galore software (<https://github.com/FelixKrueger/TrimGalore>).

### Expression Analysis

- The gene expression study will be performed with the DNASTar (ArrayStar 17) for RNA-seq analyses ([www.dnastar.com](http://www.dnastar.com)).
- Reads will be first mapped to the *Olea europaea* cv. "Picual" genome as the reference Oleur061 [3].

	Document:	D1.4. Handbook of protocols and methods		
	Author	UJAEN	Version	6
	Reference	D1.4	Date	24/03/2023

- Mapping will be undertaken using high stringency parameters, k-mer = 63 and 95% of matches.
- The default normalization method of reads per kilobase per million mapped reads (RPKM) will be employed.
- Although this is open to discussion, in our experience for comparisons between groups of samples more consistent results are obtained using a FDR = 99% and Fold Change  $\geq 8$ .

## References

-Aronesty, E. 2011. ea-utils: ‘Command-line tools for processing biological sequencing data’. [WWW document] URL. Available online: <https://github.com/ExpressionAnalysis/ea-utils> (accessed on 11 January 2017).

-Patel, R.; Jain, M. NGS QC Toolkit: A Toolkit for Quality Control of Next Generation Sequencing Data. PLoS ONE 2012, 7, e30619, doi:10.1371/journal.pone.0030619.

-Jimenez-Ruiz, J.; Ramirez-Tejero, J.A.; Fernandez-Pozo, N.; De La O Leyva-Perez, M.; Yan, H.; De La Rosa, R.; Belaj, A.; Montes, E.; Rodriguez-Ariza, M.O.; Navarro, F.; Barroso, J.B.; Beuzon, C.R.; Valpuesta, V.; Bombarely, A.; Luque, F. Transposon activation is a major driver in the genome evolution of cultivated olive trees (*Olea europaea* L.). Plant Genome 2020, e20010, doi:10.1002/tpg2.20010.

## 2. Biotic stress: pests and diseases monitoring

### WP3. Task 3.3. Monitoring for abiotic stress

Leader: Ramon Gonzalez Ruiz and J.A. Gomez Guzman (University of Jaen)


For further clarification contact: [jramonglz@ujaen.es](mailto:jramonglz@ujaen.es)

Below different protocols for the main pest and diseases are described.

### 2.1. Overview of the biology of *Bactrocera oleae*

The olive fly, *Bactrocera oleae* (Gmelin), is considered the olive key pest in Mediterranean Basin and Portugal, including the Canary Islands Azores. Their attacks are more intense in humid and temperate zones, showing great variability according to the cultivated variety. Therefore, its importance is less in areas with hot and dry summers.

This insect winters in the pupal stage, and occasionally as an adult (in areas with mild winters). In the south of Spain, adults emerge from the wintering pupae during the month of March, and together with those who have wintered as adults, a period of feeding begins,

	Document:	D1.4. Handbook of protocols and methods		
	Author	UJAEN	Version	6
	Reference	D1.4	Date	24/03/2023

based on sugary and nitrogenous substances found in plants. Although they are sexually mature, the absence of fruits available for oviposition determines the existence of this period (called "white period") that lasts until quite late in the summer (Figure 1).

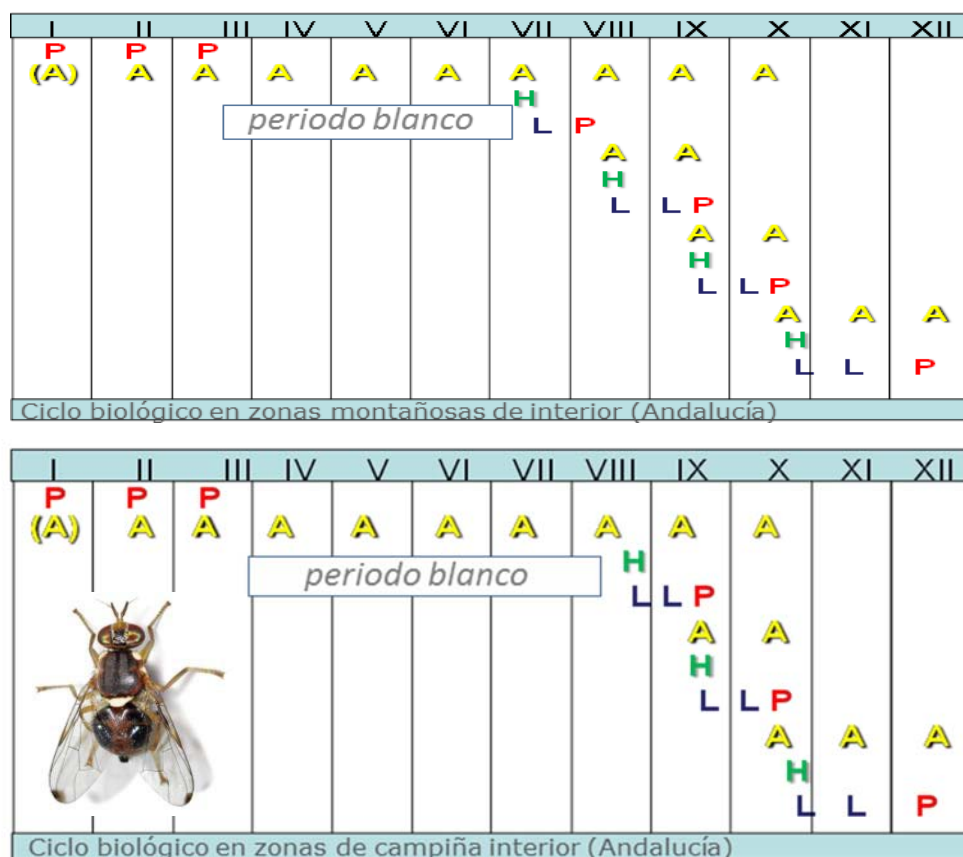



Figure 1. Biological cycle of *B. oleae* in mountainous areas (above) and countryside (below), in southern Spain. (A): Wintering adult; A: Adult; H: Egg; L: larva; P: Pupae.





	Document:	D1.4. Handbook of protocols and methods		
	Author	UJAEN	Version	6
	Reference	D1.4	Date	24/03/2023

During these months, the majority of the population is developing. Until wintering there are 3 generations, although in mountainous areas and in areas of the Mediterranean coast a fourth generation is observed.

## 2.2. Fruit sampling and processing procedure

To monitor flying populations of *B. oleae*, a device of 10 sticky yellow traps located in a central area of the plots, installed in olive trees one each other (Figure 2), would be used. This will allow us to determine and compare in a standardized way, the variations of the populations of this pest among the different countries involved.

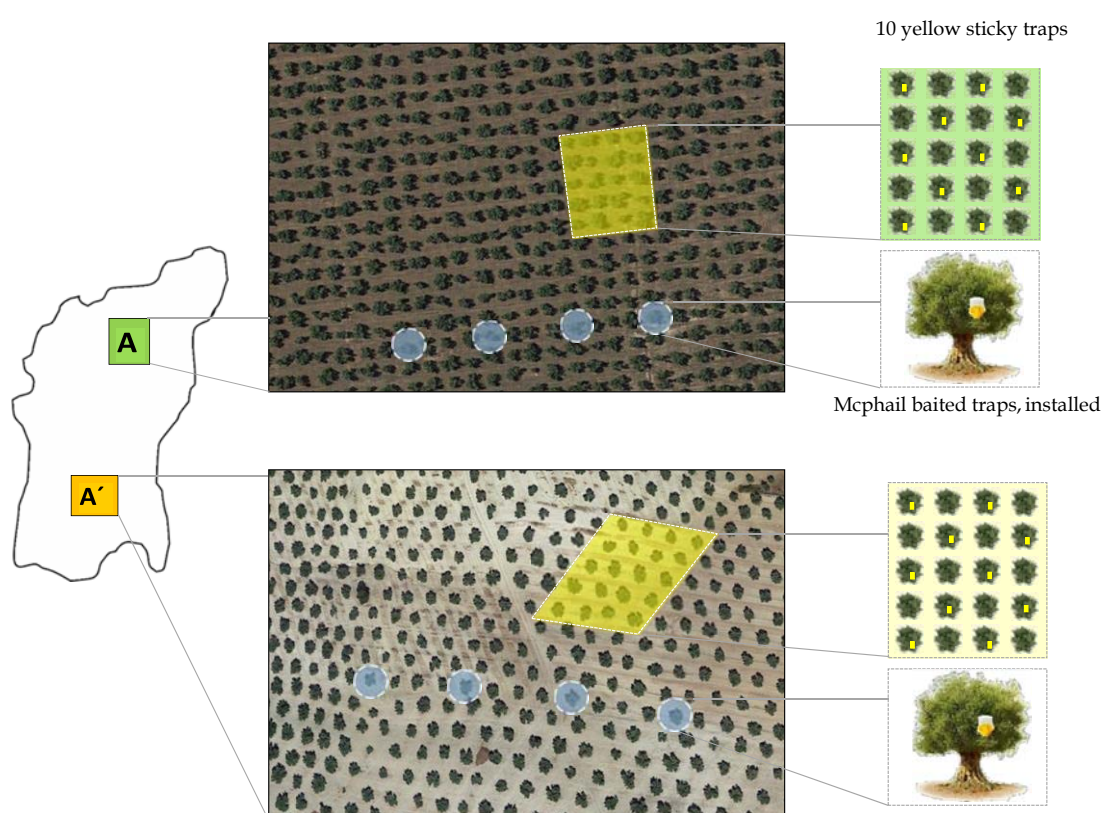



Figure 2. Sketch indicating location of sticky yellow traps and Mcphail traps on Sustainable (A) and non-sustainable plot (A').

The monitoring with sticky yellow traps of flying populations should be performed from the beginning of stage H (bone hardening) to the end of stage I (envero).

According to our available data:

- In Tunisia the interval begins in June and ends in October.
- In Greece, it begins on mid-June 15, and ends on mid-November.
- In the south of Spain, and probably in the center-south of Portugal, it begins in early August and ends in mid – November.

	Document:	D1.4. Handbook of protocols and methods		
	Author	UJAEN	Version	6
	Reference	D1.4	Date	24/03/2023

The specific start and end dates could however show variations, depending on the latitude, the altitude and the particular microclimatic of the target olive grove, but this means a total of 9 or 10 sampling intervals for sticky yellow traps. During this period, the traps can be renewed at intervals of 15 days, and at the end of each, the captured flies would be counted. It would be convenient to consider data from at least 4 pairs of plots (for instance: 2-3 pairs of plots corresponding to oil production, and 2-3 pairs of plots for production of table olives, if applicable).




Mcphail trap (left) and adult captured on sticky yellow trap (right)

However, in order to establish the equivalence between the capture levels provided by these yellow sticky traps and those that are commonly used for the decision of treatment application, based on the established population thresholds, McPhail traps can be used, baited with an attractant such as diammonium phosphate (5%). These decision thresholds (Table 2) are quite similar but slightly different among the Mediterranean countries. As indicated in Figure 2, a number of 4 units is proposed in each of the paired plots, so a total of 32 McPhail traps is required.

Table 2. Decision thresholds for the application of treatment against *B. oleae* in olive groves destined for the production of oil, and for the production of table olives in the countries participating in the SUSTAINOLIVE project. \* Please review this information, complete and, if necessary, provide the appropriate corrections.

	FRUIT FOR OIL PRODUCTION	TABLE FRUIT
	Decision threshold for treatment application	Decision threshold for treatment application
GREECE	> 1 females/trap/day & > 5% fruit infested	????
ITALY	>10 (summerr) or 30 (autumn) fem./trap/week & >10% fruit infested	>10 (summerr)-30 (autumn) fem./trap/week & >10% fruit infested
MOROCCO	????	???
PORTUGAL	> 5 females/trap/day & > 60% fertile females	> 1 Female/trap/day &/or > 1% fruit infested
SPAIN	> 5 females/trap/day & > 60% fertile females	>1 female/trap/day & >50% fertile females &/or >1% fruit infested
TUNISIA	???	???

	Document:	D1.4. Handbook of protocols and methods		
	Author	UJAEN	Version	6
	Reference	D1.4	Date	24/03/2023



Fruit sampling. Olive damaged by *B. oleae* oviposition




Oviposition injury and *Bactrocera oleae* larva


### 2.3. *B. oleae*, larvae and pupae (first generation: end-summer). Assessment of fruit infestation

Entering the data in the spreadsheet (Annex I). In the spreadsheet provided in the attached excel document, a first tab set corresponds to the data of the sticky yellow traps. For each plot, the number of individuals captured in each trap should be indicated





	Document:	D1.4. Handbook of protocols and methods		
	Author	UJAEN	Version	6
	Reference	D1.4	Date	24/03/2023

	COUNTRY										
	SITE NAME:										
	Paired plots	1									

SUSTAINABLE PLOT										
	Date 1	Date 2	Date 3	Date 5	Date 5	Date 6	Date 7	Date 8	Date 9	Date 10
	no. ind.	no. ind.	no. ind.	no. ind.	no. ind.	no. ind.	no. ind.	no. ind.	no. ind.	no. ind.
trap 1	0	0	0	0	0	0	0	0	0	0
trap 2	0	0	0	0	0	0	0	0	0	0
trap 3	0	0	0	0	0	0	0	0	0	0
trap 4	0	0	0	0	0	0	0	0	0	0
AVG/trap/day	0	0	0	0	0	0	0	0	0	0

AVG	0,000
SD	0,000

UNSUSTAINABLE PLOT										
	Date 1	Date 2	Date 3	Date 5	Date 5	Date 6	Date 7	Date 8	Date 9	Date 10
	no. ind.	no. ind.	no. ind.	no. ind.	no. ind.	no. ind.	no. ind.	no. ind.	no. ind.	no. ind.
trap 1	0	0	0	0	0	0	0	0	0	0
trap 2	0	0	0	0	0	0	0	0	0	0
trap 3	0	0	0	0	0	0	0	0	0	0
trap 4	0	0	0	0	0	0	0	0	0	0
AVG/trap/day	0	0	0	0	0	0	0	0	0	0

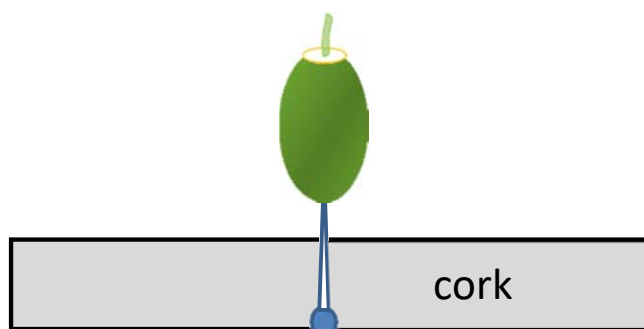
  


AVG	0,000
SD	0,000

## 2.4. Assessment of the incidence of *Prays oleae* and monitoring the impact of natural enemies

To determine the intensity of the attack of the olive moth in the study areas, and assess the effect of predation, from the start of the phenological stage G (curdled fruit) and 7-10 days after the start of this stage, 4 samplings are carried out at weekly intervals. In each one of them (and in each study area) 3 olive trees are selected at random, and 100 fruits are taken at random from each olive tree, from the four orientations and of different heights. The fruits will be placed in an opaque container (glass or plastic) and preferably in a container that protects them from solar radiation, and preferably at a temperature below ambient temperature.

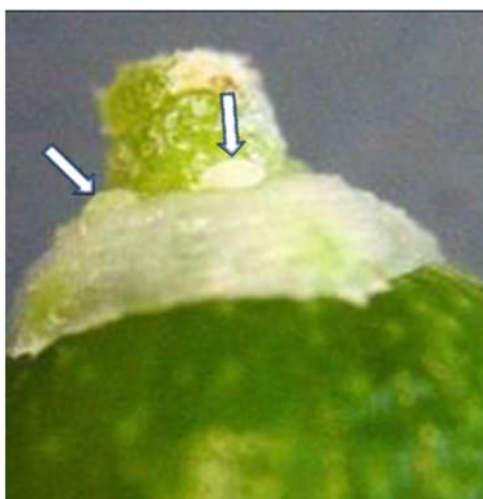
Eggs can be examined directly or they can also be preserved in the freezer. In this case, before beginning their observation, we will keep them for a few minutes at room temperature, thus allowing the evaporation of surface ice before processing. Once dried, the fruits are observed by means of a stereomicroscope, for which they can be fixed as indicated below, this allows the visualization of the calyx zone.



	Document:	D1.4. Handbook of protocols and methods		
	Author	UJAEN	Version	6
	Reference	D1.4	Date	24/03/2023

During fruit examination, we will differentiate between these three types of eggs:


**1. Live eggs.** When fresh they are milky white, not transparent. As the embryonic development progresses, they acquire a yellowish hue as the embryonic development progresses, being able, even at the end of its evolution, to observe the cephalic capsule (black color) of the larva.



**2. Predated eggs.** Generally due to the predatory activity of the larvae of the green lacewings (Chrysopidae). Of these, only the chorion remains attached to the support, as a thin and transparent layer, with its characteristic crosslinking. Its shape is irregular, very often collapsed or crushed, and it looks shiny. These types of eggs are clearly by far the most abundant, at least in Spain.



**3. Hatched eggs.** The hatched eggs have a reddish color, these eggs are bulged due to the presence under the chorion of excrement expelled by the larva, and unlike predatory eggs, the reticulation of the chorion is not appreciable.

	Document:	D1.4. Handbook of protocols and methods		
	Author	UJAEN	Version	6
	Reference	D1.4	Date	24/03/2023



When detached, the hatching hole of the larva is clearly observed.

Over the time of observations, parasitized eggs (by *Trichogramma spp*) were never found in Spain, which however have been mentioned as quite frequent in different Mediterranean areas, and which appear as dark gray, almost black coloration. In case they appear in the samples extracted in any of your olive groves, these would be counted in the excel spreadsheet as preyed eggs, thus adding to the eggs described above.

**Entering the data in the spreadsheet (Annex II).** An Excel document is attached, destined to the elaboration of the information from the data from the observation of the olives. It is recommended to make several copies in order to keep the original version always safe from any accidental modification. A pair of copies would correspond to each of the 4 weekly samplings (one for the sustainable olive grove, and one for the unsustainable olive grove).

During the observation of the fruits, the number of live (L), predated (P) and hatched (H) eggs, will be recorded for each one of the fruits. The rest of the cells should not be altered, just fill in the 3 free cells that follow the numbers.

Example: After observing the first fruit of olive tree #1 (bottom tab 1), we have found one live egg, three predated eggs and none hatched, so the spreadsheet would be as below:


It is important to bear in mind that for each one of the fruits, the three cells (L, P, H) must be filled, so that in the event that in any case there are no eggs of any of these three types, you would enter the value “0” .

Document:	D1.4. Handbook of protocols and methods		
Author	UJAEN	Version	6
Reference	D1.4	Date	24/03/2023

<b>prays oleae</b>		<b>FRUIT OBSERVATION SPREADSHEET</b>	
DATE		COUNTRY: GREECE	
ZONE		OLIVE TREE	

[illegible]

29


	Document:	D1.4. Handbook of protocols and methods		
	Author	UJAEN	Version	6
	Reference	D1.4	Date	24/03/2023

- **Population Index (P)**: Total number of eggs / 100 fruits
- **Potential attack (PA%)**, or percentage of fruits with any type of eggs (live, preyed or hatched) on them x 100 / total number of fruits observed.
- **Predation %**. It is the valuation of predatory activity, an index of the activity of natural enemies, equivalent to the number of predated eggs x 100 / total number of eggs observed.
- **FA %**. Final attack, is the percentage of fruits containing at least one hatched egg x 100 / no. total observed fruit. These fruits will be lost at the end of the summer, as a consequence of the emergence of the larva.
- **Rec%**. This parameter indicates the real efficiency of the predation, since it corresponds to the percentage of fruits in which all the eggs have been predated. Without the predatory activity of the green lacewings, these would be lost fruits. However, their action has allowed them to be recovered.

Once the fruits of the three olive trees sampled on date 1 have been processed, the data set is compiled in the fourth tab ( "TOTAL" ). On this page the information of the three olive trees is integrated, and is presented in the Table below.

<div> <div>Archivo</div> <div>InicioInsertarDiseño de páginaFórmulasDatosRevisarVista</div> <div> <div>Pegar</div> <div>Portapapeles</div> </div> <div> <div>Arial12</div> <div>NKSS</div> <div>Fuente</div> </div> <div> <div>Ajustar texto</div> <div>Combinar y centrar</div> <div>Alineación</div> </div> </div>							
	A	B	C	D	E	F	G
1							
2			Prays oleae				
3			COUNTRY	GREECE			
4			ZONE				
5			DATE	(TOTAL 3 olive trees)			
6							
7			FINAL TABLE (PARAMETERS)				
8				tree 1	tree 2	tree 3	TOTAL
9			HATCHING %	78,6	68,4	70,0	71,7
10			POPULATION	215,0	255,0	250,0	240,0
11			POT. ATTACK %	100,0	100,0	100,0	100,0
12							
13			FINAL ATTACK %	55,0	60,0	70,0	61,7
14			PREDATION %	67,4	62,7	60,0	63,2
15			RECOVERED %	30,0	25,0	20,0	25,0
16							
17			FRUITS	TREE 1	TREE 2	TREE 3	TOTAL
18			obs	20	20	20	60
19			ap	20	20	20	60
20			at	14	15	16	45
21			af	11	12	14	37
22			EGGS	TREE 1	TREE 2	TREE 3	TOTAL
23			total	43	51	50	144
24			alives	3	6	6	15
25			preyed	29	32	30	91
26			hatched	11	13	14	38
27							



	Document:	D1.4. Handbook of protocols and methods		
	Author	UJAEN	Version	6
	Reference	D1.4	Date	24/03/2023

In this final Table, the general values of the previously defined parameters are presented. Here it is observed that the value of the Population was 240 eggs / 100 fruits; the Final Attack corresponds to 61.7%, and the Predation percentage has been 63.2%, which has allowed the recovery of 25% of the fruits initially attacked (fortunately for the farmer involved, these data are fictitious;) Carrying out 4 samplings during the phenological stage G of the olive tree allows determining the percentage of predation on *Prays oleae*, as well as knowing precisely the predatory efficacy of the Green lacewings in the recovery of potentially lost fruits, and that by their action they become recovered.

Finally, it will allow to know the percentage of olive fruit drop (or Final Attack) that will occur in both sustainable and non-sustainable plots.

## 2.5. Assessment of the incidence of olive bark beetle *Phloeotribus scarabaeiodes*

Throughout its biological cycle, and in the case of healthy olive trees, this insect has two feeding periods:

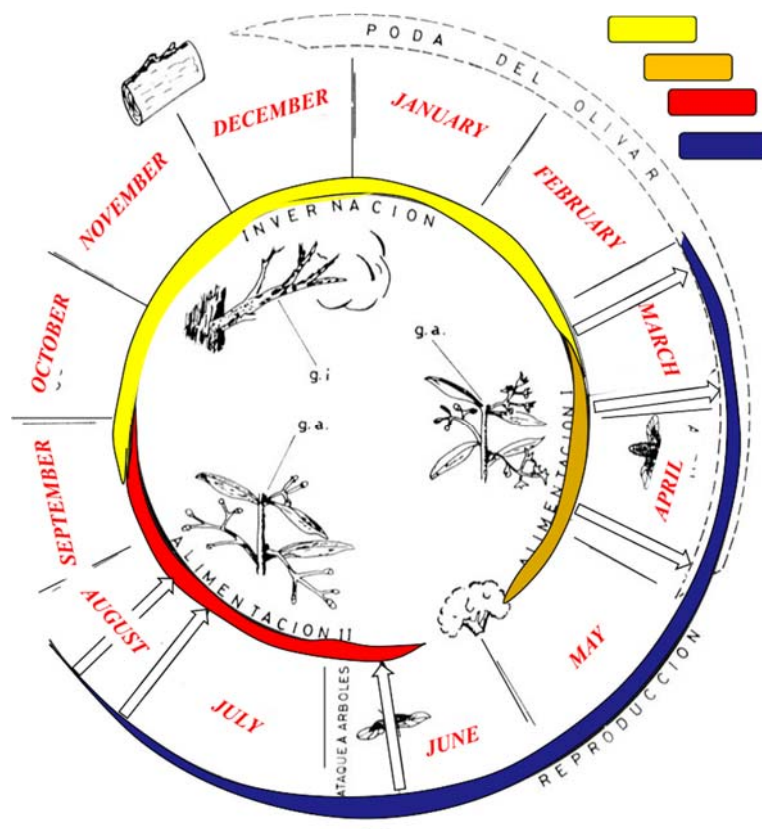



Figure 3. Life cycle of *Phloeotribus scarabaeiodes* in southern Spain. Yellow, orange, red and dark-blue periods stands for overwinter, Feeding I, Feeding II and reproduction stages.

	Document:	D1.4. Handbook of protocols and methods		
	Author	UJAEN	Version	6
	Reference	D1.4	Date	24/03/2023

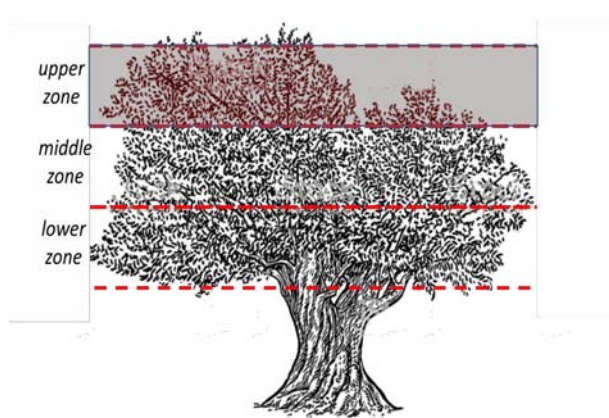
- A first period, which occurs after the overwintering of adults, and which begins at the end of winter, when the olive is at the phenological stage B (sprout). This period has a variable duration, generally up to the phenological stage G (curled fruit, end of May, in south Spain).

- A second period, of longer duration, which begins with the emergence of young adults from the pruning olive wood, what happens 15-20 days after the starting of phenological stage G of the olive tree (middle of June in south Spain). this period is maintained until the entry into winter of the adults, which takes during the stage H of the olive tree (bone hardening). At the beginning of the stage I (envero), most of beetles are in the overwintering period.

During their feeding, adults build small twig feeding galleries on the terminal branches of olive trees (Figures).


We may consider that in the case of seriously ill or dying olive trees (drought is a frequent cause), this species can reproduce directly on the branches and trunk of olive trees, which frequently triggers their death. Since this situation is atypical, the samplings expressed here focus on evaluating the activity caused by the feeding activity, and considering that this takes place in healthy olive trees.

The symptoms after a time may cause the twig to break (Figure below). However, it is also relatively frequent that these wounds could be gradually healed, although the residual marks remain.



According to the preferences of this insect, the highest density of the galleries is found in twigs whose diameter is 3mm-5mm, therefore, the evaluation of damages caused the




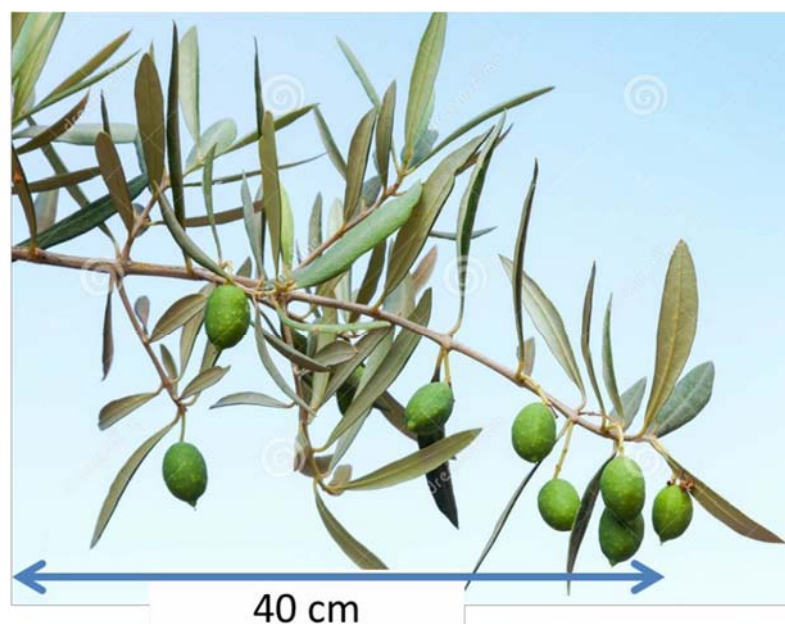
	Document:	D1.4. Handbook of protocols and methods		
	Author	UJAEN	Version	6
	Reference	D1.4	Date	24/03/2023

feeding activity must be focused on the terminal twigs. Likewise, its highest density is found in the terminal twigs of the upper third of the tree.



Since the symptoms of the feeding of this insect remain in the olive trees throughout the phenological cycle of the olive tree, the samplings can be carried out at any time of the year, although the damage density increases as the summer progresses (up to the stage I of the olives envero). Subsequently, adults begin to leave the nutritional cells, to gradually enter into the overwintering.

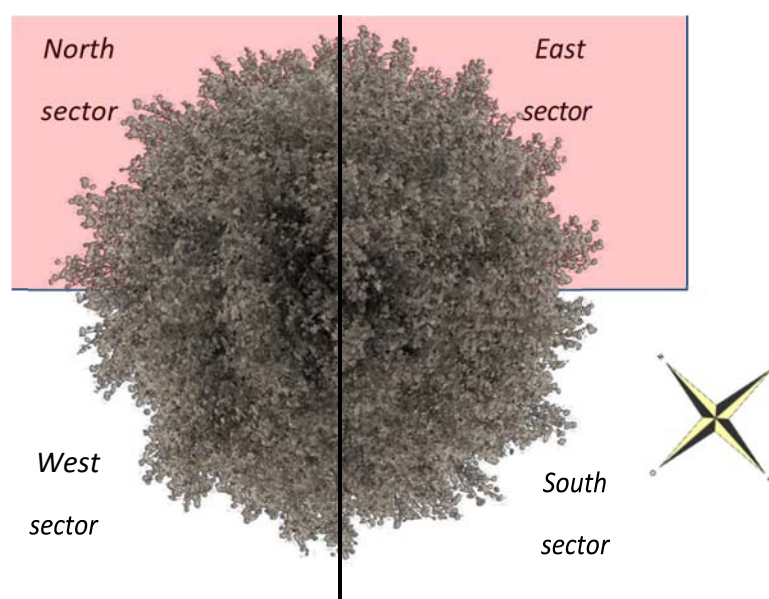
	Document:	D1.4. Handbook of protocols and methods		
	Author	UJAEN	Version	6
	Reference	D1.4	Date	24/03/2023



For each tree, the total number of damages must be noted in the first subcolumn of the spreadsheet (Twig gal.).


For the evaluation of the management practices on the impact of this pest, we recommend carrying out the samplings preferably during the summer, in the second feeding stage (which in south Spain occurs between mid-June and the end of September), carrying out a total of three sequential samplings, at 45-day intervals: First in mid-June, one second in late July, and one third sampling in mid- September.

During the summer, *P. scarabaeoides* has a clear preference to attack twigs of the Northern and Eastern sectors of the olive trees.







	Document:	D1.4. Handbook of protocols and methods		
	Author	UJAEN	Version	6
	Reference	D1.4	Date	24/03/2023

The abnormal increase in the density of the feeding symptoms is caused by the presence pruning wood stored near the olive grove (in a radius of up to about 4 km). Because of the damage caused by the scolytid bark beetles, the presence of pruning logs stored near the olive grove, is a good example of bad agricultural practice.

## 2.6. Sampling and determination of the infection rate of *Pseudomonas savastanoi*

### 2.6.1. Diagnosis


Appearance of tumors in stem and branches. Occasionally they can affect leaves and fruits. Other symptoms of the disease are chlorosis, necrosis, and premature leaf drop.

The tumors appear isolated from each other; these present an irregular surface as well as internal cavities. Symptoms occur in contiguous years, although it is common for periods of rest to occur when conditions are unfavorable for the pathogen.



### 2.6.2. Infection rate assessment

Olive trees will be observed for symptoms of tuberculosis in spring, as this is the season in which new symptoms appear.

	Document:	D1.4. Handbook of protocols and methods		
	Author	UJAEN	Version	6
	Reference	D1.4	Date	24/03/2023

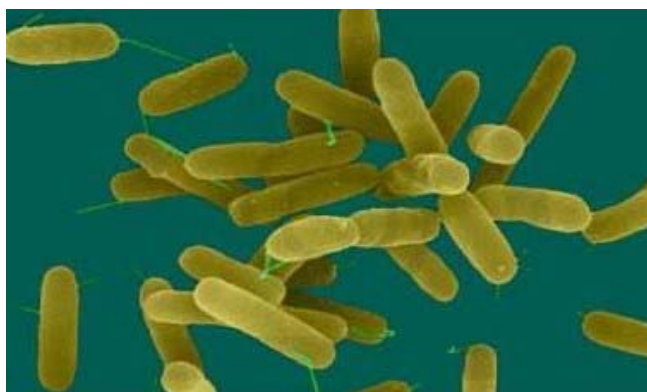
Once the affected olive trees have been detected, we proceed to calculate the percentage that they represent with respect to the total number of trees.

### 2.6.3. Isolation of the pathogen

The isolation of the pathogen can be done by immersing the tumors in sterile distilled water, for which they are immersed in a 1% sodium hypochlorite solution, for 2 minutes. An aliquot of the suspension will be seeded in Bacterial Growth Medium (LPGA).

The colonies obtained are subjected to pathogenesis tests, to select pathogenic ones. Subsequently, the relevant microbiological tests can be performed. The bacteria can be isolated.

*P. savastanoi* is a Gram negative, obligate aerobic, mobile bacterium with polar flagella.



## 3. Soil functional quality

### WP3. Task 3.4. Soil functional quality, and nutrient balance and nutrient retention


Leader: Roberto Garcia Ruiz and Julio Antonio Calero Gonzalez (University of Jaen)

For further clarification contact: [rgarcia@ujae.es](mailto:rgarcia@ujae.es) and [jcalero@ujaen.es](mailto:jcalero@ujaen.es)

### 3.1. Assessment of the diatom community in STSs and non-STSs olive farms

According to the original plan, the diatom community will only be evaluated in selected Spanish STSs and non-STSs olive farms. Nevertheless, any partner who would like to assess for diatoms community is welcome.

Diatoms have become a key source of information of the ecological quality of the environment in many countries. Their use as bioindicators has been enhanced because of

	Document:	D1.4. Handbook of protocols and methods		
	Author	UJAEN	Version	6
	Reference	D1.4	Date	24/03/2023

their sensitivity to environmental stressors (McCormick and Cairns 1994).

Terrestrial diatom communities or soil diatoms as defined by Lund (1945) are those diatoms living on substrates moistened solely by atmospheric water contribution.

## Methodology

Samples will be taken in summer period in 4 different sampling sites that will be selected considering the differences in land uses and soil composition.

1- Following the method of Barragan et al., (2018), samples will be collected by using metal cylinders ( 5.6 cm), extracting small soil cores from the upper 5 cm soil layer that will be immediately transported to the laboratory.

2- To extract diatom cells, the surface layer will be rinsed with deionized water. Sampling cylinders must be completely sealed with an impermeable film on their bottom side prior to rinsing.

3- In order to prevent cell division, Formaldehyde (4%) will be added to fix the samples. An aliquot (3-5 mL) of each of the samples has to be transferred to a new tube for treatment.

4- All samples are cleaned (digested) using concentrated hydrogen peroxide (H<sub>2</sub>O<sub>2</sub>) and heated (90 ° C) for a minimum of 48 h in a sand bath.


5- One ml of HCl is added to each tube and samples are stirred in a vortex and let settle for 2 h.

6- Afterwards, three to five repetitions of rinsing with deionized water, decantation and supernatant removal with vacuum aspiration will carried out. The final suspensions of cleaned frustules are dried on glass cover slips and mounted on permanent slides using Naphrax as mounting medium.

7- A minimum of 400 valves will be counted and identified on each slide, on random transects with a Leica DMR light microscope (LM) with a ~100 oil immersion objective.

## 3.2. Assessment of the soil quality in soils of STSs and non-STs olive farms

The estimation of soil functional quality will be performed through analysis of soil enzyme activities related to P (acid, alkaline or soil pH phosphatase activities), N (potential for N mineralisation and nitrification), S (arylsulfatase) and C (b-glucosidase) cycling. On the other hand, community level physiological profiling (CLPP) will be determined by BIOLOG system by assessing each bacterium' s usage of any of 31 different carbon sources in microtiter plates. Finally, edaphic diatom communities (only in Spain, but you are more than welcome to do it for your samples) will be characterised in some of the Spanish olive farms.

	Document:	D1.4. Handbook of protocols and methods		
	Author	UJAEN	Version	6
	Reference	D1.4	Date	24/03/2023

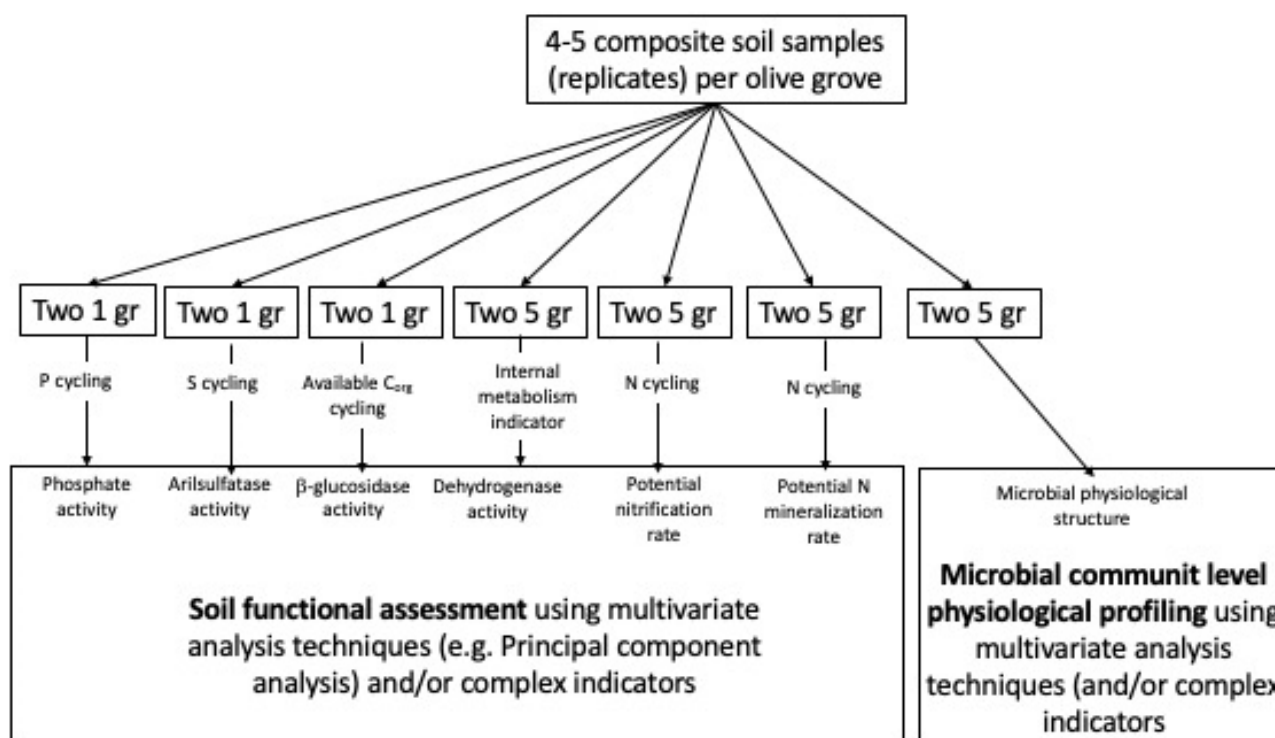


Figure 4. Overview of the indicators which refer the methods on soil functional quality specified in this section.

In case you have not the necessarily equipment and reagents, there are a couple of options.


**Option one.** One personnel of your team take the soil samples (only 100 gr of < 2 mm soils) and stay for two weeks (in two weeks of intensive work it would be possible to do all the analysis) at the University of Ja é n. Travel and accommodation expenses, microplates (see further below) and some of the reagents will be pay by you. Under this option, it would be desirable that the personnel of each of the country coincide in time. I estimate that the whole cost could be near 3000 euros (travel+accomodation+microplates+reagents) for the whole set of soil samples

**Option two.** Search in your countries for research team/lab with the adequate facilities and expertise on doing these analyses.

### 3.2.1. Acid and alkaline phosphomonoesterase activity with the substrate *p*-nitrophenyl phosphate

After the addition of a buffered *p*-nitrophenyl phosphate solution, soil samples are incubated for 1 h at 37 °C. The *p*-nitrophenol released by phosphomonoesterase activity is extracted and coloured with sodium hydroxide and determined photometrically at 400 nm. This



	Document:	D1.4. Handbook of protocols and methods		
	Author	UJAEN	Version	6
	Reference	D1.4	Date	24/03/2023

method is based on the original methods by Tabatabai and Bremner (1969) and Eivazi and Tabatabai (1977).

It will take a couple of hours to prepare the reagents and material, and a full morning or full afternoon to analyse about 50 soil samples. You will take almost the same time to analyse 5 samples than 50 samples.

### Basic laboratory equipment

1.- Substrate solution for acid phosphomonoesterase (115mM). Dissolve 4.268g of disodium *p*-nitrophenyl phosphate hexahydrate in working buffer solution for acid phosphomonoesterase, and dilute the volume to 1000ml with the same buffer in a volumetric flask. Prepare this reagent daily.

2.- Substrate solution for alkaline phosphomonoesterase (115mM). Dissolve 4.268 g of disodium *p*-nitrophenyl phosphate hexahydrate in working buffer solution for alkaline phosphomonoesterase, and dilute the volume to 1000ml with the same buffer in a volumetric flask. Prepare this reagent daily.


Alternatively, the substrate solution (same concentration) can be prepared at the measure soil pH. For that, Dissolve 4.268 g of disodium *p*-nitrophenyl phosphate hexahydrate in working buffer solution for measured soil-pH phosphomonoesterase, and dilute the volume to 1000ml with the same buffer in a volumetric flask. Prepare this reagent daily.

3.- Modified universal buffer stock solution Dissolve 12.1 g of tris (hydroxymethyl) aminomethane, 11.6 g of maleic acid, 14 g of citric acid monohydrate and 6.3 g of boric acid in 500ml of 1 M NaOH, and dilute the volume to 1000ml with distilled water in a volumetric flask. Store the solution at 4 C.

4.- Working buffer solution for acid phosphomonoesterase (pH 6.5). Mix 200 ml of modified universal buffer stock solution and 500 ml of distilled water, and adjust the pH to 6.5 with HCl. Adjust the volume to 1000 ml with distilled water in a volumetric flask.

5.- Working buffer solution for alkaline phosphomonoesterase (pH 11). Mix 200 ml of modified universal buffer stock solution and 500 ml of distilled water, and adjust the pH to 11 with NaOH. Adjust the volume to 1000 ml with distilled water in a volumetric flask.



	Document:	D1.4. Handbook of protocols and methods		
	Author	UJAEN	Version	6
	Reference	D1.4	Date	24/03/2023

Alternatively, mix 200 ml of modified universal buffer stock solution and 500 ml of distilled water, and adjust the pH near the soil pH ( $\pm 0.5$  pH units) with NaOH or HCl. Adjust the volume to 1000 ml with distilled water in a volumetric flask.

6.- Calcium chloride solution (0.5M). Dissolve 36.74g of  $\text{CaCl}_2 \cdot \text{H}_2\text{O}$  in distilled water, and dilute the volume to 500ml with distilled water in a volumetric flask.

7.- Sodium hydroxide solution (0.5 M). Dissolve 20g of NaOH in distilled water, and dilute the volume to 1000ml with distilled water in a volumetric flask.

8.- Standard stock solution (1 mg p-nitrophenol  $\text{ml}^{-1}$ ). Dissolve 1 g of p-nitrophenol in distilled water, and dilute the volume to 1000 ml with distilled water in a volumetric flask. Store the solution at 4 °C.


9.- Working standard (20  $\mu\text{g}$  p-nitrophenol  $\text{ml}^{-1}$ ). Dilute 2 ml of the standard stock solution to 100 ml with distilled water in a volumetric flask.

10. Calibration standards. Pipette 0 (reagent blank), 1, 2, 3, 4 and 5 ml of the working standard into six test tubes, adjust the volumes to 5 ml with distilled water, add 1 ml of calcium chloride solution and 4ml of sodium hydroxide solution (0.5 M), mix thoroughly, and filter through one folded filter. Calibration standards contain 0, 20, 40, 60, 80 and 100  $\mu\text{g}$  of p-nitrophenol.

### ***Procedure***

Weigh 1 g of field-moist soil (or dried soil) into two 12-15 ml test tubes. Add 1 ml of desired substrate solution (either for determination of acid or alkaline or soil-pH phosphomonoesterase) into ONE of the test tube (sample incubated with the substrate at the beginning of the incubation). Add 4 ml of the corresponding working buffer solution (either for determination of acid or for alkaline phosphomonoesterase) to the two test tubes. Shake the tubes briefly, and incubate for 1 h at 37 °C in a water bath. You can add a stopper to the test tubes.

After incubation, add 1 ml of calcium chloride solution and 4ml of sodium hydroxide solution (0.5 M) to both test tubes. Pipette additionally 1 ml of the used substrate solution (which was added to one of the test tube samples before incubation) to the test tube in which you did not add the 1 ml of substrate solution.

	Document:	D1.4. Handbook of protocols and methods		
	Author	UJAEN	Version	6
	Reference	D1.4	Date	24/03/2023

After shaking briefly, filter the contents of the tubes into new test tubes using folded filters. Measure the extinction of the yellow colour intensity of calibration standards, samples and controls with a spectrophotometer at 400 nm against the reagent blank. Take into account that if yellow colour intensity is higher than the upper limit of your spectrophotometer, you will need to dilute with distilled water.

## Calculations

Phosphomonoesterase activity is expressed as  $\mu\text{g p-nitrophenol (pNP)}$  per gram of dry soil and incubation time (1 hour). The concentration of pNP in samples and controls is calculated from the calibration curve.

$$\frac{(S-C) \times Y \times 100}{\% \text{ soil dry matter}} = \mu\text{g pNP g}^{-1} \text{ h}^{-1}$$


S: value of samples with substrate added at the beginning of the incubation ( $\mu\text{g pNP}$ )

C: value of samples with substrate added at the end of the incubation ( $\mu\text{g pNP}$ )

Y: is the factor for dilution of the yellow colour extract, only IF IS THE CASE.

## Notes

- 1.- The substrate is sensitive to light and temperature. The test tube containing the substrate solution should be covered with aluminium or incubated at low light intensity.
- 2.- Adjustment of pH values of working buffer solutions should be done at 37 °C, which is the temperature of the enzyme-substrate reaction.
- 3.- Modified universal buffer buffers in the pH range of 3-12.
- 4.- Due to the short incubation period, the addition of toluene is not necessary.
- 5.- The calibration curve is linear up to 120  $\mu\text{g}$  of p-nitrophenol.
- 6.- Use less soil, or dilute the extract, if the measured activity is outside the linear calibration range.
- 7.- Humic substances dissolve increasingly after the addition of sodium hydroxide and interfere with the determination of p-nitrophenol. Therefore, calcium chloride has to be added to the samples; it also prevents dispersion of clay minerals.
- 8.- Negative correlations between phosphomonoesterase activity and available P in soil were observed in sandy soils, in forest soils (Pang and Kolenko 1986), and in tchernozem soils.
- 9.- The relationship between soil pH and optimum pH for soil phosphomonoesterase activity was found to be soil-specific.

	Document:	D1.4. Handbook of protocols and methods		
	Author	UJAEN	Version	6
	Reference	D1.4	Date	24/03/2023

10.- Alkaline phosphomonoesterases are not excreted by plant roots. Therefore, in soils this activity is attributed to microorganisms and to the soil fauna.


### 3.2.2. $\beta$ -glucosidase activity: an enzyme involved in the easily-to-decompose organic carbon

#### Basic laboratory equipment

- 1.- Modified universal buffer stock solution. Dissolve 12.1 g of tris(hydroxymethyl)aminomethane, 11.6 g of maleic acid, 14 g of citric acid monohydrate and 6.3 g of boric acid in 500ml of 1 M NaOH, and dilute the volume to 1000 ml with distilled water in a volumetric flask. Store the solution at 4 C.
- 2.- Working buffer solution at soil pH. Mix 200 ml of modified universal buffer stock solution and 500 ml of distilled water, and adjust the pH to a pH similar to the soil pH with HCl or NaOH. Adjust the volume to 1000 ml with distilled water in a volumetric flask.
- 3.- Substrate solution for  $\beta$ -glucosidase (0.05 M). Dissolve 1.3 g of 4-nitrophenyl  $\beta$ -D-glucopyranoside in 100 ml of the working buffer solution at desirable pH. Prepare this reagent daily.
- 4.- Tris buffer (0.1 M). Dissolve 12.11 g of tris(hydroxymethyl)aminomethane in 600 ml of distilled water, and adjust with 0.5 M NaOH to pH 12. Make up the volume to 1000ml with distilled water in a volumetric flask.
- 5.- Calcium chloride solution (0.5M). Dissolve 36.74g of  $\text{CaCl}_2 \cdot \text{H}_2\text{O}$  in distilled water, and dilute the volume to 500ml with distilled water in a volumetric flask.
- 6.- Standard stock solution (1 mg p-nitrophenol  $\text{ml}^{-1}$ ). Dissolve 1 g of p-nitrophenol in distilled water, and dilute the volume to 1000 ml with distilled water in a volumetric flask. Store the solution at 4 C.
- 7.- Working standard (20  $\mu\text{g}$  p-nitrophenol  $\text{ml}^{-1}$ ). Dilute 2 ml of the standard stock solution to 100 ml with distilled water in a volumetric flask.
8. Calibration standards. Pipette 0 (reagent blank), 1, 2, 3, 4 and 5 ml of the working standard into six test tubes, adjust the volumes to 5 ml with distilled water, add 1 ml of calcium chloride solution and 4ml of the tris buffer, mix thoroughly, and filter through one folded filters. Calibration standards contain 0, 20, 40, 60, 80 and 100  $\mu\text{g}$  of p-nitrophenol.

#### Procedure

Weigh 1 g of field-moist soil (or dried soil) into two 12-15 ml test tubes. Add 1 ml of the substrate solution into ONE of the test tube (sample incubated with the substrate at the beginning of the incubation). Add 4 ml of the corresponding working buffer solution to the

	Document:	D1.4. Handbook of protocols and methods		
	Author	UJAEN	Version	6
	Reference	D1.4	Date	24/03/2023

two test tubes. Shake the tubes briefly, and incubate for 1 h at 37 °C in a water bath. You can add a stopper to the test tubes.

After incubation, add 1 ml of calcium chloride solution and 4ml of tris buffer solution to both test tubes. Pipette additionally 1 ml of the used substrate solution (which was added to one of the test tube before incubation) to the test tube in which you did not add the 1 ml of substrate solution.

After shaking briefly, filter the contents of the tubes into new test tubes using folded filters. Measure the extinction of the yellow colour intensity of calibration standards, samples and controls with a spectrophotometer at 410 nm against the reagent blank. Take into account that if yellow colour intensity is higher than the upper limit of your spectrophotometer, you will need to dilute with distilled water.

## Calculations

β-glucosidase activity is expressed as μg p-nitrophenol (pNP) per gram dry soil and incubation time (1 hour). The concentration of pNP in samples and controls is calculated from the calibration curve.

$$\frac{(S-C) \times Y \times 100}{\% \text{ soil dry matter}} = \mu\text{g pNP g}^{-1} \text{ h}^{-1}$$


S: value of samples with substrate added at the beginning of the incubation (μg pNP)

C: value of samples with substrate added at the end of the incubation (μg pNP)

Y: is the factor for dilution of the yellow colour extract, only IF IS THE CASE.

## Notes

- 1.- The substrate is sensitive to light and temperature. The test tube containing the substrate solution should be covered with aluminium or incubated at low light intensity.
- 2.- Adjustment of pH values of working buffer solutions should be done at 37 °C, which is the temperature of the enzyme-substrate reaction.
- 3.- Modified universal buffer buffers in the pH range of 3-12.
- 4.- Due to the short incubation period, the addition of toluene is not necessary.
- 5.- The calibration curve is linear up to 120 μg of p-nitrophenol.
- 6.- Use less soil, or dilute the extract, if the measured activity is outside the linear calibration range.
- 7.- Humic substances dissolve increasingly after the addition of sodium hydroxide and interfere with the determination of p-nitrophenol. Therefore, calcium chloride has to be added to the samples; it also prevents dispersion of clay minerals.

	Document:	D1.4. Handbook of protocols and methods		
	Author	UJAEN	Version	6
	Reference	D1.4	Date	24/03/2023

### 3.2.3 Arylsulfatase activity: an enzyme involved in the sulphur metabolism


Sulfatases are important for the mineralization of sulphur-containing compounds in the soils. They hydrolyze organic sulfates, and thus provide plants with available sulphur. Sulfatases are predominantly of microbial origin. In the soil, they also occur as exoenzymes, and have a close relationship to organic matter. Arylsulfatase was the first enzyme group to be discovered and has thus predominantly been investigated. It catalyzes the hydrolysis of an arylsulfate anion by splitting the O-S-bond.

After the addition of a p-nitrophenylsulfate solution, soil samples are incubated for 1h at 37 °C. Nitrophenol released by arylsulfatase activity is extracted and colored with sodium hydroxide and determined photometrically. The method is based on the original method published by Tabatabai and Bremner (1970).

It will take a couple of hours to prepare the reagents and material, and a full morning or a full afternoon to analyse about 50 soil samples. You will take almost the same time to analyse 5 samples than 50 samples.

#### Basic laboratory equipment

- 1.- Acetate buffer (0.5 M, pH 5.8). Dissolve 64g of sodium acetate trihydrate in 700ml of distilled water, adjust the pH to 5.8 with approximately 2 ml of acetic acid pipetted drop by drop, and dilute the volume to 1000 ml with distilled water in a volumetric flask.
- 2.- Substrate solution (0.02 M). Dissolve 0.515g of potassium-p-nitrophenylsulfate in acetate buffer, and dilute the volume to 100 ml with acetate buffer in a volumetric flask. Prepare this reagent daily.
- 3.- Sodium hydroxide solution (0.5M). Dissolve 20 g of NaOH in distilled water, and dilute the volume to 1000 ml with distilled water in a volumetric flask.
- 4.- Standard stock solution (1 mg p-nitrophenol ml<sup>-1</sup>). Dissolve 1g of p-nitrophenol in distilled water, and dilute the volume to 1000 ml with distilled water in a volumetric flask. Store the solution at 4 °C.
- 5.- Working standard (0.1 mg p-nitrophenol ml<sup>-1</sup>). Dilute 10ml of the standard stock solution to 100 ml with distilled water in a volumetric flask.
- 6.- Calibration standards. Pipette 0 (reagent blank), 1, 2, 3, 4 and 5 ml of the working standard in beakers, adjust the volumes to 5 ml with distilled water, and add 25ml of distilled water. Pipette 6 ml of this mixture into six test tubes, and add 4 ml of sodium hydroxide solution. Calibration standards contain 0, 20, 40, 60, 80 and 100 µg of p-nitrophenol.

	Document:	D1.4. Handbook of protocols and methods		
	Author	UJAEN	Version	6
	Reference	D1.4	Date	24/03/2023

## Procedure

Weigh 1 g of field-moist soil (or dried soil) into two 12-15 ml test tubes. Add 4 ml of acetate buffer to the two test tubes, and 1 ml of substrate solution to only one of the tube. Shake the test tubes briefly, and incubate for 1 h at 37° C.

After incubation, pipette additionally 1ml of substrate solution to the tube which did not contain the substrate at the beginning of the incubation. Shake flasks, and filter samples all the test tubes immediately.

Mix 3 ml of the filtrate and 2 ml of sodium hydroxide solution. Measure the extinction at 420nm with a spectrophotometer against the reagent blank. To prepare a calibration curve, treat calibration standards like soil filtrates.

## Calculations

Calculate the concentration of p-nitrophenol (pNP) from the calibration curve.

$$\frac{(S-C) \times 5 \times 100}{3 \times \% \text{ soil dry matter}} = \mu\text{g pNP g}^{-1} \text{ h}^{-1}$$

S: is the value of samples with substrate added at the beginning of the incubation (μ g pNP).

C: is the value of samples with substrate added at the end of the incubation (μ g pNP).

5: is the volume of extract (ml).

3: is the aliquot of filtrate (ml).

## Notes


1.- The substrate is sensitive to light and temperature. The test tube containing the substrate solution should be covered with aluminium or incubated at low light intensity.

2.- Measure the extinction within 6h.

3.- The calibration curve is linear up to 120 μ g p-nitrophenol.

4.- Tabatabai and Bremner (1970) recommended the addition of sodium hydroxide and calcium chloride prior to filtration of soil extracts, in order to prevent dissolution of humic substances under alkaline conditions. However, through the formation of Ca humate, humic substances will only partially precipitate. Thus, extinction values of humus -rich grassland soil samples can still lie outside the linear calibration range. In addition, Ca(OH) 2 will precipitate slowly upon addition of sodium hydroxide, and the turbidity of filtrates will interfere with the extinction measurement. Thus, it is recommended to add sodium hydroxide after filtration, and not to add any calcium chloride.



	Document:	D1.4. Handbook of protocols and methods		
	Author	UJAEN	Version	6
	Reference	D1.4	Date	24/03/2023

### 3.2.4. Dehydrogenase: and enzyme indicator of the intracellular metabolism

The catalase of aerobic organisms splits the toxic  $H_2O_2$  produced from the mitochondrial electron transport and from various hydroxylation and oxygenation reactions into water and oxygen.

Dehydrogenases belong to oxidoreductases, and oxidate organic compounds due to the splitting off of two hydrogen atoms. Many specific dehydrogenases transfer the separated hydrogen to one of the two co-enzymes NAD or NADP. Through these co-enzymes, hydrogen enters the respiratory chain or participates in reducing processes of biosynthesis. The dehydrogenase activity of a soil is thus the result of the activity of different dehydrogenases, which are an important component of the enzyme system of all microorganisms (enzymes of respiratory metabolism, citrate cycle, and nitrogen metabolism). Dehydrogenase activity is thus an indicator of biological redox-systems, and can be taken as a measure for the intensity of microbial metabolism in soil (Tabatabai 1982).

Lenhard (1956), Stevenson (1959), Casida et al. (1964) and Thalmann (1968) developed methods for the determination of dehydrogenase activity in soils, and used 2,3,5-triphenyltetrazolium chloride (TTC) as hydrogen receptor. Through the catalytic activity of dehydrogenases, red triphenyltetrazolium formazan (TPF) and HCl are produced.


Soil samples are suspended in a triphenyltetrazolium chloride solution and incubated for 16h at 25 °C. The triphenyl formazan (TPF) produced is extracted with acetone and measured photometrically at 485 nm. This method is similar to the standard method: ISO 23753-1:2005.

It will take a couple of hours to prepare the reagents and material, and a full morning or a full afternoon to analyse about 50 soil samples. You will take almost the same time to analyse 5 samples than 50 samples.

#### Basic laboratory equipment

In addition to basic laboratory equipment:

- 1.- Falcon tubes of 50 ml.
- 2.- Tris buffer (0.1 M). Dissolve 12.11 g of tris(hydroxymethyl)aminomethane in 600 ml of distilled water, and adjust with hydrochloric acid to pH 7.8 for acid soils (pH < 6), pH 7.6 for neutral soils (pH 6-7) or pH 7.4 for soils rich in carbonate (pH > 7). Make up the volume to 1000 ml with distilled water in a volumetric flask.

	Document:	D1.4. Handbook of protocols and methods		
	Author	UJAEN	Version	6
	Reference	D1.4	Date	24/03/2023

3.- Substrate solution. The optimum substrate concentration is between 0.1 and 2% TTC (w/v) and has to be determined for each soil type (see "Notes"). Dissolve 2,3,5-triphenyl tetrazolium chloride (TTC) in the appropriate Tris buffer. Store the solution in the dark at 4 C for up to 1 week.

5.- Methanol p.a.

6.- Standard stock solution (10 mg TPF ml<sup>-1</sup>). Dissolve 1g of triphenyl formazan (TPF) in acetone, and make up the volume to 100 ml with acetone in a volumetric flask.

7.- Working standard (0.1 mg TPF ml<sup>-1</sup>). Dilute 1 ml of the standard stock solution to 100ml with acetone.

8.- Calibration standards. Pipette 0 (reagent blank), 1, 2, 5 and 10 ml of working standard into five test tubes, and dilute to 30ml with acetone. These solutions correspond to 0, 100,200, 500 and 1000 g TPF.

## Procedure

Weigh 5 g of field-moist soil (or dried-soil) into two test tubes. Add 5 ml of substrate solution to one test tube (sample). Pipette 5 ml of Tris buffer to the second test tube (control). Mix, close the test tubes with rubber stoppers, and incubate for 16 h at 25 C.

After the incubation, and to extract the produced triphenyl formazan, add 5 ml of methanol to both samples and control. Mix, and vigorously shake the tubes for a couple of minutes. Repeat the operation adding another 5 ml of methanol. Subsequently, filter the solutions or alternatively centrifugate in a semi-dark room. Measure the extinction of the filtrates and calibration standards photometrically at 485 nm within 1h.

## Calculations

Determine the g TPF in the filtrates from the calibration curve.

$$\frac{(S-C) \times 100}{5 \times \% \text{ soil dry matter}} = \mu\text{g TFG g}^{-1} 16 \text{ h}^{-1}$$

S: is the value of the sample with substrate added at the beginning of the incubation ( $\mu$  g pNP).

C: is the value of samples with substrate added at the end of the incubation ( $\mu$  g pNP).


5: is the initial soil weight (gr).

## Notes

1.- It is recommended the following optimum substrate concentration:

For sandy, slightly humic and slightly clay soils: 0.1-0.5% TTC.

For loamy and humus soils: 0.6-1.0 % TTC.

	Document:	D1.4. Handbook of protocols and methods		
	Author	UJAEN	Version	6
	Reference	D1.4	Date	24/03/2023

For clay and humus soils: 1-2% TTC.

2.- TTC and TPF are light-sensitive. Avoid bright light during the entire reaction.

3.- The method described in this section requires strict standardization of the experimental conditions to obtain comparable results. Even the relationship between soil weight and diameter of the test tube can be important due to different aeration (Thalmann 1968).

4.- Dehydrogenase activity should not be used as a measure for soil biological activity in anaerobic soils (Glathe and Thalmann 1970). Abiotic components like iron (II) compounds or sulfides can reduce TTC.

5.- Comparative measurements of O<sub>2</sub> uptake or CO<sub>2</sub> evolution showed, however, that only 2-3% of the produced hydrogen is included in the TTC reduction (Glathe and Thalmann 1970). Possible reasons are: i) TTC inhibits the turnover because of its toxicity, ii) Not the total hydrogen is transferred to TTC, iii) TTC is competitively inhibited as a hydrogen acceptor, and the reduction takes place only after other hydrogen acceptors have been depleted, iv) A cell can take up only a restricted amount of TTC, thus limiting the TTC reduction (TPF accumulates in the cell, and can cause it to burst), and v) Additionally, oxygen interferes with the TTC reduction. The determination of dehydrogenase activity with TTC as hydrogen acceptor thus has a low reproducibility.


### 3.2.5. Potential nitrification rate

Using ammonium sulfate as substrate soil samples are incubated for 5 h at 25 °C. Nitrite released during incubation period is extracted with potassium chloride and determined colorimetrically at 520 nm. Sodium chlorate inhibits nitrite oxidation during incubation. This is a modified version of the method developed by Berg and Rosswall (1985).

#### Basic laboratory equipment

In addition to basic laboratory equipment:

- 1.- 100 ml Erlenmeyer flasks with caps.
- 2.- Substrate stock solution (10 mM). Dissolve 1.3214 g of (NH<sub>4</sub>)<sub>2</sub>SO<sub>4</sub> in distilled water and dilute the volume to 1000 ml with distilled water in a volumetric flask.
- 3.- Substrate working solution (1 mM). Dilute 100 ml of the substrate stock solution to 1000 ml with distilled water in a volumetric flask.
- 4.- Sodium chlorate solution (1.5 M). Dissolve 15.97 g of NaClO<sub>3</sub> in distilled water and dilute the volume to 100 ml with distilled water in a volumetric flask.
- 5.- Potassium chloride solution (2 M). Dissolve 149.12 g of KCl in distilled water and dilute the volume to 1000 ml with distilled water in a volumetric flask.

	Document:	D1.4. Handbook of protocols and methods		
	Author	UJAEN	Version	6
	Reference	D1.4	Date	24/03/2023

6.- Ammonium chloride buffer (0.19 M, pH 8.5). Dissolve 10 g of  $\text{NH}_4\text{Cl}$  in distilled water, adjust the pH to 8.5 with conc.  $\text{NH}_4\text{OH}$ , and dilute the volume to 1000ml with distilled water in a volumetric flask.

7.-Colour reagents. Dissolve 2 g of sulfanilamide and 0.1g of N-(1-naphthyl) - ethylenediamine hydrochloride in 150 ml of distilled water, and add 20 ml of conc. phosphoric acid. Cool the solution to room temperature and dilute the volume to 200 ml with distilled water in a volumetric flask. This solution has to be colourless and has to be prepared daily.

8.-Standard stock solution ( $1000 \text{ g NO}_2^- \text{ ml}^{-1}$ ). Dissolve 4.9257 g of  $\text{NaNO}_2$  in distilled water and dilute the volume to 1000 ml with distilled water in a volumetric flask. Store the solution at 4 °C not longer than some weeks.

9.- Working standard ( $10 \text{ g g NO}_2^- \text{ ml}^{-1}$ ). Dilute 5 ml of standard stock solution to 500 ml with distilled water in a volumetric flask.

10.- Calibration standards. Pipette 0 (reagent blank), 2, 4, 8 and 10 ml of working standard in 100 -ml volumetric flasks, add 20 ml of potassium chloride solution (2M), and make up to volume with distilled water. Calibration standards contain 0.0, 0.2, 0.4, 0.8 and 1  $\text{g NO}_2^- \text{ ml}^{-1}$ .

## Procedure


Weigh 5 g of field-moist soil into two 50 ml falcon tubes. Add 20 ml of substrate working solution (1 mM) and 0.1 ml of sodium chlorate solution, mix briefly, and close the tubes with caps.

Incubate one tube for 5 h on a rotatory shaker (samples), and store the second tube for 5 h at -20 °C (control).

After incubation thaw the control at room temperature, add 5 ml of potassium chloride solution to samples and control, mix briefly, and filter (or centrifugate) samples and control immediately.

For photometric analysis pipette 5 ml of filtrates or supernatant, 3 ml of ammonium chloride buffer and 2 ml of colour reagent into test tubes, mix, and allow to stand for 15 min at room temperature. Measure extinction of samples and control at 520 nm against the reagent blank. To prepare the calibration curve, treat 5 ml of calibration standard like the soil filtrates/supernatant.

## Calculations

	Document:	D1.4. Handbook of protocols and methods		
	Author	UJAEN	Version	6
	Reference	D1.4	Date	24/03/2023

Calculate mg N of the test solution from the calibration curve. Express potential nitrification as the amount of NO<sub>2</sub>-N released from 1 gr of soil during 5 h.

$$\frac{(S-C) \times 25 \times 1 \times 1000 \times 100}{5 \times 5 \times \% \text{ soil dry matter}} = ng \text{ N } g^{-1} 5 \text{ h}^{-1}$$

S: is the value of the sample (mg N).

25x1: volume of extract (ml).

1000: is the conversion factor from microgr to nanogr.

5: is the aliquot of filtrate (ml).

5: initial soil weight.

## Notes

1.- Transport and store soil samples after sampling at 4 °C. Avoid longer storage times.

The concentration of the inhibitor NaClO<sub>3</sub> has been optimized for arable soils with a humus content of 1.5-3.5 %. If this method is used for the estimation of potential nitrification in grassland and forest soils, increase the concentration of the inhibitor in the soil suspension because of a possible non-specific adsorption of NaClO<sub>3</sub> onto organic matter. You can test inhibitor concentration in a pre experiment.

2.- Ammonium oxidation is inhibited by high amounts of ammonium. You can test substrate concentration in a pre-experiment.

3.- If nitrite concentration of the samples exceeds that of the highest calibration standards, dilute samples with distilled water.

4.- Clean the volumetric flask containing the colour reagent with boiling water. To avoid filtration, you can centrifuge samples.

### 3.2.6. Potential soil N mineralization (waterlogged method)

Waterlogged soils are incubated for 7 days at 40 °C. NH<sub>4</sub><sup>+</sup>-N released from organic nitrogen compounds is determined.


## Basic laboratory equipment

In addition to basic laboratory equipment:

1.- Test tubes (190 x 20mm) with screw caps.

2.- Potassium chloride solution (2 M). Dissolve 149 g of KCl in distilled water, and dilute the volume to 1000 ml with distilled water in a volumetric flask.

3.- Chemicals and reagents for ammonium determination.

	Document:	D1.4. Handbook of protocols and methods		
	Author	UJAEN	Version	6
	Reference	D1.4	Date	24/03/2023

## Procedure

Weigh 5g of field-moist soil into two test tubes, and add 15 ml of distilled water. Close the tubes with caps, and shake. Incubate one tube for 7 days at 40° C (samples), and store the third tube for 7 days at -20° C (control).

After incubation, add 15ml of potassium chloride solution to samples and control, shake tubes for 30 min on a rotatory shaker, and filter (or alternatively centrifugate) samples and control. Determine ammonium content.

## Calculations

$$\frac{(S-C)}{n} = \mu g \text{ N } g^{-1} \text{ d}^{-1}$$

S: is the value of the sample (mg N g<sup>-1</sup> dry weight).

C: is the value of the control (mg N g<sup>-1</sup> dry weight).

n: is the incubation time (d).

### 3.2.7. Microbial community level physiological profiling

Soil microorganisms play a crucial role in one of the most important ecological processes: the turnover of chemical elements in an ecosystem. Soil microbes break down complex organic molecules and release inorganic nutrients which then can be used by plants. The rate of dead organic matter decay depends on the biomass and metabolic activity of microorganisms.


Microorganisms react quickly to changes in their environment because of the high surface-to-volume ratio and low homeostasis, and changes in their biomass, metabolic activity or community structure may be an early signal of alterations (also adverse alterations) in the whole ecosystem. In our context, it is expected/hypothesised that under STSs the diversity and activity of the community structure will be greater than that of the non-STSs.

In recent years, methods for studying community structure are getting popular.

The measurements of physiological activity of microorganisms represent one approach, allowing the study of different characteristics of microbial communities. The Biolog technique is one of the methods which rely on measurements of utilizing different carbon substrates by microorganisms. Measurements of substrate use enables qualifying microbial metabolic capabilities and hence functional diversity of a microbial community.

The Biolog plates method was first used to compare metabolic activity of heterotrophic microbial communities. The technique is a redox system. Various types of plates are used,



	Document:	D1.4. Handbook of protocols and methods		
	Author	UJAEN	Version	6
	Reference	D1.4	Date	24/03/2023

but Biolog GNplates for gram-negative bacteria are the most popular ones. These are plastic microtiter plates containing 95 different carbon substrates in wells, and no substrate in one well which is used as control. Among the 95 substrates one can distinguish a few groups of chemical compounds, for example, carbohydrates, amino acids, carboxylic acids, amines, amides and polymers. Additionally, each well contains a colourless tetrazolium dye.

Soil samples are shaken in a suitable solution and then the soil solution is inoculated into the plate wells. During incubation at a constant temperature, soil microorganisms oxidize substrates in the plate wells and, simultaneously, reduce colourless tetrazolium dye to a violet formazan. Colour development is measured spectrophotometrically. The rate of utilization of different substrates by different groups of microorganisms varies, so one can observe high variability in the rate of colour development and its intensity depending on the composition of a microbial community, which we expect will differ in soils of the STSs compared to that of the non-STSs. The characteristic pattern is named “metabolic fingerprint” , or “community-level physiological profile (CLPP).

There are a couple of options if you do not have the required facilities:

- 1.- Take with you the soil samples and within a week you can analyse them using the UJA facilities. In this option, you will have to pay for the travel and accommodation expenses and the microplates.
- 2.- Search for a lab /research team with capacities of doing the analysis in your country (I do have several research groups in mind in Italy and in Greece).

### Basic laboratory equipment

1.- Microplates. The microplates consist of 96 wells and purchased from a company. Cost depend of the number of microplates. If you want to do the analysis in 15 STSs and 15 comparable non-STSs the cost per microplates is about 20 euros with a final cost of 600 euros. The microplates include the tetrazolium in each well and 3 times 31 (+ one blank) sources of organic carbon (each one in a different well of the total of 96 wells) which includes:

Water –


B1 Pyruvic acid methyl ester Carbohydrates

C1 Tween 40 Polymers

D1 Tween 80 Polymers

E1  $\alpha$ -Cyclodextrin Polymers

F1 Glycogen Polymers

	Document:	D1.4. Handbook of protocols and methods		
	Author	UJAEN	Version	6
	Reference	D1.4	Date	24/03/2023


- G1 D-Cellobiose Carbohydrates
- H1  $\alpha$ -D-Lactose Carbohydrates
- A2  $\beta$ -Methyl-D-glucoside Carbohydrates
- B2 D-Xylose Carbohydrates
- C2 i-Erythritol Carbohydrates
- D2 D-Mannitol Carbohydrates
- E2 N-Acetyl-D-glucosamine Carbohydrates
- F2 D-Glucosaminic acid Carboxylic and ketonic acids
- G2 Glucose-1-phosphate Carbohydrates
- H2 D,L-  $\alpha$ -Glycerol phosphate Carbohydrates
- A3 D-Galactonic acid-  $\gamma$ -lactone Carboxylic and ketonic acids
- B3 D-Galacturonic acid Carboxylic and ketonic acids
- C3 2-Hydroxybenzoic acid Carboxylic and ketonic acids
- D3 4-Hydroxybenzoic acid Carboxylic and ketonic acids
- E3  $\gamma$ -Hydroxybutyric acid Carboxylic and ketonic acids
- F3 Itaconic acid Carboxylic and ketonic acids
- G3  $\alpha$ -Ketobutyric acid Carboxylic and ketonic acids
- H3 D-Malic acid Carboxylic and ketonic acids
- A4 L-Arginine Amino acids
- B4 L-Asparagine Amino acids
- C4 L-Phenylalanine Amino acids
- D4 L-Serine Amino acids
- E4 L-Threonine Amino acids
- F4 Glycyl-L-glutamic acid Amino acids
- G4 Phenylethylamine Amines/amides
- H4 Putrescine Amines/amides

These sources of carbon belong to: polymers, carbohydrates, carboxylic and ketonic acids, amino acids and amines and amides.

2.- Microplate reading. This is a kind of spectrometer adapted to the microplates. Absorbances are read at 590 nm.

3.- Phosphate ( $\text{KH}_2\text{PO}_4$ ; 0.05 M, pH 7.0) or tris buffer or 0.9 % NaCl solution. Because some of the phosphate might precipitate on secondary minerals of carbonate in rich-carbonate soils or on oxides of Al and Fe in low pH soil, I suggest to use the 0.9 % NaCl solution. Nevertheless, during next September and October I will do some preliminary assays to set up the best buffer/NaCl solution.

4.- 120  $\mu\text{l}$  pippete.

	Document:	D1.4. Handbook of protocols and methods		
	Author	UJAEN	Version	6
	Reference	D1.4	Date	24/03/2023

## Procedure

Soil samples should be analysis within 0-10 days of collection and always keep at about 4 °C before analysis.

Weight 5 gr of sample in 50 ml of the appropriate buffer/solution (phosphate, tris or 0.9 % NaCl) and mix in a shaking table during 30 minutes.

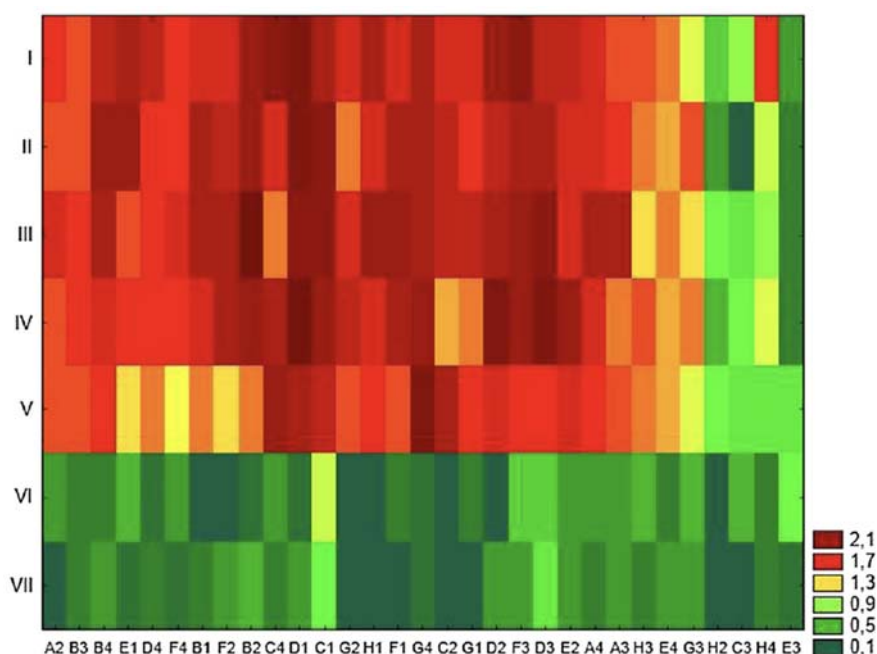
Transfer 5 ml of this solution into 50 ml of the appropriate buffer/solution and mix in a shaking table during 30 minutes. Transfer by pipetting 120 µl into each of the wells. Microplates are incubated in the dark (under aluminum fold, for instance) at 25 °C and read the absorbances (it takes about one minute to read the absorbance of each microplate) at 590 nm after 24, 48 and 72 h.


## Calculations

Absolute and relative colour intensity (indicator of microbial activity on a specific source of carbon or a family of type of carbon), Shannon diversity and Shannon evenness can be calculated.

Index	Definition	Formulae	Definitions
Average well color development		$AWCD = \sum OD_i / 31$	$p_i$ = proportional color development of the well over total color development of all wells of a plate
Shannon diversity	Measure of richness	$H = -\sum p_i (\ln p_i)$	$H$ = Shannon index of diversity
Shannon evenness	Evenness calculated from Shannon index	$E = H / \ln S$	$S$ = number of wells with color development (substrate utilization richness)

Other multivariate techniques, such principal component analysis and cluster analysis can be performed.



	Document:	D1.4. Handbook of protocols and methods		
	Author	UJAEN	Version	6
	Reference	D1.4	Date	24/03/2023

## 4. Nutrient balance and retention

### WP3. Task 3.4. Soil functional quality, and nutrient balance and nutrient retention

Leader: Roberto Garcia Ruiz and Julio Antonio Calero Gonzalez (University of Jaen)

For further clarification contact: [rgarcia@ujae.es](mailto:rgarcia@ujae.es) and [jcalero@ujaen.es](mailto:jcalero@ujaen.es)

#### 4.1. General features of the model

This model is static. It is based on recorded and measured (e.g. harvesting, fertiliser application rate...) or estimated (e.g. denitrification and  $\text{NH}_3$  volatilization for nitrogen (N) or soil phosphorus (P) and potassium (K) weathering, rainfall, or inputs of N by legumes). In this nutrient balance great attention should be pay in combining weather (specially precipitation regime), soil (soil type and main physico-chemical properties including texture features and soil content of major elements) and main management practices (such as tillage, fertilisation and harvesting) and current predictive models for key processes of the soil N, P and K cycling, which are sensitive to these type of information.

The model for the assessment of N, P and K balances in STSs and non-STSs olive farm here is a compartment-based model, static for the specific year studied and inputs and output of N, P and K in and out the considered compartments come from direct or indirect information, but others from predictions of current empirical sub model (e.g. N losses from denitrification and lixiviation).

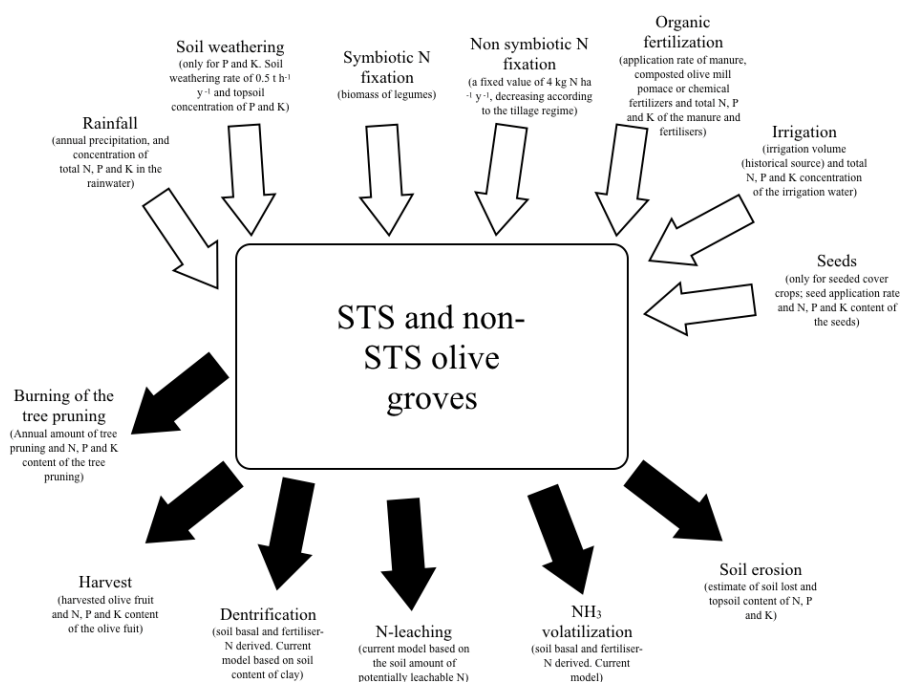



Figure 5. Input and output processes taking into account when constructing a nutrient balance.

	Document:	D1.4. Handbook of protocols and methods		
	Author	UJAEN	Version	6
	Reference	D1.4	Date	24/03/2023

During Autumn 2020, with the help of all of you, we will prepare a excel file to be fed with data and all the input and output flows, to calculate the balance and other estimates (N, P and K use efficiencies, recycled and retained N, P and K).

## 4.2. N, P and K inputs

### 4.2.1. Natural N, P and K inputs

One of the major natural routes of entry of N, P and K, in both natural and managed terrestrial ecosystems, is rainfall. However, the entry of P and K to the cropland soil by weathering of the parent material should also be considered. Although inputs of P and K from the parent material to the arable soils are not truly an entry at a farming scale, it thus at soil (and therefore at olive tree) level, and therefore it will be considered. Parent material is lacking of N, except for some type of rocks, and thus inputs by this mechanism should only be considered for P and K.


However, for N, N fixation of the atmospheric  $N_2$  by free microorganisms (non-symbiotic N fixation) and by bacteria associated with the root system of legumes in the spontaneous temporary cover crops or in the seeded cover crops should be considered.

### 4.2.2. Inputs of N, K and P by rainfall

In several attempts to develop historical balances for N in agroecosystems, the input by rainfall has been considered as a fixed value of around 5 kg N ha<sup>-1</sup> y<sup>-1</sup>. For instance, Allen (2008) used this value when analysing the retardation of the agrarian revolution in England. However, by using a rigid value, site specificity is lost which is undesirable when comparing nutrient balances for olive groves with contrasted annual precipitation.

The annual input of N, P and K by rainfall (wet deposition) can be calculated from the *volume of water* (R; L or m<sup>3</sup> = annual rainfall) per unit area (m<sup>2</sup> or ha) and the *concentration of these elements* (CN, CP and CK, respectively) in rainwater (usually expressed as mg element L<sup>-1</sup> or g element m<sup>-3</sup>). Rainfall collected could be displayed (between 3 to 5 per olive farm) and volume of water after periods of rainfall register. Annual rainfall can vary year to year (up to greater than 100 %) and therefore when doing nutrient balance, perhaps it is more convenient to use the *annual average, calculated from a comprehensive set of data of minimum 25-50 years*. For most of the development regions rainfall data are available from middle to the end of the nineteen-century. A large temporal set of data should be analysed for the possible existence of a temporal trend in the annual rainfall by using statistical test such as Mann-Kendall trend analysis (Mann, 1945; Kendall, 1975). To gain accuracy on the



	Document:	D1.4. Handbook of protocols and methods		
	Author	UJAEN	Version	6
	Reference	D1.4	Date	24/03/2023


input of these elements, only weather data of the studied area or nearby should be considered.

N, P and K dry deposition in moderate-high humid regions is negligible and usually is below an order of magnitude lower than that of wet deposition (Holland et al., 2005). Because of the difficulties in estimating dry deposition and its relatively little importance, we will not make an intend to incorporate dry deposition in the nutrient balance of our study case.

Whereas it is relatively easy to obtain information of the annual average of rainfall, *the concentration of the different elements in rainwater is more complicate*. There are two options: i) measured the concentration of total N, total P and total K in the rainfall collector used to register the volume of water, or ii) use national data base in combination with research papers. Under the latter case, levels of these elements should be inferred from current data from the studied sites or nearby. Due to the fact that rainwater concentration of these elements might differ in a seasonal scale and in different rainfall events within the same season even up to one order of magnitude, it is recommended the use of weighted annual average of N, P and K concentrations in rainfall to gain robustness in the calculations of this entry. Usually this type of information (concentration of N, P and K in rainwater) is relatively abundant in temperate regions (where there is a strong tradition of environmental monitoring stations) but annual average rainfall in these regions tends to be twice those recorded in other regions, such as the Mediterranean. Values of N, P and K inputs via rainfall are the same in the comparable pairs of STS and in the non-STs olive farms, as both of them should be nearby (e.g. same rainfall and N, P and K concentrations in the rainfall).

In one of my study cases (N, P and K balances at municipal scale in Montefrío, Spain), N and P wet depositions were calculated from the 100-year annual average of rainfall and the weighted annual average of total N and P analysed at in field rainwater collectors. The mean annual precipitation is of 6120 m<sup>3</sup> ha<sup>-1</sup>, without a significant pattern during the last 100 years, whereas the weighted mean of total N and P were of 0.57 g N-(NO<sub>3</sub><sup>-</sup>+NH<sub>4</sub><sup>+</sup>) m<sup>-3</sup> and 0.1 g P m<sup>-3</sup>, with an annual coefficient of variation between 17 to 26 %. Total K concentration in the rainwater was assumed to be 0.5 g K m<sup>3</sup>, which in the annual grand mean value analysed in rainwater for many sites of Spain by Bellot and Escarre (1989). This value is slightly smaller than the 0.8 g K m<sup>3</sup> recorded by Vázquez et al. (2003) in 14 localities of Spain. Little variations both in the rainfall volume and the rainwater potassium concentration will not affect greatly to the main results of the K balance.

Applying the same mean N, P and K concentration in the rainwater but different annual

	Document:	D1.4. Handbook of protocols and methods		
	Author	UJAEN	Version	6
	Reference	D1.4	Date	24/03/2023

rainfall (e.g. during the last 10 years), a range of variability in N, P and K inputs by rainfall, can be estimated.

$\text{RainN} = \text{Annual precipitation (m}^3 \text{ ha}^{-1} \text{ y}^{-1}) \times \text{Total N concentration in the rainwater (gr} \times \text{m}^{-3}) / 1000 \text{ (to convert gr into kg)} = \text{kg N ha}^{-1}.$


$\text{RainP} = \text{Annual precipitation (m}^3 \text{ ha}^{-1} \text{ y}^{-1}) \times \text{Total P concentration in the rainwater (gr} \times \text{m}^{-3}) / 1000 \text{ (to convert gr into kg)} = \text{kg N ha}^{-1}.$

$\text{RainK} = \text{Annual precipitation (m}^3 \text{ ha}^{-1} \text{ y}^{-1}) \times \text{Total P concentration in the rainwater (gr} \times \text{m}^{-3}) / 1000 \text{ (to convert gr into kg)} = \text{kg N ha}^{-1}.$

Take into account that these inputs account for a relatively low percentage of the total inputs, and therefore some degree of variability is assumable.

#### 4.2.3. Inputs by formation of new soil

The formation of new soil from the parent material/bedrock mobilised P and K, which are sequestered in primary minerals, to the reservoir of soil available P and K. Since the parent material/bedrock contains not significant amount of N, this entry should only be estimated for P and K. The annual inputs of P and K by weathering will be estimated from the annual formation of new soil ( $\text{Mg ha}^{-1} \text{ y}^{-1}$ ) and the content of total inorganic P and K in the soil. The formation of new soil comprises a set of processes, which transform the bedrock into soil material. In the initial stages of soil formation there is a marked predominance of physical and chemical changes by the action of weathering and water circulation affecting the bedrocks and its mineral composition. These geochemical reactions are grouped under the concept of weathering. The climatic conditions, especially rainfall and temperature regimes, together with the type of parent material, determine the magnitude and predominance of one type or another of weathering. Buol et al. (1989) showed a couple of decades ago, the relationship between climate and the extent of weathering, which has been updated by other authors (i.e. Cooke and Doornkamp, 1990). Estimates of soil formation for each pair of olive groves e need for detailed information on weather conditions and the prevailing bedrock. When geo-referentiation is not possible or information on prevailing bedrock is not possible, the best approach to estimate the soil formation rate is the analysis of the estimates reported in several studies modified depending on climatic conditions and soil type. Bedrock under climatic conditions characterized by annual precipitation values below  $600 \text{ L m}^{-2} \text{ yr}^{-1}$  and mean annual temperature above  $10^\circ \text{C}$  and a Xeric soil moisture regime, usually have low intensity of chemical and physical weathering (Cooke and Doornkamp, 1990). These conditions are fulfilled, in general, to an important area of the Mediterranean regions. Moreover, the different soil orders show varying degrees of weathering. Johnson (1987) estimated soil formation rates of between  $0.8 \text{ mm y}^{-1}$  (about

	Document:	D1.4. Handbook of protocols and methods		
	Author	UJAEN	Version	6
	Reference	D1.4	Date	24/03/2023

1 Mg ha<sup>-1</sup> y<sup>-1</sup>) and 0.25 mm y<sup>-1</sup> (<0.5 ton ha<sup>-1</sup> y<sup>-1</sup>). Moreover, Morgan (1986) considered values of soil formation rates under environmental friendly agricultural practices and in soils with medium to high weathering rate of about 1.2 ton ha<sup>-1</sup> y<sup>-1</sup>. Therefore, from your main parent material information and annual rainfall and temperature, you can estimate the annual soil weathering rate (Mg ha<sup>-1</sup> y<sup>-1</sup>). From soil total P and K concentration you can, then estimate annual entry of P and K throughout soil weathering. If it is difficult to estimate a value of P and K content in the newly formed soil. Being aware of some degree of imprecision, we believe the contents of P and K of the newly formed soil would have been close to those resulting from a weighted average for different soil orders found in the study area.

WeathP = Annual weathering rate (Mg soil ha<sup>-1</sup> y<sup>-1</sup>) x Total P concentration in the soil (kg P Mg soil<sup>-1</sup>) = kg P ha<sup>-1</sup> y<sup>-1</sup>.

WeathK = Annual weathering rate (Mg soil ha<sup>-1</sup> y<sup>-1</sup>) x Total K concentration in the soil (kg K Mg soil<sup>-1</sup>) = kg P ha<sup>-1</sup> y<sup>-1</sup>.

Take into account that these P and K inputs account for a relatively low percentage of the total inputs, and therefore some degree of variability is assumable.

The entry of N, P and K in vegetable crops of the floodplain of small-medium temporally or permanent streams, due to sedimentation of soil eroded from the surrounding hillside is difficult to quantify and will not be considered in this model.


#### 4.2.4. Inputs of N by natural N fixation

Biological dinitrogen (N<sub>2</sub>) fixation is a natural process of significant importance in current agriculture. Herridge et al. (2008) have reviewed and update long-standing and more recent estimates of biological N<sub>2</sub> fixation for the different agricultural systems, and Vitousek et al. (2002) developed and ecologically based understanding of N fixation in natural and managed ecosystems. This input can be split into symbiotic N fixation and non-symbiotic N fixation.

#### 4.2.5. Symbiotic N fixation (plant-associated)

The amount of N entering the olive groves from the atmosphere via symbiotic N<sub>2</sub>-fixing bacteria (mainly of the genus *Rhizobium*) in association with the root system of mainly legumes of seeded or spontaneous cover crops should be assessed in those olive farming with cover crops.

Estimation of the amount of atmospheric nitrogen entering the olive groves is difficult since an unknown part of the legume N of both above and belowground biomass, come from the

	Document:	D1.4. Handbook of protocols and methods		
	Author	UJAEN	Version	6
	Reference	D1.4	Date	24/03/2023


soil, and is dependent on the plant species, environmental conditions and the soil available N content, among other variables.

Currently, the most precise and accurate methodologies to determine the amount of N in legumes which come exclusively from the atmosphere are based on  $^{15}\text{N}$  analyses of legume and non legume control plants (usually grasses) growing in the same conditions, because the  $^{15}\text{N}$  isotope signal in the plant depends on whether the nitrogen comes from the soil (relatively enriched in  $^{15}\text{N}$ ) or directly from the atmosphere ( $\approx 0\text{‰}$   $^{15}\text{N}$  enrichment). These analyses require sophisticated equipment (mass spectrometer) and a high degree of technical expertise not available in most laboratories. There are a number of studies, the vast majority from temperate regions often undertaken at experimental garden or incubation chambers scales, using this technique given values of atmospheric N fixation for some species. However, the values cannot be directly extrapolated because: i) the amount of N fixed depends on the plant production and values in these experimental conditions differ of that in field conditions, and ii) generally these studies have been conducted on modern varieties of legume species.

There are many studies which show ranges of N fixation for most of the modern cultivated legume species. For example, Havlin et al. (2005) showed the range and the most characteristic value of atmospheric N fixation for 24 species of legumes with typical values ranging 55 kg N ha<sup>-1</sup> y<sup>-1</sup> for winter peas to 222 kg N ha<sup>-1</sup> y<sup>-1</sup> for alfalfa. However, these values should be taken with caution because they come from the cultivation of these species in monocultures and at optimal conditions with potentially high production levels.

Another approach, also not free of some uncertainty, is to quantify the amount of N fixed in crops or rotation types that include legume from: i) amount of N harvested in the legume species of the cover crop, ii) amount of that harvested N which come from the atmosphere (based on current information), iii) amount of N in the root system (based on current information), iv) amount of N of the root system which come from the atmosphere (based on current information), and v) N rhizodeposition (based on current information of the amount of N fixed from the atmosphere which have been mobilized directly to the soil).

Thus, using data of yield and N content of the legumes (in seeded cover crop of olive groves planted with legume or in the legumes of spontaneous cover crop), the aboveground legume N can be estimated, and after applying a coefficient which relate legume aboveground N with that in the belowground, the whole plant N (kg N per kg harvested legume) can be quantified. Finally, applying a percentage of N derived exclusively from atmospheric nitrogen (the rest comes from the soil) over the entire plant, and a percentage of plant N

	Document:	D1.4. Handbook of protocols and methods		
	Author	UJAEN	Version	6
	Reference	D1.4	Date	24/03/2023


that is mobilized directly to the soil (rhizodeposition), it is possible to quantified the amount of N fixed per kilogram aboveground net primary production.

The amount of N in the root system can be estimated from the percentage of N in the belowground biomass of several legume species (beans, alfalfa, soybeans, chickpeas ...) found by Wichern et al. (2008) and averaged 38% of total N of the whole plant. The percentage of total N in both the aerial and the root system, derived exclusively from fixed atmospheric nitrogen can be estimated, for instance, from the review of Gathumbi et al. (2002). They found an average value for the percentage of total N derived from atmospheric N ranging between 43 % (36-51 %) of *Macroptilium atropurpureum* and 79% (75-83%) of *Crotalaria grahamiana*. For all the tested species, the grand average was approximately 60%, *value that can be set to estimate atmospheric N fixation by legumes*. The rhizodeposition can be estimated in 18% of total N fixed, average value recorded by Wichern et al. (2008) after reviewing a set of studies.

The atmospheric N fixation, which remains in the olive grove after harvesting, is that of the roots system (22.8 % of the N harvested) plus that rhizodeposited (10.8 % of the N harvested).

It is difficult to estimate the amount of nitrogen fixed by the legumes in spontaneous cover crop communities because depends on the production and species composition, both attributes unique and characteristics of a particular site. However, this route of entry of N should be considered because could contribute significantly to the N budget for woody crops such as olive oil groves with a regular arrangement of the trees (between 50 - 70% of the area of one hectare can be occupied by spontaneous cover crops depending in tree density and canopy volume of the trees). There are two options to estimate the N input by legumes in cover crops. The first one it is throughout ongoing or past field studies in similar environmental and geomorphological conditions of those of the studied site, which have quantified the biomass of legumes (Mg h<sup>-1</sup>) in olive groves. Another option, the best in my opinion, is that when harvesting aboveground biomass of the spontaneous cover crop during spring 2021 with the 50 cm x 50 cm frames, a botanist or an expert with knowledge in legumes, separate legume biomass from non-legume biomass, and N is analysed in both type of biomass. By estimating the above and belowground N in legumes and taking into account that proportion taken up from the atmosphere, it is possible to upscaling that N input to a hectare.



	Document:	D1.4. Handbook of protocols and methods		
	Author	UJAEN	Version	6
	Reference	D1.4	Date	24/03/2023

NS = ((Aboveground legume biomass (kg ha<sup>-1</sup> y<sup>-1</sup>) x (N content (%)/100)+ belowground legume N (depending in aboveground legume biomass)) x (fraction of N taken up from the atmosphere) + fraction which is rhizodeposited which depends on the aboveground+belowground fixed N.


#### 4.2.6. Non symbiotic N fixation (free-living)

This route of entry of atmospheric nitrogen by biological fixation corresponded to that of autotrophic and heterotrophic organisms, which are not in direct symbiotic association with the root system of vascular plants. Details of the biochemistry, physiology and taxonomy of organisms capable of fixing atmospheric nitrogen without symbiosis can be found in Clark and Rosswall (1981), Gordon and Wheeler (1983) and Alexander (1984). The quantification of the amount of nonsymbiotic N fixation is, usually, indirect and based on incubations of soil samples in the presence of acetylene which is reduced to ethylene by the activity of nitrogenase (family of enzymes that catalyze the breakdown of the triple bond that holds the two N atoms of N<sub>2</sub>), and the subsequent determination, by gas chromatography, of the produced ethylene. Other methodologies are based upon the <sup>15</sup>N. However, none of these is entirely satisfactory.

Estimates of free N fixation in a wide range of ecosystems ranging from 0 to 30 kg N ha<sup>-1</sup> y<sup>-1</sup>, and generally higher values correspond to those measured or estimated in semi-arid regions. Unfortunately, the number of estimates of free N fixation in agricultural ecosystems, and the effects of environmental variables and management practices on the process, is scarce and incomplete. Nevertheless, intensive and frequent tillage limits the establishment of autotrophic free N-fixing organisms (such as algae) and significantly reduces the soil content of organic carbon content, which is needed for the heterotrophic free N fixation.

Boring et al. (1988) in an extensive literature review showed some estimates of free N fixation for a wide range of ecosystems. These authors presented an average of 4 kg N ha<sup>-1</sup> yr<sup>-1</sup>. This value is within the range described by Unkovich and Baldock (2008) for different types of agro-ecosystems in different climatic regions (including that Mediterranean) of Australia. However, Boring et al. (1988) and Unkovich and Baldock (2008) pointed out that levels of N that entry by this process is significantly reduced according to the intensity and frequency of tillage.

Therefore, in the absence of information from experiences in the field, it is reasonable to adopt a value of 4 kg N ha<sup>-1</sup> y<sup>-1</sup> for the atmospheric N fixed by free microorganisms. The influence of tillage in this entry can be incorporate by reducing this input according to the tillage regime using a categorical scale.

	Document:	D1.4. Handbook of protocols and methods		
	Author	UJAEN	Version	6
	Reference	D1.4	Date	24/03/2023

Input of N by free N fixation, thus, depend of the tillage regime of each olive groves.

I suggest to set up a free-living N fixation of 4 kg N ha<sup>-1</sup> y<sup>-1</sup>, for those olive groves with a soil organic matter content > 2 % no tillage or only tillage a maximum of 2 occasions per year. For those olive groves with soil organic matter content below 2 % and/or with more than 2 tillage events and/or using herbicides to control spontaneous cover crop, I suggest a value of 2 kg N ha<sup>-1</sup> y<sup>-1</sup>.

N<sub>nonS</sub> = 4, if soil organic matter content > 2 % no tillage or only tillage a maximum of 2 occasions per year or 2, if soil organic matter content is below 2 % and/or with more than 2 tillage events and/or using herbicides to control spontaneous cover crop.

#### 4.2.7. Anthropogenic N, P and K inputs

The anthropogenic routes, and therefore man-managed, of entry of N, P and K are irrigation (for those eventually and constantly irrigated crops) and fertilizers, and seed application in case of seeded cover crops.

#### 4.2.8. N, P and K entries through irrigation

Input of N, P and K by irrigation water should only be considered in irrigated olive groves. Quantifying this input require of estimates of the annual irrigation volume (m<sup>3</sup> ha<sup>-1</sup>) and water content of total N, P and K (g m<sup>-3</sup>). Concentration of P, N and K in the water should be performed in 2-5 samples collected in different moments to provide a mean and a standard deviation. I suggest to send the collected water (always keep them in a fridge at 4 °C if water samples are to be sent for analysis within 2 weeks or frozen for longer periods of time) to water laboratory analysis. The cost is about 20 euros per water sample for the three elements. Alternatively, you can search for data on N, P and K content in irrigated crops nearby to area of study and use these data to assess for these nutrient entries.


N<sub>Irr</sub> = Annual irrigation volume (m<sup>3</sup> ha<sup>-1</sup> y<sup>-1</sup>) x N concentration in the irrigated water (g N m<sup>3</sup>)/100 = kg N ha<sup>-1</sup> y<sup>-1</sup>.

P<sub>Irr</sub> = Annual irrigation volume (m<sup>3</sup> ha<sup>-1</sup> y<sup>-1</sup>) x P concentration in the irrigated water (g P m<sup>3</sup>)/100 = kg N ha<sup>-1</sup> y<sup>-1</sup>.

K<sub>Irr</sub> = Annual irrigation volume (m<sup>3</sup> ha<sup>-1</sup> y<sup>-1</sup>) x K concentration in the irrigated water (g K m<sup>3</sup>)/100 = kg N ha<sup>-1</sup> y<sup>-1</sup>.

#### 4.2.9. N, P and K entries by seeds application

Only for olive grove with seeded cover crop. This is estimated from: i) the rate of seed application (e.g. kg seeds ha<sup>-1</sup>), and ii) content of N, P and K in the seeds. Therefore, seeds

	Document:	D1.4. Handbook of protocols and methods		
	Author	UJAEN	Version	6
	Reference	D1.4	Date	24/03/2023

should be analysed for total N, P and K or alternatively literature values of N, P and K contents in seeds of this or similar species can be used. N, P and K input by seeds is rather low compared to other inputs and therefore errors in this estimation is assumable.

#### 4.2.10. N, P and K inputs by fertilization

The amount (Kg or Mg per hectare), date and way of application (e.g. applied below tree canopy, applied via foliar, applied more or less uniformly in the inter canopy area..) of any compound entering the olive grove which might have N, P and K, which includes manure, olive mill pomace, composted olive mill pomace, foliar fertilisers, should be recorded and if possible make a picture of the compounds. Always, keep a subsample (1 kg if manure or composted olive mill pomace and 10-50 grs if are concentrate nutrient products) of the material. If during the year of study, no inputs of sources of nutrients are recorded, then inform of how much manure or composted olive mill pomace the olive farmer applied and search in the area for the same material to collect a sample, and analyse for N, P and K.

Multiplying the amount applied (Mg ha<sup>-1</sup> y<sup>-1</sup> dry basis) with the concentration of N, P and K in the material (%) the N, P and K due to fertilizers is estimated.

Nfer (if three N-containing compounds are applied in a year) = (Amount applied compound 1 (Mg dry basis ha<sup>-1</sup>) x N content (%) of compound 1/100) + (Amount applied compound 2 (Mg dry basis ha<sup>-1</sup>) x N content (%) of compound 2/100) + (Amount applied compound 3 (Mg dry basis ha<sup>-1</sup>) x N content (%) of compound 3/100).


Pfer= (if three P-containing compounds are applied in a year) = (Amount applied compound 1 (Mg dry basis ha<sup>-1</sup>) x P content (%) of compound 1/100) + (Amount applied compound 2 (Mg dry basis ha<sup>-1</sup>) x P content (%) of compound 2/100) + (Amount applied compound 3 (Mg dry basis ha<sup>-1</sup>) x P content (%) of compound 3/100).

Kfer= (if three K-containing compounds are applied in a year) = (Amount applied compound 1 (Mg dry basis ha<sup>-1</sup>) x K content (%) of compound 1/100) + (Amount applied compound 2 (Mg dry basis ha<sup>-1</sup>) x K content (%) of compound 2/100) + (Amount applied compound 3 (Mg dry basis ha<sup>-1</sup>) x K content (%) of compound 3/100).

$$\text{Total N input} = \text{RainN} + \text{NS} + \text{NnonS} + \text{NIrr} + \text{Nfer}$$

$$\text{Total P input} = \text{RainP} + \text{Pirr} + \text{Pfer}$$

$$\text{Total K input} = \text{RainK} + \text{Kirr} + \text{Pirr}$$

	Document:	D1.4. Handbook of protocols and methods		
	Author	UJAEN	Version	6
	Reference	D1.4	Date	24/03/2023

### 4.3. N, P and K outputs

The main routes of outputs of N, P and K to be quantified are those due to harvesting and soil loss by erosion. However, for N net losses of N via gas ( $N_2 + N_2O$  by denitrification, and  $NH_3$  through volatilization) and by leaching, should also be taking into account.

The various transformations routes of P and K in natural and agro-ecosystems have a strong geochemical component, in which very dynamic physico-chemical processes, such as adsorption/desorption and precipitation/solubilization, are responsible for the relatively high soil retention capacity. Therefore, the P losses by leaching in agroecosystems can be considered negligible, especially when climatic conditions are characterized by annual precipitation lower than  $650 \text{ L m}^{-2} \text{ y}^{-1}$ . For K, despite in the soil solution is nearly as soluble (mobile) in water as nitrate, the losses by lixiviation is relatively low because of the soil cation exchange capacity (dynamic equilibrium in which adsorption/desorption of K in soil solution with the negative charge on the surface of clay particles and/or soil organic matter) which retain in the soil a considerable amount of K.


#### 4.3.1. N, P and K outputs by harvesting

The amount of N, P and K annually leaving the olive grove by harvesting is assessed from the harvest ( $\text{kg olive fruit harvested ha}^{-1} \text{ y}^{-1}$ ) and the contents of N, P and K at harvest. Thus, it will be needed to quantify: i) the olive fruit production, and ii) collect several 20 gr olive fruits to analyse the water content and the content of total N, P and K in the dried fruit. In my opinion analysis of N, P and K content of the dried fruit does not need to be performed in each of the olive grove. However, if harvest is performed at different periods of time between STSs and non-STSs, it is recommended to measure the water content of the olive fruit. Alternatively, N, P and K contents of the olive fruits can be estimated from literature/reports of your countries for your variety.

$$\begin{aligned}
 \text{HN} &= (\text{Fresh harvested olive fruit (kg fresh weight ha}^{-1} \text{ y}^{-1}) \times (\text{dry content of the harvested olive fruit (\%)/100}) \times (\text{N content on dry basis (\%)/100}) \\
 \text{HP} &= (\text{Fresh harvested olive fruit (kg fresh weight ha}^{-1} \text{ y}^{-1}) \times (\text{dry content of the harvested olive fruit (\%)/100}) \times (\text{P content on dry basis (\%)/100}) \\
 \text{HK} &= (\text{Fresh harvested olive fruit (kg fresh weight ha}^{-1} \text{ y}^{-1}) \times (\text{dry content of the harvested olive fruit (\%)/100}) \times (\text{K content on dry basis (\%)/100})
 \end{aligned}$$

#### 4.3.2. N outputs by burning olive tree pruning

P and K have not significant compounds in phase. Therefore, the burning of the pruning remains, does not mean an output of P and K, but a means by which P and K become more

	Document:	D1.4. Handbook of protocols and methods		
	Author	UJAEN	Version	6
	Reference	D1.4	Date	24/03/2023

available, as the fire accelerate the transference of P and K from a short-term low available pool (olive tree pruning) into a more labile forms in the soil.

However, for N, the burning of the pruning remains does mean a gaseous loss of N out of the olive grove. So, from i) the mean annual amount of tree pruning (e.g. average of three trees per farm), ii) the dry weight of the tree pruning, and iii) the N content of the tree pruning, losses by olive tree pruning can be estimated. The N content of the tree pruning does not show huge variability and thus data from literature/reports could be used.

TPN = (Fresh tree pruning (kg fresh weight per tree y<sup>-1</sup>) x number of trees per hectare (number ha<sup>-1</sup>) x (dry content of the tree pruning (%)/100) x (N content of the tree pruning on dry basis (%)/100)

#### 4.3.3. N, P and K outputs by soil erosion

Significant amount of N, P and K might be lost out the farming by soil erosion. These losses should be estimated from the total contents of N, P and K of the topsoil and annual soil loss rates.

This output will be estimated from the soil erosion (Mg ha<sup>-1</sup> y<sup>-1</sup>) calculated (see soil erosion section) and total N, P and K contents of the top 5 cm of soils. It will be assumed that enrichment ratio (of all, soil particle distribution, and total N, P and K) of the eroded material is 1.0.


EN = (Soil erosion (Mg ha<sup>-1</sup> y<sup>-1</sup>) x ((total N content (%)/100))/1000 = kg N ha<sup>-1</sup> y<sup>-1</sup>.  
 EP= (Soil erosion (Mg ha<sup>-1</sup> y<sup>-1</sup>) x ((total P content (%)/100))/1000 = kg P ha<sup>-1</sup> y<sup>-1</sup>.  
 EK= (Soil erosion (Mg ha<sup>-1</sup> y<sup>-1</sup>) x ((total K content (%)/100))/1000 = kg K ha<sup>-1</sup> y<sup>-1</sup>.

Output of K due to soil erosion can be very high as total K content in the soil can be very high.

#### 4.3.4. N outputs due to denitrification

Denitrification is a microbial process in which nitrate is reduced in an anaerobic or micro-anaerobic environment to N<sub>2</sub>O and N<sub>2</sub>, which are gases which escape to the atmosphere. Main variables controlling the magnitude and temporal pattern of this process in soils included soil nitrate and organic carbon contents, being temperature and soil water content (regulates the existence of anaerobic and/or microanaerobic environments) modulators of the process. There are two mechanisms by which N is loss by denitrification. N losses by




	Document:	D1.4. Handbook of protocols and methods		
	Author	UJAEN	Version	6
	Reference	D1.4	Date	24/03/2023

denitrification are those due to soil (baseline soil N losses) and those directly linked to fertilisation.

There is no a direct methodology to quantify with some precision the rates of N loss in the form of  $N_2$  because of the relatively huge amount of atmospheric  $N_2$  that avoid any detectable increase after an incubation period. Most techniques which assess soil N losses by denitrification are based on measuring the production of  $N_2O$  from soils (with or without fertilizer) in the presence of acetylene (which is an inhibitor of the reduction of  $N_2O$  to  $N_2$ ). Soil basal N losses by denitrification can be estimated by employing current models. There are many models to estimate the soil basal N losses and are grouped into: i) models based on the collection of many values from regions with different climatic conditions, different crops, management practices and different experimental conditions, ii) empirical model based on functional relationships between variables and few measurements of N losses by denitrification, and iii) mixed models that enshrine the former with the latter. In agroecosystems located in temperate regions, the implementation of the first group of models is recommended because they are mainly based on experiments conducted in these regions. The application of models of the second type in the reconstruction of N balance is difficult because the main input variables in these models are level of nitrate content and/or organic matter (or organic carbon) or the partial pressure of oxygen in the soil. Since the monitoring of these soil variables is complex, I suggest not to apply these methodologies.

The application of a current model for estimating the soil basal N losses should employ general soil variables relatively easy to obtain. Unfortunately, the use of general soil variables inevitably introduces some imprecision. Nevertheless, the soil N losses are specific for each crop type if those general soil variables can be described for each crop. Vinther and Hansen (2004) developed the SimD general model, which is based on a combination of average values of  $N_2$  losses, resulted from a literature review and manipulative experiments at field conditions. The model takes into account the effect of soil moisture has on the process and the relationship between soil clay content and soil hydraulic conductivity and organic carbon, and establishes a relationship between denitrification rate and clay content in soil. The model establishes a functional relationship (Michaelis-Menten type) between soil clay content and N losses as  $N_2O$ . On the other hand, the relationship between  $N_2$  and  $N_2O$  is also controlled by the clay content, and thus  $N_2$  can be estimated from those of  $N_2O$ . The amount of N annually lost by basal soil denitrification is the sum of that of  $N_2O$  and  $N_2$ .

From the soil clay content of the STS and non-STS olive groves and using the model of Vinther and Hansen (2004), we will estimate both; basal  $N_2O$  and  $N_2$  emissions, both of

	Document:	D1.4. Handbook of protocols and methods		
	Author	UJAEN	Version	6
	Reference	D1.4	Date	24/03/2023

which are taken into account to estimate the N losses due to basal denitrification.

In addition to the soil basal N losses there should be other N losses by denitrification linked to the applied N with the organic or inorganic fertiliser. N losses by denitrification due to fertilization can be measured at laboratory conditions, experimental garden and in the field. However, their analysis requires a degree of manipulation of the experimental units and a high intensity of sampling and analysis, and specialized equipment (gas chromatograph and an electron capture detector). If the necessary equipment is lacking estimates of N loss by denitrification associated to fertilization must be based on current models. The need to evaluate globally the contribution of different countries in the emission of greenhouse gases has resulted in the compilation of results and conclusions of many experiments to determine the relationship between nitrogen fertilizer use and emission of N<sub>2</sub>O (and N<sub>2</sub>) by denitrification. The result of these revisions has been the finding of a linear relationship between amount of fertilizer applied and the amount of N lost by denitrification. Following the methodology described in the IPCC (IPCC, 1997), the emission factor of N is 1.25% (1.25% organic fertilizer N lost by denitrification in the form of N<sub>2</sub>O), and therefore, this conversion coefficient is an appropriate starting point to quantify the amount of N added with the fertilizer that is lost by denitrification. However, Kasimir-Klemedsson and Klemedsson (2002) suggested after a later comprehensive literature review, an emission value of 2.5% for different types of manures. These emissions coefficients have been now revised. We will use the most recent IPCC coefficients for inorganic and organic N fertilizers to estimate the N<sub>2</sub> loss due to N fertilisers.

Den = soil basal (SDen) + fertiliser based (FDen)


SDen = f(clay content (%)) x (Cf (clay content (%))/100). “f(clay content (%))” means a function of the soil clay content and “Cf (clay content (%))” a ratio which is a function of the soil clay content.

FDen = annual amount of applied N (kg N ha<sup>-1</sup> y<sup>-1</sup>) x (IPPC fraction (%)/100)

#### 4.3.5. N losses through volatilization of NH<sub>3</sub>

The major source of NH<sub>3</sub> in the agrarian sector is volatilisation from livestock excreta, and fertilised agricultural land typically contributes approximately between one to two tenths of the total agricultural emissions.


Ammonia (NH<sub>3</sub>) is formed constantly from ammonium (NH<sub>4</sub><sup>+</sup>), which is formed from the

	Document:	D1.4. Handbook of protocols and methods		
	Author	UJAEN	Version	6
	Reference	D1.4	Date	24/03/2023

biological degradation of native organic N compounds, organic fertilizers and chemically synthesized fertilizers (such as Urea), all of these yielding  $\text{NH}_4^+$ . As it is a gas, a proportion of the  $\text{NH}_3$  present in the soil solution can volatilize to the atmosphere. Losses through volatilization of  $\text{NH}_3$  are due to the physical-chemical reaction (non-biological process) by which ammonium in the soil solution is transformed into ammonia (gas) with no change in the oxide – reduction state. The main variables governing the process are the soil ammonium content and pH. The greater of both the greater is the N loss. In addition, the degree of exposure to sunlight and soil carbonate content modulates the process; higher levels of both match with major losses. Finally, the temperature of the soil solution, the surface area exposed to the atmosphere and the resistance to  $\text{NH}_3$  transport in the atmosphere are also modulators of the process.

Main source of  $\text{NH}_3$  emission from manure management is the N excreted by livestock. Typically, more than half of the N excreted by mammalian livestock is in the urine, and between 65 and 85 % of urine-N is in the form of urea and other readily-mineralized compounds (Jarvis et al., 1989; Aarnink et al., 1997). Urea is rapidly hydrolyzed by the ureases to ammonium carbonate, and ammonium ions provide the main source of  $\text{NH}_3$ . Ammonium and compounds, including uric acid, which are readily broken down to  $\text{NH}_4^+$ , are referred to as total ammoniacal-N. In contrast, the majority of N in mammalian livestock faeces is not readily degradable (Van Faassen and Van Dijk, 1987) and only a small percentage of this N is in the form of urea or  $\text{NH}_4^+$  (Ettalla and Kreula, 1979), so  $\text{NH}_3$  emission is believed to be sufficiently small (Petersen et al., 1998). Poultry produce only faeces, a major constituent of which is uric acid and this, together with other labile compounds, may be degraded to  $\text{NH}_4^+$  after hydrolysis to urea (Groot Koerkamp, 1994).

Other described sources of  $\text{NH}_3$  emissions included the ammonium produced during the decomposing of crop residues, such as residues of cover crops in olive grove. However, its quantification is extremely uncertain, and emissions from this source are likely to be very variable, and probably vary greatly from year to year depending on environmental conditions and success of harvests. The limited experimental work (Whitehead and Lockyer 1989) found only emission from grass foliage with a high N content where much N-fertiliser had been applied, and was restricted to laboratory measurements which may overestimate


	Document:	D1.4. Handbook of protocols and methods		
	Author	UJAEN	Version	6
	Reference	D1.4	Date	24/03/2023

emission. Recent measurements have also indicated significant  $\text{NH}_3$  emissions from decomposing brassica leaves (including oilseed rape, cauliflower), especially after cutting (Sutton et al. 1996). Depending on the interpretation of results, emissions from growing vegetation and from decomposing grass herbage may be treated as an additional emission. Or they may be included together with soil emissions as a single emission factor.

Because it is a process that take place when ammonium is present in the soil solution and this is constantly produced during organic N compounds decomposition (ammonification) in natural or semi-natural ecosystems, the basal  $\text{NH}_3$  emission should be taken into account. In addition to these emissions, those derived from applied inorganic and organic fertilisers should also be considered (fertiliser-based  $\text{NH}_3$  emissions, hereafter).

Estimations of soil basal N losses by volatilization are poorly known mainly by methodological difficulties and because plants can act as both source and sink for  $\text{NH}_3$  (Schj rring, 1991). Hotan-Hartwig and Bockman (1994) in a review of a large number of studies which estimated N losses through volatilization of  $\text{NH}_3$ , found that for croplands of temperate regions, N losses by this process averaged 1 to 2 Kg N ha<sup>-1</sup> y<sup>-1</sup>. We believe that in case of lacking of further information, it is reasonable the adoption of an average of 1.5 Kg N ha<sup>-1</sup> y<sup>-1</sup> for soil basal  $\text{NH}_3$  emissions in cropland and pastureland. However, it is likely that this value is underestimated for soil with relatively high pH and carbonate, and subjected to periods of high solar radiation, as it is the case of olive cultivation in most of the areas of the Mediterranean. During next months, we will try to search for a more Mediterranean specific value.


The emissions of ammonia from the field after application of inorganic and organic N fertilizers are affected by N-fertiliser type, soil type, among others (Sommer et al. 2006). Also, the application technique and weather conditions such as temperature and wind speed have an effect on how much ammonia is emitted from the field. Most of the ammonia emissions from field-applied manure occur within two to three days after the application, a major part of the emissions may occur during the first few hours after application. In particular, the type of N-fertiliser applied has a great effect on the magnitude of emissions (Whitehead and Raistrick, 1990). Emissions are largest from urea fertiliser because it

	Document:	D1.4. Handbook of protocols and methods		
	Author	UJAEN	Version	6
	Reference	D1.4	Date	24/03/2023

hydrolyses in the soil and releases  $\text{NH}_3$ . Emissions from ammonium sulphate may also be large, but these are very dependent on soil pH, with larger emissions from calcareous soils. Other fertilisers, such as ammonium nitrate, are more neutral in pH and produce much smaller emissions. Fertilisers containing only nitrate do not emit  $\text{NH}_3$  directly. EMEP Corinair Emission Inventory Guidebook (EEA, 2007) provided default  $\text{NH}_3$  emissions factors for different chemical N-fertilisers once they have been applied. To provide a more detailed methodology it is desirable to distinguish also between the different climates and soil types of different regions within a country, as has already been done for Spain (Sanz-Cobena et al. 2014). The justification for this is well established, as crop emissions are known to be larger in warmer climates (Fenn and Hossner, 1985), while soil emissions (direct fertilizer losses) generally increase at higher soil pH (e.g. Whitehead and Raistrick, 1990). Given the need to generalize, only a broad scale approach is possible to apply these known differences in inventories. A first attempt has been applied by ECETOC (1994). Based on findings reported or collated by Misselbrook et al. (2000) and Harrison and Webb (2001) and Sutton et al. (2000, 2001, 2002) a detailed approach should consider both mean temperatures for the most important period of fertilizer application (March to May) as well as soil pH. In addition, the effect of calcareous soils should be considered through use of a multiplier on the basis of values for different areas. Thus, from the annual mean temperature of the STS and non-STS olive groves, soil pH and carbonate content, we will modulate the specific emissions factors for each type of fertiliser applied. For instance, for a spring temperature higher than 13 °C, the emission factor for Urea, anhydrous ammonia, ammonium sulphate and ammonium phosphates and ammonium nitrate, calcium ammonium nitrate and other NK and NPK, are set up 20.0 %, 4.0 %, 2.5% and 2.5 % of the N applied with the fertiliser.

Misselbrook et al. (2000) reviewed  $\text{NH}_3$  emission factors of grazing/outdoor application of manure. For land spreading manure, emissions ranged between 15 % (for solid manure of beef cattle) to 7.6 % (for sheep barn and poultry manure) of the total ammoniacal nitrogen (TAN), which is a proportion of the manure N.

Default  $\text{NH}_3$  emissions of manure land spreading was set up for different animals by SNAP (SNAP, 1999. 100900, Manure Management Regarding Nitrogen Compounds). According to table A4, 20 % of the N available for land spreading can be lost as  $\text{NH}_3$  for dairy cows,

	Document:	D1.4. Handbook of protocols and methods		
	Author	UJAEN	Version	6
	Reference	D1.4	Date	24/03/2023

other cattle, fattening pigs and sows, laying hens, broilers and other poultry, whereas values were half for sheep and horses. However, attention should be paid because these values assume that 50 % of the N in animal waste consist of mineral N (available for volatilization), while solid manure contains a lower percentage of mineral N.

Viljavuusalvelu (2008) analysed  $\text{NH}_4^+\text{-N}$  content of the manure of different livestock types. Thus, for solid manure of cattle, pigs, chickens, sheep, horses and other livestock figures were 1.6, 2.3, 7.1, 2.2, 0.9 and 6.9 kg N- $\text{NH}_4^+$  Mg<sup>-1</sup>, respectively. Thus, combining these ammonium concentrations in the solid manure of different animals with the percentage of this ammonium which is volatilized to  $\text{NH}_3$ ,  $\text{NH}_3$  emission due to land spreading of the manure into the croplands can be estimated.

$\text{VolN} = \text{soil basal (SVol)} + \text{fertiliser based (FVol)}$

$\text{SVol} = 1.5 \text{ (kg N ha}^{-1}\text{)}$


$\text{FVol} = \text{annual amount of applied N (kg N ha}^{-1} \text{ y}^{-1}) \times (\text{fraction (\%)/100})$ ; the fraction will depend on the type and characteristics of the fertilizer and some climatic (e.g. mean daily temperature when fertilizer is applied) and soil (e.g. soil pH and carbonate content).

#### 4.3.6. N losses through leaching

Nitrate is highly soluble in water and hardly is retained in the soil by geochemical mechanisms. Therefore, a great part of the nitrate in the soil solution can be lost with the water that lixiviated by gravity to deeper soil profile (deeper than the maximum root exploration depth) during periods of heavy rainfall or when the soil water content exceeds the water holding capacity. The N leaching losses depend on the concentration of nitrate in the soil solution and water flow downward throughout the soil profile. Di and Cameron (2002) compiled a series of studies evaluating N losses by leaching in grasslands, forest ecosystems, and agroecosystems with contrasted management, given a comprehensive review of the main variables, which control and modulate these losses.

In the absence of information on soil nitrate along a period of time (e.g. monthly during one year), the N leaching losses should be estimated from the current general models relating N leaching losses with general soil and meteorological variables available. We believe, the general model proposed by Di and Cameron (2000) is an adequate starting point. This empirical model relates the amount of N lost by leaching (in each 100 L m<sup>-2</sup> of lixivate water) with the amount of potentially leachable nitrogen, by mean of a quadratic function.



	Document:	D1.4. Handbook of protocols and methods		
	Author	UJAEN	Version	6
	Reference	D1.4	Date	24/03/2023

On the other hand, the amount of potentially leachable nitrogen is calculated as the sum of all N inputs (rainfall, nitrogen fixation, irrigation and input of organic fertilizer and seeds) minus the partial outputs (harvest, denitrification, ammonia volatilization and erosion). However, it should also be considered as an entry of nitrate that due to the net balance N mineralization and nitrification. Net N mineralisation and nitrification have been studied for grassland and pasture, forest ecosystems and agroecosystems, and depend heavily on the soil total N content. Generally, around 2 % of the soil organic N is annually nitrified to nitrate after being mineralised to ammonium. This percentage has been used by many authors to estimate the annual supply of available N from soil (Havlin et al., 2005). Above (protocol for potential N mineralization) we will estimate which percentage of the total N is potentially mineralizable. This, together with the total soil N data and soil bulk density (top 30 cm of soil), we can estimate the amount of nitrogen (kg N) which is mineralized. The Di and Cameron model estimates the leaching nitrate for each 100 L m<sup>-2</sup> of water lixiviated, the lixivate water volume should also be estimated. This can be done from the water balances calculated from the meteorological information of the study area. Taking into account the monthly values of rainfall and evapotranspiration, and soil water content at 100% of water field capacity, the lixiviation volume can be estimated. Annual irrigation water volume should be added to rainfall for the irrigate cropland.

Leaching N = (partial result of the N balance ((RainN+NS+NnonS+NIrr+Nfer)-(HN+TPN+EN +Den+VolN) (kg N ha<sup>-1</sup> y<sup>-1</sup>) + Mineralised N (kg N ha<sup>-1</sup> y<sup>-1</sup>)) x function of lixiviated water (which is calculated from mean monthly rainfall and evapotranspiration


Total output is calculated as the sum of all the output processes.

Total N output = HN +TPN+EN + Den + VolN +LeachingN

Total P outputs = HP+EP

Total K outputs = HK and EK

N, P and K balances in the STSs and non-STs are calculated as the difference between inputs and outputs.

	Document:	D1.4. Handbook of protocols and methods		
	Author	UJAEN	Version	6
	Reference	D1.4	Date	24/03/2023

## 5. Soil erosion

### WP3. Task 3.5. Soil erosion and carbon sequestration

Leader: Julio Antonio Calero Gonzalez and Tomas Fernandez de Castillo (University of Jaen)

For further clarification contact: jcalero@ujaen.es


#### 5.1. Introduction

Water erosion is one of the main processes of soil degradation on a global scale, particularly affecting the countries of the Mediterranean basin and one of its emblematic crops, such as the olive grove.

There are several methodologies to estimate the erosion in olive groves: i) direct measurements at the plot or hillside scale using runoff collectors or artificial rain simulators (G ó mez et al., 2009), ii) applying erosion models, which can be empirical or physical (G ó mez, 2015). Empirical models are based on the analysis of relatively easy sets of inputs obtained by calibration from experimental plots. Physical models, by contrast, are based on solving universal physical equations. Compared to physical models, empirical models are simpler and require a smaller number of input parameters. However, they are relatively unreliable in their extrapolation to situations or locations that differ markedly from where they were calibrated, leading errors when applied to large areas (Sadeghi et al., 2014).

The Universal Soil Loss Equation, in its first (USLE, Wischmeier and Smith, 1965; 1978) or later version (RUSLE, Renard et al. 1997), is one of the most applied empirical models worldwide. Moreover, USLE and its derivatives has been preferred in olive groves erosion modelling (G ó mez et al., 2003; lvarez et al., 2007, Vanwallegghem et al., 2011).

However, in addition to the uncertainty associated with its empirical nature, the main limitation of the USLE model is its scale of application, both spatial and temporal. In the first case, USLE only quantifies sheet and rill erosion at the hillslope level, leaving important processes such as gully erosion, or sediment mobilization and deposition in watersheds. On the other hand, USLE explore long-term erosive trends based on changes in average patterns of precipitation, vegetation or soil management, so the model is not sensitive to erosion associated with specific events (storms), despite the fact that these represent the largest soil losses (Merritt et al., 2003). This is because USLE does not directly implement runoff, neither discharge flow ( $\text{m}^3 \text{s}^{-1}$ ) or volume ( $\text{mm}/\text{m}^2$ ), which are the main factors of shear stress and soil particle detachment and, therefore, of erosion. Moreover, runoff flows are

	Document:	D1.4. Handbook of protocols and methods		
	Author	UJAEN	Version	6
	Reference	D1.4	Date	24/03/2023

also correlated with the transport capacity of sediments. The Sediment Delivery Ratio (SDR) concept handles both terms, removal and transport, expressing the efficiency of particle mobilization from the erosion area to the point where the sediment is measured.

Incorporating the SDR to the USLE, the effects of sediment transport and removing into the watershed may be easily accounted for, obtaining the specific sediment yield ( $\text{Mg ha}^{-1} \text{ year}^{-1}$ ). Several authors (i.e. Merritt, 2003) stated that sediment yield is a parameter more suitable to assess the whole effects of soil erosion than the potential gross erosion given by USLE. Other approaches have been developed to take into account not only the sediment transport into watersheds, but also adapted to sediment yield given by discrete events (storms). The Modified MUSLE (Williams and Berndt, 1977) estimates the sediment yield for individual storms by replacing the rain erosivity factor  $R$  of Wischmeier and Smith by a runoff factor which depend on the event runoff volume and the discharge peak in watersheds. USLE-M avoids using discharge peak, which is often not measured and difficult to predict, replacing it by the event runoff coefficient ( $Q_R$ , %) (fraction of rainfall that generates runoff), but requires a  $R$  factor for events, which must be empirically determined for each watershed.


However, the complexity of direct erosion measurements prevents the practical application on the farms of SUSTAINOLIVE, at least in this first approach to the problem. Thus, in this protocol the potential risk of soil loss ( $\text{Mg ha}^{-1} \text{ year}^{-1}$ ) will be estimated using the universal soil loss equation (USLE), modulating it with the SDR parameter in order to taking into account the sediment yield.

*The objective of this protocol* is to define a handy but rigorous GIS methodology for applying models based on the universal soil equation, both for calculating the potential risk of erosion (using USLE model) and the sediment yield by means of SDR (Sediment Delivery Ratio) parameter. This will allow us to compare the potential erosion in olive groves where Sustainable Technological Solutions (STS) were applied, as cover crops, regarding those olive groves without STS.

## 5.2. Information sources and Geographical Information System software

The basic sources of information are as follows:

a. *Orthophotography and Satellite images*. It is recommended to access and download the most up-to-date orthophotos and satellite images at the highest possible resolution. It would be highly recommended that the orthophotos have an associated near infrared (NIR) band, since their resolution is higher than the free access satellite images (i.e. Sentinel 2 or Landsat).

	Document:	D1.4. Handbook of protocols and methods		
	Author	UJAEN	Version	6
	Reference	D1.4	Date	24/03/2023

b. *Digital Elevation Models (DEM)*. This information will be basic in estimating the LS factor of USLE. As with orthophotography, the use of DEM of the highest possible resolution is recommended, since we work at the plot level. In our case, we have worked with DEM of 1.5 and 25 m resolution (tests have been made about the influence of DEM resolution on the results).

c. *Climatic Data*. The information needed to calculate the R factor, applying the equation to calculate the modified Fournier index, is the monthly average precipitation. This information can be obtained from: i) maps of average precipitation of the area (a very high resolution is not necessary, since it is assumed that the climate does not change at the plot level; we use raster files with cell size 500 m), ii) own data from the plot, or iii) extrapolation from nearby meteorological stations.

d. *Soil information*. The necessary parameters for the calculation of the K factor will be obtained from the basic soil analyses carried out on the plot. They include:

1. % Organic matter. Estimated from % O.C. (Organic Carbon).
2. Texture.
3. Structure.
4. Permeability class, which can be estimated from the texture, or from the texture and % O.C. through pedotransfer functions.

Specific recommendations on sources of information available will be made in sections 5.3.2 and 5.4.2.


As stated above, USLE is the more employed soil erosion model worldwide, so in some countries this resource is freely available (or at affordable user prices) for the user. The European Soil Data Centre (ESDAC) offers a reference point for relevant soil data that can be used by the European partners of SUSTAINOLIVE.

Among the information available in ESDAC is the European RUSLE-map of soil loss (RUSLE2015), which can be downloaded for GIS analysis in raster format (pixel size 100 m), after filling an easy request form, from the next link:

<https://esdac.jrc.ec.europa.eu/content/soil-erosion-water-rusle2015>

Technical and methodological aspects of GIS modelling and data sources for RUSLE2015 can be found in Panagos et al. (2015a), and a summary at the following link:

<https://esdac.jrc.ec.europa.eu/themes/rusle2015>

	Document:	D1.4. Handbook of protocols and methods		
	Author	UJAEN	Version	6
	Reference	D1.4	Date	24/03/2023

Likewise, each of the factor-layers from which RUSLE2015 was obtained are available, at different resolutions in ESDAC. These are discussed below, with each of the factors.

Several GIS software can be used to carry out the specific tasks of this protocol. Arc Map is the professional software that, in our opinion, provides greater versatility and power in the implementation of USLE, not only for GIS tools (data conversion, interpolation, map algebra, maps composition, etc.), but also remote sensing tools (vegetation index, image classification, etc.). However, Quantum GIS (QGIS) and SAGA are free software that can process also the USLE factors, and even include some tools and algorithms for calculating some of them. For image processing, other free software such as SNAP developed by ESA (European Space Agency) to Sentinel data. Any of the mentioned programs can be used and, in this protocol, options for all of them will be explained.

### Location and delimitation of SUSTAINOLIVE plots

Previous to the application of the USLE model, a precise geographical delimitation of the studied plots is needed. This can be done manually over the image layer (orthophotograph or satellite image), or from vector files type “cadastral parcel” provided by public administrations in some countries.

As example, in Spain all cadastral parcels referring to country properties can be downloaded in shape format, at the municipality level, at the following link <https://www.sedecatastro.gob.es/Accesos/SECACCDescargaDatos.aspx>


### USLE application in olive groves with GIS

Soil losses A ( $\text{Mg ha}^{-1} \text{ year}^{-1}$ ) of the different plots will be estimated using the USLE equation, as defined by Wischmeier and Smith (1978):

$$A = R \times K \times LS \times C \times P \text{ [eq. 5.1]}$$

Where the factors are the following:

1. R: Is the erosivity factor of the rain ( $\text{MJ mm ha}^{-1} \text{ h}^{-1} \text{ year}^{-1}$ ), which coincides with the product of kinetic energy and rain volume of all the periods of same intensity in which a storm may be divided (E), multiplied by the maximum rain intensity reached in 30 min ( $I_{30}$ ).
2. K: Is the soil erodibility ( $\text{Mg h MJ}^{-1} \text{ mm}^{-1}$ ) is the soil loss by each unit of the rain erosivity index, taking as reference a bare soil of a slope of 9% steepness and 22.1 m length.
3. L: Is the slope length factor (-). This relates soil losses for each slope length regarding a reference slope of 22.1 m length with the same soil, cover and management.

	Document:	D1.4. Handbook of protocols and methods		
	Author	UJAEN	Version	6
	Reference	D1.4	Date	24/03/2023

4. S: Is the slope steepness factor (-). This relates soil losses for each slope gradient regarding a reference slope of 9% with the same soil, cover and management.

5. C: Is the cover and management factor (-). It expresses the relationship between soil losses in a soil under a specific crop and the same under a continuous fallow.

6. P: Is the support practices factor (-). Is the ratio between soil losses in a soil in which it has been applied contour farming, strip cropping, terracing and / or subsurface drainage, and losses if the soil is plough following the steepest slope.

In sections 5.1 to 5.5 the procedures for calculating each of the USLE / RUSLE factors will be explained

### 5.3. R Factor

The R-factor is the product of kinetic energy of a rainfall event (E) and its maximum 30-min intensity ( $I_{30}$ ):

$$R = \frac{1}{n} \sum_{j=1}^n \sum_{k=1}^{m_j} (EI_{30})_k \quad [\text{eq.5.2}]$$

where R is the average annual rainfall erosivity ( $\text{MJ mm ha}^{-1} \text{ h}^{-1} \text{ yr}^{-1}$ ) for a series of n years, and E is the kinetic energy of rainfall in an event composed by r periods of equal intensity ( $i_r$ ), which arises from the product of the kinetic energy of rain drops by surface and time unit ( $e_r$ ,  $\text{MJ ha}^{-1} \text{ mm}^{-1}$ ):

$$e_r = 0.29 (1 - 0.72^{(-0.05i_r)}) \quad [\text{eq.5.3}]$$

and the total volume of the rainfall ( $v_r$ , mm),

$$E = (\sum_{r=1}^0 e_r v_r) \quad [\text{eq.5.4}]$$


considering the maximum intensity of the rainfall ( $\text{mm h}^{-1}$ ) in 30 min. ( $I_{30}$ )

$$EI = EI_{30} = (\sum_{r=1}^0 e_r v_r) I_{30} \quad [\text{eq.5.5}]$$

Since  $EI_{30}$  calculation methods require long-term rainfall intensity data, and such data are not available for all application sites, several approaches to estimate R-factor from more generalized data sources have been applied (Renard and Freimund, 1994). Probably, the most employed estimator or the R-factor be the Fourier modified index (IMF) (Arnoldus, 1977):

$$\text{IMF} = \sum_{i=1}^{12} \frac{p_t^2}{P_t} \quad [\text{eq.5.6}]$$



	Document:	D1.4. Handbook of protocols and methods		
	Author	UJAEN	Version	6
	Reference	D1.4	Date	24/03/2023

where  $p_t$  is the average monthly rainfall from January to December, and  $P_t$  is the mean annual rainfall. Arnoldus (1977) related the IMF and R factor for Morocco, obtaining the following regression model:

$$R = 0.264 \cdot IMF^{1,50} \quad [\text{eq.5.7}]$$

And Rodríguez et al. (2004) for Spain:

$$R = 2.56 \cdot IMF^{1,065} \quad [\text{eq. 5.8}]$$

Both are suitable approaches to obtain the R-factor.

For the calculation of IMF, only a raster file of every average monthly rainfall of the zone are needed. Then, using the raster calculator over the IMF raster and applying eqs. 5.7 and 5.8, a R-factor raster can be obtained for each plot, which average pixel values inside the delimited plot is the R factor in eq. 1. As rainfall is not so variable at the farm scale as other factors (i.e. soils), data with resolutions up to 1000 x 1000 m could be suitably used. In the EU a complete erosivity rainfall R-factor dataset is freely available from REDES (Rainfall Erosivity Database on the European Scale) in the following link:

<https://esdac.jrc.ec.europa.eu/content/rainfall-erosivity-european-union-and-switzerland>

Downloadable dataset includes high-resolution raster files (500 m resolution). Technical and methodological aspects of REDES can be found in at Panagos et al. (2015b).


In Spain monthly average rainfall in .shp formats, can be downloaded at the following links (resolution 500 m):

<http://centrodedescargas.cnig.es/CentroDescargas/catalogo.do?Serie=MAMOV#>

[https://descargasrediam.cica.es/repo/s/RUR?path=%2F04\\_RECURSOS\\_NATURALES%2F03\\_CLIMA%2F02\\_CARACTERIZACION\\_CLIMATICA%2F03\\_PRECIPITACION%2F01\\_PRECIPITACION%2F01\\_MEDIA%2F02\\_MENSUAL](https://descargasrediam.cica.es/repo/s/RUR?path=%2F04_RECURSOS_NATURALES%2F03_CLIMA%2F02_CARACTERIZACION_CLIMATICA%2F03_PRECIPITACION%2F01_PRECIPITACION%2F01_MEDIA%2F02_MENSUAL)

As well as the R factor in raster and at a resolution of 75 m for the region of Andalusia (South of Spain):

[http://descargasrediam.cica.es/repo/s/RUR?path=%2F06\\_RIESGOS\\_NATURALES\\_TECNOLOG%2F01\\_RIESGOS\\_NATURALES%2F03\\_EROSION%2F00\\_EROSION%2FInfGeografica%2FInfRaster%2FTIFF%2Fmedia](http://descargasrediam.cica.es/repo/s/RUR?path=%2F06_RIESGOS_NATURALES_TECNOLOG%2F01_RIESGOS_NATURALES%2F03_EROSION%2F00_EROSION%2FInfGeografica%2FInfRaster%2FTIFF%2Fmedia)

	Document:	D1.4. Handbook of protocols and methods		
	Author	UJAEN	Version	6
	Reference	D1.4	Date	24/03/2023

## 5.4. K Factor

### Calculation

The K Factor is obtained from the application of the following formula (Renard et al., 1997):

$$K = \left[ (2.1 \times 10^{-4} M^{1.14} (12 - OM) + 3.25(s - 2) + 2.5(p - 3)) / 100 \right] \times 0.1317 \quad [\text{eq. 5.9}]$$

Where OM is the organic matter (%), s a structure parameter related to the structure type and size, p the permeability class of the soil (Schoenebeger et al., 2012) and M a textural parameter, such as:

$$M = (m_{\text{silt}} + m_{\text{vfs}}) \times (100 - m_c) \quad [\text{eq. 5.10}]$$


being  $m_{\text{silt}}$  (%) the silt (0.002-0.05 mm),  $m_{\text{vfs}}$  (%) the very fine sand (0.05-0.1 mm), and  $m_c$  (%) the clay (< 0.002 mm) contents of the sample. The value of the structure parameter is codified according the following rule (Panagos et al., 2014):  $s = 1$  for very fine granular,  $s = 2$  for fine granular,  $s = 3$  for medium or coarse granular and for  $s = 4$  for the rest of structure types (blocky, platy or massive), as described in FAO (2006) and Schoenebeger et al. (2012). Permeability class can be estimated from the soil texture classes, as recommended Rawls et al. (1982) and Panagos et al. (2014), employing Table 3:

Table 3. Estimation of permeability classes from USDA texture classes.

Permeability class (p)	Texture class	Saturated hydraulic conductivity $K_s$ (mm h <sup>-1</sup> )
1 (fast and very fast)	Sand	> 61.0
2 (moderate fast)	Loamy sand, Sandy loam	20.3-61.0
3 (moderate)	Loam, Silty loam	5.1-20.3
4 (moderate slow)	Sandy clay loam, Clay loam	2.0-5.1
5 (slow)	Silty clay loam, sand clay	1.0-2.0
6 (very slow)	Silty clay, clay	<1.0

Moreover, other soil properties can be considered in addition, because they may modify strongly permeability of soils. The most important is the coarse fragment content (CF). Panagos et al. (2014) recommended taking into account the coarse fragment content of the soil because it can reduce the saturated hydraulic conductivity  $K_s$ :

$$K_{CF} = K_s(1 - CF) \quad [\text{eq. 5.11}]$$

	Document:	D1.4. Handbook of protocols and methods		
	Author	UJAEN	Version	6
	Reference	D1.4	Date	24/03/2023

being  $K_{CF}$  the modified saturated hydraulic conductivity after accounting the effect of coarse fragments (to determine CF see below).

Probably, of all the USLE factors, soil is one of the parameters that presents the largest variability at the farm scale, and the most difficult to rightly assess. For this reason, although there is a map of the K factor at the European level (500 m resolution), soil erodibility is best estimated by carrying out direct measurements from field samples: Texture analysis by the hydrometer method and Organic carbon content by the Walkey-Black Procedure. The parameters of eqs. 5.9, 5.10 and 5.11 are obtained by averaging all the plot sampling points. The Europe map of the K-Factor (Panagos et al., 2014) can be obtained from the next link: <https://esdac.jrc.ec.europa.eu/themes/soil-erodibility-europe>


### Soil sampling and pre-processing

The recommended analysis methods to calculate coarse fragments, texture and organic matter are outlined below.

Five randomly topsoil samples should be taken in each of the SUSTAINOLIVE orchards at a depth of 30 cm, because this is the representative deep for olive trees (Calero et al., 2013; L ó pez-Bellido et al., 2016). First, five inter-canopy lanes, representative of the farm, have to been selected, avoiding field borders, tracks frequently used by machinery, people or livestock, or any other unusual soil area (saline areas, eroded knolls and/or rocky outcrops, old manure piles, burn piles, fence rows, etc.). Likewise, soils should be sampled before ploughing or prior to manure or fertilizer applications. Once inside the lanes, sampling points can be selected by randomly throwing a light object (eg. a pen) into the air, within a radius of about 10 m.

In the case of olive groves, whose soils are usually stony and difficult to penetrate with probes, it is recommended to dig a soil pit with the help of a pick or shovel. Then the sample (about 1 kg) must be taken carefully from each part of the 30 cm of depth and pouring it in a clean and labelled plastic bag, to be carried to the lab.

In the lab, samples should be extended homogeneously from the bags over an absorbent paper, mixing carefully with a plastic or glass rod, but avoiding crushing the soil. Then, the sample should be dried at room temperature for several days up to reach environmental humidity, prior to chemical or physical analyses.

	Document:	D1.4. Handbook of protocols and methods		
	Author	UJAEN	Version	6
	Reference	D1.4	Date	24/03/2023

When dry, divide the final sample into four parts, which are as identical as possible, using a sample divider or by quartering. One of the parts that will be used for texture and organic carbon determinations, is weighted in a balance (0.0 g), storing the rest.

The last step in sample pre-treatment is sieving to obtain the fine earth fraction (< 2 mm). First, the sample must be gently ground to break up soil aggregates and clods, but avoiding breaking the gravel (it is recommended to use a rubber stopper). Then, the sample is passed through a 2 mm sieve, repeating the process until all the thick fragments are retained on the sieve. The sieve of the sieve is fine earth, which will be used for analysis. Finally, the sieve is placed under the tap, washing the coarse fragments, which will subsequently be dried in an oven at 110 °C for 24 h. The content of coarse fragments CF (%) of the sample is calculated with respect to the soil selected in the quartet:

$$CF = \frac{CFw}{FEw} \quad [\text{eq. 5.12}]$$

being CFw (g) the weight of coarse fragments and FEw (g) the weight of the fine earth.


### Determination of soil texture

We suggest you send the soil samples (typically about 200 gr sieved throughout 2 mm mesh) to a soil laboratory for analysis of soil texture). Nevertheless, if you want to carried out the analysis, do as follow.

Fine earth particles are separated by their sedimentation rate in water, according to Stokes' Law, using the hydrometer method (Bouyoucos, 1962). This method is as effective as the pipette method when assessing the K factor for USLE, but more rapid and simpler (Beretta et al., 2014).

### Equipment and Materials

1. Glass tube test, 1000-ml capacity
2. Thermometer, °C
3. Hydrometer (ASTM 152H, range -5 — +60 g/L, in 1 g/L)
4. Electric mixer
5. Glass beakers
6. Balance sensitive to  $\pm 0.01$  g

	Document:	D1.4. Handbook of protocols and methods		
	Author	UJAEN	Version	6
	Reference	D1.4	Date	24/03/2023

## Reagents

Dispersing solution, 10%: Dissolve 100 g of sodium polyphosphate ( $\text{Na}_6(\text{PO}_3)_6$ ) in deionized water and dilute to 1000 ml.

## Method


1. Mix 25 ml of the 10% dispersing solution and 975 ml of deionized water in a 1000 ml test tube. This mixture is the blank. Record the temperature and determine the density of the blank inserting slowly and carefully the hydrometer in the test tube. Record the hydrometer reading.
2. Weight 20 g of fine earth and transfer to a 1000 ml glass beaker. Record weight to  $\pm 0.01$  g.
3. Add  $\approx 500$  ml of deionized water and then 25-ml of 10% dispersing solution to the glass beaker.
4. Attach the glass beaker to mixer and mix the sample 60 sec.
5. Transfer the suspension quantitatively from the glass beaker to a 1000 ml test tube with the help of a plastic wash-bottle, avoiding particles from adhering to the beaker.
6. Fill to the 1000-ml mark with deionized water equilibrated to room temperature and shake the tube test 6 or 5 times to resuspend the particles adhered to the bottom, without losing liquid. After shaking, place the test tube on the table. The sedimentation time is started ( $t = 0$ ).
7. Take reading at 1 min. 8 min. For each reading, gently insert the hydrometer into the test tube, avoiding hitting the walls or the bottom. Quickly remove the hydrometer just after recording the measurement. All the subfractions of sand, except the very fine sand, has settled to the bottom of the test tube, as established by the experimental sedimentation rate values for different particle sizes.
8. Repeat step 7 at 3 min. (very fine sand), 10 min. (coarse silt), 30 min. (medium silt) and 90 min. (fine silt). After the last measurement, the density of the suspension corresponds to the clay.

## Calculations

For each time  $t$ , the density marked by the hydrometer ( $a$ ) is equal to Weight / Volume. If volume = 1 L, the hydrometer marks the weight of particles in suspension in each measure, so the percentage of particles in suspension  $s$  is:

$$\% \text{ suspension} = \frac{a}{p} \times 100 \quad [\text{eq.5.13}]$$

being  $p$  = weight of the sample ( $\pm 20$ g).

	Document:	D1.4. Handbook of protocols and methods		
	Author	UJAEN	Version	6
	Reference	D1.4	Date	24/03/2023

The percentage of particles deposited for the time (d) is: 100 -% suspension.

The percentage of particles deposited for each size class is: d at time t less d at time t-1.

The clay percentage is the % suspension at 90 min.

Results can be noted in Table 4:

Table 4. Hydrometer data to calculate texture classes.

t (times)	a* (g/L)	s (% suspension)	d (% deposited)	% particles deposited ≠ size	USDA fractions
1 min. 8 sec.					Sand (2 – 0.01 mm)
3 min.					Very fine sand (0.01 – 0.05 mm)
10 min.					Coarse silt (0.05 – 0.02 mm)
30 min.					Medium silt (0.02 – 0.005 mm)
90 min.					Fine silt (0.005 – 0.002 mm)
Total					
100 - Total					Clay (< 0.002 mm)

\* The density (g/L) of the blank should be subtracted from the density of the suspension (step 1).

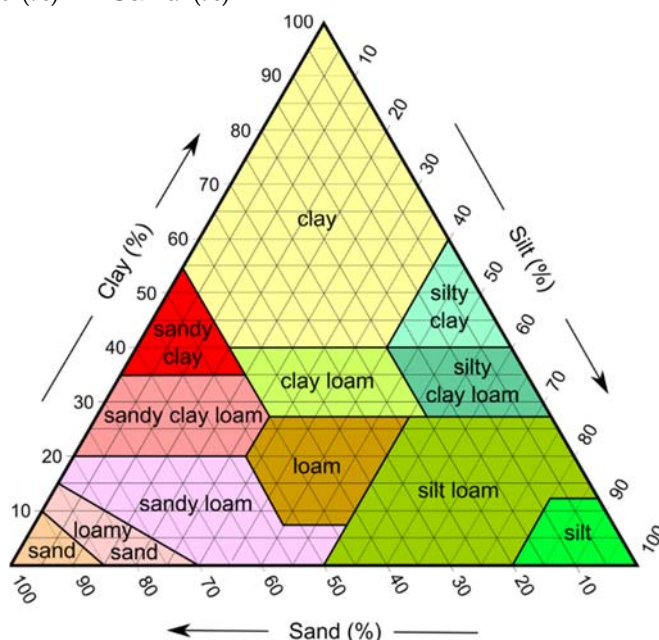
## Representation

From this table, USDA texture classes can be obtained:

Sand (%) is: sand + very fine sand (vfs).


Silt (%) is: coarse silt + medium silt + fine silt.

Clay (%) is: 100 – Silt (%) – Sand (%)



Source: [https://commons.wikimedia.org/wiki/File:SoilTexture\\_USDA.png](https://commons.wikimedia.org/wiki/File:SoilTexture_USDA.png)



	Document:	D1.4. Handbook of protocols and methods		
	Author	UJAEN	Version	6
	Reference	D1.4	Date	24/03/2023

Finally, for the calculation of the K factor (equation 4.1) the vfs and Silt fractions must be used.

### Determination of soil organic matter

We suggest you to send the soil samples (typically about 200 gr sieved throughout 2 mm mesh) to a soil laboratory for analysis of organic matter). Nevertheless, if you want to carried out the analysis, do as follow.

The organic matter content of the soil is calculated through the determination of organic carbon by the Walkey - Black method. Nevertheless, there several other methods. Contact or the easy method to rgarcia@ujaen.es. In the soil, total carbon includes inorganic carbon and organic carbon.


However, the data that are usually handled refer only to the oxidizable fraction, which only includes the organic compounds. In the Walkey - Black method, the organic matter content of the soil is calculated based on the determination of organic carbon in the soil by a wet method, based on a partial oxidation of organic carbon (O.C.) with an oxidizing agent added in excess. The degree of oxidation achieved will depend on the conditions under which the reaction takes place (fundamentally, time and temperature).

### Equipment and Materials

1. Mortar and sieve
2. Precision analytical balance
3. Magnetic stirrer
4. 500 mL Erlenmeyer
5. 1 and 20 mL pipettes
6. Test tube 250 mL
7. Burette and burette foot
8. Funnel
9. Dropper
10. Doser for concentrated H<sub>2</sub>SO<sub>4</sub>.

### Reagents

1. 1N potassium dichromate: dry the reagent in an oven at 105 ° C overnight, dissolve 49.05 g of potassium dichromate (heating slightly to favor dissolution), make up to 1000 mL with deionized water.
2. Concentrated sulphuric acid.

	Document:	D1.4. Handbook of protocols and methods		
	Author	UJAEN	Version	6
	Reference	D1.4	Date	24/03/2023

3. Deionized water.
4. Concentrated phosphoric acid.
5. Diphenylamine in sulphuric solution prepared in the following order: 0.5 g of diphenylamine in 20 mL of deionized water and 100 mL of sulphuric acid (turn from blackish brown or violet to green).
6. Salt of Morh 0.5 N:
7. 196.1 g of  $\text{Fe}(\text{NH}_4)_2\text{SO}_4 \cdot 6\text{H}_2\text{O}$  (Mohr's salt).
8. 800 mL of deionized water containing 20 mL of  $\text{H}_2\text{SO}_4$  to dissolve the salt.
9. Deionized water: bring to a volume of 1000 mL.

## Method

1. Weigh 0.5 g of dry soil and pass through a 0.5 mm sieve.
2. Place it in a 500 mL erlenmeyer flask.
3. Add 10 mL of 1N  $\text{K}_2\text{Cr}_2\text{O}_7$  and shake.
4. Add 20 mL of  $\text{H}_2\text{SO}_4$  with the dispenser slowly and shaking in an extractor hood.
5. Shake by cooling under the tap for about thirty seconds.
6. Let stand for 30 minutes on a little hot heating plate. This treatment removes carbonates.
7. Add 100 mL of deionized  $\text{H}_2\text{O}$  and allow to cool.
8. Add 10 mL of  $\text{H}_3\text{PO}_4$  (avoids possible interference with iron).
9. Add 1ml of the indicator (diphenylamine) and titrate with a 0.5N Mohr's salt solution (the end point is an almost dark black green color that turns to emerald green). If just after adding  $\text{K}_2\text{Cr}_2\text{O}_7$  1N and  $\text{H}_2\text{SO}_4$  the solution turns green, it means that all the dichromate has been reduced and the analysis must be repeated with less sample quantity.
10. Do all of the above for the blank (should consume approximately 20 mL).


## Calculations

The percentage of organic carbon will be determined with the following equation:

$$O.C. \% = (V_B - V_M) \cdot 10^{-3} \times N_{\text{Fe}} \times \frac{12}{4} \times \frac{1}{p} \times \frac{100}{(100 - \% H)} \times f \quad [\text{eq. 5.14}]$$

Where;  $V_B$ , volume of ferrous salt expended in the blank test;  $V_M$ , volume of ferrous salt expended with the sample;  $N_{\text{Fe}}$ , normality of ferrous salt;  $p$ , weight of the sample;  $f$ , recovery factor (according to the operative technique followed, in this case its value is 1.3).

The recovery factor  $f$  depends on the intensity with which the oxidation of the organic carbon takes place. In the method used, without heat input, a recovery of 77 % of organic carbon in the sample is assumed.

	Document:	D1.4. Handbook of protocols and methods		
	Author	UJAEN	Version	6
	Reference	D1.4	Date	24/03/2023

The percentage of organic matter is calculated using the "Van Bemmelen" conversion factor, whose statistically deduced value is 1.724, based on the hypothesis that 58 % of organic matter is organic carbon (this factor may vary from some soils to others).

$$\text{Organic matter, \%} = \% \text{ C} \times 1.724 \text{ [eq. 5.15]}$$

## 5.5. LS Factor

### Calculation

The LS factor represents the effect of the slope's length and steepness on sheet and rill erosion, and is defined as the ratio of expected soil losses from a field slope relative to the original USLE unit plot (22.1 m length, 0.09 m m<sup>-1</sup> steepness) (Wischmeier and Smith, 1978).


Originally, the LS factor was developed to be applied at the plot scale in unidimensional slopes, due to the methodological trouble of applying it to a complex topography landscape scale in the pre-GIS age (Benavidez et al., 2018). Thus, USLE and RUSLE use the slope length, angle and a parameter (m) that depends on the steepness of the slope in percent (Wischmeier and Smith, 1978; Renard et al., 1997).

The extension of the GIS technology also allows considering the topographic position of the plot on the slope, taking into account both the upslope contributing area and the convergence and divergence of the flow, which are also very important when assessing erosion. This is achieved from DEM, which have to be of a minimum resolution of 100 m on a large scale (studies at the watershed level), while for studies at the slope or plot level, minimum resolutions of 15 m are recommended (Benavidez et al., 2018). Several algorithms based in DEM and GIS technology has been developed to deal with complex slopes at the farm scale. Two of the most widely used are those of Moore and Burch (1986) and that of Desmet and Govers (1996), which are based on the following equations:

$$S = \left( \frac{\sin \beta}{0.09} \right)^n \text{ [eq. 5.16]}$$

$$L = \left( \frac{U}{22.13} \right)^m \text{ [eq. 5.17]}$$

$$LS = \left( \frac{U}{22.13} \right)^m \left( \frac{\sin \beta}{0.09} \right)^n \text{ [eq. 5.18]}$$

	Document:	D1.4. Handbook of protocols and methods		
	Author	UJAEN	Version	6
	Reference	D1.4	Date	24/03/2023

Where  $U$  is the upslope contributing area per unit width as indicator of discharge, and it is calculated from flow accumulation  $\times$  cell size (grid resolution in meters).  $\beta$  is the slope ( $m\ m^{-1}$ ),  $m$  a slope-length exponent parameter that is related with  $\beta$ , so that it increases with the slope steepness taking values between 0.4 to 0.72, while the steepness exponent parameter  $n$  can also vary between 1.0 and 1.3 with increasing slope.  $m$  and  $n$  are closely related to the rill / sheet erosion ratio, because with the increase in the slope steepness, rill erosion tends to predominate over sheet erosion. The method by Moore and Burch (1986) and Moore and Wilson (1993) uses a rill / sheet erosion of 1.5 (rill erosion prevailing) that yields  $m = 0.4$  and  $n = 1.3$ , so eqs. 5.16, 5.17 and 5.18 are rewritten:

$$S = \left( \frac{\sin \beta}{0.09} \right)^{1.3} \quad [\text{eq. 5.19}]$$

$$L = \left( \frac{U}{22.13} \right)^{0.4} \quad [\text{eq. 5.20}]$$

$$LS = \left( \frac{U}{22.13} \right)^{0.4} \left( \frac{\sin \beta}{0.09} \right)^{1.3} \quad [\text{eq. 5.21}]$$

Meanwhile Desmet and Govers (1996) consider a ratio of 2.58 and a  $m = 0.72$ .

The calculation of LS factor is directly implemented in the SAGA free software (Figure 6), and included in QGIS tools for SAGA. But obviously, LS factor can be computed steep by steep in ArcGIS, QGIS or SAGA through the commands sequence explained in Table 5, which is recommended for a greater control of the operations. For instance, the reclassification of flow accumulation layer in order to correct the L factor calculation has not implemented in the SAGA algorithm described in Table 6.

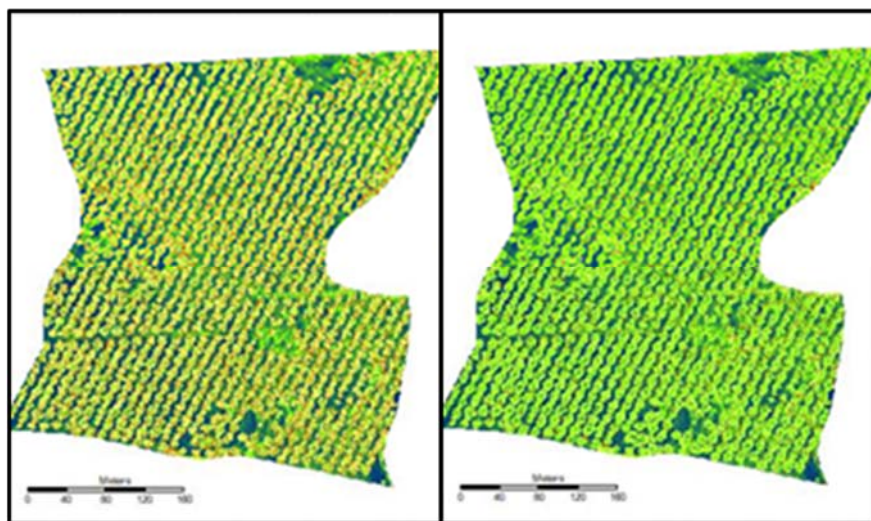


Figure 6: LS factor for The “La\_Isabelita\_with\_cover” obtained with the Moore and Burch (1986, left) and Desmet and Govers (1996, right) algorithms, at 1 m resolution (Table 5). LS factors for plots are calculated as the pixel average value of each polygon.



	Document:	D1.4. Handbook of protocols and methods		
	Author	UJAEN	Version	6
	Reference	D1.4	Date	24/03/2023

Table 5: GIS appraisal for LS calculation in ArcMap©

Pre-processing	
Inputs	• DEM
Tools	• Fill sink • Flow direction • Flow accumulation
Outputs	• Fill_DEM • fd_DEM • fac_DEM
S-FACTOR	
Inputs	• Fill_DEM
Tools	• Slope (degree) • Raster calculator (eq. 5.19)
Outputs	• Slope_fill • Rastercal_fill
L-FACTOR	
Inputs	• fac_DEM
Tools	• Reclass • Raster calculator (eq. 5.20)
Computational setups	• Reclassifying the fac_DEM grid in two classes: 0 – 250 m = 1; 250 m – max. = 0.
Outputs	• Reclass_fac • Rastercal_fac
LS-FACTOR	
Inputs	• Rastercal_fill • Rastercal_fac
Tools	• Raster calculator (eq. 5.21)
Outputs	• Rastercal_LS-Factor

Table 6: GIS appraisal for LS calculation in SAGA.

Pre-processing	
Inputs	• DEM
Tools	• Mosaicking • Fill sinks (Wang Liu) • Slope, Aspect, Curvature • Extended neighbourhoods – catchment areas (parallel)
Outputs	• Mosaic • Filled DEM • Slope • Catchment area
LS-FACTOR	
Inputs	• Slope • Catchment Area
Tools	• LS Factor
Outputs	• LS Factor

	Document:	D1.4. Handbook of protocols and methods		
	Author	UJAEN	Version	6
	Reference	D1.4	Date	24/03/2023

From the output rasters (LS Factor, Rastercal\_LS-Factor), factors are calculated as the pixel average value of each polygon delimiting each plots.

We have tested both (and other) algorithms in DEM of different resolutions in a selected site in the Municipality of Estepa (south of Spain), “La\_Isabelita” , where there are two adjacent plots, one with cover crops (CC, 14 ha.) and one without cover crops (NC, 12 ha.). The following result for the LS-factor was obtained (Table 7):

**Table 7. LS factors estimated from different calculation algorithms and grid resolutions.**

DEM resolution	Moore et al.(1993) SAGA	Desmet & Govers (1996) SAGA	Boehner & Selige (2006) SAGA	Moore and Burch (1986) ARCGIS
La Isabelita CC				
1 m (LiDAR)	4.23	2.80	5.58	2.45
5 m	1.26	0.81	0.92	0.98
25 m	1.81	1.09	1.44	1.01
La Isabelita NC				
1 m (LiDAR)	3.46	2.57	4.35	1.36
5 m	0.85	0.59	0.61	0.66
25 m	1.18	0.74	0.92	0.67


These preliminary results showed LS values rather homogeneous between the 5 and 25 m DEMs, regardless of the algorithm applied, with a clear tendency to increase the LS factor in the 1 m resolution DEM. In addition, LS factor obtained from LiDAR also showed larger variability between the different algorithms applied.

As mentioned above, for SUSTAINOLIVE plots it is recommended to use the highest resolution DEM available, preferably 1 m, because lower resolution DEM can underestimate soil losses. However, if high resolution 1 m DEM were not available, these result support the use of 25 m resolution DEM because they demonstrated few differences with 5 m DEM. In these cases, (DEM of 5 and 25 m), the procedure used to LS estimation gives similar results, but in the case of DEM of 1 m, the adequate procedure is the step-by-step application of Moore and Burch method, both in ArcGIS or QGIS. In the next section, some indications will be given on how to obtain useful information for calculating the LS factor.

## DEM and topographic products

There are world DEMs or DTMs available for downloading, being the most known SRTM (Shuttle Radar Topographic Mission), with a resolution between 30-90 m depending of the zone of the world. Data are available in: [https://dds.cr.usgs.gov/srtm/version2\\_1/](https://dds.cr.usgs.gov/srtm/version2_1/). This DEM is



	Document:	D1.4. Handbook of protocols and methods		
	Author	UJAEN	Version	6
	Reference	D1.4	Date	24/03/2023

also accessible with the STRM plugging of QGIS. However, this DEM and others (World DEM of TerraSAR-TanDEM-X, European DEM of the Global Land Monitoring Service, etc.) have not enough resolution for the purpose of this project. Thus, it is more convenient to use national or regional DEMs of the different countries:

**Spain** In the IGN download service <http://centrodedescargas.cnig.es/CentroDescargas/> different products with different resolutions are available: LiDAR coverages (1 from 2008 to 2015 and 2 from 2015 to actuality), MDT02, MDS05, MDT05, MDT25 and MDT200. Topographic maps and vectorial databases at scales 1:25.000 and 1:50.000 are also accessible.

Besides, in the download service of Institute Statistical and Cartographic of Andalusia <http://www.juntadeandalucia.es/institutodeestadisticaycartografia/lineav2/web/>, a DTM with resolution of 10 m is available. Topographic maps and vectorial databases at 1:10.000 and 1:5.000 (urban zones) are also accessible.

**Portugal:** DTMs with resolution of 50 m and 25 are available for the whole country (continental), and others with lower resolution for some territories in the National System of Geographical Information (SNIG): <https://snig.dgterritorio.gov.pt/> Besides, topographic maps and vector databases are also accessible in the same service.


**Italy:** DTMs with resolution of 20 m are available in the Geographic Military Institute (IGMI), <https://www.igmi.org/en/Home> , under payment (75€ for square of 10x10 km). The national geoportal has WFS and WCS services for downloading data: <http://www.pcn.minambiente.it/mattm/servizio-di-scaricamento-wcs/>

**Greece:** DTMs with resolution of 30-100 m are accessible in the portal of the Hellenic Military Geographical Service: [http://web.gys.gr/GeoSearch\\_EN/](http://web.gys.gr/GeoSearch_EN/) . Topographic maps at 1:50.000 scale are also available in digital format in the same portal.

**Morocco:** Topographic maps and vectorial databases are available under payment at scales 1:25.000-1:200.000 in the National Agency for Conservation of Earth, Cadastre and Cartography: <https://www.ancfcc.gov.ma/>

**Tunisia:** There is not information about DEM.

As an option, a complete LS-factor map is freely available from the European Soil Data Center (ESDAC) in the following link:

	Document:	D1.4. Handbook of protocols and methods		
	Author	UJAEN	Version	6
	Reference	D1.4	Date	24/03/2023

<https://esdac.jrc.ec.europa.eu/content/rainfall-erosivity-european-union-and-switzerland>

Downloadable datasets include a relatively high-resolution grid (25 m resolution), but it is recommended to work at higher resolutions when dealing with olive plots. The calculation method used is based on the Desmet and Govers algorithm implemented in SAGA, on the basis of a MDE of 25 m of resolution. Technical and methodological details of the LS-factor map of Europe can be found in at Panagos et al. (2015c).


## 5.6. C Factor

### Calculation

The soil erosion cover-management factor is one of most decisive USLE factors as it can reduce erosion by a factor of 1000. The C factor from RUSLE (Renard et al., 1997) summarizes a series of sub-factors (prior land-use, canopy cover, surface cover, surface roughness and soil moisture) that make quite complicated and time-consuming its application to plots of which there is no deep knowledge (Panagos et al., 2015d).

For this reason, although the RUSLE has been applied in olive groves (G ó mez et al., 2003), for the SUSTAINOLIVE plots the simplest original-USLE method developed by Wischmeier and Smith (1965) in the “handbook N 282” is recommended. This takes into account mostly the equivalent of the RUSLE canopy cover sub-factor, dealing with three parameters: i) the fraction of soil surface covered by a canopy, ii) the fraction of soil surface covered by cover crops, and iii) the average of the distance that raindrops fall after striking the canopy (related with the average canopy height). Table 8 groups and summarizes the average C values for different growth periods and cultivation practices, in this case for a non-herbaceous crop such as the olive grove (it can be consulted in Porta and Lopez-Acebedo, 2005).

Nevertheless, whether the C-RUSLE or C-USLE is applied, the goodness of the estimation depends largely on the methodological efficacy in the estimation of the air coverage (canopy cover and cover crops percentages). A simple but effective method to find the factor C is by remote sensing. Various RGB & NIR band-based indices have been applied to automatically estimate the percentages of canopy (trees) cover, herbaceous cover and bare soil in olive groves, yielding satisfactory results (Pe a-Barragan et al., 2004). Remote sensing is preferred over other kind of methods to define soil covers, as field surveys or agricultural statistics, owing to its higher precision, particularly when working at high scales (Benavidez et al., 2018). It should be noted, furthermore, that some remote sensing indices can be discriminate the bare soil from the herbaceous cover, both in summer (when grasses are

	Document:	D1.4. Handbook of protocols and methods		
	Author	UJAEN	Version	6
	Reference	D1.4	Date	24/03/2023

desiccated) and spring (when grasses are living), so the % of ground cover would also taking into account the Surface cover sub-factor from RUSLE (Table 8).


**Table 8: C-Factors for SUSTAINOLIVE olive grove plots (Wischmeier and Smith, 1965, table for grasses, scrubs and woodlands). Canopy is, here, the olive trees.**

Type and height of canopy cover		% of soil covered by cover crops <sup>1</sup>					
Canopy	% Cover	0	20	40	60	80	95
High cover not appreciable	-	0.45	0.20	0.10	0.042	0.013	0.003
High grasses or scrubs with a drop height of 45 cm	25	0.36	0.17	0.09	0.038	0.013	0.003
	50	0.26	0.13	0.07	0.035	0.012	0.003
	75	0.17	0.10	0.06	0.032	0.011	0.003
Scrubs with a drop height of about 165 cm	25	0.40	0.18	0.09	0.040	0.013	0.003
	50	0.34	0.16	0.08	0.038	0.012	0.003
	75	0.28	0.14	0.08	0.036	0.012	0.003
Trees without low height vegetation. Drop height of 3.30 m	25	0.42	0.19	0.10	0.041	0.013	0.003
	50	0.39	0.18	0.09	0.040	0.013	0.003
	75	0.36	0.17	0.09	0.039	0.012	0.003

<sup>1</sup>If a specific remote sensing procedure is applied, this would also include % of soil covered by residues (surface cover RUSLE sub-factor)

In the ideal case, the estimation of C-factor in olive groves would involve the analysis of series of historical images of at least 20 years with averaging the interannual variability from, at least, the wet (spring) and dry (summer) seasons of the year (G ó mez et al., 2003). However, as will be discussed below, it is not easy to obtain image sets that simultaneously combine high temporal (historical and seasonal series) and spatial resolutions (around 1 m or less). One solution would be to take three images from those available in the long-term average: One of the driest year, another of the wettest, and another of the year with annual rainfall closer to the long-term average ( “typical year” ). If possible, these three images should be taken at the same season, coinciding with the presence of herbaceous cover (avoiding summer). The analysis will be reduced, therefore, to three images, establishing an average value of factor C. In the case of plots without herbaceous cover, we can assume that is null thorough any year and season, so it would suffice to analyse one single image from the long-term average.

In this protocol therefore we recommended to apply the simple table of Wischmeier and Smith (1965) in combination with the precision and robustness of the Pe a-Barragan remote

	Document:	D1.4. Handbook of protocols and methods		
	Author	UJAEN	Version	6
	Reference	D1.4	Date	24/03/2023


sensing method. In the next section, the GIS method for estimating the parameters to apply Table 8 is explained.

### Image classification method to estimate ground cover in olive groves

C Factor is one the main factors and most influential of the USLE equations. Traditionally, this factor has been assessed of different ways depending on the study scale. Then, in experimental plots this factor has been estimated from the measurement of several parameters such as the percentage of vegetation cover (from bare soil to complete vegetation cover), the plants height, the root development, etc., in a time-consuming procedure (Gomez et al., 2003). Meanwhile, in regional scales (i.e European level) C-factor layer is established by using lookup tables to assign C-factor values to the land cover classes in the study area (Panagos et al., 2015d). Land use is derived from thematic maps elaborated by means of aerial/space images interpretation (photointerpretation) or digital classification (such as in Corine Landcover project), but this procedure requires a deep knowledge of the employed cartographies when using different land-cover classifications, so normally the lookup-table-based approach entails a hard and tedious harmonization work (Benavidez et al., 2018).

However, at the intermediate level considered in this project, that is farm plot, the proposed methodology is based on the analysis of orthophotographs or orthoimages of submetric resolution. In most countries (*Spain, Portugal, Italy, Morocco*, etc.) there are aerial photographs or orthophotographs with the required resolution, in some cases accessible via web (*Italy*) and even free (*Spain and Portugal*). Moreover, in some cases such as *Spain*, there are multitemporal series of orthophotographs from 1956 with a periodicity of 2-3 years in the last decades. Orthophotograph of the last years (from 2004 to actuality) are color (RGB) images, and in some cases include a NIR band. In addition, satellites images from commercial programs are available with the required resolution (0.3-0.5 m), such as World View or Pleiades, although under payment. The advantage is the wider multitemporal character of the images and also more multispectral bands incorporated, regarding the orthoimages in which this character is limited and most images are taken in summer conditions.

Thus, the methodology for C factor estimation starts with the analysis of orthophotographs/ orthoimages that leads to a land classification, which at this scale is a feature classification more than a land use classification. Then from the classification, an estimation of C factor based on the areal percentage of each class and their characteristics (height) is made as explain before (Wischmeier and Smith, 1965; Panagos et al., 2015d).

	Document:	D1.4. Handbook of protocols and methods		
	Author	UJAEN	Version	6
	Reference	D1.4	Date	24/03/2023


This analysis can be complemented with the use of satellite images of lower resolution such as those corresponding to Sentinel (Drusche et al., 2012; Frampton et al., 2013) and Landsat programs (Knight et al., 2014; Morfitt et al., 2015), whose data are free available in download services. The resolution of these images (Sentinel-2 is 10-60 m and Landsat is 30 m) is not enough to distinguish the features and land cover required. But the average values of reflectance in the different bands (13 and 10, respectively, in the visible-near infrared-short wave infrared, Vis-NIR-SWIR, spectrum) lead to a characterization of plots than can be correlated to the results obtained with the high resolution images. Moreover, these programs offer multitemporal information, that in the case of Landsat reach several decades (from the first 1980).

A simple classification method based on a pixel-based and supervised approach is proposed. It is a pixel-based and not an object-based classification (Blaschke, 2010), although finally some individual features such as olive trees are extracted, in addition to other land uses (not individual) such as grass cover and bare soil. The good results obtained in the tests made in some pilot areas do not lead to the use of more sophisticated approaches such as object-based classifications or some pixel-based such as those of deep learning (neural networks) (Zhang et al., 2016). Thus, classic statistical methods such as maximum probability and machine learning such as random forest are enough to get good results. Other approaches such as unsupervised classifications and those based on single bands of the multispectral images and indexes have been explored and can be used as alternative to the supervised classification methods.

### Image acquisition and pre-processing

First, the multispectral image has to be acquired, by means of downloading from a public service or by purchasing to a commercial company. The multispectral image can be organized in a unique file or in several files (usually one for each spectral band). Depending on the software employed and the operation applied, the image can be required in one of another type organization, but the software usually incorporate tools to transform one in to another.

The next step is to boating a spatial sample or cut of the study area. The acquired image usually extends for a larger area and it is necessary to focus the analysis in the study area. For it, the software both commercial (ArcGIS, Envi, etc.) or free (QGIS, SNAP) also include different tools to spatial sampling.

	Document:	D1.4. Handbook of protocols and methods		
	Author	UJAEN	Version	6
	Reference	D1.4	Date	24/03/2023

Once the images are open and sampled in the software, it is convenient to visualize them in colour compositions, both real colour and false colour to have a first approach to the study area. Real colour assigns a RGB palette to the corresponding bands of the multispectral image and false colour assigns this palette to other combination of bands, including infrared (NIR and SWIR) bands. In some cases, operations of contrast adjustment (image histogram) or even filter application can be necessary. The software used also provide them.

### Image classification

Supervised image classification comprises at least three phases: i) training, ii) separability analysis, and iii) pixel assignment to the different classes (Richards, 2013). Again, the different software (ArcGIS, Envi, QGIS, SNAP ...) include tools to make these operations.

Training involves the creation of sampling points or polygons in which statistic of the different bands will be calculated. An enough number of pixel from each class has to be sampled from the image. In the analysis proposed, at least three classes have to be considered: olive trees, vegetation cover (grass, bush, scrubs) and bare soil; additional classes such as water, houses roads and other constructions, etc., can be considered if they are relevant. The point or polygons can be created with the general tools to edit vector layer of the software or specific tools such as in ArcGIS, SNAP, etc. (figure 7).

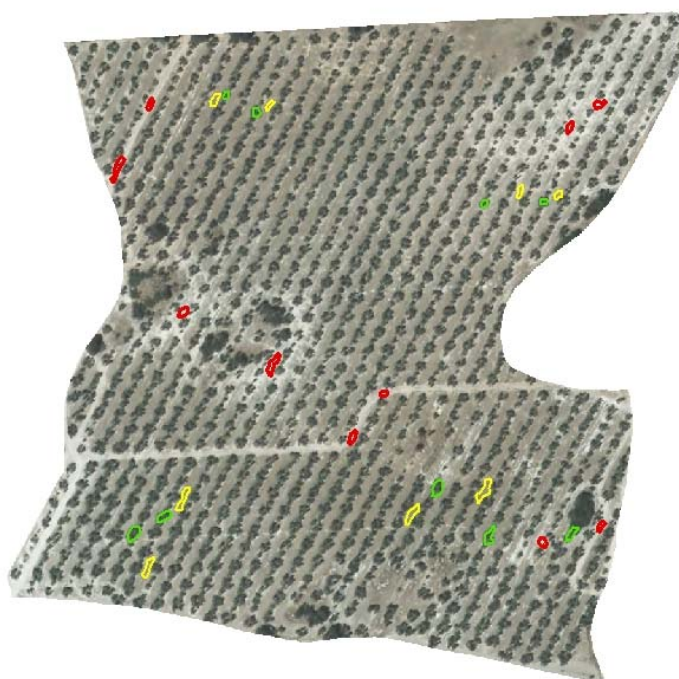



Figure 7: Multispectral image and training polygons in “La\_Isabelita\_with\_cover” farm plot.

Separability analysis consists in numerical or graphical comparison of the spectral signatures of the different classes considered. Statistical calculation (mean or average,



	Document:	D1.4. Handbook of protocols and methods		
	Author	UJAEN	Version	6
	Reference	D1.4	Date	24/03/2023

maximum, minimum, standard deviation, etc.) of each band in each class considered is the base of this analysis. Numerical or graphical comparison of average values (and also  $\pm$  maximum/minimum or the standard deviation) allows to know if the classes considered are separable or not. These graphics, known as signature diagrams (Figure 8), are usually enough to establish if the different classes are separable. Software usually allows to calculate statistics and even make the graphics, but anyway from the statistics the graphics can be drawn in spreadsheet such as Excel or Google sheets. Additionally, some software allows to calculate separability coefficients (Euclidean distance, statistical divergence, Jeffries-Matusita distance, etc.).

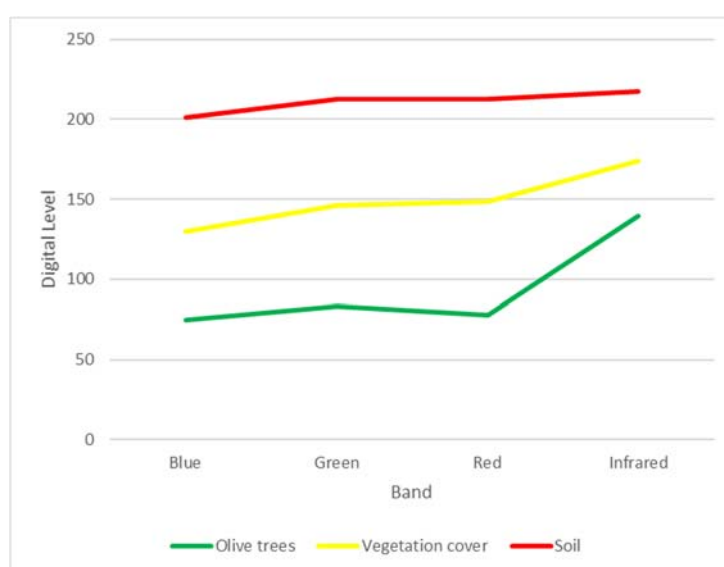



Figure 8: Signature diagram from "La\_Isabelita\_with\_cover" farm plot.

Finally, the assignment of pixels to the different classes (classification) is addressed. There are many approaches to do it, some of them based on classical statistical techniques such as minimum distance (from pixel values in each band to average values of each band in the different classes) or maximum probability to belong to a given class (Richards, 2013). Moreover, there are methods based on machine learning (decision trees, random forest, support vector machines, etc.), or even in deep learning (neural networks) (Camp-Valls, 2009; Zhang et al., 2016). For the purposes of this study and the number and nature of the classes considered, the recommendation is to use methods of easy application and availability in the software such as maximum probability and random forest. In the maximum probability method, pixels are assigned to this class with the highest probability, considering a normal distribution function (Sisodia et al., 2014). Random forest is a machine learning based on decision trees. In decision trees the pixels are assigned to a class from basic rules, for instance to have a given value of reflectance (higher, lower or within an

	Document:	D1.4. Handbook of protocols and methods		
	Author	UJAEN	Version	6
	Reference	D1.4	Date	24/03/2023

interval) in a band, other value in other bands, and so on. Random forest use many decision trees developed from different subsamples of pixels and assigns the pixels to different classes based in the rules established in each tree (Belgiu and Dragur, 2016). Finally, the pixels are definitively assigned to those classes in which they are assigned in the majority of the trees (it is like if each tree votes for each pixel to be assigned to one class and the pixel is assigned to the class with more votes). Figure 9 shows the raster layer resulting from image classification of Figure 7. Classification yield the two surface cover inputs relevant for C-factor calculation (olive trees, in green, 50% of plot surface, and cover crops, in yellow, 36% of the plot surface), while canopy height can be estimated from field observations.

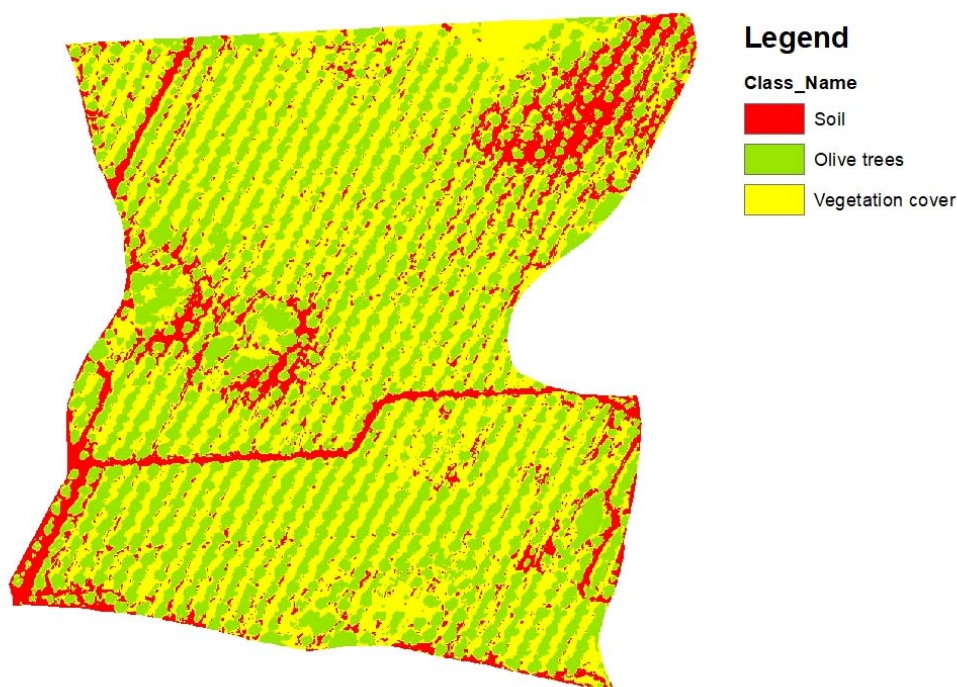



Figure 9. Classified image of the “La\_Isabelita\_with\_cover” farm plot. % Surface of each class can be easily obtained from the attribute table of the classified raster.

### Classification from bands and indexes

Other approach than can be addressed in the image classification or segmentation based on the original bands of the multispectral image or index calculations.

Multispectral image has at least three bands (RGB). This is the case of orthophotographs, although in the last years, photogrammetric cameras on board of aerial platforms incorporate a NIR band. When satellite images are used four or more bands are considered:

	Document:	D1.4. Handbook of protocols and methods		
	Author	UJAEN	Version	6
	Reference	D1.4	Date	24/03/2023

Geoeye uses 4 bands (RGB-NIR); Pleiades uses 5 bands between visible and NIR; Worldview-2 uses 8 bands between visible and NIR, etc.

From these individual bands, a classification can be made using different classification methods of variables, such as natural breaks, equal interval, quantiles, etc. The more appropriate is the natural breaks that evaluates the image-band histogram and find break points that can correspond to class limits. Usually software allows to classify bands (as layers) automatically according these methods. Nevertheless, depending on the band and the study area this classification can work or not to separate the classes considered (olives, vegetation cover and bare soil). Then, in many cases, it is necessary to change manually the limits of intervals and to observe the results visually (test and error). The test made in pilot areas show acceptable results in some bands (visible and NIR) after manual classifications.

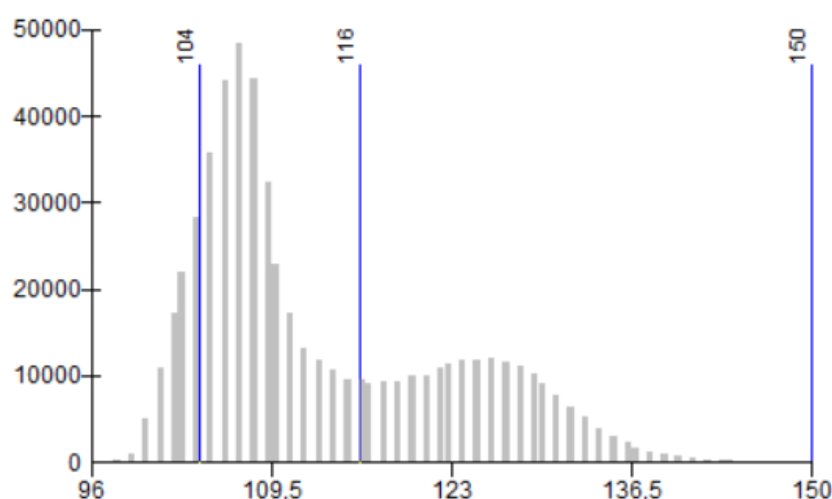



Figure 10. Image histogram and classification (own elaboration).

Index calculations allows to combine bands in an easy way. Some of these indexes are very used in fact vegetation indexes such as NDVI are probably the most extended approach analysis of remote sensing images (Rouse et al., 1974; Bannari et al., 1995). For the purposes of this work, in which three classes are considered, two of them corresponding to vegetation (olive trees and vegetation cover) and the remain class not (bare soil), vegetation index can have a certain confusion between the two first class. Then, the results do not improve those obtained in the classification from original bands, but it can be recommendable in cases where shadows appear (produced by olive trees over bare soil or vegetation cover). Vegetation index can reduce the confusion introduced by shadows in the reflectance of the different covers.

	Document:	D1.4. Handbook of protocols and methods		
	Author	UJAEN	Version	6
	Reference	D1.4	Date	24/03/2023

There are a lot of vegetation index and other such as moisture or water index that can be used. Thus, the most known and used index are NDVI (Normalized Difference Vegetation Index), that responds to the expression (Rouse et al., 1974; Bannari et al., 1995):

$$NDVI = \frac{\rho_{NIR} - \rho_{Red}}{\rho_{NIR} + \rho_{Red}} \quad [\text{eq. 5.22}]$$

Where:  $\rho_{NIR}$  and  $\rho_{Red}$  are the reflectance (or the digital level, in the case of orthophotographs).

This index, as most of the vegetation index uses the contrast in NIR and Red bands between vegetation areas (in which the index are high) and non-vegetated areas (where the index are low, close to 0, and even negative in water surfaces). This index, as other normalized indexes, ranges from -1 to 1. Thus, in addition to NDVI index with NIR and Red bands, other combinations can be applied such as NIR with the blue and green bands, and especially the green band with the blue and red band. This last option is very interesting when NIR band is not available, using the green band as NIR.

Other vegetation indexes can be tested such as (Chamard et al., 1991; Kaufman and Tanre, 1992; Bannari et al., 1995), such as ARVI (Atmospherically Resistant Vegetation Index), GCI (Green Coverage Index), SIPI (Structure Insensitive Pigment Index):

$$ARVI = \frac{\rho_{NIR} - 2\rho_{Red} + \rho_{Blue}}{\rho_{NIR} + 2\rho_{Red} + \rho_{Blue}} \quad [\text{eq. 5.23}]$$


$$GCI = \frac{\rho_{NIR}}{\rho_{Green}} - 1 \quad [\text{eq. 5.24}]$$

$$SIPI = \frac{\rho_{NIR} - \rho_{Blue}}{\rho_{NIR} - \rho_{Red}} \quad [\text{eq. 5.25}]$$

And when the NIR band is not available, an index that gives good results is the GLI (Green Leaf Index):

$$GLI = \frac{(\rho_{Green} - \rho_{Red}) + (\rho_{Green} - \rho_{Blue})}{2\rho_{Green} + \rho_{Red} + \rho_{Blue}} \quad [\text{eq. 5.26}]$$

Once the indexes are calculated, classification methods as those applied to original bands can be used (especially natural breaks or manual classification) to segment the image in the classes considered.

	Document:	D1.4. Handbook of protocols and methods		
	Author	UJAEN	Version	6
	Reference	D1.4	Date	24/03/2023

## Validation of classification

Once the image has been classified, it is convenient a certain quality control or validation. For it, besides the visual methods, some approaches such as confusion matrix are very frequently used. Confusion matrix (Congalton, 1991) compares the classification results with a ground-truth. In this type of analysis, in which usually there is not a previous map that can be used as ground-truth, it is necessary to obtain a sample of pixels that are assumed as this.

The validation sample can be obtained is a similar way as the analysis sample, by means of digitalization of point or polygons. Regarding this, it is very important that the validation sample has to be absolutely independent (different) of the analysis sample. Once the validation sample (ground-truth) has been created, the next step is the cross-correlation analysis between the classification and the ground-truth. Software incorporate different tools to do it, some of the them allowing to calculate not only the cross-table but the indexes (index of agreement, omission and commission errors, overall accuracy, etc.). When only the table is given, this table can be opened in a spreadsheet to calculate the table indexes. Index of agreement is defined as the area of the well-classified pixels (coincidence between the classification and the ground-truth) regarding the total of pixels (Congalton, 1991).

Commission and omission errors are the pixel not well-classified, from the point of view of the classes of the classification or the ground truth, respectively (Table 9).

Table 9: Image classification validation.

		Ground-truth			Commission Error	User risk
		1	2	3		
Classification	1	a11	a12	a13	$\sum a_{1i}$	$\sum a_{1i} / A$
	2	a21	a22	a23	$\sum a_{2i}$	$\sum a_{2i} / A$
	3	a31	a32	a33	$\sum a_{3i}$	$\sum a_{3i} / A$
Omission error		$\sum a_{i1}$	$\sum a_{i2}$	$\sum a_{i3}$	Agreement Index = $\sum a_{ii} / A$	
Producer risk (%)		$\sum a_{i1} / A$	$\sum a_{i2} / A$	$\sum a_{i3} / A$		

## Unsupervised classifications of single original bands

The simplest procedure to classify images is a unsupervised reclassification of each original band (RGB or RGB + NIR) through natural breaks (Table 10).


	Document:	D1.4. Handbook of protocols and methods		
	Author	UJAEN	Version	6
	Reference	D1.4	Date	24/03/2023

Table 10: GIS appraisal for C-factor calculation in *ArcMap* © by means of a single unsupervised procedure.

Inputs	<ul style="list-style-type: none"> <li>• RGB or RGB + NIR image</li> <li>• R-band raster</li> <li>• G-band raster</li> <li>• B-band raster</li> <li>• NIR-band raster</li> </ul>
Tools	<ul style="list-style-type: none"> <li>• Zone division (Spatial analyst → Reclassify)</li> </ul>
Computational setup	<ul style="list-style-type: none"> <li>• (For each input raster)</li> <li>• Number of output zones: 3</li> <li>• Method: natural breaks</li> </ul>
Outputs	<ul style="list-style-type: none"> <li>• Reclass_R-band</li> <li>• Reclass_G-band</li> <li>• Reclass_R-band</li> <li>• Reclass_NIR-band</li> </ul>

As can be appreciated visually in Figure 11, the output raster of the R-band classification (Reclass\_R-band), closely coincides with that obtained by supervised classification. Cover percentages were also similar (olive trees, in blue, 50%; cover crops, in green, 39% of the plot surface). Other bands can be tested and roughly and visually estimate which one generates the best classification.

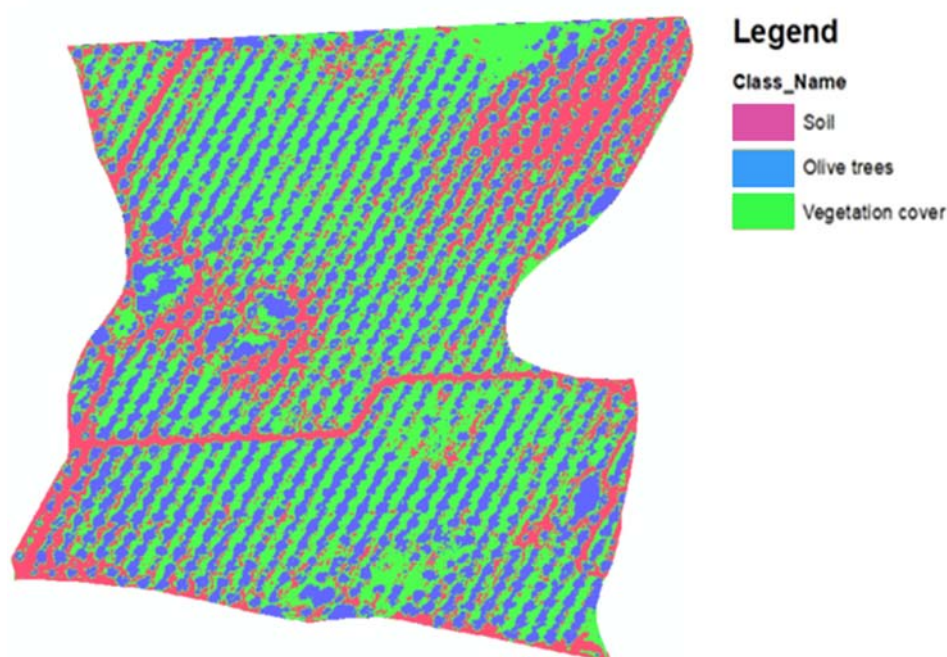



Figure 11. Unsupervised classified image of the “La\_Isabelita\_with\_cover” farm plot of the R-band. % Surface of each class can be easily obtained from the attribute table of the classified raster.



	Document:	D1.4. Handbook of protocols and methods		
	Author	UJAEN	Version	6
	Reference	D1.4	Date	24/03/2023

We suggest you to apply this last method for a first C-factor estimation and, if necessary, send the images for the supervised classification to those responsible for this task (Julio Calero and Tomas Fernandez, UJA).

### Information sources for cover-management factor estimation

To applied the remote sensing protocol, the following geoinformation is necessary.

#### i) Aerial orthophotographs

Orthophotographs or orthoimages preferably of 4 bands (RGG-NIR). Alternately 3 bands image are used if 4 bands are not available. The spatial resolution will be of about 0.5 m (maximum 1 m). If orthophotographs are not available, aerial phototographs could be used but they would require orthorectification (photogrammetric processing).

As orientation, the following sources can be consulted in the different countries:

**Spain:** At least two sources for orthoimages downloading, both on-line and free:

- Download center of IGN-CNIG (Centro de descargas Instituto Geogr á fico Nacional-Centro Nacional de Informaci ó n Geogr á fica:

<http://centrodedescargas.cnig.es/CentroDescargas/>

Orthoimages corresponding to a sheet of National Topographic Map (1:50.000), with a resolution of 0.5 m and 3 bands (RGB). Periodicity: 2-3 years in the last 15 years (from 2004, National Plan of Orthophotograph, PNOA).

- Environmental Information Network of Andalusia (Red de Informaci ó n Ambiental de Andalusia, REDIAM) - Statistical and Cartographic Instituto of Andalusia (Instituto de Estadística y Cartografía de Andaluc í a, IECA):

<http://www.juntadeandalucia.es/institutodeestadisticaycartografia/lineav2/web/>


Othoimages corresponding to a sheet of Topographic Map of Andalusia (1:10.000) with a resolution of 0.5 m and 4 bands (RGB-NIR). Periodicity of 2-3 years, in the last years (but the 4 bands are only available in the last cover of 2016). The source is the same as before (IGN-CNIG), photographs of the corresponding national aerial flight, but here the 4 bands are available. Photographs are available in the corresponding sites (photo libraries):

<http://fototeca.cnig.es/> and

<http://www.juntadeandalucia.es/institutodeestadisticaycartografia/fototeca/>

**Portugal:** Orthoimages with resolution of 0.25 m and 4 bands (RGB-NIR), corresponding to 2018. They are free for downloading in the National System of Geographical Information (Sistema Nacional de Informa ao Geogr á fica, SNIG):

<https://snig.dgterritorio.gov.pt/>

	Document:	D1.4. Handbook of protocols and methods		
	Author	UJAEN	Version	6
	Reference	D1.4	Date	24/03/2023

There are other orthoimages corresponding to previous years (2015, 2012, 2010, 2007, 1995) with resolutions of 0.5-1 m (RGB-NIR, RGB, panchromatic), some of them open to downloading, and other regional and local products at different resolutions.

**Italy:** Geographic Institute Military of Italia (Istituto Geografico Militare, IGMI) has aerial (analogic) from 1927 to 2010, most of them analogic and panchromatic, but there are also colour and false colour (with NIR band) images and orthoimages. They can be consulted and ordered by payment (100 €) in:

[https://www.igmi.org/en/geoprodotti#b\\_start=0](https://www.igmi.org/en/geoprodotti#b_start=0)

Other source is the National Geoportal (Geoportale Nazionale), with visualizers and OGC services of catalogue (CSW), query and visualization (WMS) and data downloading (WFS and WCS): <http://www.pcn.minambiente.it/mattm/>.

**Greece:** The Hellenic Military Geographical Service has aerial photographs from different years (historical), both panchromatic and colour (RGB) that can be consulted in the portal:

[http://web.gys.gr/GeoSearch\\_EN/](http://web.gys.gr/GeoSearch_EN/)

**Morocco:** The National Agency for Conservation of Earth, Cadastre and Cartography (Agence Nationale de la Conservation Fonci è re, du Cadastre et de la Cartographie, ANCFCC) offers different services on-line, among them aerial photographs and orthophotographs, both panchromatic and colour, under payment The information can be consulted in:

<https://www.ancfcc.gov.ma/>


**Tunisia:** There is not information about images and orthoimages.

## ii) Satellite images

There are many sources of satellite images, both open/free and an under payment. Free sources can be found in some of the national agencies before mentioned, where it is possible to download satellite images of different resolution and dates. However, it is more convenient to use services of direct downloading. Although there are several services, for the purposes of this project, we are focusing in the following:

-Copernicus Open Access Hub: <https://scihub.copernicus.eu/>

It is the service to open access of the Copernicus program of the European Commission and the European Space Agency (ESA), specifically for the series of Sentinel satellites. At the moment, data available are for Sentinel-1 (radar, active sensor), Sentinel-2 (with a multispectral sensor of middle-high resolution) and Sentinel 3 (with several sensors, among

	Document:	D1.4. Handbook of protocols and methods		
	Author	UJAEN	Version	6
	Reference	D1.4	Date	24/03/2023

them a multispectral of low resolution and a thermal sensor). For this project, the appropriate data are those from Sentinel-2, with 13 bands between visible, near infrared (NIR) and short-wave or middle infrared (SWIR or MIR), and resolution ranging between 10, 20 and 60 m. Temporal resolution is 5 days. Images are available from 2015.

-Earth-Explorer: <https://earthexplorer.usgs.gov/>

It is the service of Geological Survey for image downloading of Landsat project (NASA), although images of other projects such as NOAA, Hyperion or Terra (ASTER, MODIS, etc.) are available. Landsat-8 carries two sensors: OLCI, a multispectral of 8 bands between visible-NIR-SWIR with resolution of 30 m, as well as a panchromatic band with resolution of 15 m; and TIRS, a thermal sensor with 2 bands and 100 m of resolution. Temporal resolution of 15 days. Images are available from 2013. Previous satellites of Landsat project such as Landsat 5 and Landsat 7, of similar properties to Landsat 8, are available in the service, from 1980 to 2011.

In addition to these programs, images from commercial satellites can be a good alternative, especially in the cases in which orthophotographs are not available. There are several commercial programs, but the most interesting for our purposes are:

- Worldview (Digital Globe) offers different type of products from its different satellites (Worldview-1, Worldview-2, Worldview-3 and the out-of-service Worldview-4, Quickbird and Geoeye-1). The spatial resolution range from 0.3-0.5 m in panchromatic and 1.2-2 m in multispectral (Vis-NIR). The spectral resolution (multispectral) ranges from 4 bands to 8 bands in visible-NIR region, and additional bands in SWIR (in this case with lower resolutions). The images are on-demand with variable prices (24-29 \$ / km<sup>2</sup>, as reference), but there are archive images with lower prices, from 1999).

-


- Pleiades (Airbus) offers images with spatial resolution of 0.5 m in panchromatic and 2 m in multispectral, the last with 5 bands between visible and NIR. The images are on-demand (with reference prices of 26 \$ / km<sup>2</sup>), but there are also archive images from 2011.

To consult images properties and reference prices:

<http://www.landinfo.com/espanol/satellite-imagery-pricing.html>

As with other factors, C-factor layer is freely available from the European Soil Data Center (ESDAC) in the following link:

<https://esdac.jrc.ec.europa.eu/content/cover-management-factor-c-factor-eu>

	Document:	D1.4. Handbook of protocols and methods		
	Author	UJAEN	Version	6
	Reference	D1.4	Date	24/03/2023

Reference values for olive groves vary between 0.1 and 0.3 for plots without cover, and between 0.07 and 0.35 in the case of associated cover crops. Technical and methodological details of the C-factor map of Europe can be found in at Panagos et al. (2015d).

In the “La\_Isabelita” site in Spain, we probed C-factor average values from the European map with those stabilised by remote sensing and image classification. We obtained the next results (Table 11):

**Table 11: C-Factors from ESDAC and applying the method explained in this work.**

Olive grove plot	Remote sensing & Image classification <sup>1</sup>	European C-Factor 100 m res. grid <sup>2</sup>
La Isabelita with cover crops	0.08	0.22
La Isabelita without cover crops	0.16	0.23

<sup>1</sup> 0.45 m ortophotograph (RGB & NIR) (May, 2018)

These preliminary results show very little variability between adjacent plots when using the ESDAC grid. We believe this is mainly due to the relatively-lower (for the purposes of SUSTAINOLIVE) resolution of the grid, so we discouraged their use in SUSTAINOLIVE plots.

## 5.7. P Factor

The last of the factors considered in USLE is the factor support practices. This factor takes into account all those aspects of management that can be considered independent of the cover management factor (surface cover sub-factor, canopy cover sub-factor). Specifically, Wischmeier and Smith (1965, 1979) recognize the following aspects: 1) Contouring ( $P_C$  sub-factor), 2) contour Strip-cropping ( $P_{SC}$  sub-factor) and 3) Terracing ( $P_T$  sub-factor).

$$P = P_C \times P_{SC} \times P_T \quad [\text{eq. 5.27}]$$

Panagos et al., (2015e), based on an extensive review, adapt the criteria of USLE to the European environment, simplifying some aspects of the original Weischmeier and Smith tables, such as the maximum slope length for each slope range. The P-factor values proposed by Panagos et al. are showed in Tables 12 ( $P_C$  sub-factor) and 13 ( $P_{SC}$  and  $P_T$  sub-factors).

Therefore, P-factor assessments in SUSTAINOLIVE plots would require field recognition of support practices, which can be improved by means of photointerpretation of aerial or satellite images of adequate resolution ( $\approx 1$  to 5 m) to count crop strips or terraces, while the calculation of the average slope can be done using the GIS tools exposed before.


	Document:	D1.4. Handbook of protocols and methods		
	Author	UJAEN	Version	6
	Reference	D1.4	Date	24/03/2023

Table 12: Values for the Contouring sub-factor (Panagos et al., 2015).

Slope (%)	P <sub>c</sub> (Contouring sub-factor)
9 – 12	0.60
13 – 16	0.70
17 – 20	0.80
21 – 25	0.90
> 25	0.95

Table 123: Values for the Contour Stripping and Terracing sub-factors (Panagos et al., 2015).

Number of terrain features	PCS (Contour Stripping sub-factor)	PT (Terracing sub-factor)
0	1.000	1.000
1	0.853	0.707
2	0.789	0.577
3	0.750	0.500
4	0.724	0.448
5	0.704	0.408
6	0.689	0.378
7	0.677	0.354
8	0.667	0.334
> 8	0.660	0.317

The P-factor layer is also freely available from the European Soil Data Center (ESDAC) in the following link:


<https://esdac.jrc.ec.europa.eu/themes/support-practices-factor>

This applies the methodology of Panagos et al. (2015d) and yield a 1000 m resolution grid of the P-factor. Comparing with our application of the model in the “La\_Isabelita” site, we obtained the next results (Table 14):

Table 14: P-Factors from ESDAC and applying the method explained in this work.

Olive grove plot	P-Factor from field survey <sup>1</sup>	P-Factor from ESDAC
La Isabelita with cover crops	0.660	0.853
La Isabelita without cover crops	1.000	0.853

<sup>1</sup> Photogrammetric measures for the P<sub>CS</sub> sub-factor over 0.45 m ortophotograph (May, 2018). Slope averages from 1 m-resolution LiDAR DEM.

	Document:	D1.4. Handbook of protocols and methods		
	Author	UJAEN	Version	6
	Reference	D1.4	Date	24/03/2023

As is easy to know, the higher resolution of the ESDAC grid averages and homogenizes the differences between the two adjacent plots, which are subjected of different management support practices (contouring and contour stripping in “La\_Isabelita” with cover crops; none in its equivalent). Therefore, we do not recommend the use of the European map to get this factor on Sustainolive farms.

## 5.8. Sediment yield in olive groves with GIS

### Assessment of sediment transport and connectivity


Various numerical approaches are available for estimating the sediment fluxes according to the spatial and temporal scales considered in the equations, as well as the number and types of processes. In small and medium size catchments, where surface hydrology is dominated by ephemeral overland flow processes and permanent streams do not exist or are limited on time to the occurrence of intense rainfall events and/or the rainy season, the estimation of sediment transport can be achieved by using simple approaches. In this protocol, we have selected one equation and one index, namely: I) the sediment delivery ratio (SDR; %) that is defined as the ratio between gross soil erosion and catchment sediment yield during a period, usually one year (Ferro and Porto, 2000); and II) the index of sediment connectivity (IC; dimensionless) that refers to the water-mediated transfer of runoff and sediment within or between the landscape compartments (Borselli et al., 2008). Thus, sediment connectivity (SC) is a concept implicit in the approach using the SDR because low values of SDR imply a lack of connectivity (structural and/or functional). The structural connectivity evaluates the properties (topography, surface roughness, soil properties, vegetation types and patterns, tillage practices, drainage network, etc.) of a system (catchment, landscape) that control the processes of water- and sediment-transfer, and the functional connectivity results from the way those processes operate (e.g., runoff and sediment delivery).

### Calculation of the SDR

In the SEdiment Delivery Distributed (SEDD) model proposed by Ferro and Porto (2000), the SEDD model discretizes the study area into morphological units and calculates the sediment delivery ratio (SDR) for each unit. However, the SDR can be estimated using simple or complex approaches. Some examples of the simple approach can be found in USA (Fernandez et al., 2003) and Spanish (López-Vicente et al., 2011) study areas. Examples of the complex approach can be found in Italian (Di Stefano and Ferro, 2017) and Spanish (Burguet et al., 2017) sites.

In this project, and owing to the limited available input data, we have chosen the simple option. In a spatially distributed approach, each cell or pixel  $i$  of the catchment is considered



	Document:	D1.4. Handbook of protocols and methods		
	Author	UJAEN	Version	6
	Reference	D1.4	Date	24/03/2023

to be a morphological unit (area of defined aspect, length, and steepness), and thus, the sediment delivery ratio for each cell  $i$  ( $SDR_i$ ) is the fraction of the gross soil loss from cell  $i$  that reaches a user-defined flow pathway. In our case, the target of the computation will be the outlet of each plot of sub-catchment that embraces the olive grove. The  $SDR_i$  is estimated as a function of the travel time ( $t_i$ , in hours) according to Eqs. 5.28, 5.29, and 5.30 (Ferro, 1997):


$$SDR_i = \exp(-\beta \cdot t_i) \quad [\text{eq. 5.28}]$$

$$t_i = \frac{1}{3600} \sum_{i=1}^{N_p} \frac{l_i}{v_i} \quad [\text{eq. 5.29}]$$

$$v_i = d_i \cdot s_i^{0.5} \quad [\text{eq. 5.30}]$$

where  $\beta$  is the catchment-specific parameter (which primarily depends on watershed morphology and is assumed constant for a given basin),  $N_p$  is the number of cells through which the flow path traverses from cell  $i$  to the channel,  $l_i$  (m) is the length of segment  $i$  in the flow path (and is equal to the side or diagonal of a cell, depending on the flow direction in the cell),  $v_i$  ( $\text{m s}^{-1}$ ) is the flow velocity,  $d_i$  ( $\text{m s}^{-1}$ ) is a coefficient that is a measure of surface roughness characteristics, and  $s_i$  ( $\text{m m}^{-1}$ ) is the slope gradient. Equation 5.30 is derived from Manning's equation and the  $d_i$  coefficient of each grid cell is influenced by land cover. This effect on the  $d_i$  coefficient is measured by the value of Manning's roughness coefficient and the hydraulic radius (Fu et al., 2006). In this project, a map of the  $d_i$  coefficient will be generated – a unique  $d_i$  value will be associated to each land use and land cover polygon – for each site to reflect the various patterns of runoff dynamics for each management practice, ground conditions and vegetation characteristics. The travel time,  $t_i$ , for the  $N_p$  cells in Eq. 5.29 will be calculated using the Flow length tool (upwards from outlet) with weighted values (the resulting map of  $l_i / v_i$ ).

More information about flow velocity in vegetated channels can be found in Carollo et al. (2002). Regarding the catchment-specific parameter, we will assume that  $\beta = 1$ , following the method of Fernandez et al. (2003) and Fu et al. (2006) for catchments in USA and Lopez-Vicente et al. (2011) in a Spanish catchment. Therefore, we assume that  $SDR_i$  is time dependent only and that over a long period, an ephemeral or permanent stream must transport all of the sediment to the outlet.

	Document:	D1.4. Handbook of protocols and methods		
	Author	UJAEN	Version	6
	Reference	D1.4	Date	24/03/2023

### Calculation of sediment yield

In those study areas where spatially distributed values of soil erosion (calculated from USLE model, eq. 5.1) are available, the map of specific sediment yield for each cell  $i$  ( $SSY_i$ ;  $Mg\ ha^{-1}\ y^{-1}$ ) and the value of the total sediment yield per site ( $SY_i$ ;  $Mg\ y^{-1}$ ) can be calculated:

$$SSY_i = SDR_i \cdot A_i \quad [\text{eq. 5.31}]$$

The predictive ability of coupling a soil erosion model with the SDR approach for an annual cycle has been demonstrated at catchment scale under Mediterranean conditions by several authors, such as by Di Stefano and Ferro (2007) with the RUSLE equation in Italy and by L ó pez-Vicente and Navas (2010) with the Revised-MMF model in Spain. It is worth noting that the sediment transport effectiveness of a catchment decreases as  $t_i$  (see Equation 5.29) increases, and consequently, as catchment area ( $A_w$ ; ha) increases.


The annual intra-basin stored sediments ( $ISS_w$ , %) is the total amount of sediment that temporarily accumulates in the basin during the year and does not reach the basin outlet. To improve the assessment of the processes of soil redistribution in the study areas, the  $ISS_w$  is calculated as the proportion of the total eroded particles ( $E_w$ ) that are temporarily accumulated in the catchment:

$$ISS_w = 100 - \left( \frac{100 \cdot SSY_w}{E_w} \right) \quad [\text{eq. 5.32}]$$

### Calculation of IC/AIC

Among the diverse indicators to measure sediment connectivity (SC), we have chosen two approaches: I) the updated version (Ort í z-Rodr í guez et al., 2019) of the index of connectivity (IC) originally developed by Borselli et al. (2008); and II) the latest version (L ó pez-Vicente et al., 2020) of the aggregated index of connectivity (AIC) proposed by L ó pez-Vicente and Ben-Salem (2019). Indices output are dimensionless indicators that assess the probability that overland flow arrives at a user-defined target, including sinks or channels, in such a way that output values are a function of the computation target.

Both indices account for the drainage area and flow path characteristics. The downslope module ( $D_{dn}$ ) contemplates the probability that runoff and sediment arrive at a defined sink along the flow path. The upslope module ( $D_{up}$ ) represents the potential for downward routing of overland flow occurring upslope and also implements a "stream power"-like approach. In this project, the outlet of each sub-catchment will be the target. The two indices are defined in the range of  $[-\infty, +\infty]$  and connectivity increases when the index grows towards  $+\infty$ .

	Document:	D1.4. Handbook of protocols and methods		
	Author	UJAEN	Version	6
	Reference	D1.4	Date	24/03/2023

## Calculation of the IC

The **IC** is based on the following equation:

$$IC_K = \log_{10} \left( \frac{D_{up,K}}{D_{dn,K}} \right) = \log_{10} \left( \frac{\overline{W}_K \cdot \overline{S}_K \cdot \sqrt{A_K}}{\sum_{i=K,n_K} \frac{d_i}{W_i \cdot S_i}} \right) \quad [\text{eq. 5.33}]$$

where **A** (m<sup>2</sup>) is the upslope drainage area, **W** (dimensionless) is the average weighing factor of A, **S** (m / m) is the average slope gradient of A, **d<sub>i</sub>** (m) is the length of the ith cell along the downslope path, **W<sub>i</sub>** (dimensionless) is the weight of the ith cell, and **S<sub>i</sub>** (m / m) is the slope gradient of the ith cell. The subscript K indicates that each cell 'i' has its own IC value.

The weighting factor W is used to calculate the impedance to runoff and sediment fluxes due to the characteristics of the ground and land uses. For many authors, the **W** factor of eq. 5.33 is equal to the C-factor (cover-management) of the RUSLE and RUSLE2 soil erosion model. This factor enables to model the effect of tillage practices and vegetation management on the soil loss rates. In eq. 5.33, slope gradient of less than 0.005 must be adjusted to **S<sub>i</sub>** = 0.005 and higher than 1 must be set to a maximum value of **S<sub>i</sub>** = 1. The weighted flow path length and the **W**, **S** and A factors are calculated with the D-Infinity algorithm (free available in SAGA software).

## Calculation of the AIC


The AIC is based on the following equations:

$$AIC_k = \log_{10} \left( \frac{D_{up,k}}{D_{dn,k}} \right) = \log_{10} \left( \frac{\overline{R}_t \cdot \overline{RT} \cdot \overline{C}_t \cdot \overline{K}_P \cdot \overline{S} \cdot \sqrt{A_k}}{\sum_{k=i}^n \frac{d_i}{AWC_i}} \right) \quad [\text{eq. 5.34}]$$

$$AWC_i = R_{ti} \cdot RT_i \cdot C_{ti} \cdot K_{Pi} \cdot S_i \quad [\text{eq. 5.35}]$$

where **AWC** is the aggregated weighting factor at catchment scale, **R<sub>t</sub>** is the normalized rainfall erosivity factor for the period t (values between 0-1), **RT** is the residual topography factor (normalized values between 0 and 1), **C<sub>t</sub>** is the C-RUSLE factor for the period t (values between 0-1), **K<sub>P</sub>** is the soil permeability factor (normalized values between 0 and 1) and **S** is the slope gradient (m / m).

In this project, the rainfall erosivity factor, **R<sub>t</sub>** in eq. 5.34, will be set equals to 1 to avoid calculation disturbances associated to the distinct rainfall depths of the different study areas. The residual topography factor, **RT** in eq. 5.34, is obtained as the normalized and

	Document:	D1.4. Handbook of protocols and methods		
	Author	UJAEN	Version	6
	Reference	D1.4	Date	24/03/2023

inverse values of the standard deviation (SSD) of the slope gradient map (using the 'Residual Analysis (Grid)' tool included in SAGA , with a radius of 2 cells – including the centre cell – ). A minimum RT value of 0.001 is set to avoid computational errors. The  $K_P$  factor considers the influence of the soil physical properties on the sediment connectivity because the values of soil water infiltration and retention capacity can significantly vary at short and medium distance. The lowest  $K_P$  values are assigned to the unit/s with very high permeability and moderate and higher  $K_P$  values corresponded to the units with moderate and low permeability, respectively.


### Computation of the SDR and IC/AIC with GIS tools

A different number of inputs and GIS tools are required to compute the SDR and IC/AIC approaches. Most inputs will be used with the two approaches whilst others are approach-specific. Below, you can see the table 15, with the main components:

Table 15: GIS appraisal for SDR and IC/AC calculation.

Component	Approach	
	SDR	IC / AIC*
Inputs	<ul style="list-style-type: none"> <li>• DEM</li> <li>• Detailed land use map</li> <li>• Flow velocity for each LULC<sup>#</sup></li> </ul>	<ul style="list-style-type: none"> <li>• DEM</li> <li>• Detailed land use map</li> <li>• C-factor for each LULC<sup>#</sup></li> <li>• Upslope drainage area</li> <li>• Soil permeability*</li> </ul>
Computation setup	<ul style="list-style-type: none"> <li>• Define outlet</li> <li>• Define boundary</li> </ul>	<ul style="list-style-type: none"> <li>• Define outlet</li> <li>• Define boundary</li> <li>• Define working area (WA)</li> <li>• Adjust of input maps to WA</li> </ul>
Tools	<p>ArcMap®:</p> <ul style="list-style-type: none"> <li>• Convert polygon to raster</li> <li>• Flow direction</li> <li>• Basin</li> <li>• Slope gradient</li> <li>• Flow length</li> <li>• Flow accumulation (MD)</li> <li>• Raster calculator</li> </ul> <p>SAGA®:**</p> <ul style="list-style-type: none"> <li>• Sink/artifact removal</li> </ul>	<p>ArcMap®:</p> <ul style="list-style-type: none"> <li>• Convert polygon to raster</li> <li>• Flow direction</li> <li>• Basin</li> <li>• Slope gradient</li> <li>• Flow length</li> <li>• Flow accumulation (MD)</li> <li>• Raster calculator</li> <li>• Convert raster to ascii</li> </ul> <p>SAGA®:**</p> <ul style="list-style-type: none"> <li>• Sink/artifact removal</li> <li>• Local statistics</li> <li>• Flow accumulation (D-Infinity)</li> </ul>

<sup>#</sup> from tables; \* specific for the AIC; \*\* most SAGA commands have equivalent tools in ArcMap.


	Document:	D1.4. Handbook of protocols and methods		
	Author	UJAEN	Version	6
	Reference	D1.4	Date	24/03/2023

**Important remark #1!** In order to obtain comparable outputs (maps and values) between the different olive groves evaluated in this project, the C-factors and Flow velocity values have to be normalized among all sites. That means input parameterization and harmonization of the dataset must be done before running the approaches.

**Important remark #2!** Before computing the SDR and IC/AIC, the small local depressions (artifacts) of the DEMs have to be removed without adding unrepresentative flat surfaces. The Planchon and Darboux algorithm (available in SAGA software) fills the sinks and creates a minimum gradient of  $0.01^\circ$  in the new surfaces. This task ensures flow routing across the DEM. Then, the boundary of the upslope contributing area of each sub-catchment will be calculated from the location of the outlet upwards using the flow accumulation map.


## References

- Álvarez, S., Soriano, M. A., Landa, B. B. and Gómez, J.A. 2007. Soil properties in organic olive groves compared with that in natural areas in a mountainous landscape in southern Spain. *Soil Use and Management*, 23, 404–416
- Arnoldus, H.M.J., 1977. Methodology used to determine the maximum potential average annual soil loss due to sheet and rill erosion in Morocco. *FAO Soil Bull.* 34, 39-51.
- Bannari, A., Morin, D., Bonn, F. and Huete, A. R. 1995. A review of vegetation indices', *Remote Sensing Reviews*, 13: 1, 95 — 120. Download citation. <https://doi.org/10.1080/02757259509532298>.
- Belgiu, M.; Dragut, L. 2016. Random forest in remote sensing: A review of applications and future directions *ISPRS Journal of Photogrammetry and Remote Sensing*, 114, 24-31. <https://doi.org/10.1016/j.isprsjprs.2016.01.011>.
- Benavidez, R., Jackson, B., Maxwell, D., Norton, K., 2018. A review of the (Revised) Universal Soil Loss Equation ((R)USLE): with a view to increasing its global applicability and improving soil loss estimates. *Hydrol. Earth Syst. Sci.* 22, 6059-6059.
- Beretta, A.N., Silbermann, A.V., Paladino, L., Torres, D., Bassahun, D., Musselli, R. García-Lamothe, A., 2014. Soil texture analyses using a hydrometer: modification of the Bouyoucos method. *Cien. Inv. Agr.* 41263-274.
- Blaschke, T. 2010. Object based image analysis for remote sensing. *ISPRS J. Photogramm. Remote Sens.* 65, 2–16. <https://doi.org/10.1016/j.isprsjprs.2009.06.004>.
- Borselli L, Cassi P, Torri D, 2008. Prolegomena to sediment and flow connectivity in the landscape: a GIS and field numerical assessment. *Catena* 75 (3), 268–277. <https://doi.org/10.1016/j.catena.2008.07.006>
- Bouyoucos, G.J., 1962. Hydrometer method improved for making particle size analysis of soils. *Agronomy Journal* 54, 464-465.
- Burguet M, Taguas EV, Gómez JA, 2017. Exploring calibration strategies of the SEDD model in two olive orchard catchments. *Geomorphology* 290, 17–28. <https://doi.org/10.1016/j.geomorph.2017.03.034>
- Calero, J., Cordovilla, M. P., Aranda V., Borjas, R. and Aparicio, C. 2013. Effect of Organic Agriculture and Soil Forming Factors on Soil Quality and Physiology of Olive Trees. *Agroecology and Sustainable Food Systems*, 37, 193-214.
- Camp-Valls, G. 2009. Machine Learning in Remote Sensing Data Processing. *IEEE Workshop on Machine Learning for Signal Processing (MLSP09)*. <https://doi.org/10.1109/MLSP.2009.5306233>.
- Carollo FG, Ferro V, Termini D, 2002. Flow Velocity Measurements in Vegetated Channels. *Journal of Hydraulic Engineering* 128 (7), 664–673. [https://doi.org/10.1061/\(ASCE\)0733-9429\(2002\)128:7\(664\)](https://doi.org/10.1061/(ASCE)0733-9429(2002)128:7(664))
- Chamard, P., Courel, M. F., Ducousso, M., Guénégo, M. C., Le Rhun, J., Levasseur, J. E., Loisel, C. and Togola, M. 1991. Utilisation des bandes spectrales du vert et du rouge pour une meilleure évaluation des formations végétales actives. *Téléédétection et Cartographie*, Éd. AUPELF-UREF, 203-209.
- Congalton, R., 1991. A review of assessing the accuracy of classifications of remotely sensed data. *Remote Sensing of Environment*, Vol. 37, pp. 35-46. [https://doi.org/10.1016/0034-4257\(91\)90048-B](https://doi.org/10.1016/0034-4257(91)90048-B).


	Document:	D1.4. Handbook of protocols and methods		
	Author	UJAEN	Version	6
	Reference	D1.4	Date	24/03/2023

- Desmet, P.J.J., Govers, G., 1996. A GIS procedure for automatically calculating the USLE LS factor on topographically complex landscape units. *J. Soil Water Cons.* 51, 427-433.
- Di Stefano C, Ferro V, 2007. Evaluation of the SEDD model for predicting sediment yield at the Sicilian experimental SPA2 basin. *Earth Surface Processes and Landforms* 32 (7), 1094–1109. <https://doi.org/10.1002/esp.1465>
- Di Stefano C, Ferro V, 2017. Testing Sediment Connectivity at the Experimental SPA2 Basin, Sicily (Italy). *Land Degradation & Development* 28 (7), 1992–2000. <https://doi.org/10.1002/ldr.2722>
- Drusch, M., U. Del Bello, S. Carlier, O. Colin, V. Fernandez, F. Gascon, B. Hoersch, C. Isola, P. Laberinti and P. Martimort. 2012. "Sentinel-2: ESA's optical high-resolution mission for GMES operational services." *Remote Sensing of Environment* 120: 25-36. <https://doi.org/10.1016/j.rse.2011.11.026>.
- FAO, 2006. Guidelines for Soil Description, 6th edition. Food and Agriculture Organization of the United Nation, Rome.
- Fernandez C, Wu JQ, McCool DK, Stöckle CO, 2003. Estimating water erosion and sediment yield with GIS, RUSLE, and SEDD. *Journal of Soil and Water Conservation* 58 (3), 128–136. <https://www.jswnonline.org/content/58/3/128/tab-article-info>
- Ferro V, 1997. Further remarks on a distributed approach to sediment delivery. *Hydrological Sciences Journal* 42 (5), 633–647. <https://doi.org/10.1080/02626669709492063>
- Ferro V, Porto P, 2000. Sediment delivery distributed (SEDD) model. *Journal of Hydrologic Engineering* 5 (4), 411–422. [https://doi.org/10.1061/\(ASCE\)1084-0699\(2000\)5:4\(411\)](https://doi.org/10.1061/(ASCE)1084-0699(2000)5:4(411))
- Frampton, W.J.; Watmough, G. Milton, E.J. 2013. Evaluating the capabilities of Sentinel-2 for quantitative estimation of biophysical variables in vegetation. *ISPRS Journal of Photogrammetry and Remote Sensing*, 82, 83-92. <https://doi.org/10.1016/j.isprsjprs.2013.04.007>.
- Fu G, Chen S, McCool DK, 2006. Modeling the impacts of no-till practice on soil erosion and sediment yield with RUSLE, SEDD, and ArcView GIS. *Soil & Tillage Research* 85 (1-2), 38–49. <https://doi.org/10.1016/j.still.2004.11.009>
- Gómez, J.A., 2015. Procesos erosivos en olivar en Andalucía a diferentes escalas: entendimiento, magnitud, implicaciones e intentos de control. *Proc. IV Jornadas de Ingeniería del Agua* 145-154. (In Spanish)
- Gómez, J.A. Battany, M., Renschler, C.S. and Fereres, E. 2003. Evaluating the impact of soil management on soil loss in olive orchards. *Soil Use and Management* 19, 127-134.
- Gómez, J.A., Sobrinho, T.A., Giráldez, J.V. and Fereres, E. 2009. Soil management effects on runoff, erosion and soil properties in an olive grove of Southern Spain. *Soil & Tillage Research* 102, 5–13
- Kaufman, Y. J. and Tanré, D. 1992. Atmospherically Resistant Vegetation Index (ARVI) for EOS-MODIS. *IEEE Transactions on Geoscience and Remote Sensing* 30 (2): 261-270. <https://doi.org/10.1109/36.134076>.
- Knight, E.J.; Kvaran, G. 2014. Landsat-8 operational land imager design, characterization, and performance. *Remote Sens.* 6 (11):10286-10305. <https://www.mdpi.com/2072-4292/6/11/10286>.
- López-Bellido, P.J., López-Bellido, L., Fernández-García, P., Muñoz-Romero, V., López-Bellido, F., 2016. Assessment of carbon sequestration and the carbon footprint in olive groves in Southern Spain. *Carbon Management* 7 (3-4), 161-170.
- López Vicente M, González Romero J, Lucas Borja ME, 2020. Forest fire effects on sediment connectivity in headwater sub-catchments: Evaluation of indices performance. *Science of the Total Environment* 732, article 139206. <https://doi.org/10.1016/j.scitotenv.2020.139206>
- López-Vicente M, Ben-Salem N, 2019. Computing structural and functional flow and sediment connectivity with a new aggregated index: A case study in a large Mediterranean catchment. *Science of the Total Environment* 651 (Part 1), 179–191. <https://doi.org/10.1016/j.scitotenv.2018.09.170>
- López-Vicente M, Lana-Renault N, García-Ruiz JM, Navas A, 2011. Assessing the potential effect of different land cover management practices on sediment yield from an abandoned farmland catchment in the Spanish Pyrenees. *Journal of Soils and Sediments* 11 (8), 1440–1455. <https://doi.org/10.1007/s11368-011-0428-2>
- Merritt, W.S., Letcher, R.A., Jakeman A.J., 2003. A review of erosion and sediment transport models. *Environmental Modelling & Software*, 18, 761–799
- Moore, I.D., Burch, G.J., 1986. Physical basis of the length-slope factor in the Universal Soil Loss Equation. *Soil Sci. Soc. Am. J.* 50, 1294-1298.
- Moore, D., Wilson, J.P., 1993. Length-slope factors for the Revised Universal Soil Loss Equation: Simplified method of estimation. *J. Soil Water Cons.* 47, 423-428.



	Document:	D1.4. Handbook of protocols and methods		
	Author	UJAEN	Version	6
	Reference	D1.4	Date	24/03/2023

- Morfitt, R.; Barsi, J.; Levy, R.; Markham, B.; Micijevic, E.; Ong, L.; Scaramuzza, P.; Vanderwerff, K. 2015. Landsat-8 Operational Land Imager (OLI) Radiometric Performance On-Orbit. *Remote Sens.* 7, 2208-2237.. <https://www.mdpi.com/2072-4292/7/2/2208>.
- Ortíz-Rodríguez AJ, Muñoz-Robles C, Borselli L, 2019. Changes in connectivity and hydrological efficiency following wildland fires in Sierra Madre Oriental, Mexico. *Science of the Total Environment* 655, 112–128. <https://doi.org/10.1016/j.scitotenv.2018.11.236>
- Panagos, P., Meusburger, K., Ballabio, P., Borrelli, P., Alewel, C., 2014. Soil erodibility in Europe: A high-resolution dataset base on LUCAS. *Science of the Total Environment* 479-480, 189-200.
- Panagos, P., Borrelli, P., Poesen, J., Ballabio, C., Lugato, E., Montanarella, L., Alewell, C., 2015a. The new assessment of soil loss by water erosion in Europe. *Environmental Science & Policy* 54, 438-447.
- Panagos, P., Ballabio, C., Borrelli, P., Meusburger, K., Klik, A., Percec-Tadic, M., et al., 2015b. Rainfall erosivity in Europe. *Science of the Total Environment* 511, 801-814.
- Panagos, P., Borrelli, P., Meusburger, K., 2015c. A new Slope Length and Steepness Factor (LS-Factor) for Modeling Soil Erosion by Water. *Geosciences* 2015 5, 117-126.
- Panagos, P., Borrelli, P., Meusburger, K., Alewel, C., Lugato, E., Montanarella, L., 2015d. Estimating the soil erosion cover-management factor at the European scale. *Land Use Policy* 48, 38-50.
- Panagos, P., Borrelli, P., Meusburger, K., van der Zanden, E.H., Poesen, J., Alewell, C., 2015e. Modelling the effect of support practices (P-factor) on the reduction of soil erosion by water at European scale. *Environmental Science and Policy* 51, 23-34.
- Peña-Barragán, J.M., Jurado-Exposito, M., López-Granados, F., Atenciano, S., Sánchez-de la Orden, M., García-Ferrer, A., García-Torres, L., 2004. Assessing land-use in olive groves from aerial photographs. *Agriculture, Ecosystems and Environment* 103, 117-122.
- Porta, J., López-Acebedo, M., 2005. Agenda de Campo de Suelos, información de suelos para agricultura y el medio ambiente. Mundi-Prensa, Madrid. (In Spanish).
- Rawls, W.J., Brakensiek, C.L., Saxton, K.E., 1982. Estimation of soil water properties. *Trans. Am. Soc. Agric. Eng.* 25, 1316-1320.
- Renard, K.G., Freimund, J.R., 1994. Using monthly precipitation data to estimate the R-factor in the revised USLE. *Journal of Hydrology* 157, 287-306.
- Renard, K.G., Foster, G.R., Weesies, G.A., McCool, D.K. & Yoder, D.C. 1997. Predicting soil erosion by water: a guide to conservation planning with the revised universal soil loss equation (RUSLE). US Department of Agriculture, Washington, DC.
- Richards, J.A. 1994. Remote Sensing Digital Image Analysis: an Introduction. 5ª Ed. Springer-Verlag. Berlín. 340 p.
- Rodríguez, M.F., Florentino, A., Gallardo, J., De Antonio, R., 2004. Sistemas de Información Geográfica en la evaluación de la erosión hídrica en Badajoz-España aplicando la metodología USLE. *Agronomía Tro.* 54, 391-410 (In Spanish).
- Rouse, J. W., Haas, R. W., Schell, J. A., Deering, D. W. and Harlan, J. C. 1974. Monitoring the vernal advancement and retrogradation (Greenwave effect) of natural vegetatioa NASA/GSFCT Type III Final Report, Greenbelt, MD, USA.
- Sadeghi, S.H.R., Gholami, L., Khaledi-Darvishan, A.K., Saeidi, P., 2014. A review of the application of the MUSLE model worldwide. *Hydrological Sciences Journal* 59, 365-375.
- Schoenebeger, P., Wysocki, D.A., Benham, E.C., Broderson, W.D., 2012. Field Book for Describing and Sampling Soils. NRCS, National Soil Survey Center, Lincoln, NE.
- Sisodia, P.S.; Tiwari, V.; Kumar, A. 2014. Analysis of Supervised Maximum Likelihood Classification for remote sensing image. *IEEE International Conference on Recent Advances and Innovations in Engineering (ICRAIE-2014)*. <https://doi.org/10.1109/ICRAIE.2014.6909319>.
- Vanwalleghem, T., Juan Infante-Amate, J., González de Molina, M., Soto-Fernández, D. and Gómez, J.A. 2011. Quantifying the effect of historical soil management on soil erosion rates in Mediterranean olive orchards. *Agriculture, Ecosystems and Environment* 142, 341– 351.
- Williams, J.R., Berndt, H.D., 1977. Sediment delivery rations determined with sediment and runoff models. In: *Erosion and solid matter transport in inland water. Proceedings of Paris Symposium, July 1997*, IAHS Publication, 122. Wallingford: IAHS Press, 169-179.

	Document:	D1.4. Handbook of protocols and methods		
	Author	UJAEN	Version	6
	Reference	D1.4	Date	24/03/2023

Weischmeier, W.H., Smith, D.D., 1965. Predicting rainfall-erosion losses from cropland east of the Rocky Mountains. Guide for Selection of Practices for Soil and Water Conservation. Agriculture Handbook 282, Washington DC., Agricultural Research Service, 49 pp.

Wischmeier, W.H., Smith, D.D., 1978. Predicting rainfall erosion losses, a guide to conservation planning. Agriculture Handbook 537, Washington DC., U.S. Department of Agriculture, 58 pp.

Zhang, L.; Zhang, L.; Du, B. 2016. Deep Learning for Remote Sensing Data: A Technical Tutorial on the State of the Art. IEEE Geoscience and Remote Sensing Magazine, 4, 2.:  
<https://doi.org/10.1109/MGRS.2016.2540798>.

## 6. Carbon sequestration and C-footprint

### WP3. Task 3.5. Soil erosion and carbon sequestration

Leader: Julio Antonio Calero Gonzalez, Roberto García Ruiz and Milagros Torrus Castillo

For further clarification contact: [jcalero@ujaen.es](mailto:jcalero@ujaen.es)


During months of Autumn 2020, we, with the help of all of you, will prepare an excel file to be fed with data and all the input and output of carbon, to calculate the C footprint at olive farm scale (e.g. net annual amount of CO<sub>2</sub> released to the atmosphere per kg of olive fruit produced or net annual amount of CO<sub>2</sub> taken up from the atmosphere per kg of olive fruit produced).

### 6.1. Introduction

In this section, we will try identify, and how to quantify them, the main processes to assess for carbon (C) sequestration and C footprint in STS and non-STS olive groves of Portugal, Spain, Italy, Greece, Tunisia and Morocco.

The model to assess C footprint is based on the annual gross C input and output in the studied olive groves, resulting in an annual net C balance (which can be positive; gross C input is higher than gross C outputs, or negative; gross C input is higher than gross C outputs or close to zero; gross C input is similar to gross C outputs) which can be normalized by kg of harvested olive fruit (e.g. assuming a gross C input of 4500 kg C-CO<sub>2</sub> ha<sup>-1</sup> y<sup>-1</sup> and a gross C output of 3780 kg C-CO<sub>2</sub> ha<sup>-1</sup> y<sup>-1</sup>, the net balance -inputs - outputs- is 720 kg C-CO<sub>2</sub> ha<sup>-1</sup> y<sup>-1</sup>).

If the harvested olive is 2890 kg ha<sup>-1</sup> y<sup>-1</sup>, then per each kg of olive fruit, it has been taking up from the atmosphere to olive grove about 750 kg C-CO<sub>2</sub> ha<sup>-1</sup> y<sup>-1</sup> / 2890 kg olive fruit ha<sup>-1</sup> y<sup>-1</sup> = 0.249 kg C-CO<sub>2</sub> kg<sup>-1</sup> harvested olive fruit. Please, take into account that 1.0 kg C-CO<sub>2</sub> is equivalent to 3.66 kg CO<sub>2</sub>, and thus the 0.249 kg C-CO<sub>2</sub> kg<sup>-1</sup> harvested olive fruit is the

	Document:	D1.4. Handbook of protocols and methods		
	Author	UJAEN	Version	6
	Reference	D1.4	Date	24/03/2023

equivalent of  $0.912 \text{ kg CO}_2 \text{ kg}^{-1}$  harvested olive fruit. Some studies which have tried to assess for a kind of C footprint are Proietti et al. (2014), Ilarioni et al. (2013) and L ó pez-Bellido et al. (2016). The magnitude of the inputs and outputs of carbon are subjected to the production, tree density and age and managements, and therefore differences between STS and non-STs are expected.


C sequestration will be assessed by accounting for the difference in the soil protected C (physically-chemically protected C and chemically protected carbon) between STS and comparable but non-STs olive groves. This will be done by taking a top 30 cm soil samples and determination of the physically-chemically protected C and chemically protected carbon.

## 6.2. Carbon footprint

As mentioned above, C footprint will be calculated from and annual carbon balance in SUSTAINOLIVE olive farms. The following fluxes should be taking account on annual basis and at olive farm scale, taking as reference one hectare:

**Inputs:** this includes: a) annual net inputs of C which is storage in the woody and other permanent structures of the olive tree (trunk, roots, branches) ( $C_{intree}$ ,  $\text{kg C ha}^{-1} \text{ y}^{-1}$ ), b) annual inputs of C in the olive fruit ( $C_{inolivefruit}$ ), c) annual inputs of C in the herbaceous cover, which could be spontaneous or seeded ( $C_{incovercrop}$ ,  $\text{kg C ha}^{-1} \text{ y}^{-1}$ ) in case olive grove applies this soil management, and d) annual input of C with the organic fertilizer ( $C_{inferti}$ ).

**Outputs:** this include direct and indirect (externalised C outputs) and the following should be considered: a) (direct) C output due to the harvested olive fruit ( $C_{outolivefruit}$ ). Please, take into account that the C input which is mobilized to the olive fruit is considered as an input, but also as an output resulting in a net  $C_{olivefruit}$  balance of zero, b) (direct) C-CO<sub>2</sub> emission from the decomposition of herbaceous cover crop residue ( $C_{outcovercrop}$ , (this will be a fraction of the  $C_{incovercrop}$ ), c) (direct) C-CO<sub>2</sub> emission from the decomposition of the organic fertiliser ( $C_{outferti}$ ) (this will be a fraction of the  $C_{inferti}$ ), d) C-CO<sub>2</sub> emitted only in case the tree pruning is burned, as it will be the case for some of the non-STs Spanish olive groves, or the CO<sub>2</sub> emitted during the decomposition of the tree pruning remains is these are deployed on top of the soil ( $C_{outpruning}$ ), e) (direct) C-CO<sub>2</sub> emission from the soil by basal soil respiration ( $C_{outsoil}$ ) which will be a fraction of the top 30 cm SOC ( $\text{Mg SOC ha}^{-1}$ ) and climate conditions, f) (direct) eroded C ( $C_{eroded}$ ), g) (indirect) C-CO<sub>2</sub> which has been emitted during the production of herbicides, insecticides, fungicides and chemical fertilisers ( $C_{outinsumes}$ ), h) (direct) C-CO<sub>2</sub> which has been emitted during soil operations (e.g. tillage, spontaneous cover crop cut...

	Document:	D1.4. Handbook of protocols and methods		
	Author	UJAEN	Version	6
	Reference	D1.4	Date	24/03/2023

( $C_{outsoilmanag}$ ), i) (direct) C-CO<sub>2</sub> which has been emitted during harvesting ( $C_{outharv}$ ) by using machineries, j) (direct) C-CO<sub>2</sub> which has been emitted during tree pruning ( $C_{outprun}$ ) by using machineries, and k) (indirect) C-CO<sub>2</sub> which has been emitted during irrigation if pumps are needed.

For some of the in-and-outflows the estimation will be based on models (e.g.  $C_{outsoil}$ ) others on well-described coefficient (e.g.  $C_{outinsumes}$ ; C-CO<sub>2</sub> emitted from each kg of N-Urea produced), whereas others from measurement (e.g.  $C_{intree}$ ,  $C_{inolivefruit}$ ,  $C_{incovercrop}$ ,  $C_{inferti}$ ).

### 6.2.1. Annual C inflows


$C_{intree}$  (kg C ha<sup>-1</sup> y<sup>-1</sup>). As mentioned above this is the annual net inputs of C which is storage in the woody and other permanent structures of the olive tree (trunk, roots, branches). This will be estimated from: i) measurement of three biovolume (three trees per olive grove. If in the olive groves there are trees of different ages, then, three trees per each age class), ii) converting tree biovolume into kg of tree and from here to kg of C in each tree taking into account the C content of branches, and iii) age of the tree. Although, the annual rate of tree-C increase is not linear along many years (e.g. first 50 years), for the time being we will assume so (now, a Master Thesis student is studying this function which related age with tree C in different rainfed and irrigated tree densities).

So, the annual C accumulation (kg C ha<sup>-1</sup> y<sup>-1</sup>) in the olive trees of one hectare ( $C_{intree}$ ) can be calculated as:

$C_{intree} = (\text{Volume of the tree (m}^3 \text{ tree}^{-1}) \times \text{tree density (kg m}^{-3}) \text{ on dry mass basis} \times (\text{organic carbon content (\%)/100}) \times \text{number of trees in one hectare (trees ha}^{-1}) / \text{age of the tree (y)}).$

### 6.2.2. Volume of trees

The volume of the trees is estimated from the average volume of, at least, three (five should be desirable) representative trees (this is the case if there is only one age class. If there are two or three age classes, then biovolume should be measured in three trees of each age classes), of the olive groves. To determine the biovolume of tress (m<sup>3</sup> tree<sup>-1</sup>), tree-to-five trees in the plots will be randomly selected among the most representative trees. In each of them: i) measure the diameter of the trunk at the root collar, and at the birth of the primary tree branches, with the help of a tree caliper, and ii) the length between both diameters. Do the same with the primary, secondary and tertiary branches if these have a diameter of  $\geq 2$

	Document:	D1.4. Handbook of protocols and methods		
	Author	UJAEN	Version	6
	Reference	D1.4	Date	24/03/2023

cm. The volume of the trunk and the various strata of branches ( $V_s$ ) will be modelled by a truncated cone following this formula:

$$V_s = \frac{1}{3} \pi h (R^2 + r^2 + R r) \quad [\text{eq.6.1}]$$

where  $R$  and  $r$  are the major and minor diameter, respectively, which usually coincide the trunk diameter at the root collar and the trunk diameter at the birth of primary branches; and  $h$  the length between  $R$  and  $r$ . The total volume of the above-ground part of the tree is the sum of the volumes of all the measured  $n$  branches:

$$V_{\text{tree}} = \sum_{i=1}^n V_s \quad [\text{eq.6.2}]$$

### 6.2.3. Wood density

In the field, after making the biovolume measurement, collect some wood samples to calculate the wood density. There are two options. Option 1: collect one core of the trunk and primary branches from Pressler borer. Option 2: when pruning the tree, take cylindrical parts (and easy to measure the volume) of the tree pruning. Once in the laboratory, the samples are weighed on the balance (0.01 g) and dried in the oven for 4 days at 50 C. Once dried, they will be weighed again, recording the dry weight ( $W_s$ ). Subsequently, the volume of the cores (if option 1) or of the pruned branches (option 2) are calculated determined from the truncated cone equation, eq.3.2 ( $V_{sd}$ ). The density of the wood is determined by the ratio of the dry weight and the resulting volume of each branch:


$$D_{\text{tree}} = \frac{W_s}{V_{sd}} \quad [\text{eq.6.3}]$$

### 6.2.4. Tree biovolume and mass

From the wood density and above-ground volume of trees, we can calculate the aerial biomass of trees ( $B_{\text{aerial}}$ , kg ha<sup>-1</sup>):

$$B_{\text{aerial}} = V_{\text{tree}} \times D_{\text{tree}} \quad [\text{eq.6.4}]$$

However, there is another biomass which we cannot account for; the root biomass. We will apply an expansion factor based on empirical relationships between above-ground / below-ground biomass of olive trees ( $F_r$ ). We recommended the ratio (above-to-below ground

	Document:	D1.4. Handbook of protocols and methods		
	Author	UJAEN	Version	6
	Reference	D1.4	Date	24/03/2023

biomass) of 4.2 estimated by Lopez-Bellido et al. (2016) for Picual and Arbequina varieties. Illarioni et al (2013) for the Leccino variety found that this ratio was close to 7.2:

$$B_{\text{tree}} = B_{\text{aerial}} + B_{\text{root}} (= \frac{B_{\text{aerial}}}{4.2}) \quad [\text{eq.6.5}]$$

Note #1: The relationship between the main trunk and main branches (primary branches), which are easily and quick to measured, and the remain biovolume (secondary, tertiary and so on, which take much longer time to be measured) is relatively constants. Velazquez-Martí et al. (2014) stated that trunk plus primary branches accounted for the 77% of tree volume and the 75% of its biomass, so an expansion factor of 1.25 might be used to get the total aerial volume of trees from trunk and primary branches determination. Moreover, in our preliminary assessment of olive trees in the SUSTAINOLIVE plots in Spain, we found a ratio of 1.23 (CV = 11%) between total volume / trunk + primary branches, which can be also used as a factor to estimate total volume from the trunk + primary branches measures. Anyway, its highly recommended to measure all branches with a diameter  $\geq 2$  mm and to apply eq.6.2, carefully pointing to which stratum they belong each one.

Note #2: The relationship between permanent (wood) to non-permanent (leaves) biomass. According with Proietti et al. (2014) or López-Bellido et al. (2016), leaves biomass represents less than 10% of tree biomass so, taking into account the great difficulty of its measurement, it can be discarded assuming the error. However, the expansion factor of 1.13 (F<sub>i</sub>) can be used (Illarioni et al., 2013), so eq.6.5 can be modified as follow:

$$B_{\text{tree}} = (B_{\text{aerial}} + B_{\text{root}} (= \frac{B_{\text{aerial}}}{4.2})) \times 1.13 \quad [\text{eq.6.6}]$$


Finally, the biomass of all the olive trees in the plot is obtained multiplying the biomass of the representative tress by the number of tress of the plot (N<sub>trees</sub>):

$$B_{\text{trees}}(\text{per hectare}) = B_{\text{tree}} \times N_{\text{trees}} (\text{per hectare}) \quad [\text{eq.6.7}]$$

#### 6.2.5. Annual C accumulation rate

An aliquot of the core (option 1) or from different parts of the tree pruning (option 2) is milled (once dried) and analysed for total carbon and Nitrogen, for instance by using CNHS analyser. The cost of one carbon analysis in a soil laboratory might cost  $5 \pm 3$  euros per sample. As an option, data on olive tree content (on dry basis) can be taken from the



	Document:	D1.4. Handbook of protocols and methods		
	Author	UJAEN	Version	6
	Reference	D1.4	Date	24/03/2023

literature, as, usually, is a variable which shows little variability.  $B_{\text{trees}}$  (per hectare) x (carbon content (%)/100) =  $C_{\text{trees}}$ .


Finally, if  $C_{\text{trees}}$  (kg C ha<sup>-1</sup>) is divided by the tree age (y<sup>-1</sup>), the annual C accumulation rate ( $C_{\text{intree}}$ ) is calculated. Please, take into account that calculations differ slightly if trees of the olive farm have different age classes.

$C_{\text{inolivefruit}}$  = olive fruit yield per hectare (kg ha<sup>-1</sup>) x (dry weight of the olive fruit (%)/100) x (carbon content (%)/100). For dry weight, collect some olive fruits at harvest, fresh weight and dried at 50 ° C during 4-5 days and calculate the percentage of dry weight respect to the fresh weight. Take an aliquot of the dried olive fruit, mill it and analysed for total C and N in a CNH autoanalyzer. The cost of one carbon analysis in a soil laboratory might cost 5 ± 3 euros per sample.

$C_{\text{incovercrop}}$  = Annual C input within the cover (spontaneous or seeded) crop. This will be based on measuring aboveground cover crop biomass and the C content of the aboveground biomass. This should be measured just before cut the cover crop, each time is cut within a growing year. For instance, in Spain it is relatively usual to cut the spontaneous cover crop in two occasions (e.g. in March and later late in April) per year: Measuring the aboveground biomass (in this case net primary production) in these two occasions, we will calculate the whole amount of aboveground biomass which has been produced during that year. Samples should be taking in different area within the studied olive grove where cover crop is growing by throwing at least 5 times and randomly a square of 0.5 x 0.5 m size (0.25 m<sup>2</sup>). Then, the whole biomass at ground level is cut at kept in a plastic bag. If the cover crops grow in bands of specific dimension between tree lines, then measure the band width and the number of bands in one hectare (this can be done at your room previously).

The collected biomass in the plastic bag are taken to the lab, fresh weighed and dried in a ventilated oven a 50 °C until constant weight (4-5 days) and then weight. Once the materials are dried, weighed again to calculated dry biomass in the square of 0.5 x 0.5 m size (0.25 m<sup>2</sup>) (then you can scale the biomass in one hectare of your olive grove), and mill an aliquot and analyse for carbon and nitrogen in a CNHS autoanalyzer. The annual aboveground C input is calculated as dry biomass per hectare x ((carbon content (%)/100).

To estimate root biomass of cover crops, there are two option: Option 1: use some literature coefficients which related aboveground/belowground biomass (sometimes carbon) in similar types of plant communities. We do have some. Option 2: Convert some of squares of 0.5 x 0.5 m size (0.25 m<sup>2</sup>) into a cubic samples of 20 x 20 x 20 cm. Placed the soil samples

	Document:	D1.4. Handbook of protocols and methods		
	Author	UJAEN	Version	6
	Reference	D1.4	Date	24/03/2023

in a robust plastic bag (the sample will weigh more than 10 kg) and once in the lab carefully washed to remove adhering soil. It is recommended the washing be carried out over a sieve (# 1 mm) to avoid losing fine roots. Separate the roots from the aboveground biomass, dried them (50 °C for 4-5 days) and weight to obtain belowground biomass in 0.25 m<sup>2</sup> and to calculate the aboveground-to-belowground biomass. By analysing the carbon content once the dried roots are milled, then, root-C (in 0.25 m<sup>2</sup> and thus you can scale up to one hectare) and ratio aboveground-to-belowground C are calculated. You do not need to determine using Option 2 the root biomass and root C in each of the olive grove with cover crop. Just, several replicates in a couple of olive groves with cover crop.

To estimate the annual C input per hectare (kg C ha<sup>-1</sup> y<sup>-1</sup>), we have to know the percentage of the cover crops (m<sup>2</sup> / m<sup>2</sup>) in the plot. This can be attained following the methodology proposed in section 5.6 (supervised or unsupervised image classification).


*C<sub>inferti</sub>* = Annual C input due to organic fertilizer. This estimate is based on annual amount of organic fertilizer is applied. Take 3 – 5 subsamples (about 50 – 100 gr) of the organic fertilizer, fresh weight, dry in an oven at 50 °C during 4-5 days, weight them again to know water content, mill a subsample (about 5 – 10 grs) and analyse for total carbon and nitrogen using, for instance a CNHS autoanalyser.

$C_{inferti} = \text{Annual fresh amount of organic fertilizer (kg ha}^{-1} \text{ y}^{-1}) \times ((100 - \text{water content (\%)})) / 100) \times (\text{content of carbon (\%)} / 100) = \text{kg C ha}^{-1} \text{ y}^{-1}$ .

### 6.2.6. Annual C outflows

*C<sub>outolivefruit</sub>* = this is the carbon that goes out the olive farm due to the harvested olive fruit. This has been C-CO<sub>2</sub> taken from the atmosphere within the olive grove but get out of the olive groves. This is the same value than *C<sub>inolivefruit</sub>*.

*C<sub>outcovercrop</sub>* = This is the annual amount of carbon emitted as CO<sub>2</sub> during the decomposition of the cover crop residues. This will be estimated as a fraction of the cover crop-C. There are now in the literature several isohumic coefficients (e.g. a fraction of organic carbon of a source of organic carbon -cover crop residues in this case- which remains in the soil at longer term after decomposition) we might use. In addition, we are doing our own experiments (in the lab at optimal conditions and in the field; litter bags technique) to provide these isohumic coefficients. In addition, we will provide (using double exponential 4 parametric functions) the decomposition rate of the labile-C and refractory-C for a couple of types of cover crop. This will be calculated as:  $C_{incovercrop} \text{ (kg C ha}^{-1} \text{ y}^{-1}) \times \text{isohumic fraction (a value between 0 to 1)} \times \text{a one-year fraction of the number of years the isohumic coefficient are applied (eg. if a residue takes 3 years to decompose, the one-year fraction of the$

	Document:	D1.4. Handbook of protocols and methods		
	Author	UJAEN	Version	6
	Reference	D1.4	Date	24/03/2023

isohumic coefficient for the first year can be 0.5 (50%), 0.35 (35%) for the second and 0.15 (15%) for the third).


$C_{outferti}$  = This is the annual amount of carbon emitted as CO<sub>2</sub> during the decomposition of the organic fertilizer. This will be estimated as a fraction of the organic fertiliser-C. There are now in the literature several isohumic coefficients (e.g. a fraction of organic carbon of a source of organic carbon (organic fertiliser in this case) with remains in the soil at longer term after decomposition) for many types of manures, and composted olive mill pomace, we might use. This will be calculated as:  $C_{inferti}$  (kg C ha<sup>-1</sup> y<sup>-1</sup>) x isohumic fraction (a value between 0 to 1) x a one-year fraction of the number of years the isohumic coefficient are applied.

$C_{outpruning}$  = This is the annual amount of carbon emitted as CO<sub>2</sub> due to: i) olive tree pruning residues if these are burned. In this case  $C_{outpruning}$  = Annual fresh amount of tree pruning (kg ha<sup>-1</sup> y<sup>-1</sup>) x ((100-water content (%)/100) x (carbon content (%) of the olive tree pruning/100), or ii) during the decomposition of the olive tree pruning residues. This will be estimated as a fraction of the olive tree pruning-C. There are now in the literature several isohumic coefficients (e.g. a fraction of organic carbon of a source of organic carbon (olive tree pruning in this case) with remains in the soil at longer term after decomposition), we might use. This will be calculated as: Annual fresh amount of tree pruning (kg ha<sup>-1</sup> y<sup>-1</sup>) x ((100-water content (%)/100) x (carbon content (%) of the olive tree pruning/100), x isohumic fraction (a value between 0 to 1) x a one-year fraction of the number of years the isohumic coefficient are applied.

$C_{outsoil}$  = This is the annual C-CO<sub>2</sub> emitted out of the soil by basal soil respiration. This will be estimated throughout different models. Hopefully, by next autumn we will be able to describe the specific model we will use. Nevertheless, the model will be based on: i) SOC stock of the soil, ii) mean monthly temperature and rainfall, and iii) some indicator of soil texture. The type of models we might use will be similar to that of the RothC. By using the model, the annual amount of C-CO<sub>2</sub> emitted can be estimated

$C_{eroded}$  = This is the annual C loss due to soil erosion. This carbon is not necessarily emitted as CO<sub>2</sub>, but it does leave the olive grove to another ecosystem; e.g. nearby olive groves or a water courses. This flow is calculated as: soil erosion (Mg ha<sup>-1</sup> y<sup>-1</sup>) x (top 5 cm soil total (organic + inorganic) C content (%)/100).

$C_{outinsumes}$  = This is the indirect annual CO<sub>2</sub> emitted due to the production of insecticides, fungicides and herbicides. According to the type (active principle) of product the emitted CO<sub>2</sub> to product a given amount can be obtained for specific tables already published. This annual outflow is calculated as following: (amount (g) of herbicide of active principle A

	Document:	D1.4. Handbook of protocols and methods		
	Author	UJAEN	Version	6
	Reference	D1.4	Date	24/03/2023

applied in one hectare and year x amount of C-CO<sub>2</sub> emitted (kg) per gr of active principle) + (amount (g) of insecticide of active principle B applied in one hectare and year x amount of C-CO<sub>2</sub> emitted (kg) per g of active principle) + (amount (g) of fungicide of active principle C applied in one hectare and year x amount of C-CO<sub>2</sub> emitted (kg) per g of active principle).

*C<sub>outsoilmana</sub>* = this is a direct annual CO<sub>2</sub> emission due to any fuel consumption in the soil operations (tillage, cover crop control, etc.) and it is calculated from the diesel consumption. Therefore, olive farm has to record the number of liters of diesel spent per hectare and year in these operations.

*C<sub>outharv</sub>* = This is a direct annual CO<sub>2</sub> emission due to any fuel consumption in the harvest operations and it is calculated from the diesel consumption. Therefore, olive farm has to record the number of liters of diesel spent per hectare and year in harvesting.

*C<sub>outprun</sub>* = This is a direct annual CO<sub>2</sub> emission due to any fuel consumption in the tree pruning operations and it is calculated from the petrol consumption. Therefore, olive farm has to record the number of liters of petrol spent per hectare and year in pruning.

*C<sub>outirrig</sub>* = This is an indirect annual C-CO<sub>2</sub> emission due to the CO<sub>2</sub> emitted in producing the electricity (is irrigation pump work with electricity) or by petrol consumption is the pumps works with petrol. Therefore, olive farm has to record the energy (kWh) and the name of the company (according to the company the percentual distribution of the sources of the energy differ and thus the CO<sub>2</sub> emitted per kWh) or liters of petrol spent per hectare and year in irrigation.


C-footprint (+ if more CO<sub>2</sub> is directly or indirectly emitted per one hectare than that taking up or - if less CO<sub>2</sub> is directly or indirectly emitted per one hectare than that taking up) =

$$\{((C_{outolivefruit} + C_{outcovercrop} + C_{outferti} + C_{outpruning} + C_{outsoil} + C_{eroded} + C_{outinsumes} + C_{outsoilmana} + C_{outharv} + C_{outprun} + C_{outirrig}) - (C_{intree} + C_{inolivefruit} + C_{incovercrop} + C_{inferti})\} / \text{fresh harvested olive fruit (kg fresh olive fruit ha}^{-1} \text{ y}^{-1}) = \text{kg C-CO}_2 \text{ kg}^{-1} \text{ fresh harvested olive fruit or } 3.66 \times \text{kg CO}_2 \text{ kg}^{-1} \text{ fresh harvested olive fruit}$$

### 6.3. Carbon sequestration

This will be estimated using three complementary approaches:

1.- By calculating the amount of C that enters the soil annually (e.g. isohumic carbon from cover crops, tree pruning residues and organic fertilisers) and will be expressed as kg SOC ha<sup>-1</sup> y<sup>-1</sup>.

	Document:	D1.4. Handbook of protocols and methods		
	Author	UJAEN	Version	6
	Reference	D1.4	Date	24/03/2023

2.- By the difference in SOC ( $\text{Mg C ha}^{-1}$ ) (taking into account the SOC (%) in the top 30 cm of soils and bulk density after removing the weight of the soil > 2 mm) between each pair of STS and non-STS olive groves and taking into account the number of year with STS.

3.- By analysing the protected SOC ( $\text{Mg protected C ha}^{-1}$ ) in each pair of STS and non-STS. Top 30 cm of soil samples should be air-dried, pass throughout 2 mm mesh. And then, 100 gr of < 2 mm soil is passed on wet basis throughout a 250 and 53  $\mu\text{m}$  meshes. The collected material (between 250 – 2000, between 53 to 250 and < 53  $\mu\text{m}$  is dried, weighed and organic carbon is determined in each of the fraction. The amount of organic carbon in the 53 – 250  $\mu\text{m}$  is the physically-chemically protected C, whereas that < 53  $\mu\text{m}$  is the chemically-biochemically protected C. By comparing the protected C between each pair of STS and non-STS olive farm and taking into account the number of years under STS, the annual C sequestration can be estimated.


This section explains the soil sampling for physico-chemical, biological (soil functional quality indicators) and soil organic carbon (SOC) determinations.

For each STS and non-STS two types of sampling are required: 1) whole disturbed sample for the top 30 cm of soil, and 2) undisturbed cores from 0-5 cm and 15-20 cm, as representative of the 0-30 cm bulk density.

### 6.3.1. Disturbed samples (top 30 cm)

A minimum of three (each one composed of 4. Select a point in the inter-row area and collected 4 soil samples about 10-20 cm of that point following in the north, south, east and west parts. The four soil samples are put in the same bag; this is one soil sample composed of four) randomly topsoil samples should be taken in each plots at a depth of 30 cm. Avoid field borders, tracks frequently used by machinery, people or livestock, or any other unusual soil area (saline areas, eroded knolls and/or rocky outcrops, old manure piles, burn piles, fence rows, etc.). Likewise, soils should be sampled on spring and no operation should have been done during the last two – three weeks of soil sampling.

In the case of olive groves, whose soils are usually stony and difficult to penetrate with probes, it is recommended to dig a soil pit with the help of a pick or shovel, carefully taking the sample (about 1 kg) from each part of the 30 cm of depth and pouring it in a clean and labelled plastic bag, to be carried to the lab.

	Document:	D1.4. Handbook of protocols and methods		
	Author	UJAEN	Version	6
	Reference	D1.4	Date	24/03/2023

In the lab, samples should be extended homogeneously from the bags over an absorbent paper, mixing carefully with a plastic or glass rod, but avoiding crushing the soil. Then, the sample should be dried at room temperature for several days up to reach environmental humidity, prior to chemical or physical analyses.

When dry, divide the final sample into four parts, which are as identical as possible, using a sample divider or by quartering. One of the parts that will be used for organic carbon and equivalent calcium carbonate determinations, is weighted in a balance (0.0 g), storing the rest.

The last step in sample pre-treatment is sieving to obtain the fine earth fraction (< 2mm). All analyses should be carried out over this fraction. First, the sample must be gently ground to break up soil aggregates and clods, but avoiding breaking the gravel (it is recommended to use a rubber stopper). Then, the sample is passed through a 2 mm sieve, repeating the process until all the thick fragments are retained on the sieve. The sieve of the sieve is fine earth, which will be used for analysis. Finally, the sieve is placed under the tap, washing the coarse fragments, which will subsequently be dried in an oven at 110 ° C for 24 h. The content of coarse fragments CF (%) of the sample is calculated with respect to the soil selected in the quartet:

$$CF = \frac{CF_w}{FE_w} \times 100 \quad [\text{eq. 6.8}]$$

being CF<sub>w</sub> (g) the weight of coarse fragments and FE<sub>w</sub> (g) the weight of the fine earth. For soils having more than 35% coarse fragments (skeletal soils), the following correction factor for bulk density is recommended (Lal, 2005):


$$C_m = \frac{D_g \times \left(1 - \frac{CF}{100}\right)}{D_g \times \left(1 - \frac{CF}{100}\right) + \left(B_D \times \frac{CF}{100}\right)} \quad [\text{eq. 6.9}]$$

where D<sub>g</sub> is the density of the coarse fragments (it can be supposed 2.65 g cm<sup>-3</sup> for average mineral soils), CF is the % weight of coarse fragments and BD the bulk density, as defined below (eq.5.3).

### 6.3.2. Undisturbed samples and bulk density sampling and determination

The bulk density of a soil is the ratio of the solid mass to the total volume occupied by the soil particles plus the pore space. The mass is determined by weighing the dried sample at



	Document:	D1.4. Handbook of protocols and methods		
	Author	UJAEN	Version	6
	Reference	D1.4	Date	24/03/2023

105 ° C for one day, and the total volume is deduced from the volume of the testing apparatus employed in the field (core).

Topsoil undisturbed samples could be taken in the same 30-cm pits made for the disturbed samples. In this case, it should be done after sampling the latter. Field borders, tracks and other unusual areas, as well as freshly tilled soils, must be avoided. Two cores from the surface (0 – 5 cm) and subsurface soil (15 – 20 cm) should be collected as explained bellow.

The following material is needed (Figure 12):

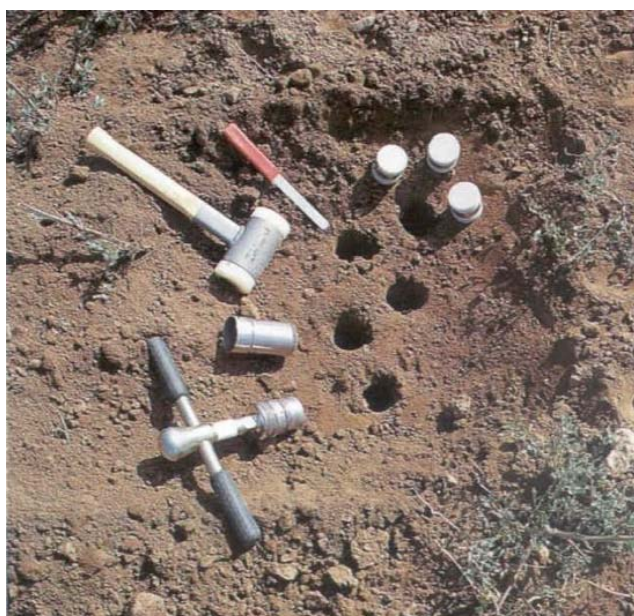



Figure 12. Material for sampling undisturbed cores in the field.

1. Soil core sampler (Kopeki cylinder, 5-cm diameter and height ring).



2. Hand mace
3. Flat-bladed knife
4. Sealable bags and marker pen
5. Porcelain vessel (250 ml)
6. Balance (0.01 g)

	Document:	D1.4. Handbook of protocols and methods		
	Author	UJAEN	Version	6
	Reference	D1.4	Date	24/03/2023

## Method and Calculations

1. Using the hand mace, drive the kopeki cylinder, with the beveled edge down, to a depth of 5 cm.



2. Removing of the cylinder: dig around the ring with the knife or trowel underneath it, carefully lift it out to prevent any loss of soil.



3. Remove excess soil from the sample with the knife. The bottom of the sample should be flat and even with the edges of the ring.




4. Using the knife, push out the sample into a plastic sealable bag. Make sure the entire sample is placed in the plastic bag. Seal and label the bag and take to the lab.

5. Weight the fresh soil and dried it using an oven at 105 C for 24 h.

6. The mass is determined by weighing the dried sample ( $D_s$ ) and dividing by the volume of the kopeky cylinder ( $V_B$ , 98.175 cm<sup>3</sup>):

$$B_D = \frac{D_s}{V_B} \quad [\text{eq. 6.10}]$$

	Document:	D1.4. Handbook of protocols and methods		
	Author	UJAEN	Version	6
	Reference	D1.4	Date	24/03/2023

For soils rich in coarse fragments, bulk density can be multiplied by the correction factor for skeletal soils, as define in eq.6.9.

### 6.3.3. Determination of soil organic matter

The organic matter content of the soil is calculated through the determination of organic carbon by: i) CNHS autoanalyser (this will determine total C which include organic and inorganic C), or ii) the Walkey - Black method.


However, the data that are usually handled refer only to the oxidizable fraction, which only includes the organic compounds. In the Walkey - Black method, the organic matter content of the soil is calculated based on the determination of organic carbon in the soil by a wet method, based on a partial oxidation of organic carbon with an oxidizing agent added in excess. The degree of oxidation achieved will depend on the conditions under which the reaction takes place (fundamentally, time and temperature).

### Equipment and Materials

1. Precision analytical balance
2. Magnetic stirrer
3. 500 mL Erlenmeyer
4. 1 and 20 mL pipettes
5. Test tube 250 mL
6. Burette and burette foot
7. Funnel
8. Dropper
9. Doser for concentrated  $H_2SO_4$
10. Mortar
11. Sieve (2 mm)

### Reagents

10. 1N potassium dichromate: dry the reagent in an oven at  $105^{\circ} C$  overnight, dissolve 49.05 g of potassium dichromate (heating slightly to favor dissolution), make up to 1000 mL with deionized water.
11. Concentrated sulphuric acid.
12. Deionized water.
13. Concentrated phosphoric acid.

	Document:	D1.4. Handbook of protocols and methods		
	Author	UJAEN	Version	6
	Reference	D1.4	Date	24/03/2023

14. Diphenylamine in sulphuric solution prepared in the following order: 0.5 g of diphenylamine in 20 mL of deionized water and 100 mL of sulphuric acid (turn from blackish brown or violet to green).

15. Salt of Morh 0.5 N:

16. 196.1 g of  $\text{Fe}(\text{NH}_4)_2\text{SO}_4 \cdot 6\text{H}_2\text{O}$  (Mohr's salt).

17. 800 mL of deionized water containing 20 mL of  $\text{H}_2\text{SO}_4$  to dissolve the salt.

18. Deionized water: bring to a volume of 1000 mL.

## Method

1. Weigh 0.5 g of the fine earth fraction of dry soil (< 2 mm) and pass through a 0.5 mm sieve.
2. Place it in a 500 mL erlenmeyer flask.
3. Add 10 mL of 1N  $\text{K}_2\text{Cr}_2\text{O}_7$  and shake.
4. Add 20 mL of  $\text{H}_2\text{SO}_4$  with the dispenser slowly and shaking in an extractor hood.
5. Shake by cooling under the tap for about thirty seconds.
6. Let stand for 30 minutes on a little hot heating plate. This treatment removes carbonates.
7. Add 100 mL of deionized  $\text{H}_2\text{O}$  and allow to cool.
8. Add 10 mL of  $\text{H}_3\text{PO}_4$  (avoids possible interference with iron).
9. Add 1ml of the indicator (diphenylamine) and titrate with a 0.5N Mohr's salt solution (the end point is an almost dark black green color that turns to emerald green). If just after adding  $\text{K}_2\text{Cr}_2\text{O}_7$  1N and  $\text{H}_2\text{SO}_4$  the solution turns green, it means that all the dichromate has been reduced and the analysis must be repeated with less sample quantity.
10. Do all of the above for the blank (should consume approximately 20 mL).

## Calculations


The percentage of organic carbon will be determined with the following equation:

$$\text{SOC, \%} = (\text{VB} - \text{VM}) \cdot 10^{-3} \times N_{\text{Fe}} \times \frac{12}{4} \times \frac{1}{p} \times \frac{100}{(100 - \% \text{H})} \times f \quad [\text{eq.6.11}]$$

Where;

VB, volume of ferrous salt expended in the blank test; VM, volume of ferrous salt expended with the sample;  $N_{\text{Fe}}$ , normality of ferrous salt; p, weight of the sample; f, recovery factor (according to the operative technique followed, in this case its value is 1.3).

The recovery factor f depends on the intensity with which the oxidation of the organic carbon takes place. In the method used, without heat input, a recovery of 77 % of organic carbon in the sample is assumed.

	Document:	D1.4. Handbook of protocols and methods		
	Author	UJAEN	Version	6
	Reference	D1.4	Date	24/03/2023

The percentage of organic matter is calculated using the "Van Bemmelen" conversion factor, whose statistically deduced value is 1.72, based on the hypothesis that 58 % of organic matter is organic carbon (this factor may vary from some soils to others).

$$\text{Organic matter, \%} = \% \text{ SOC} \times 1.724 \quad [\text{eq. 6.12}]$$

#### 6.3.4. Determination of equivalent calcium carbonate

The determination of calcium carbonate equivalent (total carbonate content expressed in  $\text{CaCO}_3$ ) is carried out by measuring the amount of  $\text{CO}_2$  released that is produced by reacting the carbonates of the soil with a strong acid ( $\text{HCl}$  1: 1). The assessment can be done in two ways:

- Collecting the  $\text{CO}_2$  released in a  $\text{NaOH}$  solution and subsequently assessed.
  - Measuring the amount of  $\text{CO}_2$  released by manometric (pressure) or volumetric methods.
- Here we will apply the volumetric method. The amount of  $\text{CO}_2$  released will be measured by the pressure it exerts on a solution, saturated with  $\text{CO}_2$ , in a gas burette, a set called Bernard's Calcimeter (Figure 13):

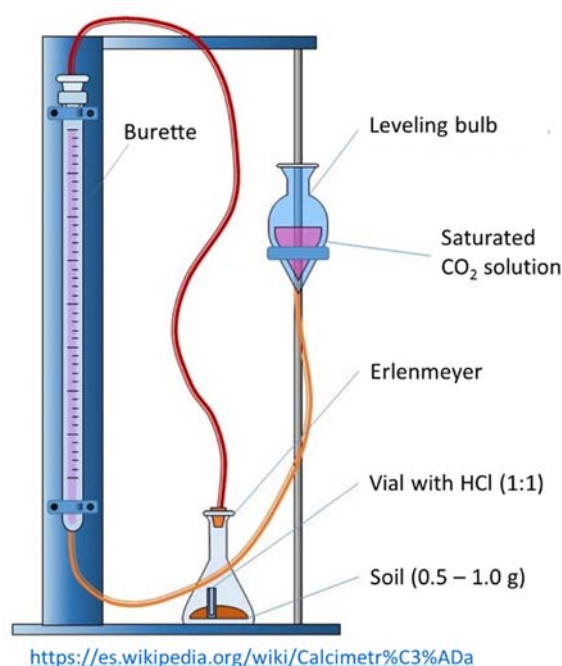



Figure 13. Bernard Calcimeter

#### Equipment and Materials

1. Bernard Calcimeter (volumetric calcimeter)
2. Frosted Mouth Erlenmeyer Flask
3. Plastic or glass tube closed at one end (vial)
4. Balance (0.001 g)

	Document:	D1.4. Handbook of protocols and methods		
	Author	UJAEN	Version	6
	Reference	D1.4	Date	24/03/2023

## 5. Agate mortar and pestle

### Reagents

1.  $\text{CaCO}_3$  standard (specifically labeled: for analysis)
2. Hydrochloric Acid (1: 1)
3. Saturated  $\text{CO}_2$  solution: 100g  $\text{NaCl}$  + 1g  $\text{NaHCO}_3$  in 300 mL of distilled water. Diluted  $\text{H}_2\text{SO}_4$  (2N) is gradually added to this solution until weak acid reaction (check with indicator paper).  $\text{H}_2\text{SO}_4$  2N: 53.3 mL  $\text{H}_2\text{SO}_4$  in 1L distilled water.


### Method

1. Fill the calcimeter with saturated  $\text{CO}_2$  solution to avoid that part of the  $\text{CO}_2$  released when the carbonate reacts with the  $\text{HCl}$  can be dissolved, which would decrease the volume measured in the burette.
2. Weigh exactly 0.2 g of pure  $\text{CaCO}_3$  on the balance (be  $W_p$ ) and placed in a (perfectly dry) Erlenmeyer flask with care that  $\text{CaCO}_3$  does not adhere to the walls of the flask.
3. Ground finely (0.03 mm) about 2 g of fine earth in the agate mortar.
4. Weigh 0.2 g to 1 g of the well ground fine soil on the balance and record (let  $W$ ). Approximately 0.2 g should be weighed if the sample is assumed to be rich in carbonates; Approximately 1 g if the sample is assumed to have no significant carbonate content; and intermediate quantities will be weighed in other cases. Beforehand, a qualitative determination of the carbonate content of the sample can be made by adding to it a few drops of  $\text{HCl}$  1:10 and observing if effervescence occurs.
5. Introduced the sample into the centre of the flask, which must be very dry. Place the vial filled with  $\text{HCl}$  and dry on the outside inside the flask, taking care not to spill it and make it splash over the sample. Close the flask tightly with the stopper connected to the calcimeter using a silicone tube (use silicon or grease). Level the level bulb and burette levels on the calcimeter (equalize the pressure), writing down the L1 reading.
6. Turn the flask upside down by shaking it gently so that the  $\text{HCl}$  reacts with the sample, and shake for about 5 minutes. Re-level the level bulb and burette levels and record the L2 reading.
7. Repeat the steps 5 – 6 with the  $\text{CaCO}_3$  standar; in this case the readings will be  $L_{p1}$  and  $L_{p2}$ .

IMPORTANT REMARK: flasks should never be handled with full hands. They must be touched the least to avoid transmitting heat that would modify the results.

### *Calculations*



	Document:	D1.4. Handbook of protocols and methods		
	Author	UJAEN	Version	6
	Reference	D1.4	Date	24/03/2023

The carbonate content of the sample can be expressed as a percentage of CaCO<sub>3</sub> that is subtitled equivalent. (Not all carbonates in the soil have to be calcium. With this experience we make all the carbonates present "equivalent" to CaCO<sub>3</sub>).

$$\text{CaCO}_3\% = \frac{W_p \times (L_1 - L_2)}{W \times (L_{2p} - L_{1p})} \times 100 \quad [\text{eq. 6.12}]$$

- W = grams of sample
- L1 = reading before HCl reaction
- L2 = reading after reacting with HCl
- Wp = grams of standard CaCO<sub>3</sub> (0.2 g)
- Lp1 = standard reading before HCl reaction
- Lp1 = standard reading after reacting with HCl

### 6.3.5. Carbon stocks

The inorganic carbon stock (Mg ha<sup>-1</sup>) is calculated from calcium carbonate equivalent (CaCO<sub>3</sub>, Mg Mg<sup>-1</sup>), the volume of one hectare at 30 cm depth (topsoil), 3 x 10<sup>-3</sup> m<sup>3</sup>, and the Bulk density of the soil (B<sub>D</sub>, Mg m<sup>-3</sup>):


$$\text{CS}_{\text{inorg}} = \text{CaCO}_3 \times 3 \cdot 10^3 \times B_D \quad [\text{eq.6.13}]$$

And, in the same way, the stock of organic carbon (Mg ha<sup>-1</sup>), employing here the SOC (Mg Mg<sup>-1</sup>):


$$\text{CS}_{\text{org}} = \text{SOC} \times 3 \cdot 10^3 \times B_D \quad [\text{eq.6.14}]$$

### Key References

- Alburquerque J.A., Gonzalvez J., Garcia D., Cegarra J., 2007. Effects of a compost made from the solid by-product ("alperujo") of the two-phase centrifugation system for olive oil extraction and cotton gin waste on growth and nutrient content of ryegrass (*Lolium perenne* L.). *Bioresource Technology* 98(4): 940-945
- Bannari, A., Morin, D., Bonn, F. and Huete, A. R. 1995. A review of vegetation indices', *Remote Sensing Reviews*, 13: 1, 95 — 120
- Bechini, L., Castoldi, N., 2009. On farm monitoring of economic and environmental performances of cropping systems: Results of a 2-year study at the field scale in northern Italy. *Ecological Indicators* 9, 1096 – 1113.
- Belgiu, M.; Dragut, L. 2016. Random forest in remote sensing: A review of applications and future directions *ISPRS Journal of Photogrammetry and Remote Sensing*, 114, 24-31
- Blaschke, T. 2010. Object based image analysis for remote sensing. *ISPRS J. Photogramm. Remote Sens.* 65, 2–16.
- Camp-Valls, G., 2009. Machine Learning in Remote Sensing Data Processing. *IEEE Workshop on Machine Learning for Signal Processing (MLSP09)*. 10.1109/MLSP.2009.5306233
- Calero, J., Cordovilla, M. P., Aranda V., Borjas, R. and Aparicio, C. 2013. Effect of Organic Agriculture and Soil Forming Factors on Soil Quality and Physiology of Olive Trees. *Agroecology and Sustainable Food Systems*, 37, 193-214.

	Document:	D1.4. Handbook of protocols and methods		
	Author	UJAEN	Version	6
	Reference	D1.4	Date	24/03/2023

- Chamard, P., Courel, M. F., Ducouso, M., Guénégou, M. C., Le Rhun, J., Levasseur, J. E., Loisel, C. and Togola, M. 1991. Utilisation des bandes spectrales du vert et du rouge pour une meilleure évaluation des formations végétales actives. Télédétection et Cartographie, Éd. AUPELF-UREF, 203-209.
- Congalton, R., 1991. A review of assessing the accuracy of classifications of remotely sensed data. Remote Sensing of Environment, Vol. 37, pp. 35-46.
- Delgado G., Aranda V., Pérez-Lomas A.L., Martín-García J.M., Calero J., Delgado R., 2012. Evolution of available heavy metals in soils amended with sewage sludge co-compost. A microcosm experiment. Compost Science & Utilization, 20: 1-12.
- Drusch, M., U. Del Bello, S. Carlier, O. Colin, V. Fernandez, F. Gascon, B. Hoersch, C. Isola, P. Laberinti and P. Martimort. 2012. "Sentinel-2: ESA's optical high-resolution mission for GMES operational services." Remote Sensing of Environment 120: 25-36.
- Frampton, W.J.; Watmough, G. Milton, E.J. 2013. Evaluating the capabilities of Sentinel-2 for quantitative estimation of biophysical variables in vegetation. ISPRS Journal of Photogrammetry and Remote Sensing, 82, 83-92.
- Gómez H.F., Pomares A., García C., Baixauli J.M., Aguilar J.L., Porcuna M.J., Verdú A., Hermoso F., Tarazona M., Estela B., Cabot T., Campos D., Gómez de Barreda R., Coscollá. R., 2000. Evaluación de un sistema de producción ecológica de cultivos hortícolas en Valencia. Fundación Cátedra Iberoamericana. Colección cursos y conferencias. 4
- Gómez-Muñoz, B., Valero-Valenzuela, J.D., Hinojosa, B., García-Ruiz, R., 2016. Management of tree pruning residues to improve soil organic carbon in olive groves.
- Guzmán, G.I., González de Molina, M., 2017. Energy in Agroecosystems: A Tool for Assessing Sustainability. Advances in Agroecology. CRC Press.
- Guzmán G., Alonso-Mielgo, A., 2004. Fertilización en el olivar ecológico. In: Manual de olivicultura ecológica Ed., Instituto de Sociología y Estudios Campesinos ISEC. (2004). Universidad de Córdoba, Córdoba, 174 pp.
- Ilarioni, L., Nasini, L., Brunori, A., Proietti, P., 2013. Experimental measurement of the biomass of Olea europea L. African Journal of Biotechnology 12, 1216 – 1222.
- Kaufman, Y. J. and Tanré, D. 1992. Atmospherically Resistant Vegetation Index (ARVI) for EOS-MODIS. IEEE Transactions on Geoscience and Remote Sensing 30 (2): 261-270.
- Knight, E.J.; Kvaran, G. 2014. Landsat-8 operational land imager design, characterization, and performance. Remote Sens. 6 (11):10286-10305
- Lal R. & Shukla, M. (2004). Principles of Soil Physic. Marcel-Dekker, Inc. New York-Basel
- López-Bellido, P.J., López-Bellido, L., Fernández-García, P., Muñoz-Romero, V., López-Bellido, F., 2016. Assessment of carbon sequestration and the carbon footprint in olive groves in Southern Spain. Carbon Management 7, 161 – 170.
- Morfitt, R.; Barsi, J.; Levy, R.; Markham, B.; Micijevic, E.; Ong, L.; Scaramuzza, P.; Vanderwerff, K. 2015. Landsat-8 Operational Land Imager (OLI) Radiometric Performance On-Orbit. Remote Sens. 7, 2208-2237.
- Pappalardo, S.E., Gislimberti, L., Ferrarese, F., De Marchi, M & Mozzi, P. (2019). Estimation of potencial soil erosion in the Prosecco DOCG area (NE Italy), toward a soil footprint of bottled sparkling wine production in different land-management scenarios. Plos One (2019).
- Proietti, S., Sdringola, P., Desideri, U., Zepparelli, F., Brunori, A., Ilarioni, L., Nasini, L., Regni, L., Proietti, P., 2014. Carbon footprint of an olive tree grove. Applied Energy 127, 115 – 124.
- Richards, J.A. 1994. Remote Sensing Digital Image Analysis: an Introduction. 5ª Ed. Springer-Verlag. Berlín. 340 p.
- Rouse, J. W., Haas, R. W., Schell, J. A., Deering, D. W. and Harlan, J. C. 1974. Monitoring the vernal advancement and retrogradation (Greenwave effect) of natural vegetation NASA/GSFC Type III Final Report, Greenbelt, MD, USA.
- Sánchez-Martín et al., 2010 Sanchez-Martín, L., A. Meijide, L. Garcia-Torres y A. Vallejo. 2010. Combination of drip irrigation and organic fertilizer for mitigating emissions of nitrogenoxides in semiarid climate. Agriculture, Ecosystems & Environment 137(1-2): 99-107.
- Sánchez-Monedero M.A., Cayuela M.L., Mondini C., Serramia N., Roig A., 2008. Potential of olive mill wastes for soil C sequestration. Waste Management 28, 767-773.

	Document:	D1.4. Handbook of protocols and methods		
	Author	UJAEN	Version	6
	Reference	D1.4	Date	24/03/2023

Sisodia, P.S.; Tiwari, V.; Kumar, A. 2014. Analysis of Supervised Maximum Likelihood Classification for remote sensing image IEEE International Conference on Recent Advances and Innovations in Engineering (ICRAIE-2014).DOI: 10.1109/ICRAIE.2014.6909319.

Sofo, A., Nuzzo, V., Palese, A.M., Xiloyanis, C., Celano, G., Zukowskyi, P. and Dichio, B., 2005. Net CO<sub>2</sub> storage in mediterranean olive and peach orchards. *Scientia Horticulturae* 107, 17–24

Therios, I., 2009. Olives. CPRS in Horticulture Series 18. CABI, Wallingford, UK, 426 pp.

Urbano-Terrón, P. (1992). Tratado de fitotecnia general. Mundi-Prensa, Madrid.

Velazquez-Martí, B., Fernández-González, E., López-Cortés, I., Salazar-Hernández, D.M., 2011. Quantification of the residual biomass obtained from pruning of trees in Mediterranean olive groves.

Velazquez-Martí, B., López-Cortés, I., Salazar-Hernández, D.M., 2014. Dendrometric analysis of olive trees biomass quantification in Mediterranean orchards. *Agroforest Systems* 88, 755-765. *Biomass and Bioenergy* 35, 3208 – 3217.

Zhang, L.; Zhang, L.; Du, B. 2016. Deep Learning for Remote Sensing Data: A Technical Tutorial on the State of the Art. *IEEE Geoscience and Remote Sensing Magazine*, 4, 2.

## 7. Assessment of resilience to climate change

### WP3. Task 3.7. Assessment of resilience to climate change

Leader: Ignacio Jesus Lorite Torres (IFAPA)

For further clarification contact: [ignacioj.lorite@juntadeandalucia.es](mailto:ignacioj.lorite@juntadeandalucia.es) or


lorite.torres@gmail.com

Partners do not need to evaluate or analyse anything. IFAPA will work on the data partners will provide IFAPA.

### 7.1. General considerations

In order to develop the activities included in Tasks 3.7 (WP3) “Assessment of the resilience to climate change”, an accurate characterization of the field experiments considered by each partner of SUSTAINOLIVE project is required, and includes:

1. Coordinates UTM of the field experiments
2. Olive cultivar and age of the plantation
3. Flowering phenology and oil accumulation curve as described below.
4. Irrigation supply: Annual irrigation supply for each experiment is required (m<sup>3</sup> per ha). If more frequent measures are available, please provide them.
5. Irrigation method.
6. Cover crop: It would be necessary the type, sowing date (if seeded cover crop), % of soil covered and date of removal of the cover crop.
7. Soil characteristics (texture and depth). It would be desirable to collect data from at least 3 depths.
8. Density (trees per ha), size of the tree and % of soil covered by the olive canopy.
9. Yield.

	Document:	D1.4. Handbook of protocols and methods		
	Author	UJAEN	Version	6
	Reference	D1.4	Date	24/03/2023

10. Pests and diseases identified in the experimental fields.

11. Weather data from a close weather station including: Daily maximum and minimum temperature, rainfall, air humidity, solar radiation and wind speed. The distance from the field experiment to the weather station is also required.

12. Other agricultural practices carried out in the field experiments (such as pruning, etc.) and occurrence of alternate bearing.

13. Pictures of the experiments are recommended.

Please, take into account that data to fulfil most of these requirements have already been taking in other tasks.

The methodology to assess for climate change resilience is based on following the flowering phenology and oil quantity and quality, combined with soil and climate data.

## 7.2. Flowering phenology evaluation

Reproductive phenological data will be observed each 3-4 days for four groups of three trees per olive grove. Only trees with significant flowering will be considered. The international standardized BBCH numerical scale for olive (Sanz-Cortes et al. 2002) will be used, with observations starting with stage 57 (the corolla, green-colored, is longer than the calyx) and ending with 68 (majority of petals fallen or faded). For each group of three trees and date, the earliest, most common, and latest stages will be recorded. With this information, three phenological parameters will be calculated:


**Flowering period (FP):** Defined as the period (number of days) from the first time for stage 61 (first flower open) to appear as earliest stage, until, the first time for stage 68 (majority of petals fallen) to appear as most common stage.

**Full bloom period (FBP):** Period (number of days) within the flowering period defined as starting at the first time for stage 61 to appear as most common, until last time for stage 65 (full bloom, at least 50% of flowers open) as most common.

**Full bloom date (FB):** The average date found for the full bloom period, expressed as DOY (Day of the Year).

## 7.3. Fruit traits and oil quality assessment






*Sampling.* A random sample of 500 g of olive will be harvest for four groups of three trees per cultivar during the harvest season every 10 days; approximately days 5, 15 and 25 of

	Document:	D1.4. Handbook of protocols and methods		
	Author	UJAEN	Version	6
	Reference	D1.4	Date	24/03/2023

September, October, November and December. No any discrimination on olive skin color will be performed at sampling harvest.

**Ripening index.** External color of the pulp will be recorded in a random sample of 30 fruits per tree, using the following scale (Table 16).

Table 16. Skin color for ripening index (Frías et al., 1991)

Olive	Color	Index
	Green	0
	Light-green	1
	Purple spots in less than half of fruit skin	2
	Purple spots in more than half of fruit skin	3
	Violet-black skin	4

**Oil content and fruit traits.** From the 500 gr sample, three random subsamples of around 25-30 g will be selected. The number of fruits will be counted. Each subsample will be placed in a glass petri dish with a fireproof paper (Figure 12). Each subsample will be weighted independently to calculate fruit weight. Then, samples will be transferred to an air-forced oven at 105 during a minimum of 42 hours. The subsamples will be again weighted to calculate fruit dry weight. Each three subsamples of the same tree will be stored together until evaluation (Figure 13).



Figure 12. Subsamples prepared for drying in the air-forced oven.




Figure 13. Subsamples packed after oven-dry

Oil content will be evaluated using a Nuclear Magnetic Resonance previously calibrated for the range of variation of oil content of olive cultivars.

**Oil quality.** We are searching for other alternatives to assess for the fatty oil quality. Fatty acid composition of oil could be efficiently estimated from fruit analysis (Figure 4). For that



	Document:	D1.4. Handbook of protocols and methods		
	Author	UJAEN	Version	6
	Reference	D1.4	Date	24/03/2023

purpose, a sample of 10 representative olives of the 500 sample should be chosen. They should be stored at -20 °C until analysis. Olives should be healthy and without any visible damage.

- 1.- Prepare methylation solution: methanol : toluene : dimethoxypropane : sulphuric acid in a 39:20:5:2 proportion.
- 2.- Prepare 10 ml reaction tubes. Tubes should be prepared to resist 100 °C using volatile substances. They should have Teflon caps
- 3.- Remove fruit skin with a scalpel and then take 50-100 mg of pulp (Figure 14-A). 4.- Place the pulp in a reaction tube and then add 4 ml of the methylation solution and 2 ml of heptane (Figure 14-B,C). The person taking the 50-100 mg of pulp should make an initial practice in order to standardize the size of the pulp sample.
- 5.- Tubes should be nicely closed and gently shaken. Any tube not closing perfectly or having any leak should be discarded.
- 6.- Keep the tubes, with the pulp, methylation solution and heptane, in a water bath for 2 hours to 80 °C (Figure 14-B).
- 7.- Then remove tubes from the bath and leave for a while to reach room temperature.
- 8.- Take 1.5 ml from the upper, transparent phase (Figure 14-C) and put in a gas-chromatograph tube (Figure 14-D). Take special care not to take any from the lower yellowish phase as it could damage the chromatograph injector or column.

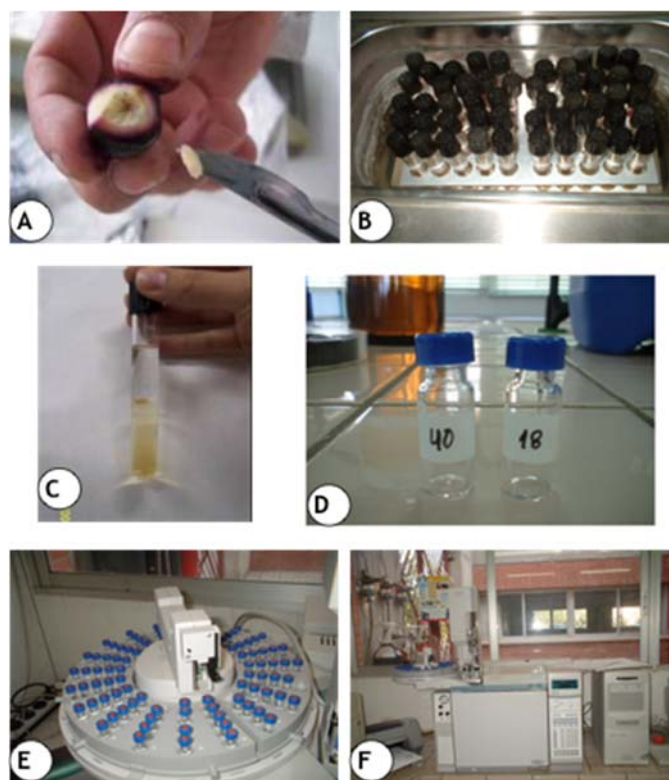



Figure 14. Protocol for fatty acid determination directly of olive fruits.



	Document:	D1.4. Handbook of protocols and methods		
	Author	UJAEN	Version	6
	Reference	D1.4	Date	24/03/2023

9.-Gas-liquid chromatography (GLC) could be performed on a Perkin Elmer Clarus 600 GC (Perkin Elmer Inc, Waltham, MA, USA) equipped with a BPX70 30 m x 0.25 mm internal diameter x 0.25 m film thickness capillary column (SGE Analytical Science Pty Ltd, Ringwood, Australia). Hydrogen should be used as carrier gas at a constant flow of 0.8 mL min<sup>-1</sup>. Split injector and flame ionization detector are maintained at 300 °C. The initial oven temperature was 140 °C maintained for two minutes, followed by a rate increase of 20 °C min<sup>-1</sup> up to 250 °C, maintained for 2 minutes.

## 8. Social agrarian metabolism, social life cycle and life cycle sustainability assessments

### WP5. Tasks of this WP


Leader: Anna Irene De Luca and Manuel Gonzalez de Molina

For further clarification contact: [anna.deluca@unirc.it](mailto:anna.deluca@unirc.it) and [mgonnav@upo.es](mailto:mgonnav@upo.es)

### 8.1. General introduction to WP5 methodologies

In the Mediterranean basin, olive growing is considered a main component of their socio-economic and cultural life, shaping the rural natural landscapes of many of their regions and preventing rural depopulations, as well as being an important source of income. In addition, olive groves is the predominant landscape of many villages of the Mediterranean basin, and therefore changes in the set of managements might have not only socio-economic but also environmental consequences. Nevertheless, olive systems are characterized by many critical aspects, such as high production costs and low market prices of olive oil. If on the one hand, the intensification of olive production processes has tried to solve these problems, on the other hand, that resulted in simplified landscapes with low-nature-value, driving greater negative environmental impacts.


Producing high-quality, healthy and socially responsible products, while containing production costs, is a challenge which need to be solved. Therefore, evaluation tools are of utmost importance to help farmers shaping management practices to obtain competitive products. Furthermore, balancing profitability while reducing environmental impacts is of utmost importance, and it requires suitable tools for farmers to organize and manage their business to reach these purposes (De Luca et al, 2018; Iofrida et al, 2020). Preserving the environment, as well as the agricultural ecosystems, meeting consumers' needs, paying attention to workers' wellbeing and other social issues, by adapting or modifying managerial and organizational features is the real challenge for current agri-food

	Document:	D1.4. Handbook of protocols and methods		
	Author	UJAEN	Version	6
	Reference	D1.4	Date	24/03/2023

productions. For this purpose, it is still necessary today to implement agroecology practices aimed “to optimize ecological processes, environmental and public health and well-being, and minimize social-ecological costs from agriculture such as soil degradation, water contamination, greenhouse gas emissions, exhaustion of non-renewable resources, and inequitable social structures” (Bezner Kerr et al, 2021:1). Until today, the concept of “agroecology” remains deliberately broad and multilayered, concerning at once scientific disciplines, practice and social movements (Wezel et al., 2009; Gonzales de Molina & Lopez-Garcia, 2021). Scholars, international organizations and peasant activist associations have long recognized and proven the multiple and positive externalities of agroecology, not only in terms of environment, but also concerning biodiversity, farmers’ incomes, resilience, and mitigation of climate change (van der Ploeg et al, 2019). Nevertheless, because of the broad fields of application, there is still a great deal of inhomogeneity which needs to be overcome by harmonizing evaluation methods and indicators for measuring the sustainability of agroecology linked to various dimensions and contexts and to compare performances (FAO, 2019).

The academic research constantly exploring new paths to assess the implications of agroecology as comprehensively as possible, and various approaches exist according as the scale of application (crop plot / farm / landscape / regional levels), the objectives of the evaluation (which dimensions of sustainability) and the opportunity to incorporate into models or to integrate models involving cross-disciplinary issues. Despite a wide assortment of definitions, indicators, guidelines exist in scientific literature and technical reports (Mottet et al, 2020), some scholars glimpse a lack of approaches to combine different perspectives on sustainability, to clarify economic and social aspects (D’ Annolfo et al, 2017; Landert et al, 2020).

Pairwise, few studies exist that refers to environmental loads of agroecological systems from a life cycle or energetic point of view. In this context, an international project called “SUSTAINOLIVE” (Novel approaches to promote the SUSTAINability of OLIVE cultivation in the Mediterranean) has been activated by a Consortium of 22 entities from Spain, Portugal, Italy, Greece, Tunisia and Morocco, and funded by PRIMA (Partnership for Research and Innovation in the Mediterranean Area) programme, and co-funded by Horizon 2020. The main objective of the project is to improve the sustainability of the olive oil sector, through the implementation and promotion of a set of innovative sustainable management solutions, based on agroecological concepts, as well as on the exchange of knowledge and participation of multiple stakeholders and final users. Among the project activities, a specific work package is devoted to the socio-economic and environmental evaluation of the

	Document:	D1.4. Handbook of protocols and methods		
	Author	UJAEN	Version	6
	Reference	D1.4	Date	24/03/2023

potential impacts in terms of environmental burdens, economic benefits and social repercussions and, finally, the overall sustainability of specific “olive farms case studies” in the countries partners. In particular, this contribution presents a new methodological proposal for sustainability assessment based on the Social Agrarian Metabolism (SAM) and Life Cycle approaches to evaluate environmental and socio-economic performances of different olive farms (in Spain, Italy, Greece, Portugal, Tunisia, and Morocco) - by comparing “agro-ecological” (i.e., Sustainable Technological Solutions - STSs) and “ordinary” (i.e., non-STSs) management principles. This report illustrates the rationale behind the research design and application of the two methodological approaches.

Among the scientific activities of the project, WP5 is focused on applying a holistic approach using joint environmental and socio-economic criteria to assess the overall sustainability and to identify key environmental, economic and social constraints of current and potential olive grove and oil production alternatives. From a managerial point of view, these project activities will contribute in improving the effectiveness of farm processes, also by the co-construction of novel knowledge that can be useful to key actors in the olive-oil sector.

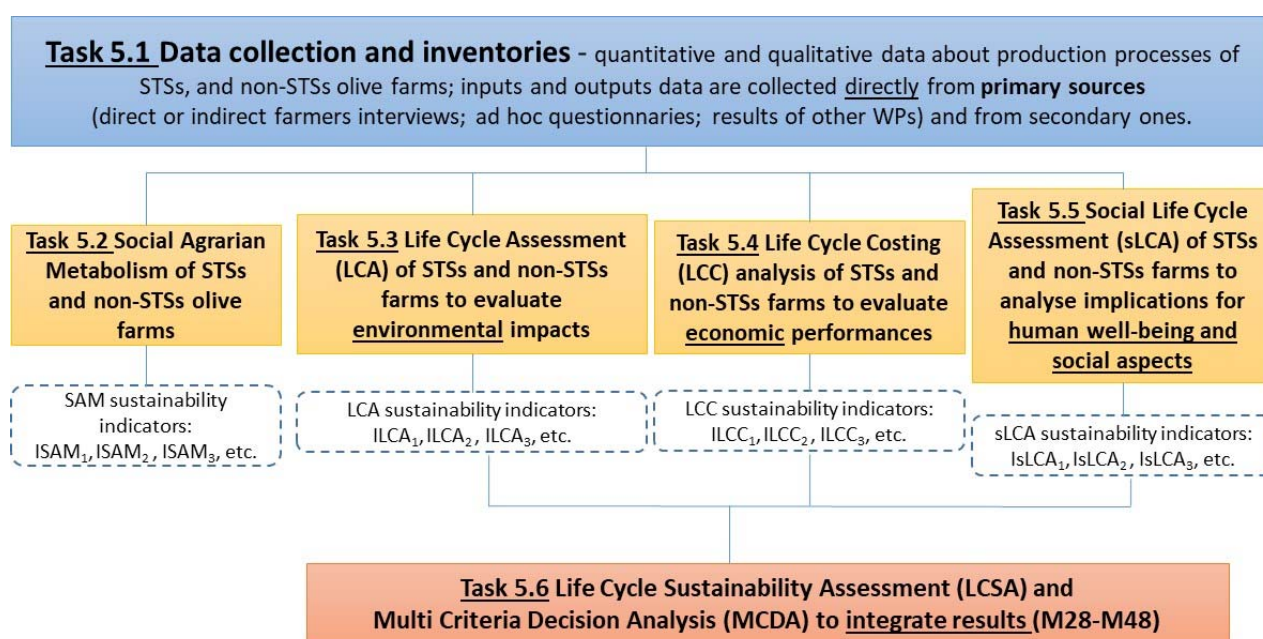



Figure 15. WP5 framework


In particular, the WP5’ s general aim is to provide an assessment of environmental and socio-economic impacts - i.e., a measurement of olive farms sustainability by comparing scenarios with and without STSs in selected contexts for each involved partner countries (Italy, Greece, Portugal, Spain, Morocco, and Tunisia) in close collaboration with key actors in the different areas. This is carried out by applying and integrating different

	Document:	D1.4. Handbook of protocols and methods		
	Author	UJAEN	Version	6
	Reference	D1.4	Date	24/03/2023

methodological approaches in order to analyze the environmental, economic and social dimensions of sustainability. Data provided by WP2 and WP3 and the olive farmer associations will feed WP5 methodologies, whose environmental and socio-economic results will be integrated through multi-criteria techniques to identify the main hot-spots within a overall sustainability framework and a comprehensive overview of STSs potential implications. The specific WP5’ s framework is illustrated in Figure 15.

The rationale behind the WP5 is based on the integration different scientific approaches: the Social Agrarian Metabolism (SAM) and the Life Cycle methodologies. The first approach recalls the concept of “biophysical accounting” to measure the mutual dependences incurred during the interaction between nature and society by measuring biophysical fund-flow integrated and reproductive (Gonzales de Molina et al, 2020) to identify the optimal configuration of land uses, livestock densities, and other elements characterizing agrarian systems. The implementation of SAM will provide information on biophysical functioning and will produce synthetic indicators of sustainability that can be easily monitored. Flows (e.g. production of goods and services) and funds (e.g., reproduction and improvement of the series of processes required for the production and consumption of goods and services) will be evaluated to assess whether STSs and comparable non-STSs are sustainable. SAM also will analyse the role played by energy flows within olive groves, taking into account not only the harvested olives but also the produced biomass which is not harvested, which is essential to fuel the heterotrophic components providing ecosystem services to olive farmers. Jointly with SAM an implementation of Life Cycle-based approaches (Life Cycle Assessment - LCA, Life Cycle Costing - LCC and Social Life Cycle Assessment - sLCA) will be carried out to assess the sustainability performances of STSs and non-STSs scenarios.

As it is known, LCA is a standardized methodology (ISO 14040-14044:2006) that enable to evaluate impacts and uncover burden shifts during the whole life cycle of a product or service, from cradle to grave. LCC is aimed at the accounting of every cost generated all along the functioning of the life cycle, allowing a long-term evaluation of the cost-effectiveness. It allows to highlight and quantify the main cost items, but also financial indicators of investment, throughout the life cycle stages, by classifying them in terms of initial costs, periodical maintenance costs, operational costs and end of life disposal costs or residual value. LCC also analyses all costs associated that are directly covered by one, or more, of the actors involved in the products life cycle, including externalities that are anticipated to be internalized in the decision-relevant future. sLCA will be carried out to assess for the social impacts of olive farmers with STSs and without STSs. The impacts will be assessed in terms of psychosocial risk factors (PRF) i.e., the hours of potential exposure

	Document:	D1.4. Handbook of protocols and methods		
	Author	UJAEN	Version	6
	Reference	D1.4	Date	24/03/2023

to working conditions that can lead to health problems, especially for workers directly involved, but also local communities and consumers that can be affected. These risks are measured, according to the scientific literature, in terms of the odds ratio (OR) and they will be classified by strength of association. Each farming task will be related to one or more working condition (such as noise, vibrations, stress, open-air work, use of chemicals, work load, etc.). Finally, a Life Cycle Sustainability Assessment (LCSA) by means of Multi Criteria Decision techniques (according to De Luca et al, 2018) could be applied for a comprehensive evaluation of STSs and non-STSs for each olive farm case studies.


## 8.2. Social Agrarian Metabolism (SAM)

### 8.2.1. Origin, background, and theoretical principles

Social Metabolism (SM) refers to the set of theories and methodological tools that allow analysing a society' s biophysical behaviour (Aadrianse, 1997; Matthews et al., 2000; Haberl, 2001; Weisz et al., 2006). It provides valuable information to assess a society' s environmental sustainability and has even turned into a new perspective on human beings' relationships with their physical environment, that is, with flows of energy, materials and information (Fischer-Kowalsky & Haberl, 1997, 2007; Sieferle, 2011; Gonz á lez de Molina & Toledo, 2011, 2014). Social Metabolism can be defined, therefore, as the way in which human societies organize their exchanges of energy and materials with their natural environment (Fisher-Kowalski & Haberl, 1993; Fisher-Kowalsky 1998; Giampietro & Mayumi, 2000; Giampietro et al., 2011) with the purpose of reversing the entropic process they are subject to, like all living beings (Gonz á lez de Molina & Toledo, 2014). In this sense, human societies carry out two basic material tasks: on the one hand, they produce goods and services and distribute them among society' s individuals; on the other, they reproduce the conditions that make production possible, thus gaining stability over time. A substantial share of social relations is therefore oriented towards the organization and maintenance of exchanges of energy, materials and information. This is metabolic activity. Its mission is to configure and feed the "funds" (Georgescu-Roegen, 1971) that societies build to generate goods and services, i.e. to counteract the law of entropy and thus generate order. Such funds are fed, that is, they are maintained and reproduced through the exchange of energy and materials with the environment.

SM is thus an analytical tool applied to socio-ecological relationships, whatever their scale or territorial scope. It can therefore be applied to agriculture. Consequently, *Social Agrarian Metabolism* (SAM) can be described as the exchange of energy, materials and information



	Document:	D1.4. Handbook of protocols and methods		
	Author	UJAEN	Version	6
	Reference	D1.4	Date	24/03/2023


that agroecosystems perform with their socio-ecological environment. The purpose of metabolic activity is that of appropriating biomass to satisfy human species' endosomatic consumption directly or indirectly through livestock while providing basic ecosystem services. SAM has also tried to satisfy the exosomatic demand (raw materials and energy) of societies with an organic metabolism and continues to do so, to a lesser extent, in industrial societies. To accomplish this, society colonizes or seizes a part of the available land. Within this territory, it establishes varying degrees of intervention or interference in the ecosystems' structure, functioning and dynamics, giving rise to different types of agroecosystems. In other words, SAM refers to the appropriation of biomass by members of a society by managing the agroecosystems present on the land (Guzmán Casado & Gonzalez de Molina, 2017). Each of the SAM's forms of organization leaves their *particular mark* on the territory, configuring specific landscapes and specific agroecosystem arrangements. The landscape is the visible mark left on the territory, although hidden marks may materialize in a different, sometimes distant territory, from which natural resources (*land embodied, virtual land*) are imported (Guzmán & González de Molina, 2009; Guzman et al., 2011; Infante et al., 2018a).

### 8.2.2. Funds and flows in Agrarian Metabolism

The metabolic exchange is composed of flows that go in and out of agroecosystems, as described in the EW-MEFA methodology. However, our proposal not only quantifies these flows but also carefully measures whether or not these flows maintain the dissipative structures or fund elements they are endowed with. The distinction between flows and funds was borrowed from Nicolas Georgescu-Roegen (1971) and Mario Giampietro and colleagues (Giampietro et al., 2014) who incorporated it into the MuSIASEM methodology. According to Georgescu-Roegen, the economy's ultimate goal is not the production and consumption of goods and services, but the reproduction and improvement of the processes necessary for their production and consumption. This different understanding of economic activity's main objective implies that from a biophysical point of view, we need to shift our attention away from energy and material flows and instead focus on fund elements, in this case SAM: we must centre our analysis on whether fund elements are improved or at least reproduced during each productive cycle. In other words, our focus switches from the production and consumption of goods and services to sustainability, and whether both production and consumption can be maintained indefinitely.

Accordingly, it is essential to distinguish between flows and funds. Flows include energy and materials that are consumed or dissipated during the metabolic process, such as raw




	Document:	D1.4. Handbook of protocols and methods		
	Author	UJAEN	Version	6
	Reference	D1.4	Date	24/03/2023

materials or fossil fuels. The rhythm of these flows is controlled by external factors - relating to the accessibility of the environment's resources in which the metabolic activity unfolds - and by internal factors - related to the processing capacity of energy and materials, relying in turn on the technology used and the knowledge to manage it. For their part, fund elements are dissipative structures that use inputs to transform them into goods, services and waste, i.e. into outputs, within a given time scale; they remain constant during the dissipative process (Scheidel & Sorman, 2012). They process energy, materials and information at a rate determined by their own structure and function. To do so, they need to be periodically renewed or reproduced. This means that part of the inputs must be used in the construction, maintenance and reproduction of the fund elements, limiting, of course, their own processing rhythm (Giampietro et al., 2008a). The quantities of energy and materials invested in the maintenance and reproduction of the fund elements cannot be employed for end uses. These types of elements can even be improved over time, when energy and materials are allocated for this purpose.

Agroecosystems are, as we have said, dissipative structures that can be decomposed, in turn, into other structures, be they social or ecological. For the purposes of this research, four fund elements were taken into account: land, livestock, agrarian population and technical means of production or technical capital. The four funds are closely connected and represent the fullest manifestation of the socio-ecological relationships at the heart of each agroecosystem and at the centre of the metabolic exchange. The articulation between the four fund elements is fundamental, as we shall see later, to explain metabolic dynamics.

Each fund element has a different nature, either biophysical or social, and therefore each fund element works with different quality flows and different metrics. As pointed out by Giampietro et al. (2014, 29), the flows' characteristics are closely related to the fund they come from. A territory is colonized or land is appropriated by society to generate useful biomass flows; it is usually measured in hectares and subdivided into different uses that produce vegetal biomass, expressed in tons of vegetal biomass per hectare ( $t\ ha^{-1}$ ) – or its equivalent in energy,  $MJ\ ha^{-1}$  – or net primary productivity (NPP). The livestock fund element is the source of flows directed to society as well as to the agroecosystem itself, providing animal biomass for raw materials, food and, to a much lesser degree, energy or services such as traction or manure. It is usually measured in standard livestock units of 500 kg ( $LU_{500}$ ) and the flows it generates are expressed in kg or t of animal biomass  $ha^{-1}$  or LU or  $MJ\ ha^{-1}$  if the flows are expressed in energy units. The agrarian population is the fund element that generates the human work flows. They are usually measured in hours or days of work (hours or days/year<sup>-1</sup>). Finally, the "means of production" fund brings together the

	Document:	D1.4. Handbook of protocols and methods		
	Author	UJAEN	Version	6
	Reference	D1.4	Date	24/03/2023


supply of production tools that generate mechanical work flows or vegetal health services and other services. It is usually measured, for example, in terms of installed capacity, expressed in Kw of power or cv, and its flows in Kw hour<sup>-1</sup> or MJ ha<sup>-1</sup>, etc.

In SAM not only biophysical flows are exchanged, but also flows of information. These flows have the capacity to order and organize components of physical, biological and social systems. As they cannot all be taken into account given their inherent complexity, we selected the information flows with the biggest explanatory capacity regarding farmers' decisions. Agricultural work is also considered as a workflow containing decisive information that organizes agroecosystem structure and functioning. Consequently, we assumed that these decisions were directly influenced by the monetary remuneration that farmers receive in exchange for the sale of their products. Therefore, they constitute a suitable proxy for synthesized information flows. In other words, for the purposes of this research, information flows are defined as follow: flows originating in the agrarian population fund element, in the form of work and incorporated management decisions; and monetary flows stemming from the agroecosystem' s social environment and ending up in this population fund in the form of money obtained in exchange for production. The prices received by farmers, the prices paid for inputs and agricultural income will constitute the main information flows in this research.

To summarize, the four fund elements of agroecosystems we have defined receive flows of energy, materials and originate, in turn, outflows in the form of biomass that society remunerates through monetary flows. These monetary flows, which are also information flows, stop at farmers, who through their agricultural labour, that is, through their tasks, maintain and reproduce the funds. Monetary flows are input information flows and agroecosystem management decisions are output flows. Consequently, energy and material flows, both inputs and outputs, can be broken down into productive, reproductive or maintenance flows of fund elements; meanwhile, information flows are composed of monetary flows (input) and human work flows (output) and normally have a reproductive role. The reproductive capacity of these latter flows determines the dynamics of agroecosystems and the dynamics of the agrarian sector as a whole.

### 8.2.3. The organization and dynamics of agrarian metabolism

The four fund elements that operate in SAM mutually affect each other. This interrelation is expressed in each metabolic arrangement in a particular fashion, giving rise to a sort of unstable equilibrium that makes the AM function as a whole in a specific way. The ability to

	Document:	D1.4. Handbook of protocols and methods		
	Author	UJAEN	Version	6
	Reference	D1.4	Date	24/03/2023

process energy and materials that each fund element has determines not only the magnitude of the flows it generates but also generates restrictions for others. Land availability and its capacity to produce biomass have a direct impact on the magnitude of the flows originating in human work, livestock or means of production. Low availability of human work can, for example, limit the capacity of the land to produce useful biomass, favouring, for example, livestock use of the land and vice versa; very strong traction power can lead to a more intensive agricultural use of the land that would not correspond to the size of the population and its capacity to work; while an excessive volume of the technical means of production or livestock may require importing energy from the outside, in the form of biomass or fossil fuels.

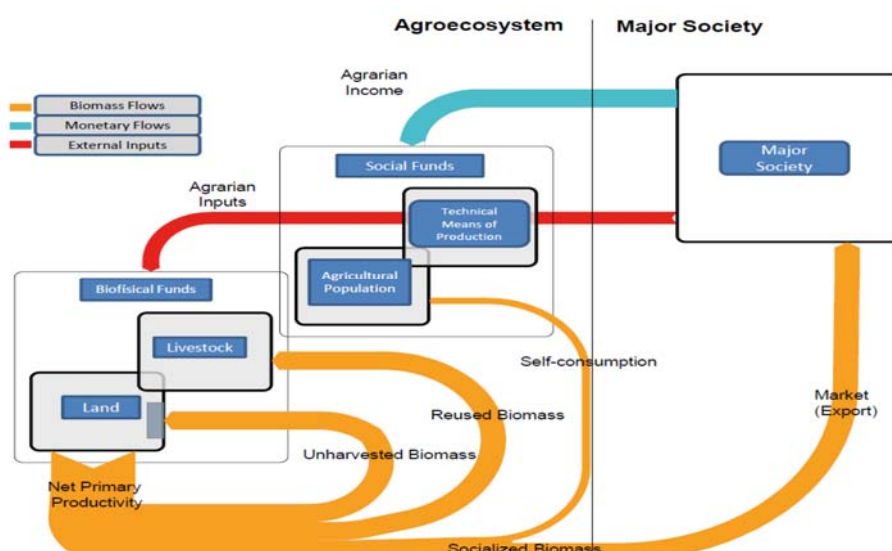



Figure 16. Flowchart of Agrarian Metabolism

The fund elements mutual dependence not only explains the structure, functioning and dynamics of AM, but also constitutes the key to its degree of sustainability i.e., whether if each fund element is capable of providing the services required by SAM itself to function (Giampietro et al., 2014 and 2019) and to do so in a balanced manner over time. The imbalance between each fund' s capacity and the generated flows can make it necessary to seek a new equilibrium, thus causing changes that compromise the medium and long-term viability of the established metabolic arrangement. This consistency between flows and funds and among funds themselves has been made operational through the so-called "sudoku effect" (Giampietro et al., 2014; Giampietro & Bukkens, 2015).

We incorporated this idea into our SAM proposition to evaluate the sustainability or at least get an idea of it: a variable part of the energy and material flows must necessarily be invested in the maintenance and reproduction of the funds and these in turn must preserve the

	Document:	D1.4. Handbook of protocols and methods		
	Author	UJAEN	Version	6
	Reference	D1.4	Date	24/03/2023


necessary relation of congruity in such a way that the flows originated in one fund can help the others to function and vice versa. In our view, the imbalances or lack of correspondence between the funds and their flows explain the metabolic dynamics and, therefore, tendencies towards unsustainability and towards metabolic change.

#### 8.2.4. State of the art of SAM in agricultural field and its application to olive growing

The most widespread SM methodology is the Economy Wide Material and Energy Flow Accounting (EW-MEFA) methodology (Eurostat, 2001; Bringezu et al. 2003). This tool has been largely developed by the SERI, the Wuperthal Institute and the IFF-Social Ecology of Vienna. EW-MEFA is designed to obtain data that support the analysis of the biophysical trajectories of economies and societies, both today and throughout history. It also measures the biophysical relationships between territories, describe and characterize resource consumption and the ways in which resources are appropriated. Sufficiently consistent data can be obtained allowing to evaluate the degree of sustainability of the relations between a given society and its environment. MEFA thus constitutes an appropriate instrument to study the material aspects of society. Economic and social aspects are not incorporated in this methodology. Not many studies have adopted this methodology to analyse biomass production and its role in the economy at large (Schandl & Schultz, 2002; Krausmann et al., 2008; Kovanda & Hak, 2011; Krausmann et al. al., 2011; Gierlinger & Krausmann, 2012; Singh et al, 2012; Infante et al 2015). Most studies focus on the present and their time frame of analysis is fairly limited (Risku Norka, 1999; Risku-Norja & Mäenpää, 2007; for a review of the state of the art, see Infante et al., 2017). Estimates of food system metabolisms (Wirsenius, 2003) or agri-food (Heller & Keoleian, 2003, Infante et al., 2018b; Tello & González de Molina, 2017) and analyses of global and continental biomass flows (Krausmann et al., 2008) have also been carried out. Nevertheless, none of these works applied the methodology to the agricultural sector, nor have they gone into sufficient historical depth to study the transition to the industrial metabolic regime. One exception is the recent study on Social Metabolism of Czech Agriculture in the period 1830-2010 (Greslova et al., 2015).

In the last years, some papers have also been published under the umbrella of the Sustainable Farm System (SFS) project on agricultural case-studies from Austria, USA, Colombia, Catalonia and Canada<sup>1</sup>. These works share a similar approach that highlights the application of metabolic methodologies to agriculture in these countries with both a current

<sup>1</sup> The references can be found at <https://www.researchgate.net/project/Sustainable-Farm-Systems-Long-Term-Socio-Ecological-Metabolism-of-Western-Agriculture>.


	Document:	D1.4. Handbook of protocols and methods		
	Author	UJAEN	Version	6
	Reference	D1.4	Date	24/03/2023

and historical perspective. The research group that composes the Agroecosystems History Lab (AHL), also part of the SFS and Sustainolive projects, has adopted the same approach but with a clearly agroecological orientation. As a result of this, the book *The Spanish Metabolism of Spanish Agriculture, 1900-2010* (Gonzalez de Molina et al., 2020) has been published, in which the SAM is applied to Spanish case.

In this section is presented a preliminary calculation method adapted to the distinctive features of agriculture. This method combines different metabolic traditions (EW-MEFA, MuSIASEM, etc.) with the arsenal of knowledge, theories and concepts proper to Agroecology. Firstly, in accordance with the importance we have attributed to the fund element of reproduction, special attention is paid to what happens inside agroecosystems. We thus developed a specific methodology for calculating net primary productivity (NPP), taking into account all the NPP, both aerial and root parts. From the SAM perspective, the NPP is of interest as a whole since it supports trophic chains. NPP establishes the limits of the maintenance capacity of heterotrophic populations: all members of the animal kingdom (human population, domesticated animals and wild fauna), the fungi, a large part of the bacteria and the archaea. Therefore, appropriation by human societies of NPP affects the maintenance of the rest of heterotrophic organism populations that depend on the same resources.

The standard methodology (E-W MEFA) is based on distinguishing fresh matter products from dry matter products (mainly pastures and forage plants) (Eurostat, 2015), thus adding different kinds of weights. The most rigorous way to consider all types of biomass is to reduce them all to dry matter, as commonly done in specific studies on agriculture from a biophysical perspective (Krausmann et al., 2008; Smil, 2013). Crops with greater water content have become highly relevant, to the detriment of others crops with lesser water content. Therefore, considering the dry weight avoids distortions produced by the different water contents among types of biomass.

Secondly, in line with the Agroecology definition of agroecosystem, the SAM proposition includes economic aspects that have been left out until now. This integration is performed via the study of the monetary flows that enter and leave the system. Society remunerates the agrarian sector for its products, whether agricultural, livestock or forestry products, and this remuneration constitutes the main inflow. Expenditures outside the sector, including expenses related to current means of production acquired on markets (commercial seeds and seedlings, that are not farm-reproduced nor exchanged between farmers, fuels and lubricants, fertilizers and amendments, feed, phytosanitary ware, material maintenance

	Document:	D1.4. Handbook of protocols and methods		
	Author	UJAEN	Version	6
	Reference	D1.4	Date	24/03/2023


expenses, etc.) constitute the outflows. To quantify both flows, we used the data provided by questionnaires (see below). The difference between both flows constitutes the gross value added (GVA) produced within agroecosystem boundaries. Agrarian income is obtained once depreciations, land taxes, fixed assets, or employed labour have been deducted, and the subsidies added together. This constitutes the flow of money with which to reproduce and improve, where appropriate, agrarian metabolism fund elements and, especially, the agrarian population. In this way, the SAM proposal also integrates information flows that traditional methodologies do not contemplate.

Thirdly and last, our proposal makes it possible, unlike other methodologies, to measure both the social and environmental impacts generated by a specific metabolic arrangement on agroecosystems. The perspective we adopted here is as follows: an agroecosystem will be more sustainable if its fund elements are reproduced adequately through energy flows, materials and information. This means that the agroecosystem's capacity to maintain biomass production in the long term, without relying on external inputs, is the chief manifestation of sustainable management. So far, methods for assessing agricultural sustainability have mainly relied on a battery of indicators of potential natural resource degradation problems e.g. the “Framework to Assess Natural Resources Management Systems incorporating Sustainability Indicators” (*Marco para la Evaluación de Sistemas de Gestión de Recursos Naturales que Incorporan Indicadores de Sostenibilidad*, López-Ridaura et al., 2002) or the Sustainability Assessment of Farming and the Environment (SAFE) (van Cauwenbergh et al., 2007). However, their usefulness is limited because they do not reflect the functioning of the agroecosystem or describe the funds' reproduction mechanisms and, therefore, they do not reveal much about the processes that cause degradation or the interrelationships between them. Specific modes of calculation are detailed later on.

#### 8.2.5. Methodological application to SUSTAINOLIVE project

In this work, the methodology and conceptual framework of Agrarian Metabolism have been applied to Mediterranean olive groves according to the methodological guidelines proposed in *Energy in Agroecosystems* (Guzmán and González de Molina, 2017; González de Molina et al., 2020). This work sets out how the material and energy flows accounting in agroecosystems should be done. The different considerations on biomass fluxes (NPPact partitioning), the material and energy converters used (see below) and the energy indicators calculated (EROIs) have been extracted from it. Although this book is the most comprehensive academic work on the application of Agrarian Metabolism to case studies, it



	Document:	D1.4. Handbook of protocols and methods		
	Author	UJAEN	Version	6
	Reference	D1.4	Date	24/03/2023


includes two works whose contribution has to be highlighted, those of Aguilera et al. (2015) and Guzmán et al. (2014). The former develops a comprehensive review and proposal for the assessment of energy incorporated in industrial inputs, whereas the latter compile a database of NPP converters to estimate biomass partitioning and determine the gross energy contained in the different biomass portions of main herbaceous and fruit trees, but also in industrial and livestock products.

The methodology of Agrarian Metabolism proposed in the aforementioned works is suitable for any scale - from farm scale to global scale. However, as authors establish, the converters and reference values gathered in these works need to be updated according to new research and adapted to each case study. Indeed, field data and historical data must always be the preferred source of information. When field or historical data cannot be obtained, they can be replaced by results produced in studies under similar conditions or modelled from proper equations.

During 2020 and 2021, samples of biomass, organic amendments and soil were taken in many of the SUSTAINOLIVE olive grove plots and analyzed in laboratory. Additionally, an extensive interview was conducted. The results of both procedures were used as input data in the Agrarian Metabolism model (i.e. the excel spreadsheet below described).

In all the SUSTAINOLIVE plots, samples of soil were taken to determine its density, organic matter content, and other physico-chemical characteristics by lab methods. The aerial biomass production of olive trees was calculated by direct measures in several olive trees of some SUSTAINOLIVE plots. The biomass of permanent structures – trunk and main branches - was obtained by the biovolume method, consisting on measuring the volume of the wood and transforming it to dry weight applying a density factor. Pruning material was weighted just after cutting and some samples were taken. The volume and weight of these fresh samples were measured, and they were dried in an oven to determine the density (green volume – dry weight) and the dry matter content.

A long term experiment was conducted in four Spanish olive groves plots to determine the biomass of leaves, flowers and fruits naturally falling throughout the year and also during harvest. The biomass fell from the tree was collected in boxes, sampled every 3 months during a year, and dried in an oven. In addition, biomass residues falling during the harvest were also measured and samples were taken to determine its dry matter content. The aerial biomass produced per tree was extended to one hectare by multiplying by the tree density. For the olive groves where fractions of this aerial biomass can not be measured, it was

	Document:	D1.4. Handbook of protocols and methods		
	Author	UJAEN	Version	6
	Reference	D1.4	Date	24/03/2023


estimated from similar plots or modelled. The aerial biomass of cover crops was measured in most of the SUSTAINOLIVE plots where they are left to grow. In these plots, cover crop was harvest in five random squares of 0.25 m<sup>2</sup>, and the obtained biomass was dried in an oven. The productivity calculated was assigned to the area really covered by the cover crop to know the aerial biomass production of cover crops per hectare. Other material flows were modelled or estimated from converters proposed by Guzmán and González de Molina (2017). Soil losses by erosion were determined from RUSLE model and material flows involving livestock were determined – feed consumption and excreta – by the animal dietary balance. Data from the interview were used to adjust the measured and modelled flows and to entirely estimate some of the material flows such as the organic amendments or the olive yield. Energy flows were determined based on the material flows and the energy converters proposed by Guzman and Gonzalez de Molina (2017). They will be further explained.

Together with the material and energy flows accounting, an economic study was performed. To this purpose, economic data were required in the interview. The results of the economic study were used integrated on the final analysis of the sustainability of the farm. From now on, we will focus on the biophysical (material and energy) exchanges.

To perform the calculations in an orderly and, to some extent, automatic manner, the Excel Microsoft program was chosen. The model created is divided into four excel sheets. Two spreadsheets have been dedicated to the calculations of material and energy flows, while the other two are associated respectively with the previous ones and contain the converters and factors needed for the calculations. In the following, we will go deeper into the description of each excel sheet as well as the calculations performed.

### Material flow spreadsheet


This spreadsheet is divided into sections following the classification of Agrarian Metabolism. Since internal cycles of material and energy are registered as well as inputs and outputs, different sections or specific material flows can be expressing different phases of the same flow, that is, different physical expressions of the same energy. At the end of the spreadsheet we provide indicators in which this aspect was considered to avoid double accounting. All data are expressed per hectare and year.

	Document:	D1.4. Handbook of protocols and methods		
	Author	UJAEN	Version	6
	Reference	D1.4	Date	24/03/2023

The first sheet section contains the basic characteristics of the plot, namely the area in hectares, the farming system (traditional, intensive or superintensive) and the type of management (organic, conventional or integrated).

The Net Primary Productivity (NPP) section below includes the breakdown of the different components or biomass categories produced in the plot. Each biomass category is required in fresh matter and then transformed into dry matter by applying dry matter converters (from “Material converters” spreadsheet, see below). *Socialized Vegetable Biomass* (SVB) (A1) is the phytomass that is directly appropriated by society, considered as it is extracted from the agroecosystem, prior to its industrial processing. It includes the olive fruits, the wood, the light pruning (when is exported for electricity production) and the cereal grain and straw (when cereal is grown between olive rows). Following Agrarian Metabolism concepts, the *Reused Biomass* (RB) is the phytomass that is intentionally returned to the agroecosystem by the farmer. Therefore, it does not cross the agroecosystem boundaries. Within this category, we differentiated two components.

*Reused Biomass* (B1) refers to the residual biomass that is intentionally incorporated to the soil (composted or not). In this category, we have included the following residues that are usually generated in Mediterranean olive groves: light pruning (burned or shredded); leaves (those that fall during the harvest process and go to the olive mill mixed with the olives); stems (fallen due to the harvest process); cereal residues (if cereal is grown); vegetation cover (spontaneous weed that is left to be grown in the orchard and then cut and incorporated to the soil before dry season); green manure; and any other source of organic matter coming from other plots of the same farm. *Reused biomass used as feed* (B2) includes the biomass considered as residue that is intentionally given as feed to livestock. The following items are included: light pruning, leaves (returned from the processing plant, see B1), cereal residues and the spontaneous weed that are allowed to grow to feed grazing animals. The next category, *Unharvested Biomass* (UhB), contains all the biomass that is not intentionally managed but is left in the soil without any human work. Flowers, leaves and fruits that naturally fall to the soil along the season and the dying roots of the olive trees, as well as the belowground biomass of cereals, spontaneous vegetation cover and green manure are the items included as unharvested biomass. Finally, *Accumulated biomass* (E) is the portion of biomass incorporated to perennial plant structures, both aboveground (trunk and main branches) and belowground (living roots).


	Document:	D1.4. Handbook of protocols and methods		
	Author	UJAEN	Version	6
	Reference	D1.4	Date	24/03/2023

The third section account for the *Socialized animal biomass* (SAB)(A2). This is the animal biomass directly appropriated by the society, in this case, milk, live weight of meat at the farm gate and eggs (depending on what type of animal makes up the livestock herd).

The fourth section, *On farm animal inputs* (F) is dedicated to the animal inputs whose origin is within farm boundaries and not brought from the outside, that is, excreta and/or manure that recirculates within the agroecosystems. This section is divided into feces (F1), urine (F2) and feces and urine together (F3), to be fulfilled according to the methods of management of livestock and excreta. The animals from which these residues commonly originate in Mediterranean olive groves are: pig, poultry, cow, horse and sheep.

The fifth section is *Industrial Inputs*. This one is dedicated to inputs incorporated in the olive grove that have an industrial origin, that is, they are manufactured or produced in factories or processing plants. In the first place, the *Inorganic fertilizer* (G) section details the name, the quantity applied and the content of the main nutrients. Secondly, *Pesticides* (H) are divided into *Herbicides*, *Insecticides*, and *Fungicides*. For each product, the name and the related active matter, the amount applied by the farmer and the content of active matter have been registered. The next inorganic input is the *plot fuel consumption* (I), referring to the direct fuel consumption at the farm gate due to the realization of farming tasks. It covers all the farm tasks typical of Mediterranean olive groves, classifying them according to the type of energy carrier consumed. Data are requested in litres of diesel and gasoline per hectare and then converted to kg per hectare by multiplying them by the fuel density (in “Material converters” spreadsheet). For decades, all tractors run on diesel, so tasks run by diesel are those performed with tractors such as harvest by trunk shaking, soil tasks, fertilization, and so on. In turn, manual powered tools as chainsaws for pruning, manual shakers and blower machines for harvest, and brush cutters run on a mix of gasoline and oil or they are electrically powered. Therefore, task run by gasoline are those executed by manual tools. The tasks that can be performed with electrical power have been also included although this flow do not account for the material flow.

The last industrial input to be taken into account is *Machinery* (J). In this case, we have calculated the kilograms of weight of the most commonly used machinery that can be virtually imputed to one hectare of the farmland, according to the time taken for each task. For the self-propelled machinery (tractor, olive harvester, cereal harvester, buggy, bobcat, ATV and cars) data required is the installed power (kW), the machine weight (kg) and the useful life (h); then the weight per hour is calculated. In the case where these data are not available, we provide some standardized data from literature in “energy converters”

	Document:	D1.4. Handbook of protocols and methods		
	Author	UJAEN	Version	6
	Reference	D1.4	Date	24/03/2023

spreadsheet (see below). For the agricultural implements, the weight (kg) and the lifetime (h) were assumed to be the same for all the cases.

By multiplying the weight per hour calculated by the time employed in each task, we know the kilograms of machinery attributable to one hectare of the olive grove.


To calculate the total working time per hectare of each self-propelled machine and implements, we have registered the following information for each task: frequency of the task, operation time of every piece of equipment, number of workers, and total human hours. The task and subtasks listed are the following: harvest (olive harvest and cereal harvest), pruning (pruning, stacking of pruning, light pruning shredding and wood gathering), weed control (herbicide application, weed mowing with tractor and manual weed clearing), soil (disk harrow, cultivator, drag harrow, and roller), fertilization (centrifugal broadcaster, atomizer, manure spreader and slurry tank), and others (ex. alperujo recovery, composting,...).

The seventh section included in the material flow accounting is *Non-industrial inputs*. Contrarily to the section described above, this section contains data of inputs of non-industrial origin brought in from outside the farm boundaries. Within this last section we included 7 categories of inputs. First of all, we consider the manure brought from the outside of the farmland (*Off-farm manure inputs*, K1) classified by animal species. Then, *Other organic inputs*, K2, such as olive pomace ( “alperujo” ); other compost, organic fertilizers, leaves, straw, sludge and others. *Animal feed/bedding* (L) differentiates between grain, fodder, cereal straw and mixed feed. The next section, *Seeds* (M), introduces cereal and green manure seed sown between olive rows. The final sections account for water inputs for *Irrigation* (N1), *Water for animals* (N2) and *Human labor* (O) employed per hectare per year. This last three sections are not material flows but have been registered for calculation purposes.

Finally, the *Soil losses by erosion* (P) section details the amount of soil loss yearly by erosion and its content in organic matter.

Once fulfilled all these sections, the different indicators and categories of Agrarian Metabolism are calculated. Some of the categories included in the energy flow accounting are not contained in the material flows given that they do not have a material equivalent. The spreadsheet automatically calculates the following components:

Socialized Vegetable Biomass (SVB): the vegetable biomass directly appropriated by society.

	Document:	D1.4. Handbook of protocols and methods		
	Author	UJAEN	Version	6
	Reference	D1.4	Date	24/03/2023

Socialized Animal Biomass (SAB): the animal biomass directly appropriated by society. This category does not sum for NPPact as it is not of vegetable origin.

Socialized Biomass (SB): is the sum of the SVB and SAB.

Reused Biomass (RuB) is the result of adding all the residues intentionally incorporated to the soil and those given as feed to livestock (as long as they do not cross agroecosystem boundaries).

Unharvested Biomass (UhB) accounts for aerial and root biomass abandoned in the agroecosystem.

Recycled biomass (RcB) is the sum of RuB and UhB, and represents all the biomass that recirculates within the system no matter if it is intentionally or not intentionally incorporated.

Accumulated Biomass (AB) results of adding aerial perennial structures accumulated in one year and those accumulated belowground.

$NPPact = SVB + RuB + UhB + AB$

Inorganic input: is the sum of the inorganic fertilizers, pesticides, fuel use and machinery involved.

Organic input: is the sum of organic inputs such as external manure or compost.

External input (EI): is the sum of organic and inorganic inputs. Human labor and water are not considered material flows.

Total Inputs Consumed (TIC): is the sum of EI and RcB

Although in the SAM methodology, soil losses are not usually taken into account when applied at a larger scale than the farm, due to the difficulties involved in their calculation, soil losses are also calculated in this case: is the total amount of soil lost by erosion (both organic and inorganic matter).

As stated by Soto et al. (2016), correction factors to consider biomass losses due to pests, etc. in the estimation of NPP have a high degree of uncertainty, and thus they were not considered.

We have calculated also the main metabolic indicator from the Economy-wide Material Flow Accounting (EW-MEFA) methodology.

Domestic extraction (DE): is the sum of SVB and RuB. It reflects the biomass directly or indirectly appropriated by society.


Imports: all the external flows that enter in the agroecosystem.

Exports: all the flows that leaves the agroecosystem.

Physical trade balance (PTB): it is obtained by the difference between Imports and Exports.

Domestic material consumption (DMC): It is calculated by adding DE and PTB.



	Document:	D1.4. Handbook of protocols and methods		
	Author	UJAEN	Version	6
	Reference	D1.4	Date	24/03/2023

## Material converters

Briefly, material conversion factors allow us to:

- convert the fresh matter into dry matter and vice versa
- estimate different categories of biomass of the NPP
- estimate the food intake and excreta of livestock

Dry matter converters transform fresh matter into dry matter. Most of this converters come from Guzman and Gonzalez de Molina (2017), and the rest from our experimental data or reviewed field studies.

Biomass partitioning factors included in this spreadsheet are the residue index and the root to shoot ratio. The residue index calculates the fresh weight of the residues produced from the fresh weight of the corresponding products. In the case of olive trees, an equation and some reference values are provided to estimate the production of wood and light pruning from the olive production. Similarly, conversion factors to estimate the straw production from grain production in cereals are shown.

The root to shoot ratio shows the relation between the aerial part (excluding fruits) and the belowground portion, and it is commonly expressed in dry matter. This conversion factor is provided for olive trees, weeds and cereals.


We also provide a set of reference values of biomass produced by cover crops, biomass accumulated in the trees annually and others.

Besides biomass partitioning factors, material converters also include the different percentages of nutrient content (N, P<sub>2</sub>O<sub>5</sub>, K<sub>2</sub>O, SO<sub>3</sub>) of most common fertilizers (Ammonia, Ammonium Nitrate, Ammonium Sulfate, Calcium-Ammonium Nitrate, Calcium Nitrate, Urea, Potassium Nitrate, ...).

Finally, manure nutrient contents are provided along with calculations to assess the livestock balance (daily kg of dry matter food/kg of body weight, daily kg dry matter manure/kg body weight, and daily kg dry matter excreta/kg body weight).

## Energy flow spreadsheet

Once we have calculated the materials flows, and by applying the energy converters (see following section), the energy flows of the olive groves are calculated. All the data in this spreadsheet are given in joules (or a multiple) per hectare and year.

	Document:	D1.4. Handbook of protocols and methods		
	Author	UJAEN	Version	6
	Reference	D1.4	Date	24/03/2023

This spreadsheet covers the same sections than the Material flow spreadhseet.

The NPP components, the Socialized Animal Biomass, the biomass recirculation through livestock excreta, and the soil losses, express the gross energy of their equivalent material flows. Meanwhile, the energy flow of external organic inputs reflects the gross energy of their equivalent material flow plus the energy required in processing and transporting them (embodied energy). It is important to clarify that energy flow of external organic inputs (seed, feed, organic residues, etc.) do not account for the energy required in their production process, since that energy is imputed to the agroecosystem in which they were produced. On the other hand, the energy flow of human labour reflects the total energy per hour. Finally, the energy flow of industrial inputs accounts for the energy requirements for i) the extraction of raw materials (including the energy carriers used in the manufacture process), ii) the manufacture and processing, iii) the distribution and transport to the farm and, if applicable, iv) the maintenance. In the case of energy carriers (fossil fuels and electricity), the gross energy of the element itself is added to the embodied energy.

At the end of the spreadsheet, a list of indicators has been included. All indicators are equivalent to those of the material flow spreadsheet, but energy flows attributable to water flows and human work, which don't have a material equivalent, have also been added as components of External input.

In addition, there are specific indicators for energy flows:

Non-Renewable Energy (NRE): it reflects the energy flows from non-renewable sources, that is, the embodied energy of industrial input and water flows.

Renewable Energy (NRE): it reflects the energy flows from renewable sources. It is calculated as the sum of energy flows from organic input (only gross energy) and human labor.


Finally, the energy efficiency as a proxy of agroecosystem sustainability is assessed by using the EROIs proposed by Tello et al., (2016) and Guzmán and González de Molina (2017):

i) Economic EROIs: These EROIs have traditionally been calculated on the sole basis of supply services, given that these have a direct impact on society or the farmer, ignoring the fact that regulation and maintenance services are essential for supply services to survive over time (Tello et al, 2016).

Final EROI tells us the return on the energy investment made by society.

$$FEROI = SB/(RuB+EI)$$

External final EROI relates EI to the final output crossing the agroecosystem boundaries, and assesses to what extent the agroecosystem analyzed becomes a net provider or rather a net consumer of energy.

	Document:	D1.4. Handbook of protocols and methods		
	Author	UJAEN	Version	6
	Reference	D1.4	Date	24/03/2023

$EFEROI = SB/EI$

Internal final EROI tells us the efficiency with which the biomass that is intentionally returned to the agroecosystem is transformed into a product that is useful to society.

$IFEROI = SB/RuB$

ii) Agroecological EROIs: These EROIs have been developed to inform about the sustainability of the agroecosystem (Guzmán and González de Molina, 2015).

NPPact EROI estimates the real productive capacity of the agroecosystem, whatever the origin of the energy it receives, i.e., solar for the biomass or fossil for an important portion of the EIs. This is an indicator that provides integrative information on the state of the agroecosystem, beyond the particular situation of each fund element. A decreasing trend in NPPact EROI values of an agroecosystem over time indicates degradation of the productive capacity (Guzmán et al. 2018).

$NPPact\ EROI = NPPact/TIC$ , (Total Input Consumed =  $RuB + UhB + EI$ ).

Biodiversity EROI provides useful information on the extent to which energy invested in the agroecosystem contributes to sustaining food chains of heterotrophic species (Guzmán et al. 2018).

$Biodiversity\ EROI = UhB/TIC$

Woodening EROI estimates whether the energy added to the system is contributing to the storing of energy in the system as AB. A decreasing trend in this EROI indicates a deterioration of the woodland fund element (Guzmán et al. 2018).

$Woodening\ EROI = AB/TIC$


Further information about the calculation in energy terms of NPPact and its components, and of the external inputs, can be found in detail in Guzmán Casado and González de Molina (2017) and Guzmán et al. (2017).

## Energy converters

These factors allow us:

- to convert the biomass (dry matter) into gross energy.
- to calculate embodied energy of the industrial inputs.
- to calculate embodied energy of organic external inputs.

The first group of converters has been taken from the work of Guzmán and González de Molina (2017). Gross energy values of biomass were obtained from its composition and standardized energy values of fats, proteins, and carbohydrates. Since biomass produced in olive groves (olives, pruning, weeds,...) is highly stable in terms of composition, this is a fair approach to calculate the gross energy.

	Document:	D1.4. Handbook of protocols and methods		
	Author	UJAEN	Version	6
	Reference	D1.4	Date	24/03/2023


To detail the origin and suitability of the energy converters of the industrial inputs, they have been classified as follows:

*Agrochemicals.* Guzman and Gonzalez de Molina (2017) provide a set of energy converters to calculate the embodied energy of different fertilizers and pesticides. In the case of fertilizers, embodied energy can be calculated from the content of the different nutrients (N, P<sub>2</sub>O<sub>5</sub> and K<sub>2</sub>O) according to their chemical formulation. In the case of pesticides, it can be calculated from the content of active matter. When data about specific fertilizers or active matters of pesticides were not available in this work, the embodied energy of these products was obtained from LCA studies or some of the SimaPro databases.

*Fossil fuels.* The energy converters for fossil fuels were entirely obtained from the work of Guzman and Gonzalez de Molina (2017).

*Machinery and implements.* Leaving aside the fuel consumed during field operations, the embodied energy of machinery and implements can be broken down into i) energy attributable to the extraction and processing of raw materials (including fossil fuels) ii) energy attributable to equipment manufacture, iii) energy attributable to the transport of this equipment from the manufacture location to its destination and iv) energy attributable to the maintenance. The work of Guzman and Gonzalez de Molina (2017) provides historical data of energy requirements of each process for three categories: tractors, tillage implements and other implements. For tractors and tillage implements, the energy converter we used was the total embodied energy in MJ per kg of machinery. The mass and useful life of tractors were calculated from a general specific weight for tractors (kg per kW of power) and field-based estimations of useful life, respectively. The mass of tillage implements was estimated from catalogs of manufacturers. As the agricultural implements under the heading "other implements" can be very different from each other, we recalculate the energy requirements attributed to raw materials when the material composition of these implements was known or could be estimated. The energy requirements of other processes were kept. Thus, for the non-tillage implements, the energy converter of total embodied energy in MJ per kg of machinery with little modification was used. The mass of these implements was estimated from catalogs of manufacturers.

*Irrigation.* Energy requirements for irrigation can be very variable according to the energy requirements of water extraction and the embodied energy of irrigation infrastructure. Average values of energy requirements of irrigation infrastructure from Guzman and Gonzalez de Molina (2017) were used in all the plots, and, when direct energy consumption

	Document:	D1.4. Handbook of protocols and methods		
	Author	UJAEN	Version	6
	Reference	D1.4	Date	24/03/2023

of water pumping was not available, the energy requirement for water extraction was calculated from the well depth and the energy converter from Guzman and Gonzalez de Molina (2017).


*Organic external inputs.* The embodied energy of organic external inputs was calculated as the sum of their gross energy and the energy required in processing (composting) and transporting them. Guzman and Gonzalez de Molina (2017) provide reference values for both the gross energy and the processing and transporting energy for different products.

### 8.3. Life Cycle Methodologies (LCA, LCC, sLCA)

#### 8.3.1. Origin, background, and theoretical principles

Within the theoretical framework of Life Cycle Thinking (LCT) (Heiskanen, 2002), many methodologies have been developed to assess the sustainability impacts of the production and consumption of goods and services, all throughout their life cycle, i.e. from the "cradle" (e.g., the planning phase) to the "grave" (e.g., the disposal phase). More in details, Life Cycle Costing (LCC) was the first methodology to be developed, applied since the fifties for industrial investments appraisals; Life Cycle Assessment (LCA) is the one that mostly attracted the attention of researchers and practitioners, it now a renowned and standardized methodology (ISO, 2021); it assesses the environmental impacts of products or processes referring to specific midpoint or endpoint impact categories, concerning human health, ecosystem quality and resource use (Horne et al., 2009). Social Life Cycle Assessment (SLCA) is the latest tool developed with the LCT framework, and it is aimed at assessing the social impacts deriving from the life cycle of products and services; a specific ISO norm (num. 14075) is currently under development. The process of standardization is being long and difficult due to the multiparadigmatic characteristics of social sciences (Iofrida et al., 2018). Almost recently, Social Organizational Life Cycle Assessment (SOLCA) has been proposed to assess the behaviour - in terms of social performances - of companies.

LCA was developed the first time inspired by the economic appraisal of projects life cycle (first applications of LCC) in the industry sector, to assess the impacts of product or service considering all phases of the life cycle (from cradle to grave), helping to highlight, and therefore prevent, possible burden shift among phases. During the nineties, SETAC improved the already existing Resource and Environmental Profile Analysis (REPA) method (precursor of LCA) and proposed for the first time a life cycle model for environmental impacts assessment in order to (Curran, 1996) objectively evaluate the environmental

	Document:	D1.4. Handbook of protocols and methods		
	Author	UJAEN	Version	6
	Reference	D1.4	Date	24/03/2023

burdens associated to a product, process or activity by identifying all inputs (mass and energy) and outputs such as products, wastes, emissions (Fava et al., 1991).

The LCA methodology is standardized by specific ISO norms since 1997, which have been constantly updated (ISO, 2006; 2021). The perspective of assessment can differ according to the aim of evaluation: attributional LCA is aimed at describing environmentally relevant physical flows between a life cycle and its subsystems, while consequential LCA describes how environmentally relevant flows will change in response to possible decisions (Ekvall, 2019).


The ISO (2021) standards describe four different and iterative steps to conduct an LCA study, which are a reference also for the other life cycle methodologies, as an umbrella procedure to homogenize the evaluations:

1. *Goal and scope.* This step entails the definition of the purpose of the evaluation, the width of the system boundaries, the outline of the foreground and background systems, the choice of cut-off and allocation criteria as well as the Functional Unit (FU), which is the measure unit to which refer all impact and is needed to compare life cycle phases or different scenarios.

2. *Life Cycle Inventory.* In this step, quantitative and qualitative data are collected; inbound and outbound flows of energy, materials and emissions are accounted and validated. This is useful especially when circular systems are under assessment; indeed, circularity indicators are usually based on the account of balances of mass and energy. Data quality check is of utmost importance to ensure the reliability of results. Primary data can be collected by means of the typical methods of social research: questionnaires, interviews, surveys, focus groups, Delphi method with the eventual participation of stakeholders involved with different degrees of intensity. Secondary environmental data are available for many productive sectors: the main used for agricultural systems are Ecoinvent, Agri-footprint, World Food LCA Database.

3. *Impact assessment of product or service life cycle.* This step is done by means of recognized environmental characterization models that allow estimating midpoint and endpoint impacts such as ReCiPe2016 (Goedkoop et al., 2013; Huijbregts et al., 2016), LC-Impact (Verones et al., 2016) and Impact World+ (Bulle et al., 2019). Impact categories are selected and, for all of them, relevant indicators allow implementing the contribution analysis of individual processes within the cycle under study.



	Document:	D1.4. Handbook of protocols and methods		
	Author	UJAEN	Version	6
	Reference	D1.4	Date	24/03/2023

4. *Interpretation of results.* This is a critical step aimed at identifying, checking, and comparing information from the results obtained to retrieve new knowledge; inventory and impacts assessment results are summarized, and insights are inferred, in order to provide conclusions and recommendations for readers in an exhaustive and comprehensive way (Hernandez et al., 2019). Therefore, interpreting life cycle results means identifying significant issues, comparing life cycle phases and/or productive scenarios to draw conclusions while identifying limitations and further research needs.


LCA evolved over the years, through a process of refining and consensus building at academic level, being constantly improved and adapted. For example, characterization factors and emission estimation models are constantly updated (e.g. USEtox and PestLCI) according to the advancements of scientific research (see Fantke, 2019).

Today, LCA-based methods have been implemented to serve certification standards such as Environmental Footprint of Product (PEF), Environmental Product Declaration (EPD), Global GreenTag's LCARate certification, but also the Carbon Footprint (BSI, 2011; ISO, 2006c, 2013), Water Footprint (ISO, 2014), Ecological Footprint (GFN, 2009).

LCC' s first purpose is to account for all financial costs across the life cycle phases; the main difference with LCA is that there are no specific standardized norms, neither databases nor characterization models. Moreover, three possible approaches exist, namely financial or conventional LCC (C-LCC), environmental LCC (E-LCC) and societal LCC (S-LCC) (Stillitano et al., 2022).

C-LCC is a quasi-dynamic model (De Luca et al., 2015) that evaluates internal costs like the total cost of ownership (TCO); it takes into account many kind of stakeholders such as consumers, manufacturers, or project managers, i.e. those who are directly involved in the cash flows.

E-LCC, in addition to direct monetary flows of the life cycle, assesses externalities' monetary values (i.e., the environmental impacts in monetary terms). It summarizes all costs(real money flows) associated with the life cycle of a product or service that are directly covered by those actors involved in the life cycle, such as producers and consumers, including externalities that are expected to be internalized in future decisions. The E-LCC is not a stand-alone evaluation process but is considered as complementary to LCA, and it extends the purposes of C-LCC to be consistent with the system boundaries and functional


	Document:	D1.4. Handbook of protocols and methods		
	Author	UJAEN	Version	6
	Reference	D1.4	Date	24/03/2023

unit (FU) and other main elements of life cycle evaluations according to the ISO (2021) norms (Mayanti and Helo, 2022). E-LCC allows estimating the external costs in terms of monetary value of indirect damages that are not marketable (goods or services without a market) (Stillitano et al., 2022).

S-LCC includes the monetary value of externalities corresponding to environmental and social impacts and can provide interesting insights for public authorities and policy decision makers (Stillitano et al., 2022). Societal LCC also aims to assess the socio-economic efficiency of given scenarios by estimating welfare loss or gain (Ylyas et al., 2021).

Social LCA (SLCA) is the latest tool developed within the Life Cycle Thinking methods, with a first publication in 1997 (O’ Brien et al., 1997); its principal aim is to evaluate social impacts deriving from products or services’ life cycles, affecting different typologies of stakeholders, such as workers, local communities, value chain actors, consumers, societies, and children (UNEP, 2020). The general methodological setting to assess social impacts is the same that of LCA for the environmental ones (the four steps above mentioned); but while LCA is regulated by specific ISO norms (2021), SLCA is still not consensually defined, and the most diverse methodologies have been proposed in literature (Iofrida et al., 2018). A specific standard, the ISO norm 14075 “Principles and framework for social life cycle assessment” , is under development (in preparatory phase). After approximatively ten years, UNEP (2020) updated the Guidelines for SLCA, and the Methodological Sheets for subcategories in SLCA (UNEP, 2021), providing some guidance for social evaluations of life cycles, such as a list of possible impact categories, subcategories and indicators per each stakeholders’ groups. According to them, there are two main families of approaches, corresponding to different impact assessment procedures and each of them responding to different practical research aims: the Reference Scale Approach (Type I), and the Impact Pathway Approach (Type II). SLCA Type I assesses the social performance of companies of organizations involved in the product system, by comparing their behaviour to a reference scenario (for example, specific legal regulations).


The comparison is made according to specific primary or secondary data, information or stakeholders opinions, and therefore the evaluation consists in the description of a current status and not in the accounting of the links between the life cycle and long-term impacts. Therefore, the characterization process is based on interpretation. On the other hand, SLCA Type II evaluates social impacts through causal or correlation/regression-based relationships between the product or service life cycle. The characterization process is based on an analytical and quantifiable identification of the consequences of the life cycle.

	Document:	D1.4. Handbook of protocols and methods		
	Author	UJAEN	Version	6
	Reference	D1.4	Date	24/03/2023

Examples of SLCA type II methodologies can be found for example in the Preston pathway (Feschet et al., 2013), in the Wilkinson pathway (Bocoum et al., 2015) and in the Psychosocial Risk Factors pathway (Iofrida et al., 2019). According to UNEP (2020) the SLCA Type II is epistemologically and methodologically more in line with environmental LCA, where inventory inputs are quantitatively linked with environmental impacts. This duality of procedure is due to the multiparadigmatic characteristics of social sciences: actually, in SLCA, both interpretivist and post-positivist epistemological positions have been applied in scientific literature (Iofrida et al., 2018).

Most of the studies published are framed within the interpretivist paradigms, evaluating in a qualitative or normative way a wide range of impact categories mostly linked to companies' behaviour (e.g. child labour, corruption, fair salary, etc.), rather than to the life cycle functioning. Few studies can be found in literature framed in the post-positivist paradigms, i.e. quantifying cause-effect relationships between life cycle functioning and Areas of Protection (AoP) in an objective and generalizable way. Concerning the assessment of companies' behaviours, recently a specific tool has been proposed within the life cycle methodologies: Social Organisational Life Cycle Assessment (SOLCA) is aimed at assessing the socio-economic and social aspects of the activities of a whole organisation (or a portion of it) through a life cycle perspective (Martínez-Blanco et al. 2015; UNEP 2020; D'Eusano et al., 2022). The methodological framework of SOLCA derives from an integration of SLCA and O-LCA (ISO/TS 2014), and therefore, shares the same phases of LCA (i.e., Goal and Scope Definition, Inventory, Impact Assessment, and Interpretation). Thus, SLCA does not have a unique impact assessment method nor characterization models, but some specific databases and methods have been set up to assess social risks within the SLCA type I approach, like Product Social Impact Life Cycle Assessment (PSILCA) and the Social Hotspot Database (SHDB), which can be used with the LCA software (SimaPro, Open LCA, etc.).

However, recent literature reviews put in evidence that SLCA still remains a young and immature method, suffering many barriers such as the variety of impact categories, the lacking of linking life cycle structures to social phenomena or the difficulty of tracking social impact pathways (Pollock et al., 2021). Concerning in particular type II SLCA, some authors highlighted that many models need to better clarify cause-and-effect chains, relationships with social sciences, and more explicit measurement models. Most of them do not present ready-to-use characterization factors, and only a few models consider the time lag between cause and effect. Finally, several models are not always connected to company data. Furthermore, there is a lack of literature specifically focused on socio-economic life cycle

	Document:	D1.4. Handbook of protocols and methods		
	Author	UJAEN	Version	6
	Reference	D1.4	Date	24/03/2023

assessment: few authors paid attention to the possible synergies of combining S-LCA and LCC, such as for example Barke et al. (2020).


Finally, Life Cycle Sustainability Assessment emerged in the academic panorama to meet the requirement of an overall assessment methodology, able to cover all aspects of sustainability. Many procedures have been proposed for a comprehensive assessment methodology that can cover all dimensions of sustainability, called Life Cycle Sustainability Assessment (LCSA); among them, the most implemented procedure is represented by the equation  $LCSA = LCA + LCC + SLCA$ . The integration or combination of sustainability results can be made in many ways. According to de Luca et al. (2017), Multicriteria Decision Analysis (MCDA) can help LC practitioners to overcome trade-offs among the different dimensions of sustainability, but also to deal with subjective assumptions in an objective way, and to take into consideration stakeholders' values and desiderata.

### 8.3.2 State of the art in agricultural field and olive growing

Olive oil production is a relevant agri-industrial sector in terms of both production and consumption in Europe. However, although being so widespread and having a relevant impact on economy and the market (Stillitano et al., 2016), olive oil production is associated with several adverse effects on the environment that cause resource depletion, land degradation, air emissions and waste generation (Strano et al., 2014). The impacts may vary significantly as a result of the practices and techniques employed (Iofrida et al., 2018) in olive cultivation and olive oil production as well as with the analysis techniques adopted in the study and its assumptions (De Luca et al., 2018).

Several approaches are available concerning economic aspects as in (Stillitano et al., 2017) as well as about the long term feasibility of such systems (Stillitano et al., 2018) and/or social aspects, to account the complexity on such a relevant and cross-cutting market aspect. A well-recognised and solid approach towards the environmental sustainability of the olive oil sector is widely recognised in the Life Cycle Assessment (LCA) methodology (De Luca et al., 2018b), that can be applied within the framework of a more integrated sustainability performance evaluation (Büyükoçkan and Karabulut, 2018), or in combination of the aforementioned methods (Kyriakopoulos, 2008).

Based on mass and energy balances developed in steady state, LCA aims at computing all flows in the life cycle of a product or of a service, through its “cradle” to its “grave” ,


	Document:	D1.4. Handbook of protocols and methods		
	Author	UJAEN	Version	6
	Reference	D1.4	Date	24/03/2023

and at translating them into impacts, being either human hazards for safety and health, environmental impacts, primary energy use, etc. (Kyriakopoulos, 2007).

LCA applications to the olive oil sector in the Mediterranean area has seen several previous applications in literature; the widest variety of studies are traced for Italy and are here briefly summarized. Rinaldi et al. (2014) analysed the cradle to grave carbon footprint and energy footprint of extra virgin olive oil produced in central Italy (Perugia – Umbria, Italy). System boundaries include olive orchard cultivation, oil extraction, bottling, packaging, storage at  $-18^{\circ}\text{C}$  and distribution. The aim of the study was to establish the most environmentally intensive stages of the life cycle of the product. The functional unit chosen was 1 L of extra virgin olive oil, ready for distribution. Environmental hotspots are mainly identified in the distribution stage, due to the preference in air-transport. Secondary hotspots can be found in the olive orchard fertilization, storage in the pre-distribution stage and lastly the manufacture of glass bottles. Authors suggest modifications in the transportation policies of the product as well as the use of lighter glass bottles. Proietti et al. (2014) analysed the life cycle of a “Leccino” cultivar in Central Italy.

The environmental impacts associated with the management processes were evaluated with the LCA methodology within the use of standards UNI EN ISO 14040 and 14,044. A comparison between sequestered CO<sub>2</sub> and emissions is also developed in the paper. Results identify the highest GWP100 value traceable in the first year of cultivation, as well as the highest weight of fertilizers in the overall cultivation environmental impacts. The breakeven point between sequestration and emission is between 4 and 5 years, after which sequestered CO<sub>2</sub> reaches 5 to 6 times the value of emissions after year 10. In Salomone and Ioppolo (2012), authors performed a LCA analysis of olive oil production in the province of Messina, in Italy, in the southern island of Sicily. The study focused on the whole province with the aim of giving an insight toward the development of eco-design actions within the olive oil production sector, including different combinations of cultivation practices, olive oil extraction methods and olive oil mill waste treatments. The analysis shows higher environmental impacts for conventional scenarios (except for impact categories associated with land use), and important environmental loads associated with some sub-processes (such as fertilization, the use of pesticides and the combustion of exhausted pomace), as well as significant positive contributions associated with the use of by products as fuels or fertilizers.


In order to have further positive local impacts on the whole supply chain, authors also suggest to enhance the particular qualities of local products, e.g. by exploiting the

	Document:	D1.4. Handbook of protocols and methods		
	Author	UJAEN	Version	6
	Reference	D1.4	Date	24/03/2023

appropriate promotion and marketing strategies as well as developing circular economy and industrial symbiosis synergies between different actors and quality, traceability and environmental management systems with strong product orientation. The study also highlights some issues, most of all the poor availability of site-specific data. De Gennaro et al. (2012) reports an analysis of olive growing models and their environmental sustainability assessment: the two models analysed are “high density” (HDO) and “Super high density” (SHDO) orchards. Life cycle assessment and life cycle costing were applied to the two systems. The results highlighted that the HDO configuration performed consistently better for all impact categories, due to lower use of energy and chemicals as well as higher production yield. Results for several environmental categories are shown only for the orchard stage and they report variable highest contributions among fuel and lubricant, fertilizers and pesticides. Pattara et al. (2016) proposes five case studies in Abruzzo (central Italy) analysed through carbon footprint, in order to estimate greenhouse gas emissions due to the cultivation of olives and production of olive oil. Functional unit was chosen as 5 l of extra virgin olive oil with primary and secondary packaging. Results for the agricultural stage range from 3.34 to 7.74 kg CO<sub>2</sub> eq/FU (with a high share due to fertilizers and pesticides) while the packaging process in the industrial phase has a significant impact reaching 1.13 kg-3.20 kg of CO<sub>2</sub> eq. Proietti et al. (2017) describes a carbon footprint calculated through life cycle assessment of olive oil in Umbria (central Italy) starting from cultivation up to transformation and packaging, starting from data from different companies. The functional unit is 1 l of olive oil. Results are very variable from around 1 kgCO<sub>2</sub> eq/FU up to 4.5 kgCO<sub>2</sub> eq/FU but in all cases the olive grove phase represents the most significant contribution to the overall life cycle environmental impacts. Iraldo et al., (2014) proposes the results of an LCA based on the production of extra virgin oil in Val di Cornia (Tuscany, central Italy), using 1 kg of extra virgin olive oil as functional unit. Impact assessment was performed according to CML 2001 using several environmental impact categories as well as cumulative energy demand.

Results mark a nearly complete predominance of the agricultural stage with percentages as high as nearly 94% in the case of the eutrophication that are instead in the lowest case equal to 60% for the case of photochemical oxidation. It is worth mentioning that for acidification and eutrophication the most relevant contribution are fertilisers which cause more than 80% of the impacts highlighted by the indicator, while the other indicators mark mixed trends. In Accorsi et al. (2015), authors explore the operations of a global supply chain for extra-virgin olive oil (EVOO) in Italy according to a (LCA) methodology. The LCA assessment methodology is applied to determine the environmental impact categories associated with the bottled EVOO life cycle, focusing on packaging decisions. The study analyzes the most




	Document:	D1.4. Handbook of protocols and methods		
	Author	UJAEN	Version	6
	Reference	D1.4	Date	24/03/2023

relevant hot-spots in the supply chain supporting decisions towards more efficient and environmentally-friendly operations. Results highlight the potential of bottles in reducing the environmental impact of EVOO supply chains and identify hotspots. To a more limited extent, also in other countries the topic of LCA of olive oil has been tackled. In Spain Romero-Gamez et al. (2017), analyses the environmental impacts of olive fruit production systems in Andalusia (Southern Spain) aiming to the environmental sustainability assessment of different olive oil growing systems. The analysis considered only crop production up to the farm gate when the olive is harvested and transported to the oil mill, thus choosing 1 ton of olives as functional unit. Regional data from twelve different scenarios are described including studies from different sources. Climate change, acidification, eutrophication, ecotoxicity, land use and water resource depletion were chosen as impact categories. Results mark once more the high impact of fertilizers within most of the impact categories. Authors conclude that the manufacture and application of fertilizers contributed to the highest burdens in all impact categories and cropping systems, therefore, the reduction and optimization of fertilizers would be the most efficient way to improve the process environmentally.

The most innovative systems (intensive and super-intensive) offered the worse environmental results caused by the high level of mechanization, the large volumes of water and energy used for irrigation and high doses of fertilizers and pesticides applied. The high productivity obtained in the intensive and super-intensive systems did not justify the largest environmental impact for most categories. These innovative systems should be optimally designed to minimize the impact of their mechanization. Lastly, authors suggest the use of renewable energy generation systems to improve the eco-profile of the olive oil and an optimization of the use of fertilizers and pesticides as top priority. Navarro et al. (2018) focus instead the role of packaging within the Life Cycle Assessment of Virgin Olive Oil, through a ISO 14044 study, performed with the CML impact assessment methodology, in different case studies in Spain. The stages included in the system boundaries are: Olive production, oil making, packaging, distribution and end of life, for three different types of bottles: glass, PET and Tin, using a wide range of environmental indicators and primary energy from cumulative energy demand. The functional unit is however different than most previous cases and considers instead 0.5 L of oil and its packaging. Glass and tin packaging are the ones adding more impact (average of 58% and 37% respectively) to most of the impact categories, while PET adds about 13% of impact.


In Avraamides and Fatta (2008), LCA was used to evaluate the use of raw materials and emissions of pollutants from olive oil production in Cyprus and to identify the processes

	Document:	D1.4. Handbook of protocols and methods		
	Author	UJAEN	Version	6
	Reference	D1.4	Date	24/03/2023

causing the highest environmental impacts. The analysis is developed as “cradle to gate” and all results refer to a FU of 1 l of olive oil. The results were organised in a classification of the individual processes in priority categories according to their potential optimization: fertilization and olive oil extraction processes should be considered as priority 1 processes, irrigation and pruning are classified in priority 2, pest control and olive oil management in priority 3 and tree planting, collection and transportation of olives to the processing unit (as their contribution to all the environmental flows considered was less than 0.5%) in priority 4. The production of the inorganic fertilisers used in the agricultural stage of olive oil production and the disposal of liquid effluent from olive mills to evaporation ponds were found to be ‘ ‘hot-spot’ ’ processes. However, the study does not fully develop environmental indicators, mainly focusing instead on “hot spots” processes, making fully fledged comparisons with previously described literature difficult and potentially non-relevant.

In Busset et al. (2012) a LCA study of the French olive oil production sector is proposed, aimed at reducing the carbon footprint and optimising the waste management of the olive oil sector in the SUDOE area (Spain, Portugal and France). The results defined different scenarios for olive oil production in France based on the different olive production techniques (with or without irrigation, mechanical or not, organic or not), different extraction processes (pressing, centrifugation in two phases or centrifugation in three phases) and different waste management schemes (incineration or spreading). The expected result was a comparison of all the scenarios in order to identify the parameters that influence the environmental consequences of olive oil production.


In Tsarouhas et al. (2015) a case study of olive oil production in Greece is presented. LCA has been used to quantify the environmental performance of olive oil production in Gerakini, Chalkidiki region, Greece. The FU is 1 lt of olive oil using a plastic bottle. Fourteen sub-systems of the overall olive oil production are investigated. All key parameters that are associated with the life cycle of olive oil production are studied and environmental “hotspots” are diagnosed. Cultivation of olive trees and production of olive oil are the sub-systems that are responsible for the majority of the environmental impacts and thus authors conclude that any effort to minimize the overall life cycle impact from olive oil production should include them. Concerning climate change emissions as example, in comparison to the 1.1 kg CO<sub>2</sub> eq representing the overall climate change impacts for the life cycle examined, the cultivation of olives itself has an impact of around 40%. In El Hanandeh and Gharaibeh (2016), authors performed a comparison of different olive oil production practices in the Mediterranean region through a LCA study. Five environmental

	Document:	D1.4. Handbook of protocols and methods		
	Author	UJAEN	Version	6
	Reference	D1.4	Date	24/03/2023

impact categories relevant in the context of Jordan were assessed: acidification (AP); particulate matter formation (PM10); human toxicity (HTP); climate change (GWP100) and agricultural land occupation (AGLO).

Authors claimed that olive oil production in the northern region of Jordan is environmentally efficient when compared to large scale production practices common in other Mediterranean olive oil producing countries. In relation to the UF of 1 kg of olive oil, the life cycle includes all agricultural stages from the cultivation of the olive tree, harvesting, milling and oil extraction, as well as packaging and transportation. Life Cycle impacts are reported as average on a large number of small and micro-scale farmers in Jordan: Climate change is equal to 0.57 kg CO<sub>2</sub> eq, Acidification is equal to 11.83 g SO<sub>2</sub> eq, Particulate matter is 5.99 g PM<sub>10</sub> eq Human toxicity is equal to 0.774 kg 1.4 dB eq. Rajaeifar et al. (2014) analysed energy and economic flows and greenhouse gas (GHG) emissions of olive oil production in Iran through a LCA with considering four main stages of agricultural olive production, olive transportation, olive oil extraction and its olive oil transportation to the customer centres. Data were collected from 150 olive growers in the Guilan province of Iran. Energy and economic flows and greenhouse gas (GHG) emissions of olive oil production in Iran were investigated considering four main stages of agricultural olive production, olive transportation, olive oil extraction and transportation to the customer centres. The agricultural production stage ranked the first in GHG emissions among the four stages with the share of 93.81% of total GHG emissions. Some final and summarizing remarks can be formulated: The use of conventional technologies in the olive oil generation scenarios is usually tied with higher environmental impacts. Intensive production has usually higher environmental impacts, while extensive cultivation scenarios are characterized by lower productivity per area. It is also worth mentioning, that most LCA studies cannot take in consideration some aspects, such as the better organoleptic quality of organic materials, the higher level of antioxidants, longer shelf life than non-organic materials, and this should be kept in mind when comparing mere impact data tables (Longo et al., 2017).


Different hot spots are also traced in the production and treatment phases throughout the different studies of the olive oil stage (Bernardi et al., 2018) The result trends are variable with the localization and the techniques used in the olive oil production stages as in (De Luca et al., 2018a). Similar trends and results can be traced within the three main producers in EU, Italy, Spain and Greece. Although a wide set of indicators were chosen for the LCAs as well as different functional units that make comparisons difficult, the following Fig. 1 includes the results achieved within the most used indicator (GWP) and functional unit (1 l

	Document:	D1.4. Handbook of protocols and methods		
	Author	UJAEN	Version	6
	Reference	D1.4	Date	24/03/2023

of olive oil). Sustainability became the catchword of academic research in the last decades. This is mainly due to the growing interest of consumers, entrepreneurs, politicians and many other private and public actors in reduce human impacts on natural resources. However, environmental sustainability is not the only concern: economic and social consequences of anthropic activities are felt as important to satisfy social necessities and human well-being.

Life Cycle Thinking (LCT) tools stand out for their ability to prevent burden shifts by considering all phases of the life cycle of a product, from planning to disposal or reuse (De Luca et al., 2015a, 2015c). Organic production is widely recognized for being less impacting; therefore, some studies tried to implement in olive growing production also Life Cycle Costing (LCC) and social Life Cycle Assessment (sLCA). The first tool is aimed at the accounting of every cost generated all along the functioning of the life cycle, allowing a long-term evaluation of the cost-effectiveness (ISO, 2008; Stillitano et al., 2016). The second one, is the most recent and controversial methodology among this family of evaluation tools; indeed, it is striving to reach consensus on many issues, such as the purposes of the assessment, the source of impacts to be considered, the impact assessment method and the epistemological bases underpinning the methodological choices (Iofrida et al., 2018a). The present study applies a Psychosocial Risk Factors (PRF) pathway (Gasnier, 2012; Silveri et al., 2014; Iofrida et al., 2018b), that allows predicting damages on health on the workers directly involved in the life cycle of a product. Decent work, especially in agriculture, has been the among the first goals of international organizations (such as ILO, the International Labour Organization) and policies; indeed, many conditions can threaten the safety of workers, in terms of ergonomics, exposure to hazardous products, diseases and accidents, and psychosocial risks. Concerning these last, one of the most diffused definitions describes PRF as “those aspects of work planning and management - and their relative social and environmental contexts - that can potentially lead to physical or psychological damages” (Cox and Griffiths 1995:69). Until now, few studies have focused on olive production systems applying LCC (De Gennaro et al., 2012; Ramez et al., 2014; Notarnicola et al., 2004; Stillitano et al., 2016, 2017b2018) and only De Luca et al. (2018a, 2018b) integrated more life cycle tools to the olive growing sector, i.e. LCA and SLCA.

Based on the results of previous research (Stillitano et al., 2016, 2017b2018), this study represents a further development by assessing the social and economic impacts of Italian olive growing in the study area of the Plain of Lamezia Terme, in South Italy. Plains are commonly preferred for agricultural activities: in fact, in this kind of areas, it is concentrated the highest percentage of Calabrian olive orchards. In particular, the aim is to compare


	Document:	D1.4. Handbook of protocols and methods		
	Author	UJAEN	Version	6
	Reference	D1.4	Date	24/03/2023

organic and conventional olive growing practices, to highlight differences in terms of long-term profitability and impacts on workers' health.

### 8.3.3 Methodological application to Sustainolive project

The environmental impact analysis is carried out through an LCA that is applied according to ISO norms (ISO, 2006a, ISO, 2006b). The functional units (FU) are 1 ha of cultivated surface and 1 kg of olive harvested, and the system boundary consisted of the agricultural production “from cradle to farm gate”. In the Life Cycle studies, the choice of FU is at the discretion of the practitioner, but it strongly depends on the objectives of the assessment, the addressees of the study, and the typology of the investigation. According to a review by Cerutti et al. (2015), surface FUs are preferred when management practices are under discussion. Data for foreground processes were directly collected from the experimental design and included the fuel, lubricants and water consumption, typology of water distribution and related energy consumption, quantity, type, period and distribution modality of fertilizers and pesticides, distances of transport and masses of products dislocated, waste typology, mass and disposal modality, and all the inputs and outputs linked to weed control. Data on nitrous oxide and ammonia emissions were estimated according to Brentrup et al. (2000). The herbicide emissions were estimated as 100% of the active ingredient (Nemecek and Kägi, 2007). Data on the background processes were obtained from the Eco-invent V. 3.2 database (Wernet et al., 2016), and they were related to the fuel, lubricant, energy, fertilizers, pesticides, herbicides and capital goods production as well as waste processes. LCA elaborations were performed with SimaPro software (PR è , 2016). To identify the environmental impacts of each agricultural operation, three impact categories were selected. First, the Climate Change from the IPCC 100a - 2013 method to highlight the impact related to the mechanical operations.

The Toxicity (the sum of human, fresh water aquatic, marine aquatic and terrestrial ecotoxicity) was found using the CML baseline V3.03 method to uncover the effects of chemical herbicide use and Land Use (the sum of agricultural and urban land occupations) from the ReCiPe midpoint method to consider the area that was subjected to alterations during the orchard life cycle. Other impact categories should be considered, but the selection was limited to three to harmonize the integration of the different life cycle tools. A sensitivity analysis was performed by varying the principal inputs connected to the agricultural operation. To identify the economic insights, a Conventional LCC (Ciroth et al., 2016) is applied. The system boundary and the functional unit were similar to those of the LCA. This approach is based on a cash flow model (ISO, 2008), and it allows for the


	Document:	D1.4. Handbook of protocols and methods		
	Author	UJAEN	Version	6
	Reference	D1.4	Date	24/03/2023

rationalization of the long-term decision-making process when different investment alternatives are available. Because the study followed a farms perspective, only the real money flows were considered (Swarr et al., 2011, Martínez-Blanco et al., 2014). As a first step in the analysis, all of the costs occurring over the life cycle of each weeding scenario were calculated. For this purpose, an economic inventory was created through the monetization of all the collected inputs and outputs. This collection was performed by multiplying the measured quantities by the unit prices of the last year. Therefore, this economic inventory was fully complementary to the environmental one, because each unitary process cost was split into its elementary components (Falcone et al., 2016); in particular, costs related to the planting (investment costs) and operating costs of each production stage and disposal costs were analysed.

The total cost was classified into variable and fixed costs. The following variable costs were accounted for in the production process: fertilizers, pesticides, herbicides, fuels and lubricant consumption by machinery, human labour costs needed during agricultural operations, outsourced cost items (e.g., expert consultancies, transport and outsourced cultivation practices), and interests on advanced capital. The fixed costs included the ownership costs of the machinery and land investments (i.e., the depreciation, insurance and maintenance), rent for land use, interests on capital goods, taxes and administrative overheads (De Luca et al., 2015b, Falcone et al., 2015, Stillitano et al., 2017). Here, the input cost was calculated according to the current market prices. The family labour cost was estimated in terms of the opportunity cost and was equalized to the employment of casual workers according to the local current wage. The rental cost for land use was deduced from the average local rental prices while accounting for the interests on advance capital and capital goods, where interest rates of 4.5% and 2% were applied, respectively. The administrative overheads were estimated to be 5% of the gross production value, which corresponds to the annual total revenues (Stillitano et al., 2016). The total revenues for the entire life cycle of each scenario were then calculated by multiplying the olive yield by its market price, which referred to the last harvest season (De Gennaro et al., 2012, Mohamad et al., 2014), including EU Agricultural Policy subsidies.

All of the costs and revenues were discounted for the entire life cycle of olive plant but also are calculated in terms cost/revenues per year. To select a discount rate, the opportunity cost approach in terms of alternative investments with a similar risk and time was used. During the life cycle, we assumed constant prices, and therefore, we could exclude adjustments for inflation (Emblemsvåg, 2003, Hussain et al., 2005). Thus, three economic categories were identified, i.e., Profitability, Life cycle costs and Investment feasibility, which




	Document:	D1.4. Handbook of protocols and methods		
	Author	UJAEN	Version	6
	Reference	D1.4	Date	24/03/2023

corresponded to the following indicators: the Gross Margin (GM), Discounted Life Cycle Costs (DLCC) and Net Present Value (NPV). The first indicator was calculated by subtracting the variable costs from the total revenues. The discounted life cycle costs were determined by summing up the investment costs, the present value of the operating costs of each production phase, and disposal costs; this indicator has been applied to estimate the overall cost of the different scenarios, with the purpose of recognizing the primary processes responsible for most of the economic impacts. The cash flow assessments generated at different stages of the project lifespan can provide information on its viability; thus, the NPV was chosen as an indicator of the investment feasibility and represents the sum of discounted future cash flows incurred during the whole life cycle. It is also one of the most frequently applied and appropriate indicators in the LCC literature (Foolmaun and Ramjeawon, 2013, Hossaini et al., 2014, Yu and Halog, 2015).

The selected indicators were able to assess the primary economic hotspots during the entire life of the olive growing systems, and therefore, they provided information on more effective management for long-term sustainability. As a final step, sensitivity analyses were performed by changing the olive selling prices, the discount rate, and the primary input used in the agricultural phases to demonstrate how the economic results are related to these variables. The sensitivity analysis concerning the olive price change was performed by assuming a specific range and by excluding public subsidies, to reflect the market price dynamics in a free market.


The LCA and LCC have their roots in disciplines belonging to the so-called “hard sciences”, and therefore, post-positivist paradigms are predominant (Iofrida et al., 2016). This approach is probably the primary reason why the LCA and LCC first reached a methodological consensus, and standardized procedures were established in ISO 14040:2006 and ISO 14044:2006 for LCA and in ISO 15686-5:2008 and Norwegian standard NS 3454 for LCC, but only for buildings and constructed assets. This is not the case for sLCA, which, despite being proposed during the nineties, did not yet have a common methodological procedure. A broad number of different methodological proposals have been set up with attention to the most diverse aspects, such as company responsibilities or impacts derived from the very nature of the life cycle, a local perspective or global one, with lists of primarily static indicators that were chosen according to very different criteria. The sLCA proposed here has been conceived to be epistemologically near the other methodologies, to facilitate their integration from a holistic perspective. Therefore, the assessment methodology chosen here belongs to mixed-methods research (Tashakkori and Teddlie, 2010), i.e., it combines an “impact pathway” (Feschet et al., 2013, Macombe et

	Document:	D1.4. Handbook of protocols and methods		
	Author	UJAEN	Version	6
	Reference	D1.4	Date	24/03/2023


al., 2013, Silveri et al., 2014, Bocoum et al., 2015, Iofrida, 2016) and a type 1 impact assessment (e.g., UNEP-SETAC, 2009, De Luca et al., 2015b, De Luca et al., 2015a). Both positive and negative indicators could be chosen (Di Cesare et al., 2016). In detail, the “social health” impact category is used for people who are directly involved in the life cycle, i.e., all types of workers, such as farmers, experts, employees, and labourers. Consumers have been excluded in accordance with the system boundaries of the other LC tools. Here, the source of impacts under consideration is the very nature of the life cycle, and farm responsibilities (organization, management, decisions, and internal policies) are not taken into account. The impacts found here are assessed in terms of psychosocial risk factors (Cox et al., 2000, Gasnier, 2012, Silveri et al., 2014, Amiri et al., 2015), i.e., the hours of potential exposure when someone works under conditions that can lead to health problems. These risks are measured in terms of the odds ratio (OR) and are classified by the strength of association. For each life cycle phase, an inventory sheet reported how many hours of work were necessary (the average of the interview data) for each task. Each task was then related to one or more working condition (noise, vibrations, stress, open-air work, and use of chemicals) (Callea et al., 2014). A literature review has been conducted to gather those studies and correlate these conditions with the psychosocial risks.

## 8.4. Bibliographical references


- ADRIAANSE, A.; BRINGEZU, S.; HAMMOND, A.; MORIGUCHI, Y.; RODENBURG, E.; ROGICH, D. and SCHÜTZ, H. (1997): Resource flows: The material basis of industrial economies. Washington, DC: World Resources Institute.
- AGUILERA, E., GUZMÁN, G.I., INFANTE-AMATE, J., SOTO, D., GARCÍA-RUIZ, R., HERRERA, A., VILLA, I., TORREMOCHA, E., CARRANZA, G., GONZÁLEZ DE MOLINA, P. (2015). Embodied energy in agricultural inputs. Incorporating a historical perspective. *DT-SEHA* 1507.
- BEZNER KERR, R, MADSEN, S, STÜBER, M, LIEBERT, J, ENLOE, S, BORGHINO, N, PARROS, P, MUTYAMBAI, D M, PRUDHON, M, WEZEL, A, 2021. Can agroecology improve food security and nutrition? A review. *Global Food Security*. 29, 100540. <https://doi.org/10.1016/j.gfs.2021.100540>.
- BRINGEZU, S., H. SCHÜTZ Y S. MOLL (2003), Rationale for and interpretation of economy-wide materials flow analysis and derived indicators. *Journal of Industrial Ecology* 7(2): 43–64.
- D'ANNOLFO, R, GEMMILL-HERREN, B, GRAEUB, B, GARIBALDI LA. 2017. A review of social and economic performance of agroecology. *International Journal of Agricultural Sustainability*. 15:6, 632-644.
- DE LUCA, AI, FALCONE, G, STILLITANO, T, IOFRIDA, N, STRANO, A, GULISANO, G, 2018. Evaluation of sustainable innovations in olive growing systems: A Life Cycle Sustainability Assessment case study in southern Italy. *Journal of Cleaner Production*. 171, 1187-1202. <https://doi.org/10.1016/j.jclepro.2017.10.119>.
- EUROSTAT (2001), Economy-wide material flow accounts and derived indicators: A methodological guide. Eurostat, European Commission, Luxembourg: Eurostat, 2001;
- EUROSTAT (2015), Economy-wide Material Flow Accounts (EW-MFA). Compilation Guide 2013. Luxembourg: European Statistical Office.
- FAO. TAPE Tool for Agroecology Performance Evaluation 2019 - Process of development and guidelines for application. Test version. Rome. Available on <http://www.fao.org/3/ca7407en/CA7407EN.pdf> (accessed 01 May 2021).

	Document:	D1.4. Handbook of protocols and methods		
	Author	UJAEN	Version	6
	Reference	D1.4	Date	24/03/2023

- FISCHER-KOWALSKI M (1998) Society's metabolism: the intellectual history of materials flow analysis, part I, 1860–1970. *J Ind Ecol* 2:61–77
- FISCHER-KOWALSKI, M. and HABERL, H. (1993): "Metabolism and colonization. Modes of production and the physical exchange between societies and nature. Innovation", in *The European Journal of Social Science Research*, nº 6, vol. 4, pp. 415–442.
- FISCHER-KOWALSKI, M. and HABERL, H. (2007): *Socioecological transitions and global change: Trajectories of social metabolism and land use*. Institute of Social Ecology. Vienna (Austria). Edward Elgar Publishing.
- FISCHER-KOWALSKI, M. Y HABERL H., 1997. Tons, joules and money: modes of production and their sustainability problems. *Society and Natural Resources* 10(1): 61–85.
- GEORGESCU-ROGEN, N. (1971), *The entropy law and the economic process*. Cambridge. Harvard University Press.
- GIAMPIETRO, M. and BUKKENS, S. (2015): "Analogy between Sudoku and the multi-scale integrated analysis of societal metabolism", in *Ecological Informatics*, nº 26, vol. 1, pp. 18–28.
- GIAMPIETRO, M. and MAYUMI, K. (2000): "Multiple-scale integrated assessment of societal metabolism: introducing the approach", in *Population and Environment*, nº 22, pp. 109–154.
- GIAMPIETRO, M., MAYUMI, K. and RAMOS-MARTIN, J. (2008a): "Multi-Scale Integrated Analysis of Societal and Ecosystem Metabolism (MUSIASEM). An Outline of Rationale and Theory", in *Document de treball, Departament d'Economia Aplicada de la Universitat Autònoma de Barcelona*. Barcelona.
- GIAMPIETRO, M.; ASPINALLIS, R. J.; RAMOS-MARTIN, J. and BUKKEN, S. G. F. (eds), (2014): *Resource Accounting for Sustainability Assessment: the nexus between energy, food, water and land use*. London. Routledge.
- GIAMPIETRO, M.; MAYUMI, K.; and SORMAN, A. H. (2011), *The metabolic pattern of societies: where economists fall short*. London. Routledge.
- GIERLINGER, S. and KRAUSMANN, F. (2012): "The Physical Economy of United States of America", in *Journal of Industrial Ecology*, nº 16, vol. 3, pp. 365–377.
- GONZÁLEZ DE MOLINA, M, LOPEZ-GARCIA, D, 2021. Principles for designing Agroecology-based Local (territorial) Agri-food Systems: a critical revision. *Agroecology and Sustainable Food Systems*, DOI: 10.1080/21683565.2021.1913690
- GONZÁLEZ DE MOLINA, M, SOTO FERNÁNDEZ, D, GUZMÁN CASADO, G, INFANTE-AMATE, J, AGUILERA FERNÁNDEZ, E, VILA TRAVER, J, GARCÍA RUIZ, R, 2020. Agrarian Metabolism: The Metabolic Approach Applied to Agriculture, in: González de Molina, M, Soto Fernández, D, Guzmán Casado, G, Infante-Amate, J, Aguilera Fernández, E, Vila Traver, J, García Ruiz, R, (Ed.), *The Social Metabolism of Spanish Agriculture, 1900–2008. The Mediterranean Way Towards Industrialization*. Environmental History, 10. Springer Open. <https://doi.org/10.1007/978-3-030-20900-1>
- GONZÁLEZ DE MOLINA, M. and TOLEDO, V. (2011): *Metabolismos, naturaleza e historia. Una teoría de las transformaciones socio-ecológicas*. Barcelona. Icaria.
- GONZÁLEZ DE MOLINA, M. and TOLEDO, V. (2014): *Social Metabolism: A Theory on Socio-Ecological Transformations*. New York. Springer. González de Molina & Toledo, 2011, 2014
- GONZÁLEZ DE MOLINA, MANUEL, DAVID SOTO FERNÁNDEZ, GLORIA GUZMÁN CASADO, JUAN INFANTE-AMATE, EDUARDO AGUILERA FERNÁNDEZ, JAIME VILA TRAVER and ROBERTO GARCÍA RUIZ, eds. *The Social Metabolism of Spanish Agriculture, 1900–2008*. Berlin: Springer, 2020.
- GREŠLOVÁ, P.; GINGRICH, S.; KRAUSMANN, F.; CHROMÝ, P. and JANČÁK, V. (2015): "Social metabolism of Czech agriculture in the period 1830–2010", in *AUC Geographica*, nº 50, vol. 1, pp. 23–35.
- GUZMÁN CASADO, G. I. and GONZÁLEZ DE MOLINA, M. (2009): "Preindustrial agriculture versus organic agriculture: The land cost of sustainability", in *Land Use Policy*, nº 26, pp. 502–510.
- GUZMÁN G. I. and GONZÁLEZ DE MOLINA, M. (2017): *Energy in Agroecosystems: a Tool for Assessing Sustainability*. Boca Raton (FL). CRC Press.
- GUZMÁN, G. I., AGUILERA, E., GARCÍA-RUIZ, R., TORREMOCHA, E., SOTO-FERNÁNDEZ, D., INFANTE-AMATE, J., GONZÁLEZ DE MOLINA, M. (2018). The agrarian metabolism as a tool for assessing agrarian sustainability, and its application to Spanish agriculture (1960–2008). *Ecology and Society*, 23(1).
- GUZMÁN, G. I., GONZÁLEZ DE MOLINA, M. (2015). Energy efficiency in agrarian systems from an agroecological perspective. *Agroecology and Sustainable Food Systems*, 39(8), 924–952.

	Document:	D1.4. Handbook of protocols and methods		
	Author	UJAEN	Version	6
	Reference	D1.4	Date	24/03/2023

- GUZMÁN, G. I., GONZÁLEZ DE MOLINA, M., SOTO FERNÁNDEZ, D., INFANTE-AMATE, J., AGUILERA, E. (2017). Spanish agriculture from 1900 to 2008: a long-term perspective on agroecosystem energy from an agroecological approach. *Regional Environmental Change*, 18(4), 995-1008.
- GUZMÁN, G. I.; GONZÁLEZ DE MOLINA, M. and ALONSO, A. M. (2011): "The land cost of agrarian sustainability: an assessment", in *Land Use Policy*, nº 28, 825-835.
- GUZMÁN, G., AGUILERA, E., SOTO, D., CID, A., INFANTE-AMATE, J., GARCÍA RUIZ, R., HERRERA, A., VILLA, I., GONZÁLEZ DE MOLINA, M. (2014). Methodology and Conversion Factors to Estimate the Net Primary Productivity of Historical and Contemporary Agroecosystems. *DT-SEHA* 1407.
- HABERL, H. (2001): "The energetic metabolism of societies. I: Accounting concepts", in *Journal of Industrial Ecology*, nº 5, pp. 11-33.
- HELLER, M. C. and KEOLEIAN, G. A. (2003): "Assessing the sustainability of the US food system: a life cycle perspective", in *Agricultural Systems*, nº 76, pp. 1007-1041.
- INFANTE-AMATE, J., AGUILERA FERNÁNDEZ, E. & GONZÁLEZ DE MOLINA, M (2018b), Energy transition in Agri-food systems. Structural change, drivers and policy implications (Spain, 1960–2010). *Energy policy*, vol. 122, pp. 570-579.
- INFANTE-AMATE, J.; AGUILERA, E.; PALMERI, F.; GUZMÁN, G.; SOTO, D.; GARCÍA-RUIZ, R. and GONZÁLEZ DE MOLINA, M. (2018a): "Land embodied in Spain's biomass trade and consumption (1900–2008): Historical changes, drivers and impacts", in *Land Use Policy*, nº 78, pp. 493-502.
- INFANTE-AMATE, J.; GONZÁLEZ DE MOLINA, M.; TOLEDO, V. (2017), El metabolismo social. Historia, métodos y principales aportaciones. *Revista Iberoamericana de Economía Ecológica* Vol. 27: 130-152.
- INFANTE-AMATE, J.; SOTO, D.; AGUILERA, E.; GARCÍA RUIZ, R.; GUZMÁN, G.; CID, A. and GONZÁLEZ DE MOLINA, M. (2015): "The Spanish Transition to Industrial Metabolism Long-Term Material Flow Analysis (1860-2010)", in *Journal of Industrial Ecology*, nº 19, vol. 5, pp. 866-876. Available in: <https://doi.org/10.1111/jiec.12261>
- IOFRIDA, N, STILLITANO, T, FALCONE, G, GULISANO, G, NICOLÒ, BF, DE LUCA, AI, 2020. The socio-economic impacts of organic and conventional olive growing in Italy. *New Medit.* 1, 117-131. <https://doi.org/10.30682/nm2001h>.
- KOVANDA, J. and HAK, T. (2011): "Historical perspectives of material use in Czechoslovakia in 1855-2007", in *Ecological Indicators*, nº 11, vol. 5, pp. 1375-1384.
- KRAUSMANN, F.; ERB, K. E.; GRINGRICH, S.; LAUK, C. and HABERL, H. (2008): "Global patterns of socioeconomic biomass flows in the year 2000: a comprehensive assessment of supply, consumption and constraints", in *Ecological Economics*, nº 65, pp. 471-487.
- KRAUSMANN, F.; GRINGRICH, S. and NOURBAKHCH-SABET, R. (2011): "The Metabolic Transition in Japan", in *Journal of Industrial Ecology*, nº 15, vol. 6, pp. 877-892.
- LANDERT, J, PFEIFER, C, CAROLUS, J, SCHWARZ, G, ALBANITO, F, MULLER, A, SMITH, P, SANDERS, J, SCHADER, C, VANNI, F, PRAZAN, J, BAUMGART, L, BLOCKEEL, J, WEISSHAIDINGER, R, BARTEL-KRATOCHVIL, R, HOLLAUS, A, MAYER, A, HRABALOVA, A, HELIN, J, AAKKULA, J, SVELS, K, GUISEPELLI, E, SMYRNIOTOPOULOU, A, VLAHOS, G, IORDANIDIS, Y, SZILÁGYI, A, PODMANICZKY, L, BALÁZS, K, GALIOTO, F, LONGHITANO, D, ROSSIGNOLO, L, POVELLATO, A, ŽILĀNS, A, JEJELEVIČIUS, G, FRĂȚILĂ, M, YOLDI, UI, MASSA, CA, BIENZOBAS ADRIÁN, J, SAHLIN, KR, RÖÖS, E, FRICK, R, BIRCHER, R, AALDERS, I, IRVINE, KN, KYLE, C, MILLER, D, 2020. Assessing agro-ecological practices using a combination of three sustainability assessment tools. *Landbauforschung*, 70, 2:129-144. <https://doi.org/10.3220/LBF1612794225000>.
- LÓPEZ-RIDAURA, M.; MASERA, O. and ASTIER, M. (2002): "Evaluating the sustainability of complex socio-environmental systems. The MESMIS framework", in *Ecological Indicators*, nº 2, vol. 1-2, pp. 135-148.
- MATTHEWS, E. (2000), *The Weight of Nations: material outflows from industrial economies*. Washington DC. World Resources Institute.
- MOTTET, A, BICKSLER, A, LUCANTONI, D, DE ROSA, F, SCHERF, B, SCOPEL, E, LÓPEZ-RIDAURA, S, GEMMIL-HERREN, B, BEZNER KERR, R, SOURISSEAU, J-M, PETERSEN, P, CHOTTE, J-L, LOCONTO, A, TITTONELL, P, 2020. Assessing Transitions to Sustainable Agricultural and Food Systems: A Tool for Agroecology Performance Evaluation (TAPE). *Front. Sustain. Food Syst.* 4:579154. <https://doi.org/10.3389/fsufs.2020.579154>.
- RISKU-NORJA, H. (1999): "The total material requirement-concept applied to agriculture: a case study from Finland", in *Agricultural and Food Science in Finland*, nº 8, pp. 393-410.

	Document:	D1.4. Handbook of protocols and methods		
	Author	UJAEN	Version	6
	Reference	D1.4	Date	24/03/2023

- RISKU-NORJA, H. and MÄENPÄÄ (2007): "MFA model to assess economic and environmental consequences of food production and consumption", in *Ecological Economics*, nº 60, vol. 4, pp. 700-711. Available in: <https://doi.org/10.1016/j.ecolecon.2006.05.001>
- SCHANDL, H. and SCHULZ, N. (2002): "Changes in the United Kingdom's natural relations in terms of society's metabolism and land-use from 1850 to the present day", in *Ecological Economics*, nº 41, vol. 2, pp. 203-221.
- SCHEIDEL, A. and SORMAN, A. H. (2012): "Energy transitions and the global land rush: Ultimate drivers and persistent consequences", in *Global Environmental Change*, nº 22, vol. 3, pp. 559-794.
- SIEFERLE R. P. (2011): Cultural evolution and social metabolism, in *Geografiska Annaler. Series B, Human Geography*, nº 93, vol. 4, pp. 315-324.
- SINGH, S. J.; KRAUSMANN, F.; GINGRICH, S.; HABERL, H.; ERB, K. H. and LANZ, P. (2012): "India's biophysical economy, 1961-2008. Sustainability in a national and global context", in *Ecological Economics*, nº 76, pp. 60-69.
- SMIL, V. (2013): *Harvesting the Biosphere: What We Have Taken from Nature*. London. The MIT Press.
- SOTO, D., INFANTE-AMATE, J., GUZMÁN, G.I., CID, A., AGUILERA, E., GARCÍA, R., GONZÁLEZ DE MOLINA, M. (2016). The social metabolism of biomass in Spain, 1900–2008: From food to feed-oriented changes in the agro-ecosystems. *Ecological Economics*, 128, 130-138.
- SUSTAINOLIVE, 2019. Grant Agreement "SUSTAINOLIVE – Novel approaches to promote the sustainability of olive groves in the Mediterranean", Grant Agreement Number 1811 (Call 2018 Section 1 Farming). Partnership for Research and Innovation in the Mediterranean Area Programme (PRIMA).
- TELLO, E. & GONZÁLEZ DE MOLINA, M. (2017), Methodological Challenges and General Criteria for Assessing and Designing Local Sustainable Agri-Food Systems: A Socio-Ecological Approach at Landscape Level. In Fraňková, E.; Haas, W.; Singh, J. S. (2017), *Socio-metabolic Perspectives on the Sustainability of Local Food Systems. Insights for Science, Policy and Practice*. Berlin: Springer, pp. 27-68.
- TELLO, E. GALÁN, V. SACRISTÁN, G. CUNFER, G.I. GUZMÁN, M. GONZÁLEZ DE MOLINA, F. KRAUSMANN, S. GINGRICH, R. PADRÓ, I. MARCO, D. MORENO-DELGADO (2016), Opening the black box of energy throughputs in farm systems: A decomposition analysis between the energy returns to external inputs, internal biomass reuses and total inputs consumed (the Vallès County, Catalonia, c.1860 and 1999). *Ecological Economics*. 121: 160–174
- VAN CAUWENBERGH, N.; BIALA, K.; BIELDERS, C. (2007): "SAFE – a hierarchical framework for assessing the sustainability of agricultural systems", in *Agriculture, Ecosystems and Environment*, nº 120, vol. 2-4, pp. 229-242.
- VAN DER PLOEG, JD, BARJOLLE, D, BRUIL, J, BRUNORI, G, COSTA MADUREIRA, LM, DESSEIN, J, DRĄG, Z, FINK-KESSLER, A, GASSELIN, P, GONZALEZ DE MOLINA, M, GORLACH, K, JÜRGENS, K, KINSELLA, J, KIRWAN, J, KNICKEL, K, LUCAS, V, MARSDEN, T, MAYE, D, MIGLIORINI, P, MILONE, P, NOE, E, NOWAK, P, PARROTT, N, PEETERS, A, ROSSI, A, SCHERMER, M, VENTURA, F, VISSER, M, WEZEL, A, 2019. The economic potential of agroecology: Empirical evidence from Europe. *Journal of Rural Studies*. 71, 46-61. <https://doi.org/10.1016/j.jrurstud.2019.09.003>.
- WEISZ, H.; KRAUSMANN, F.; AMANN, C.; EISENMENGER, N.; ERB, K. H.; HUBACEK, K. and FISCHER-KOWALSKI, M. (2006): "The physical economy of the European Union: crosscountry comparison and determinants of material consumption", in *Ecological Economics*, nº 58, vol. 4, pp. 676-698
- WEZEL, A, BELLON, S, DORÉ, T, FRANCIS, C, VALLOD, D, DAVID, C, 2009. Agroecology as a science, a movement and a practice. A review. *Agronomy for Sustainable Development*. 29, 503-515. <https://doi.org/10.1051/agro/2009004>.
- WIRSENIUS, S. (2003): "The Biomass Metabolism of the Food System. A Model-Based Survey of the Global and Regional Turnover of Food Biomass", in *Journal of Industrial Ecology*, nº 7, vol. 1, pp. 47-80.